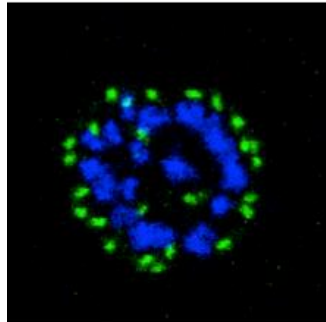


**Identification and characterization of invasion-related  
proteins of the malaria parasite *Plasmodium falciparum*  
(Welch, 1892)**



Dissertation with the aim of achieving a doctoral degree of the faculty of  
Mathematics, Informatics and Natural Sciences

Department of Biology

University of Hamburg

Submitted by

Louisa Wilcke

Hamburg, 2018

Dissertationsgutachter: Prof. Dr. Tim-Wolf Gilberger

Dr. Tobias Spielmann

Datum der Disputation: 23.03.2018

## **Eidesstattliche Versicherung**

Hiermit erkläre ich an Eides statt, dass ich die vorliegende Dissertationsschrift selbst verfasst und keine anderen als die angegebenen Quellen und Hilfsmittel benutzt habe.

Hamburg, 22.02.2018

Louisa Wilcke

**Language certificate**

I am a native speaker, have read the present PhD thesis and hereby confirm that it complies with the rules of the English language.

A handwritten signature in black ink, reading "Mackenzie Jonscher". The signature is written in a cursive style with a large initial 'M' and 'J'.

Hamburg, February 14<sup>th</sup>, 2018

Mackenzie Jonscher

## Summary

Malaria is a vector-borne disease, which is caused by a protist of the *Plasmodium* genus. *Plasmodium spp.* are obligate intracellular parasites with a complex life cycle that alters between a vertebrate and a mosquito host.

One of the essential steps in the vertebrate host is the asexual proliferation within the erythrocytes that allows the exponential multiplication of the pathogen and is responsible for all clinical symptoms in humans. To survive and multiply the parasite invades its host cell rapidly. It relies on an orchestrated cascade of molecular interactions between parasite ligands and surface structure on the erythrocyte. The aim of this work is i) to probe into the role of putative phosphorylation sites in the cytoplasmic domain of one well established parasite ligand called “Erythrocyte Binding Antigen 175” (EBA175) and ii) to identify novel parasite proteins that are secreted and might function as ligands during the invasion process.

Towards the first sub aim – I assessed six predicted phosphorylation sites within the cytoplasmic domain. To do so, I generated a transgenic parasite line with six amino acid exchanges targeting each of these putative phosphorylation sites. Using an assay that allows the quantification of EBA175 function, I could show that – in contrast to other parasite ligands – none of these putative phosphorylation sites are essential for protein function.

The second sub aim of my project focused on the identification of novel secreted proteins playing a role in the invasion process. Candidates were identified using bioinformatics tools that identified genes with i) a transcriptional profile similar to known parasite ligands and other host cell invasion related proteins and ii) encompass a predicted sequence coding for a signal peptide. This resulted in a list of 289 genes fulfilling these criteria out of which 156 were not characterized. Out of these, 38 genes with unpublished function were selected for further analyses. The first step in the

functional investigation was the tagging of the genes of interest at the 3' end with GFP, which resulted in 29 transgenic parasite lines with a gene specific GFP tag. Using fluorescence microscopy in live parasites expression and localization of the fusion proteins were investigated and subdivided into five categories. 15 proteins could be localized to the invasion relevant compartments surface, inner membrane or basal complex, and apical organelles. In order to analyze the function of these 15 proteins a gene knock-out approach was initiated that already reveals that 6 proteins of these are redundant and 4 appear to be likely essential. Taking together, this approach allows the rapid identification of novel candidate gene that might play an important role in erythrocyte invasion.

## Zusammenfassung

Malaria ist eine durch einen Vektor übertragene Infektionskrankheit, die durch einen intrazellulären Parasiten der Gattung *Plasmodium* ausgelöst wird. Plasmodien haben einen komplexen Lebenszyklus, der zwischen Wirbeltieren und Mücken alterniert. Ein wesentlicher Schritt dieses Lebenszyklus ist die asexuelle Vermehrung, die innerhalb von Erythrozyten im Wirbeltier-Wirt stattfindet. Sie ermöglicht eine exponentielle Vermehrung des Parasiten und ist für das Krankheitsbild der Malaria verantwortlich. Um zu überleben, ist eine schnelle Invasion in die Wirtszelle notwendig. Der Invasionsprozess ist sehr komplex und umfasst viele streng regulierte Wechselwirkungen zwischen Liganden des Parasiten und Rezeptoren auf der Oberfläche der Wirtszelle.

Ein wichtiger und gut charakterisierter Invasionsligand ist „Erythrocyte Binding Antigen 175“ (EBA175). Ziel dieser Arbeit war es zum einen, die Rolle von putativen Phosphorylierungsstellen innerhalb der zytoplasmatischen Domäne von EBA175 zu untersuchen. Zum anderen sollten neue sekretierte Parasitenproteine identifiziert werden, die als Invasionsliganden in Frage kommen.

Um die Phosphorylierung der zytoplasmatischen Domäne von EBA175 zu untersuchen, wurde eine Zelllinie generiert, in welcher sechs vorhergesagte Phosphorylierungsstellen ausgetauscht wurden, um deren Phosphorylierung zu unterbinden. Mit Hilfe eines Invasionsassays wurde gezeigt, dass – im Gegensatz zu anderen Invasionsliganden des Parasiten – keine dieser putativen Phosphorylierungsstellen einen essentiellen Einfluss auf die Funktionalität des Liganden hat.

Das zweite Projekt zielte auf die Identifikation neuer sekretierter Proteine ab, die eine Rolle im Invasionsprozess spielen. Von anderen Invasionsliganden und Proteinen, die an der Invasion beteiligt sind, ist ein spätes Transkriptionsprofil bekannt. Mit Hilfe eines bioinformatischen Ansatzes wurde nach Kandidatengen gesucht, die ein solches Profil

und zusätzlich ein vorhergesagtes Signalpeptid aufweisen. Aus einer Liste von zunächst 289 Genen wurden 38 Kandidaten mit unbekannter oder nicht veröffentlichter Funktion ausgesucht, um diese weiter zu charakterisieren. Alle Kandidaten wurden zunächst C-terminal mit GFP fusioniert. Es konnten 29 transgene Zelllinien generiert werden, die fluoreszenzmikroskopisch untersucht wurden. Anhand ihrer Lokalisation und Expressionsrate wurden die Fusionsproteine in fünf Gruppen eingeteilt. 15 der Proteine wurden auf der Parasitenoberfläche, an dem Inneren Membran- und Basalkomplex, oder in den apikalen sekretorischen Organellen lokalisiert. All diese Kompartimente können mit der Invasion in Verbindung gebracht werden. Zur weiteren funktionellen Analyse wurde ein Gen-Knock-Out initiiert. Sechs der untersuchten Proteine konnten bereits als redundant eingestuft werden und vier der Kandidaten haben möglicherweise eine essentielle Funktion für den Parasiten.

Zusammenfassend ermöglicht dieser bioinformatische Ansatz die schnelle Identifizierung neuer Kandidatengene, die eine wichtige Rolle bei der Invasion des Parasiten in die Wirtszelle spielen könnten.



# TABLE OF CONTENTS

<b>SUMMARY</b>	<b>V</b>
<b>ZUSAMMENFASSUNG</b>	<b>VII</b>
<b>LIST OF FIGURES</b>	<b>XI</b>
<b>LIST OF TABLES</b>	<b>XIII</b>
<b>ABBREVIATIONS</b>	<b>XIV</b>
<b>1 INTRODUCTION</b>	<b>1</b>
1.1 MALARIA – A VECTOR-BORN DISEASE	1
1.1.1 EPIDEMIOLOGY	1
1.1.2 CLINIC	3
1.1.3 TREATMENT AND PREVENTION	5
1.2 PARASITE BIOLOGY	10
1.2.1 SYSTEMATIC CLASSIFICATION	10
1.2.2 THE LIFE CYCLE	10
1.3 INVASION	16
1.3.1 MEROZOITES – THE ERYTHROCYTE-INVADING PARASITE STAGE	16
1.3.2 THE APICAL COMPLEX	18
1.3.3 THE PROCESS OF INVAISON	18
1.3.4 MOLECULAR BASIS FOR INVASION – RECEPTOR-LIGAND INTERACTION	25
1.4 POST-TRANSLATIONAL MODIFICATIONS	31
1.5 THE INVADOME	34
1.6 AIMS OF THIS WORK	36
<b>2 MATERIAL AND METHODS</b>	<b>37</b>
2.1 MATERIAL	37
2.1.1 CHEMICALS AND BIOLOGICAL REAGENTS	37
2.1.2 LABWARE AND DISPOSABLES:	39
2.1.3 TECHNICAL AND MECHANICAL DEVICES	40
2.1.4 KITS AND STANDARDS	42
2.1.5 SOFTWARE, DATA BASES AND BIOINFORMATICAL TOOLS	42
2.1.6 STOCK SOLUTIONS, BUFFERS AND MEDIA	43
2.1.7 BIOCHEMICAL WORK	48
2.1.8 BACTERIAL AND PARASITE STRAINS	49
2.1.9 ANTIBODIES	50
2.1.10 FLUORESCENCE DYES	51
2.1.11 ENZYMES AND POLYMERASES	51
2.1.12 PLASMIDS	51
2.1.13 OLIGONUCLEOTIDES	52

<b>2.2</b>	<b>METHODS</b>	<b>53</b>
2.2.1	MOLECULAR BIOLOGICAL METHODS	53
2.2.2	BIOCHEMICAL TECHNIQS	59
2.2.3	CELL CULTURES TECHNIQS FOR <i>PLASMODIUM FALCIPARUM</i>	61
2.2.4	LIVE CELL AND FLUORESCENCE IMAGING	67
2.2.5	NEURAMINIDASE INVASION ASSAY	67
2.2.6	FLOW CYTOMETRY FACS	67
2.2.7	GENE IDENTIFICATION	68
<b>3</b>	<b>RESULTS</b>	<b>69</b>
<b>3.1</b>	<b>REGULATORY STEPS IN INVASION – PHOSPHORYLATION OF EBA175 CPD</b>	<b>69</b>
3.1.1	GENERATION OF EBA175 MUTANTS	69
3.1.2	LOCALIZATION OF EBA175 <sub>WT</sub> -GFP AND EBA175 <sub>PHOSPHO</sub> -GFP	73
3.1.3	FUNCTIONAL ANALYSIS OF EBA175 <sub>WT</sub> -GFP AND EBA175 <sub>PHOSPHO</sub> -GFP	75
<b>3.2</b>	<b>BIOINFORMATIC SCREEN FOR NOVEL, SECRETED PROTEINS IMPLICATED IN ERYTHROCYTE INVASION</b>	<b>79</b>
3.2.1	EXPERIMENTAL VALIDATION OF CANDIDATE GENES	81
3.2.2	CANDIDATE EXPRESSION AND LOCALIZATION	84
3.2.3	CANDIDATE ESSENTIALITY IN THE BLOOD STAGES	113
<b>4</b>	<b>DISCUSSION</b>	<b>116</b>
<b>4.1</b>	<b>REGULATORY STEPS IN INVASION – PHOSPHORYLATION OF EBA175 CPD</b>	<b>116</b>
<b>4.2</b>	<b>NOVEL PUTATIVE CANDIDATES FOR ERYTHROCYTE INVASION</b>	<b>119</b>
4.2.1	IDENTIFICATION OF NOVEL CANDIDATES	120
4.2.2	FUNCTIONAL DOMAINS WITHIN THE LOCALIZED CANDIDATE GENES	121
4.2.3	CRITICAL ASPECTS	129
<b>4.3</b>	<b>CONCLUSION AND OUTLOOK</b>	<b>131</b>
<b>BIBLIOGRAPHY</b>		<b>133</b>
<b>APPENDIX</b>		<b>157</b>
<b>DANKSAGUNG</b>		<b>170</b>

## List of Figures

FIGURE 1: COUNTRIES ENDEMIC FOR MALARIA IN 2000 AND 2016.....	2
FIGURE 2: DIFFERENT INFLUENCES ON THE CLINICAL OUTCOME OF MALARIA INFECTION (MILLER, 2002).....	5
FIGURE 3: SCHEMATIC REPRESENTATION OF THE LIFE CYCLE OF P. FALCIPARUM. ....	12
FIGURE 4: PLASMODIUM SPP. ASEXUAL ERYTHROCYTIC STAGES.....	14
FIGURE 5: REPRESENTATION OF THE DIFFERENT STAGES DURING GAMETOCYTOGENESIS. ....	15
FIGURE 6: 3D REPRESENTATION OF A FREE MEROZOITE AND ITS CORE SECRETORY ORGANELLES.....	17
FIGURE 7: SCHEMATIC DESCRIPTION OF THE STEPS OF MEROZOITE INVASION FROM EGRESS UNTIL POST-INVASION WHEN THE VACUOLE IS SEALED. ....	20
FIGURE 8: SCHEMATIC REPRESENTATION OF THE INVASION ASSOCIATED ORGANELLES OF AN INVASIVE MEROZOITE. .....	23
FIGURE 9: GLIDING MOTILITY AND THE MOTOR COMPLEX. ....	25
FIGURE 10: SCHEMATIC REPRESENTATION OF THE GENE STRUCTURE OF EBL FAMILY MEMBERS OF P. FALCIPARUM AND P. VIVAX REPRESENTED BY THE EXON STRUCTURES.. ....	29
FIGURE 11: SCHEMATIC STRUCTURE OF THE TYPE I TRANSMEMBRANE PROTEIN PfEBA175. ....	30
FIGURE 12: PUTATIVE PHOSPHORYLATION SITES OF EBA175. ....	70
FIGURE 13: SCHEMATIC REPRESENTATION OF THE PCR-BASED MUTATION STRATEGY AND INTEGRATION OF THE PLASMIDS INTO THE ENDOGENOUS EBA175 LOCUS. ....	72
FIGURE 14: EVIDENCE FOR CORRECT INTEGRATION AND EXPRESSION OF THE EBA175 WILD TYPE AND PHOSPHO- MUTANT. ....	73
FIGURE 15: LOCALIZATION OF EBA175 <sub>WT</sub> GFP.....	74
FIGURE 16: LOCALIZATION OF EBA175 <sub>PHOSPHO</sub> GFP. ....	75
FIGURE 17: NEURAMINIDASE INVASION ASSAY COMPARING PARENTAL 3D7, W2MEF AND TRANSGENIC W2MEF- EBA175 <sub>WT</sub> GFP PARASITEMIA AFTER 72 H.....	77
FIGURE 18: NEURAMINIDASE INVASION ASSAY COMPARING THE PARASITEMIA OF PARENTAL W2MEF, TRANSGENIC W2MEF-EBA175 <sub>WT</sub> GFP AND -EBA175 <sub>p0</sub> GFP PARASITES AFTER 48 HOURS. ....	78
FIGURE 19: SCHEMATIC DESCRIPTION OF THE SEARCH STRATEGY FOR NOVEL INVASION ASSOCIATED CANDIDATES AND EXPRESSION PROFILES.....	80
FIGURE 20: SCHEMATIC DESCRIPTION OF THE INTEGRATION STRATEGY FOR NOVEL INVASION ASSOCIATED CANDIDATES.....	82
FIGURE 21: PCR ANALYSIS OF CORRECTLY INTEGRATED CANDIDATES. ....	83
FIGURE 22: REPRESENTATION OF SELECTED AND LOCALIZED CANDIDATES.....	84

FIGURE 23: SCHEMATIC REPRESENTATION OF SURFACE LOCALIZED PROTEINS IN LATE SCHIZONTS AND FREE MEROZOITES. ....	86
FIGURE 24: ANALYSIS OF PF3D7_1136200 LOCALIZATION. ....	87
FIGURE 25: ANALYSIS OF PF3D7_1143200 LOCALIZATION. ....	88
FIGURE 26: ANALYSIS OF PF3D7_1229300 LOCALIZAION. ....	89
FIGURE 27: ANALYSIS OF PF3D7_1421900-GFP LOCALIZATION.....	90
FIGURE 28: SCHEMATIC REPRESENTATION OF IMC OR BC LOCALIZED PROTEINS IN T1 AND T3 PHASE OF LATE SCHIZONTS. ....	91
FIGURE 29: ANALYSIS OF PF3D7_0530300 LOCALIZATION. ....	92
FIGURE 30: ANALYSIS OF PF3D7_ LOCALIZATION.. ....	93
FIGURE 31: SCHEMATIC REPRESENTATION OF PROTEINS WITH APICAL LOCALIZATION. ....	94
FIGURE 32: ANALYSIS OF PF3D7_0105400.1 LOCALIZATION.. ....	95
FIGURE 33: ANALYSIS OF PF3D7_0811600 LOCALIZATION.. ....	96
FIGURE 34: ANALYSIS OF PF3D7_1014100-GFP LOCALIZATION.....	97
FIGURE 35: ANALYSIS OF PF3D7_1115600 LOCALIZATION ....	98
FIGURE 36: ANALYSIS OF PF3D7_1310200-GFP LOCALIZATION.....	99
FIGURE 37: ANALYSIS OF PF3D7_1404700-GFP LOCALIZATION.....	100
FIGURE 38: ANALYSIS OF PF3D7_1404900 EXPRESSION AND LOCALIZATION.. ....	101
FIGURE 39: ANALYSIS OF PF3D7_1463900 LOCALIZATION. ....	102
FIGURE 40: ANALYSIS OF PF3D7_1035900-GFP EXPRESSION AND LOCALIZATION.....	103
FIGURE 41: ANALYSIS OF PF3D7_0316300.2 LOCALIZATION.. ....	105
FIGURE 42: ANALYSIS OF PF3D7_0404800-GFP LOCALIZATION.....	105
FIGURE 43: ANALYSIS OF PF3D7_0625400-GFP LOCALIZATION.....	106
FIGURE 44: ANALYSIS OF PF3D7_1105300 LOCALIZATION. ....	107
FIGURE 45: ANALYSIS OF PF3D7_1334600 LOCALIZATION. ....	108
FIGURE 46: ANALYSIS OF PF3D7_1472600-GFP LOCALIZATION.....	110
FIGURE 47: ANALYSIS OF PF3D7_0419400-GFP EXPRESSION AND LOCALIZATION.....	110
FIGURE 48: SCHEMATIC OF TARGETED GENE DISRUPTION STRATEGY USING SLI (SLI-TGD).....	114
FIGURE 49: PCR ANALYSIS OF CORRECTLY INTEGRATED TGD CONSTRUCTS. ....	115
FIGURE 50: SCHEMATIC REPRESENTATION OF A MEROZOITE AND CANDIDATE GENES THAT WERE LOCALIZED TO THE INVASION RELATED COMPARTMENTS. ....	121
FIGURE 51: ANNOTATED FUNCTIONAL DOMAINS WITHIN THE 15 LOCALIZED CANDIDATES. ....	122

FIGURE 52: ALIGNMENT OF PF3D7\_1143200 WITH KNOWN HSP PROTEINS..... 124

FIGURE 53: EXPRESSION VALUES OF THE CANDIDATE GENES. .... 128

## List of Tables

TABLE 1: LOCALIZED CANDIDATES. .... 85

TABLE 2: BLOOD STAGE ESSENTIALITY OF LOCALIZED CANDIDATES. .... 114

TABLE 3: LIST OF OLIGONUCLEOTIDES THAT WERE USED TO GENERATE THE EBA175 CONSTRUCTS AND FOR  
VALIDATION OF THEIR INTEGRATION INTO THE ENDOGENOUS LOCUS. .... 157

TABLE 4: LIST OF OLIGONUCLEOTIDES THAT WERE USED FOR CLONING AND INTEGRATION ANALYSIS OF THE  
CANDIDATE GENE CONSTRUCTS..... 161

TABLE 5: LIST OF OLIGONUCLEOTIDES THAT WERE USED FOR SEQUENCING OF THE PLASMIDS THAT WERE  
GENERATED FOR THIS STUDY. .... 161

TABLE 6: LIST OF GENES THAT WERE USED AS CONTROL FOR THE EXPRESSION PROFILES OF CANDIDATE GENES  
SELECTED IN THE BIOINFORMATIC SCREENING APPROACH AND THE ACCORDING REFERENCE PUBLICATIONS.162

TABLE 7: LIST OF ALL 289 GENES THAT WERE IDENTIFIED BY THE BIOINFORMATICS SCREEN..... 169

## Abbreviations

%	percent	hpi	hours post infection
AA	amino acids	HR	homology region
AIDS	acquired immune deficiency syndrome	HSP	heat shock protein
ACT	Artemisinin combination therapy	IMC	inner membrane complex
AMA1	apical membrane antigen 1	iRBC	infected red blood cell
AQ	Amodiaquine	IRS	indoor residual spraying
ATP	adenosine triphosphate	ITNs	insecticide-treated mosquito nets
BC	basal complex	kb	kilo base
bp	base pair	kDa	kilo Dalton
BSD	blasticidin S deminase	MAP	mitogen-activated protein
CLAMP	claudin-like apicomplexan microneme protein	MC	maurer's clefts
CPD	cytoplasmic doamin	MDR1	multi drug resistance reporter 1
CR1	complement receptor 1	µg	microgram
CQ	Chloroquine	mg	milligram
CSP	circumsporozoite protein	µl	microliter
DARC	Duffy antigen receptor for chemokines	ml	milliliter
DBL	Duffy binding-like	µm	micrometer
DHFR	dihydrofolat reductase	mM	millimolar
DNA	desoxyribonucleic acid	MSP1	merozoite surface protein 1
EBA	erythrocyte binding antigen	MT	microtubules
EBL	erythrocyte binding-like	NC	nucleus
<i>E. coli</i>	<i>Escherichia coli</i>	PCR	polymerase chain reaction
eIF2	eukaryotic translation initiation factor	<i>Pf</i>	<i>Plasmodium falciparum</i>
EMA	European Medicine Agency	<i>PfCRT</i>	<i>P. falciparum</i> CQ transporter
EMP1	erythrocyte membrane protein 1	<i>PfCRT</i>	<i>P. falciparum</i> circumsporozoite protein
EtOH	Ethanol	<i>PfSPZ</i>	<i>P.m falciparum</i> sporozoites
FV	food vacuole	PKA	protein kinase A
GAP45	glideosome associated protein 45	PK2	protein kinase 2
gDNA	genomic DNA	PM	plasma membrane
		<i>P. spp.</i>	<i>Plasmodium</i> species

GFP	green fluorescent protein	PTM	post-translational modification
GLURP	glutamate-rich protein	PV	parasitophorous vacuole
GlyAB/C	Glycophorin A/B/C	PVM	parasitophorous vacuole membrane
GSK3	glycogen synthase kinase 3	RBC	red blood cell
HIV	human immunodeficiency	RBL	reticulocyte binding-like
Rh	reticulocyte binding homologue	T	threonine
Ripr	Rh5 interacting protein	TBV	transmission blocking vaccines
RNA	ribonucleic acid	TGD	targeted gene disruption
ROM4	rhomboid-like protease 4	<i>T.</i>	<i>Toxoplasma gondii</i>
RON	rhoptry neck protein	<i>gondii</i>	
PPM	parasite plasma membrane	TM	transmembrane domain
RT	room temperature	TVM	tubovesicular membrane network
S	serine	TRAP	thrombospondin-related anonymous protein
SDS	sodium dodecyl sulfate	UPR	unfolded protein response
SLI	selection linked integration	Puf	Pumillo family of proteins
SP	signal peptide	WHO	World Health Organisation
SUB2	subtilisin-like sheddase 2	XA	xanthurenic acid
		Y	tyrosine

# 1 Introduction

## 1.1 Malaria – a vector-borne disease

With the first Chinese documentation almost 5000 years ago (2700 BC) malaria has been known ever since (Cox, 2010). Even the old Greeks knew about the fevers although back then it was thought to be caused by bad air rising from the swamps giving the disease its name (mala:bad, aer:air). In the late 19<sup>th</sup> century the parasites were discovered in the blood of malaria patients when Alphonse Laveran could show for the first time that it is a protozoan parasite. It also was the first time that a protozoan was found to be able to inhabit human blood cells (Cox, 2010; Laveran, 1881, 1884).

Malaria is a vector-borne disease caused by a protist of the *Plasmodium* genus. *Plasmodium* spp. are obligate intracellular parasites with a complex life cycle that alters between a vertebrate and a mosquito host. Over 200 *Plasmodium* species exist but only five of them are known to infect humans: *P. vivax*, *P. ovale*, *P. malariae*, *P. knowlesi*, and *P. falciparum* – the most virulent out of all causing the severest form, *falciparum* malaria (Keeling and Rayner, 2015). *Plasmodium* spp. are part of the phylum *Apicomplexa*, which are known to be obligate intracellular parasites. And although *P. falciparum* is the most virulent out of them, *P. vivax* is gaining attention as infection rates caused by this species have significantly increased over the last few years (Ahmed and Cox-Singh, 2015; White et al., 2014). *P. knowlesi* was predominantly known as a zoonotic parasite but a rising number of *Knowlesi*-infections of human has been reported recently in South-East Asia (Ahmed and Cox-Singh, 2015).

### 1.1.1 Epidemiology

Malaria is a disease endemic in mostly the poor and underdeveloped countries. It predominantly occurs in the tropical and subtropical regions with the highest infection



rates seen in the Sub-Saharan African region (114 million people in 2015). Besides AIDS/HIV and tuberculosis malaria is the disease with the highest mortality rate worldwide. The malaria incidence is continually decreasing (21% from 2010 to 2015) and the mortality rate has fallen about 29% between 2010 and 2015 (62% between 2000 and 2015). Therefore the number of countries and territories considered to be endemic has changed from 108 to 91 over the last 15 to 20 years (Figure 1) (WHO, 2016). Nonetheless, half of the world population still lives at risk of malaria infection (with 216 million estimated cases in 2016) and over 400 000 people are dying every year (445 000 in 2016), with two thirds being children under the age of five (WHO, 2016; WHO malaria report, 2017). Globally *P. falciparum* is responsible for most of the malaria infections while not more than about 4% can be referred to *P. vivax*. Similar can be reported for the estimated deaths caused by malaria infections. Of the globally 429 000 deaths in 2015, 92% occurred in the Sub-Saharan African region with the vast majority of 99% being caused by *P. falciparum* (WHO Malaria report, 2016).

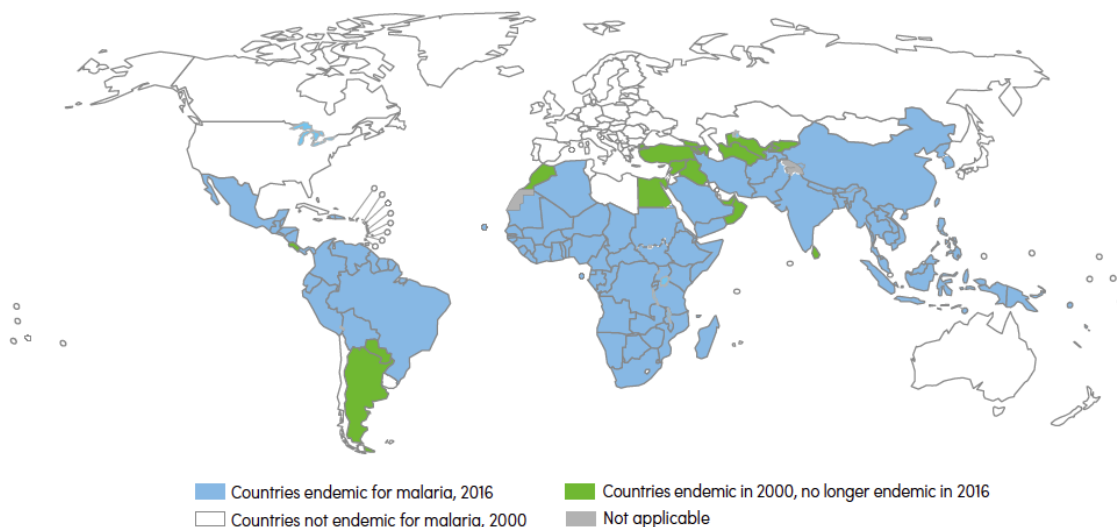


**Figure 1: Countries endemic for malaria in 2000 and 2016.** Countries with 3 consecutive years of zero indigenous cases are considered to have eliminated malaria (WHO, 2016).

### 1.1.2 Clinic

Malaria infection of human happens due to a bite of a parasite-carrying female *Anopheles* mosquito. Via the bloodstream the parasite migrates to the liver, where it invades hepatocytes and transforms into an erythrocyte-invading merozoite, that is released into the blood stream (Cowman and Crabb, 2006). All symptoms of a malaria infection are caused by the blood stage of the parasite life cycle when newly formed parasites are released from the erythrocytes, which causes the malaria descriptive fever (for detailed description of the parasite life cycle see section 1.2.2). The preceding liver stage in contrast remains without symptoms as only a small number of hepatocytes are infected. Nonetheless, the liver stage strongly influences the incubation period, which in general varies between 9 and 30 days (*P. falciparum* and *P. malariae*, respectively) (Bartoloni and Zammarschi, 2012). The duration of this period depends on the infecting species and the way of transmission as well as the general immune status of the infected person.

#### 1.1.1.1 Infecting species and clinical outcome

The course of disease can be differentiated into uncomplicated and severe malaria, depending on different factors such as the host and the infecting parasite, as well as geographic and social factors (Figure 2; reviewed in Miller, 2002). The clinical malaria symptoms are rather diverse and the severity ranges from mild headache to serious complications that may lead to death if not treated properly. The first symptoms are common to all malaria species. They emerge as rather unspecific flu-like symptoms including headache, backache, lassitude, dizziness, anorexia and vomiting pursued by recurring fever.

Malaria infections caused by *P. vivax* and *P. ovalae* mostly develop uncomplicated. They both come with a fever occurring every three days (tertian fever), which is defined by first a cold stage, followed by a hot stage of fever ending in sweating. The parasitemia

usually does not exceed 2%. Both strains are able to form dormant stages, called hypnozoites, which upon activation develop into hepatic schizonts (late, multinucleated parasite stages). Depending on strain, origin and previous treatment these relapses may occur even years after the primary infection. Severe malaria cases caused by these species have been barely reported. Although increasing evidence of severe *P. vivax* malaria has recently been reported (Bartoloni and Zammarchi, 2012; Guerra et al., 2010; Price et al., 2007). *P. malariae* causes the mildest but the most enduring form of the disease. Even though *P. malariae* is not able to form dormant stages relapses may occur up to 50 years after the primary infection from persisting blood stages. The incubation period differs from at least 18 days up to 40 days and the fever intervals typically recur every 72 hours (due to the 72h-life cycle of the parasite; quartan malaria) and parasitemia usually does not exceed 1%. Infection caused by *P. falciparum* significantly differs in its clinical outcome. Because of the asynchronous growth of the blood stage parasites the fever occurs irregular as a quotidian (daily) fever, tertian or in 36-hour intervals (subtertian malaria). Due to specific host cell modification infected red blood cells (iRBC) bind to the endothelium (cytoadherence) or other RBCs (called rosetting). This sequestration results in blockage of the microvasculature and may contribute to severe malaria (Rogerson et al., 1997; Gamain et al., 2001; Miller, 2002). A change from a mild to a severe form may develop at any stage and rapid if not treated properly. Severe malaria affects the central nervous system resulting in cerebral malaria, the pulmonary system leading to respiratory failure, the renal system, which results in acute renal failure, as well as the hematopoietic system, which subsequently leads to severe anaemia and may result in death (Bartoloni and Zammarchi, 2012). The species that was most recently discovered as a human pathogen is *P. knowlesi*, which usually infects primates (Garnham, 1966). The clinical disease equals *P. falciparum* and *P. vivax* infection (Daneshvar et al., 2009).

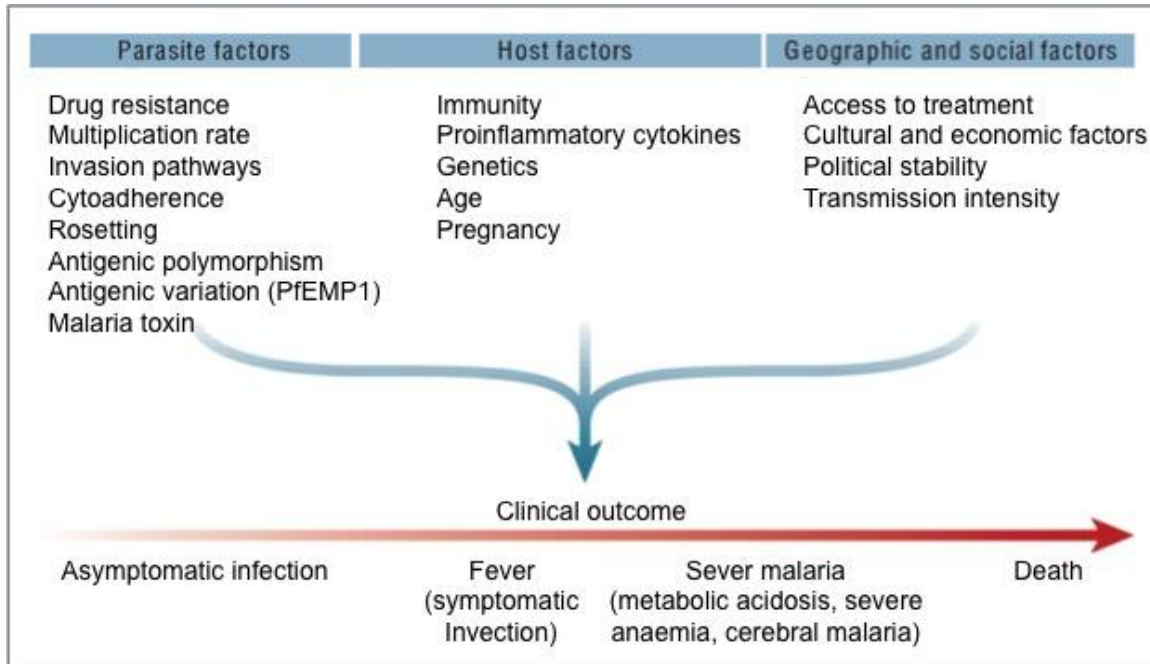


Figure 2: Different influences on the clinical outcome of malaria infection (Miller, 2002).

### 1.1.3 Treatment and prevention

#### 1.1.3.1 Drugs

Quinine was the first antimalarial drug, extracted from the bark of the Cinchona tree in the early 19<sup>th</sup> century. It was found to be highly efficient against late blood stages. In *P. vivax* and *P. ovale* it was also shown to have a weak effect against gametocytes, the sexual form of the parasite (see section 1.2.2.2). Chloroquine (CQ) and amodiaquine (AQ) are derivatives of quinine. They both are 4-aminoquinolones, the most widely used class of drugs against malaria these days (WHO, 2016; Winzeler, 2008). The intraerythrocytic parasite digests the haemoglobin of the RBC in the so-called food vacuole (FV), a compartment to safely store metabolic waste products. This process serves as its main source of nutrition. During this process haemoglobin gets degraded into amino acids and heme (ferriprotoporphyrin IX), which is a toxic side product and therefore has to be turned into hemozoin. CQ inhibits this conversion resulting in the death of the parasite (Parhizgar and Tahghighi, 2015).

Currently, the treatment mostly recommended by the WHO is artemisinin-based combination therapies (ACTs) (WHO, 2016). Artemisinins are short-acting antimalarial drugs, which are active against asexual blood stage parasites as well as sexual gametocytes. ACT is a therapy combined of two antimalarial compounds, with one of them being artemisinin or its derivatives. In combination with long-acting drugs the development of *P. falciparum* resistance is supposed to be delayed (Parhizgar and Tahghighi, 2015). The hallmark of artemisinin activation is the generation of highly reactive radicals upon peroxide cleavage, however, the exact mechanisms are not known to date (Meshnick et al., 1993; O'Neill et al., 2010). The access to ACTs in endemic areas has expanded in recent years with the negative side effect of emerging parasite resistances (Dondorp et al., 2009).

### 1.1.3.2 Drug resistance

Increasing drug resistance is one of the major problems that have been of high interest over the last years (Miller, 2002). To date parasite resistance to antimalarial drugs has been documented in already three of the five human-infecting malaria species, namely *P. falciparum*, *P. vivax* and *P. malariae*, which seems to result from cross resistances (WHO, 2016).

In the 1950s the first resistance to CQ was reported from South-America and South-East Asia (Payne, 1987; D'Alessandro and Buttiens, 2001). Mutation in the *P. falciparum* CQ transporter (*PfCRT*) (at amino acid 76) was shown to reduce CQ uptake into the FV. And further reduction of CQ import results from a mutation in the multi-drug resistant protein-1 (*PfMDR1*) (Fidock et al., 2000; Sidhu et al., 2002; Sanchez et al., 2008). Although not entered yet or completed all clinical phases, new analogues based in 4-aminoquinolones are currently tested to overcome resistance and toxicity issues (reviewed in Parhizgar and Tahghighi, 2015). Additionally, increasing drug resistance against artemisinin has already been reported in five countries in the Greater Mekong subregion. It is assumed to account for additional 100 000 deaths per year (Lubell et al.,

2014; WHO, 2016). To date more than 200 mutations in the *Pfkelch13* gene originating from multiple independent emergence events have been reported (WHO malaria report, 2017). However, C580Y is the most frequent mutation in the *PfKelch13* protein and considered as a primary marker for artemisinin resistance (Ariey et al., 2014). The underlying molecular mechanisms are unknown, although they have been discussed controversially. Wang and colleagues suggested the activation to be haem dependent (J. Wang et al., 2015) upon haemoglobin digestion as the main haem source in later parasite stages. Other studies designate artemisinin as an inhibitor of *P. falciparum* phosphatidylinositol-3-kinase (*PfPI3K*) or associated artemisinin resistance with increased expression of unfolded protein response (UPR) pathways involving the major PROSC and TRiC chaperone complexes (Mbengue et al., 2015; Mok et al., 2015).

### 1.1.3.3 Vaccine development

During their life cycle malaria parasites pass through multiple stages implicating intra- and extraerythrocytic phases, as well as different hosts (section 1.2.2). Also, they express a variety of antigens each specific to the different stages. These specific parasite features make the development of effective malaria vaccines challenging. In fact there is no vaccine available to date to prevent humans from any parasitic infection thus not against malaria (Hoffman et al., 2015). Only one vaccine has been progressed through phase 3 clinical trial to date, termed RTS,S/AS01 (also known as Mosquirix®). RTS,S is an injectable, recombinant vaccine that targets the pre-erythrocytic parasite. More precisely, it targets the *Plasmodium falciparum* circumsporozoite protein (*PfCSP*), which is present on the sporozoite surface and is expressed by early liver stages. It was shown to reduce the incidence of clinical malaria by ~51% over the first 14 months among children 5-17 months old when receiving the first of three doses. However protection waned over time. Among children (5-17 months) who completed four doses clinical incidence was reduced by 39% and severe malaria by 31.5% (RTS,S Clinical Trials partnership and Agnandji et al., 2012; RTS,S Clinical Trials partnership, 2015; Oyen et al.,

2017). Although this is a big step in malaria vaccine development RTS,S displays relatively little efficacy and continued efforts are required and undertaken to enhance efficacy and duration of protection. So far, WHO and the European Medicine Agency (EMA) strongly consider RTS,S as a complementary malaria control tool that could be added to the usual prevention and treatment procedure (Oyen et al., 2017; WHO, 2016).

A further approach is the immunisation against pre-erythrocytic stages due to bites of irradiated mosquitoes infected with *Plasmodium falciparum* sporozoites (PfSPZ). It has been known for over 40 years that high levels of immunity can be reached with this method (Nussenzweig et al., 1969; Seder et al., 2013). The first PfSPZ vaccine candidates were designed for subcutaneous or intradermal application, which led to low immune responses and minimal protection. Intravenous administration of attenuated, aseptic, purified, cryopreserved PfSPZ vaccine composition was recently shown to establish high-level protection (Seder et al., 2013). This approach is of high interest, as immune responses against PfSPZ would prevent blood stage infection and thereby stopping gametocyte production thus preventing from further transmission. But the challenge for high-scale sporozoite extraction from mosquito salivary glands still must be mastered.

Transmission blocking vaccines (TBV) target antigens present on early sexual erythrocytic stages and early mosquito stages during transmission. Such antigens are for example Pfs25 and Pfs28. So far TBVs are poorly immunogenic but a newly designed vaccine combination is currently tested in phase 1a clinical trial (Moreno and Joyner, 2015).

Blood stage vaccines target antigens present on the merozoite surface such as the merozoite surface protein 1 (MSP1) and apical membrane antigen 1 (AMA1), which is also expressed in sporozoites. The time before merozoite invasion into the RBC is the only time of the blood cycle when the parasite is exposed to the human immune system and therefore antigens present on the merozoite surface are highly interesting targets. Despite several attempts to date no statistically significant efficacy was observed. But the chimeric protein GMZ2 is currently tested in phase 2b clinical trial. GMZ2 results

from fusing the glutamate-rich protein (GLURP) to the merozoite surface protein 3 (MSP3), and is a promising candidate as in phase 1 trials immunization inhibited parasite growth *in vitro* (Audran et al., 2005; reviewed in Moreno and Joyner, 2015).

Another promising candidate for blood stage vaccines is the reticulocyte binding homologue 5 (Rh5) that was recently found to be essential for blood stage invasion. It exhibits limited genetic diversity and binds to a receptor on the erythrocyte surface (Crosnier et al., 2011). Rh5-specific human antibodies were shown to block parasite growth *in vitro* and are linked to a reduced risk of malaria in Mali (Tran et al., 2014). This makes Rh5 an attractive new vaccine candidate (Moreno and Joyner, 2015).

### 1.1.3.4 Control strategies

Current vector control strategies to prevent infections are mainly the use of insecticide-treated mosquito nets (ITNs) and indoor residual spraying (IRS). In the Sub-Saharan African region up to 53% of the people at risk sleep under ITNs but still one fifth of the households do not have access to treated nets or at least not all people living in one household have ITNs (WHO, 2016). Further increasing mosquito resistance against insecticides has already been reported. There are currently four insecticide classes used for ITN treatment and IRS, namely pyrethroids, organochlorine (DDT), carbamates, and organophosphates. Out of the 73 countries that provide monitoring data already 60 reported resistance to at least one, and 50 countries reported resistance to two or more insecticide classes (data from 2010; WHO (2016)).

All together these data clearly demonstrate the urgent need for the development of new prevention strategies, vaccines and especially new effective antimalarial drugs.



### 1.2 Parasite biology

#### 1.2.1 Systematic classification

*Plasmodium* species belong to the genus *Plasmodium* and are members of the family *Plasmodiidae* in the order of *Haemosporidae*. They are part of the phylum *Apicomplexa* (Storch and Welch, 2003), which are known to be obligate intracellular parasites. Beside *Plasmodium* spp. other *Apicomplexan* parasites are *Toxoplasma gondii*, *Cryptosporidium* spp., *Theileria* spp., and *Eimeria* spp. (Levine, 1988).

A common feature of all *Apicomplexa* is the apical complex comprising specialized organelles, namely rhoptries, micronemes and dense granules, situated at the apical pole of the parasite. A second *Apicomplexa* characteristic is the apicoplast. It is a plastid that was acquired via secondary endosymbiosis of a red algae and therefore is encompassed by four membranes. The apicoplast has lost its ability to perform photosynthesis but has still essential functions for the parasite such as the synthesis of isoprenoid precursors (L. Lim and McFadden, 2010; Ralph et al., 2004).

Together with *Dinoflagelata* and *Ciliata*, the *Apicomplexa* form the super-phylum of *Alveolata*, which are phylogenetically linked by different features such as a double membrane structure underlying the plasma membrane called inner membrane complex (IMC) and a conserved protein family termed “alveolins” (Cavalier-Smith, 1993; Gould et al., 2008).

#### 1.2.2 The life cycle

The life cycle of *P. falciparum* parasites is a complex process that takes place in different hosts, alternating between mosquitoes and humans. It is divided into asexual replication in the human host and sexual reproduction in the vector (mosquito) (Figure 3). The infection of a human starts with the bite of a *Plasmodium*-infected female *Anopheles* mosquito. Sporozoites, the motile and infective form of the parasite, are injected into

the blood stream. As *Plasmodium* parasites can only survive inside a host cell, sporozoites use the blood stream to migrate to the liver where they pass through several Kupffer cells before they actively invade hepatocytes, endothelial liver cells (Mota et al., 2001). In the hepatocytes sporozoites rapidly multiply in a process called hepatic schizogony during which they develop into liver merozoites. In a so-called merosome, a host cell membrane-derived vesicle protecting merozoites from host cell immune responses, thousands of hepatic merozoites are released into the blood stream. Upon rupture the extracellular merozoites start to invade erythrocytes thereby beginning the asexual erythrocytic phase of the life cycle (Sturm et al., 2006). The parasites develop within erythrocytes over 36 to 48 hours from ring stages to trophozoites into schizonts. Due to rupture of the major schizonts up to 32 newly formed daughter-merozoites are released into the blood stream and the invasion immediately starts again (the blood cycle is described in section 1.2.3) (Bannister and Mitchell, 2003; Bannister et al., 2000).

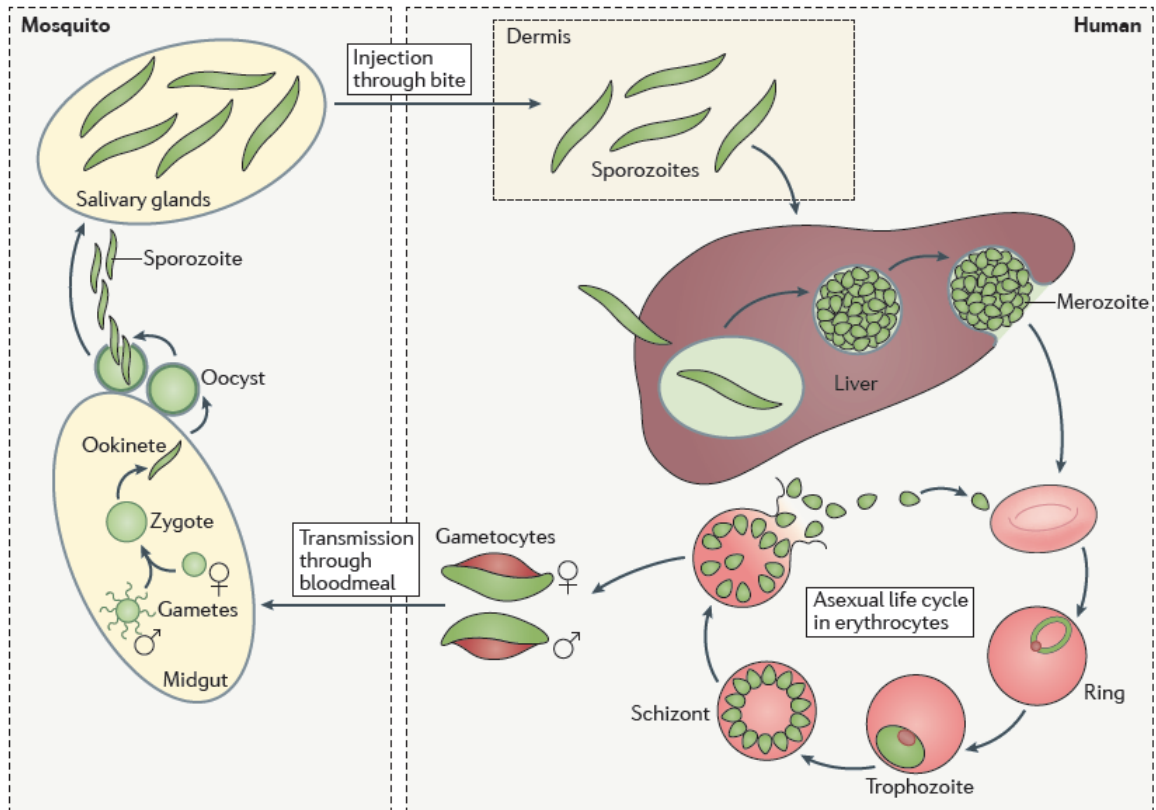


**Figure 3: Schematic representation of the life cycle of *P. falciparum*.** With the bite of an infected *Anopheles* mosquito sporozoites are injected into the dermis. Via the blood stream the sporozoites migrate to the liver and invade hepatocytes. Here they develop into thousands of merozoites, which are released into the blood stream to infect erythrocytes. The parasite undergoes asexual replication. A small proportion develops into gametocytes, the sexual form of the parasite (see section 1.2.2.2). With a second blood meal gametocytes can be taken up by an *Anopheles* mosquito and undergo a sexual reproduction (Frénal et al., 2017).

### 1.2.2.1 The asexual blood stage

During invasion into the erythrocyte the asexual blood-stage parasites establish a parasitophorous vacuole (PV), which derives from an invagination of the host cell plasma membrane (PM) during the invasion process. Herein the parasites develop morphologically. From the ring stage the parasite transforms into a trophozoite, the stage in which the parasite mainly grows. As the parasite needs access to essential nutrients from the RBC cytosol to grow and reproduce it establishes its own tubovesicular membrane network (TVM) inside the iRBC. The TVM is used to import nutrients and to dispose waste products (Elmendorf and Halder, 1993; 1994; Elford and Ferguson, 1993; Grellier et al., 1991; Pouvelle et al., 1991). To maintain growth and

asexual replication over 80% of the erythrocyte haemoglobin is digested by the parasite (Ginsburg, 1990). Haemoglobin uptake occurs due to cytosomes but the detailed process is not clarified to (Aikawa et al., 1966). Due to the toxicity of the iron ions in the heme group of metabolized haemoglobin, the resulting ferromagnetic hemozoin has to be stored safely in the lysosome-like FV, the parasite's "safety cabinet", whereby the globin is used as a source for amino acid metabolism (Ashong et al., 1989; Lazarus et al., 2008; Goldberg et al., 1990). This conversion can be inhibited by CQ, which results in the death of the parasite (see section 1.1.2.1) (Golan et al., 2011; Parhizgar and Tahghighi, 2015). To avoid clearance by macrophages in the spleen some further remodelling is necessary. Therefore the parasite exports numerous proteins to modify the host cell suitable for its own needs. The *P. falciparum* erythrocyte membrane protein 1 (*PfEMP1*), which is encoded by members of the *var* gene family, is expressed at the erythrocyte surface. This results in adherence of the iRBCs to the endothelial cell wall (Baruch et al., 1995; Deitsch and Wellems, 1996; Howard et al., 1988; Su et al., 1995). Further, the attachment of several uninfected RBC to one iRBC, called rosetting, as well as autoagglutination of iRBCs help the parasite to escape clearance by the spleen and are thought to be implemented in the pathology of cerebral malaria (Wahlgren et al., 1994; Roberts et al., 1992; Berendt et al., 1994). By the end of its growth phase the parasite matures into a schizont and starts to replicate. In a process called schizogony nuclear division takes place resulting in a multinuclear schizont holding up to 32 newly formed daughter merozoites, which upon rupture of the erythrocyte are released into the blood stream. They invade uninfected RBCs and the cycle restarts (Figure 4) (Bannister, 2003; Sturm et al., 2006).

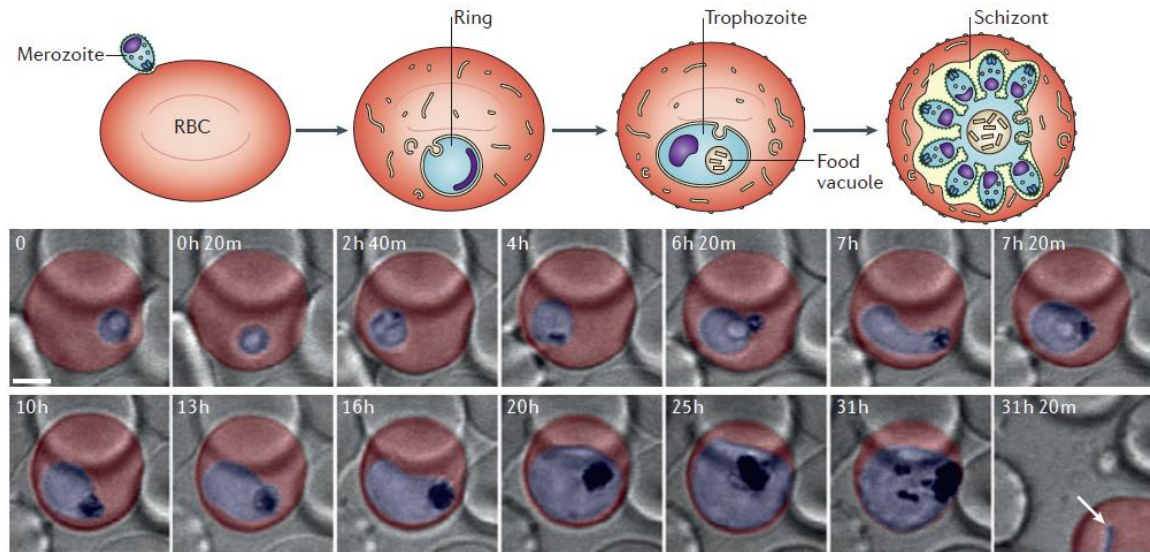


**Figure 4: *Plasmodium* spp. asexual erythrocytic stages.** The upper panel graphically represents the four main blood stages merozoite, ring, trophozoite, and schizont. The lower panel shows 4D imaging of a developing parasite (blue) in an erythrocyte (red) via confocal microscopy. The development is shown from ring stage to schizont stage; the white arrow (31h 20m) indicates a freshly invaded ring; scale bar, 2  $\mu\text{m}$  (De Niz et al., 2016).

### 1.2.2.2 Gametocytogenesis – the development of sexual stages

A small proportion of the invaded merozoites start to differentiate into male and female gametocytes (micro- and macrogametes, respectively), the sexual forms of the parasite. This process, called gametocytogenesis, is the essential part of the life cycle to ensure further transmission of the parasite to the next host defining the elusive role of gametocytes (Janse et al., 1986; Taylor and Read, 1997; Guttery et al., 2015). Gametocyte production in *P. falciparum* takes approximately 10 to 12 days whereby all merozoites of one schizont are committed to either develop into gametes or continue their asexual cycle (Bruce et al., 1900; Silvestrini et al., 2000; Guttery et al., 2015). The exact circumstances that trigger these differentiations are not clear to date but it is suggested that stressors such as high parasitaemia or nutrition depletion result in a higher production of sexual parasite forms (Dixon et al., 2008; Smith et al., 2000; Alano, 2014; Carter and Miller, 1979; Williams, 1999). Gametocytes develop through five morphologically distinct stages (I-V) resulting in crescent-shaped mature gametocytes (Figure 5). Early gametocyte stages (I-IIa) are morphologically rather similar to early

asexual stages. During development the gametocytes undergo drastic changes. In stage IIb they start to elongate and one side straightens resulting in a D-shaped form (stage III). The gametocytes further elongate and their ends become rounded (stage IV and V). The sexual parasite uses about 75% of the haemoglobin and covers about half of the erythrocyte's volume (Hanssen et al., 2012; Hawking et al., 1971, Dixon et al., 2012). Notably only stage V gametocytes can be found circulating in the blood stream as all other stages, protected from clearance by the spleen, are thought to develop in the bone marrow (Joice et al., 2014; Farfour et al., 2012; Aguilar et al., 2014).

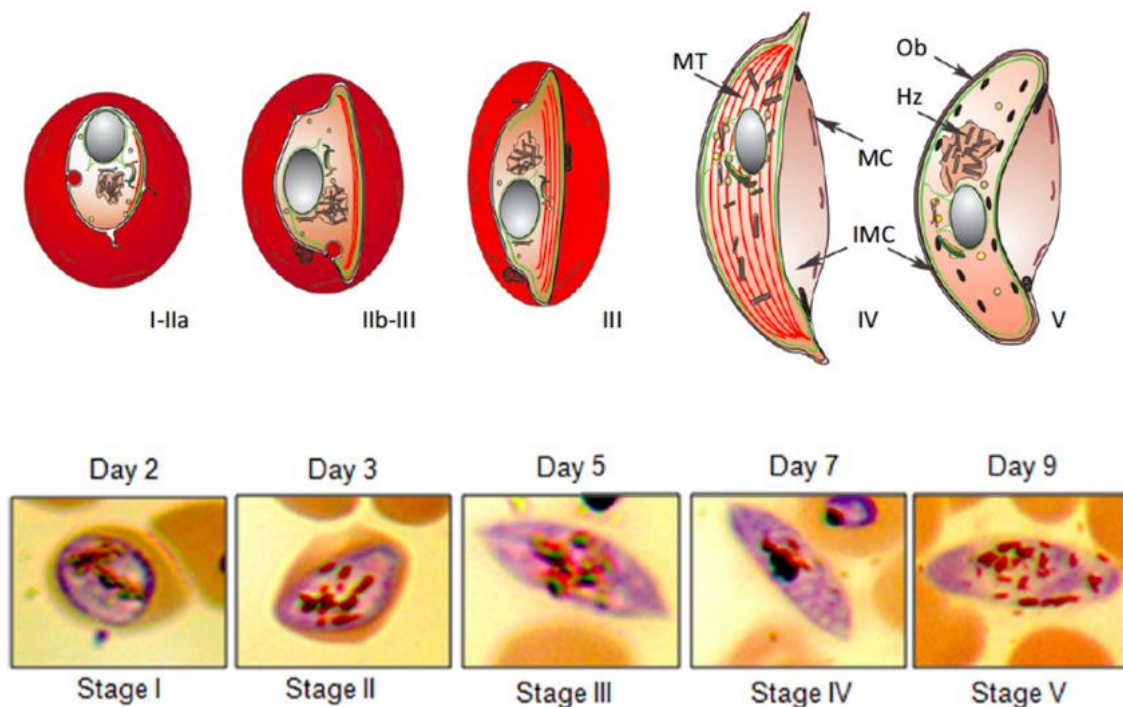


**Figure 5: Representation of the different stages during gametocytogenesis.** The gametocytes develop through five distinct stages (I-V) during which they elongate (stage IIb-II) and become their defining banana-shaped form (stage V). Upper panel: schematic representation including the nucleus, osmophilic bodies (Ob), aggregated hemozoin crystals (Hz), Maurer's clefts (MC), IMC, and microtubules (MT). Lower panel: Giemsa-stained blood smears of infected erythrocytes showing the different stages from day 2 to day 9 of development (Graphic modified from Dixon et al., 2012, upper panel and Chaubey et al., 2014, lower panel).

### 1.2.2.3 The sexual phase of the life cycle

Once gametocytogenesis is completed, mature male and female stage-V-gametocytes can be taken up during the blood meal of a female *Anopheles* mosquito. The gametocytes are ingested in the mosquito midgut where the sexual replication takes place. Compared to the human body the temperature as well as the pH is significantly lower in *Anopheles* mosquitoes. Together with the exposure to xanthurenic acid (XA), which is present in the midgut, these changes subsequently trigger the maturation of the gametocytes into gametes (Taylor and Read, 1997; Billker et al., 1998; Guttery et al., 2015). It takes about 12 minutes for a haploid male gametocyte to develop into eight flagellated sexually competent male gametes. These octoploid gametes are released during a process called exflagellation (Janse et al., 1988; Guttery et al., 2015; Sinden, 2015). Meanwhile female gametocytes develop into fertile macrogamete. Upon fertilization haploid male and female gametes fuse to a diploid zygote, subsequently developing into a tetraploid ookinete in which meiotic recombination occurs (Sinden, 1983). In this form the parasite is able to traverse the mid-gut epithelial cell wall where an oocyst is formed. Its rupture results in the release of sporozoites. These haploid sporozoites actively migrate through the haemocoel into the salivary glands where they remain until the next blood meal of the mosquito, through which they are transmitted to the next human host (Figure 3, left panel).

## 1.3 Invasion

### 1.3.1 Merozoites – the erythrocyte-invading parasite stage

Two invasive forms are found in *Plasmodia*: the hepatocyte-invading sporozoites and the erythrocyte-invading merozoites. Both are highly specialized, as they are responsible to ensure the parasites ability to find a new host cell where it can hide from the host immune system. Even though sporozoites and merozoites invade completely different

cell types they use the same molecular background. The erythrocyte invading merozoites (Figure 6) are 1-2  $\mu\text{m}$  in size and are the smallest cells of the parasites life cycle and one of the smallest eukaryotic cells at all (Bannister et al., 1986; Cowman et al., 2012). They encompass two rhoptries and a few micronemes. Sporozoites in contrast are significantly larger and contain a higher number of micronemes, which correlates with their motility (Carruthers and Tomley, 2008). Erythrocytes do not possess a nucleus or any other organelles. *Plasmodium* spp. therefore bring their own invasion machinery and express all proteins involved in invasion on their own. Because the extracellular parasite is directly exposed to the human immune system the invasion process needs to be rapid and takes less than 30 seconds (M. Treeck et al., 2009). Also over 400 proteins are involved in this process (Hu et al., 2009), which makes it even more necessary to be tightly coordinated.

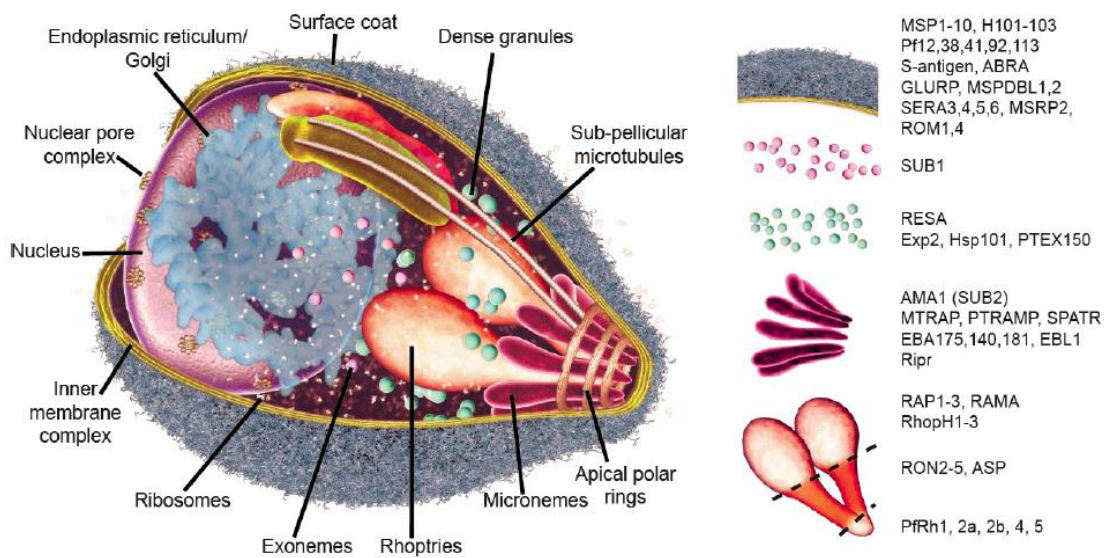


**Figure 6: 3D representation of a free merozoite and its core secretory organelles.** Organelles are listed beside with core molecular compounds of key invasion-related compartments (Cowman et al., 2012).



### 1.3.2 The apical complex

The apical complex is a special feature of the phylum *Apicomplexa*. It comprises four secretory apical organelles, namely rhoptries, micronemes, dense granules, and exonemes that were added recently (Yeoh et al., 2007). All motile and invasive stages of *Apicomplexa* – sporozoites, tachyzoites, merozoites and ookinets – are all highly polarized and comprise secretory organelles at their apical pole. The content of these organelles is secreted depending on the step of invasion or motility. While micronemes are present in all motile stages, rhoptries are restricted to invading forms and thus are absent in ookinets (Carruthers et al., 2008; Frénil et al. 2017).

The rhoptries are the biggest of the organelles. They are built very late during the last hours of schizogony and are situated in a pairwise arrangement. Among other proteins members of the Rh family are stored in these organelles (Bannister et al., 2000). Micronemes store invasion related proteins such as members of the erythrocyte binding-like (EBL) family, which are secreted to the surface during invasion (Cowman and Crabb, 2006; Carruthers and Sibley, 1999). Dense granules are supposed to secrete their protein content into the freshly established PV during the final phase of invasion (Bannister et al., 1975; Aikawa et al., 1990) (Figure 6 and Figure 8A). Exonemes are dense granule-like organelles that are released into the PV. They are suggested to mediate protease dependent rupture and egress from the iRBC (Yeoh et al., 2007).

### 1.3.3 The process of invasion

*Apicomplexa* invade their host cell in an active process, which significantly differs from other parasites. The stepwise invasion process of the parasite into the RBC is tightly organized (Figure 7). Although it is not completely resolved to date, the current state suggests the involvement of external signals that are passed through internal pathways resulting in successful invasion. The process starts after egress of the merozoites, which requires disruption of the erythrocyte cytoskeleton as well as the rupture of first the parasitophorous vacuole membrane (PVM) and subsequently of the erythrocyte PM

(Riglar et al., 2011; Salmon et al., 2001; Wickham et al., 2003). Egress is followed by the initial step of invasion, which is the attachment of the parasite to the erythrocyte surface. This is supposed to be triggered by the sudden exposure of the merozoites to the low ionic conditions of the blood plasma. Low potassium levels may lead to the release of intracellular  $\text{Ca}^{2+}$  stores resulting in secretion of microneme proteins such as the erythrocyte binding ligand 175 (EBA175) and AMA1 onto the parasite surface (Singh et al., 2010; Treck et al., 2009). Importantly only microneme proteins are secreted at that stage. Rhoptry proteins are not yet affected. While there are contradictory theories suggesting rhoptry proteins such as the *P. falciparum* reticulocyte homologue 1 (*PfRh1*) to be responsible for microneme secretion (Gao et al., 2013), it rather seems to be the other way around. At least for *T. gondii* it was shown that secreted microneme proteins might trigger the release of rhoptry proteins, once more demonstrating the strict order of the invasion process (Kessler et al., 2008). Following microneme secretion, the first attachment of the parasite to an erythrocyte is a weak and reversible binding to surface receptors, which occurs randomly and is likely mediated by merozoite surface proteins such as the glycosylphosphatidylinositol (GPI)-anchored MSP-1 (Cowman and Crabb, 2006). Interaction of the C-terminus of MSP-1 with band 3 receptor on the host cell surface is supposed to result in a non-covalent binding (Gerold et al., 1996; Holder et al., 1992; Goel et al., 2003).

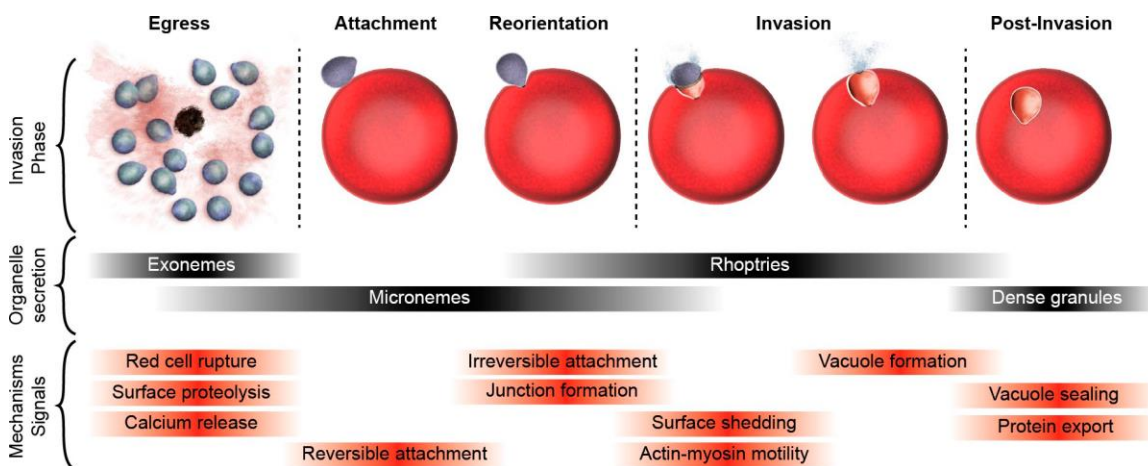


**Figure 7: Schematic description of the steps of merozoite invasion** from egress until post-invasion when the vacuole is sealed. The invasive phase is depicted with the associated steps of invasion and the signals triggering the single steps. Following egress the free merozoite attaches to the RBC and reorientates. After formation of a tight junction the active process of invasion is powered by the actin-myosin motor driving the parasite through the moving junction into the host cell. In the last step the membrane is sealed behind the parasite and the PV is established due to dense granule secretion (Cowman et al., 2012).

As all invasion-relevant organelles are located at the apical pole, the parasite reorientates to ensure that the apical end is directly located to the host cell surface (Preiser et al., 2000; Dvorak and Miller, 1975; Gilson and Crabb, 2009). Adhesion proteins stored in the micronemes are now in close proximity to the erythrocyte surface to enable binding to host cell receptors. The ligand EBA175 (see section 1.2.8.2), a member of the EBL family, is a well-characterized invasion ligand during this step. It interacts with the Glycophorin A (GlyA) receptor, which is present on the RBC surface (Camus and Hadley, 1985; Sim et al., 1994). This binding subsequently restores basal  $\text{Ca}^{2+}$  levels as mentioned before, triggering the discharge of rhoptry proteins (Singh et al., 2010; Singh and Chitnis, 2017, review). Due to interaction of these proteins with receptors on the RBC surface the weak initial binding changes to an irreversible connection, called “tight junction”, due to which the parasite finally commits to invasion. One essential receptor-ligand interaction at this stage is the binding of AMA1 to a complex of rhoptry neck proteins (RONs) (Srinivasan et al., 2011; Tonkin et al., 2011). Following upstream triggers the rhoptry proteins RON2, RON4, RON5, and RON8 are translocated into the host cell membrane. RON4, 5 and 8 hereby seem to fix the complex to the erythrocyte cytoskeleton whereas RON2 is inserted as an integral membrane protein. Thereby it acts as the anchor for the membrane antigen (Besteiro et al., 2009). Recent data proofed the interaction of AMA1 with RON2 to be essential for *T. gondii* as well as for *P. falciparum* invasion as it triggers tight junction formation (Lamarque et al., 2011; P Srinivasan et al., 2011). Specific prevention of AMA1-RON2 interaction disables junction formation and further blocks the induction of the PV. The tight junction is considered as the last checkpoint for an on-going coordinated invasion process (Riglar et al., 2011). This master switch triggers all downstream invasion steps

that are organized sequentially with rhoptry contents being secreted in a strict order (Singh et al., 2005; Riglar et al., 2011). Albeit this interaction is important for on-going invasion it does not seem to be the only event contributing to tight junction formation. In *T. gondii* another tight junction protein was discovered recently, called claudin-like apicomplexan microneme protein (CLAMP) (Sidik et al., 2016). While its role in *P. falciparum* is not completely resolved, absence of this protein in *T. gondii* leads to interruption of the invasion process due to the inability to form a tight junction.

To finally invade the RBC, the tight junction is transformed into a 'moving junction' – the actin-myosin motor of the parasite actively moves the parasite into the RBC (Miller et al., 1979; Heintzelman, 2003; Baum et al., 2006). During this process the tight junction is pulled across the merozoite surface until the parasite is completely enclosed by the PVM, which finally seals due to fusion of the membranes (Bannister et al., 1986; Lingelbach and Joiner, 1998; Riglar et al., 2011). To enable moving irreversible receptor-ligand interactions have to be broken and processed. This so-called shedding of the merozoite surface coat is suggested to happen due to the proteolytic processing of the surface ligands. The cleavage is performed by proteases such as the *P. falciparum* serine protease subtilisin-like sheddase 2 (*PfSUB2*) and *P. falciparum* rhomboid-like protease 4 (*PfROM4*) (Aikawa et al., 1978; Ladda et al., 1969). *PfSUB2* hereby cleaves the binding of MSP1 as well as the binding of AMA1 to RON2 (Baker et al., 2006; Olivieri et al., 2011). MSP1 is processed already early in invasion but shedding itself does not occur before invasion is close to completion while the parasite runs through the moving junction (Boyle et al., 2010; Riglar et al., 2011). The membrane associated *PfROM4* removes binding of EBA175 to the erythrocyte receptor GlyA (O'Donnell et al., 2006). With the last step of invasion, the sealing of the membrane, the parasite "closes the door behind" and is now perfectly hidden from the human immune system. The dense granules can now secrete their content into the newly formed PVM starting to modify the host cell immediately after invasion (Aikawa et al., 1990; review: de Koning-Ward, 2016).

### 1.3.3.1 Gliding motility and the motor complex

All motile forms of the parasite rely on an exclusive mode of substrate-dependent locomotion, called gliding motility. This process is mediated by a unique machinery called the glideosome, which enables active migration across biological membranes and host cell invasion.

The glideosome is composed of the actin-myosin motor underlying the PM. Stage specific adapter proteins, such as proteins that are structurally related to the sporozoite thrombospondin related analogous protein (TRAP), interconnect the motor system with the three-layered pellicle of the merozoite encompassing the PM and the underlying IMC. The necessary force to drive the parasite into the host cell is generated by anchoring of the glideosome to the IMC membranes (Siddall et al., 1997; Morrissette et al., 1997; Morrissette and Sibley, 2002; Opitz and Soldati, 2002; Aikawa et al., 1978; Blackman and Carruthers, 2013; Baum et al., 2008). The IMC is a Golgi-derived double membrane structure composed of small flattened vesicular sacs and is interconnected with the cytoskeleton (Figure 8A and Figure 8) (Striepen et al., 2007; Aikawa et al., 1981). This interconnection to the subpellicular microtubules is mediated by so-called alveolins, a network of intermediated filament-like proteins. It mainly confers stability and shape to the cell and was shown to play a central role in cytokinesis and invasion (Aikawa et al., 1981; Meszoely et al., 1987; Kono et al., 2012).

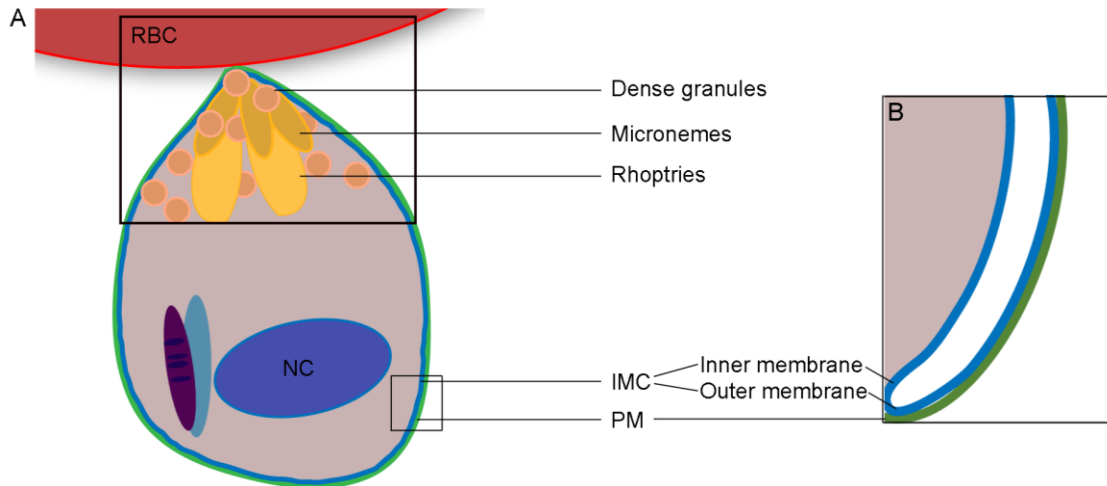


**Figure 8: Schematic representation of the invasion associated organelles of an invasive merozoite. A.** The black box highlights the apical pole of the merozoite attaching to the RBC (illustrated in red). Depicted are the apical organelles: dense granules (circles in light orange), micronemes (light brown) and the two rhoptries (yellow). The IMC (blue), the PM (green), mitochondrion (purple), apicoplast (light blue), and the nucleus (NC, dark blue) (adapted from Hu et al., 2008). **B.** Schematic zoom of the inner and outer membrane of the IMC underlying the PM, which together form the pellicle of the merozoite.

### 1.3.3.2 The motor complex

The motor complex itself is composed of myosin A (MyoA), the associated protein myosin A tail domain interacting protein (MTIP) (Bergman et al., 2003), and the three gliding associated proteins GAP45, GAP50, and GAP40 (Gaskins et al., 2004; Baum et al., 2006; Fréchal et al., 2010) that act as secure anchors linking myosin to the cholesterol-rich membranes of the IMC (Johnson et al., 2007). MyoA acts as fast motor converting the chemical energy that is released by ATP (adenosine triphosphate) hydrolysis into direct movement along actin filaments (Fréchal et al., 2017) (Figure 9).

Therefore MTIP binds to MyoA, which acts as a lever arm and converts energy into movement (Bosch et al., 2007; Green et al., 2006). GAP45 is targeted to the PM by N-terminal acylation. The C-terminal domain in contrast associates with the IMC. By recruiting MyoA to the IMC it forms a bridge between the IMC and the PM (Fréchal et al., 2010; Ridzuan et al., 2012). GAP50 and GAP40 possibly anchor MyoA to the parasite cytoskeleton. A family of glideosome-associated proteins with multiple-membrane

spans (GAPMs) that reside in the IMC interact with alveolins and GAP50 thereby linking the glideosome to the underlying cytoskeleton, which probably enables the generation of traction forces (Bullen et al., 2009) (Figure 9B and C). During the process of invasion the principal task of the motor complex is the tight and moving junction. The junction consists of intimate molecular connections between the parasite and the host cell membranes, for example due to receptor binding of AMA1 to the RON complex (Baum et al., 2008; Srinivasan et al., 2011). Actin filaments distributed at the tight junction interact with myosin heads thereby generating the force to move the parasite into the host cell right into the space which is generated due to rhoptry release. To enable movement into the host cell adhesins are cleaved in their transmembrane domain (TM). This cleavage occurs due to proteases such as SUB1, SUB2 and ROM4 and leads to disengagement of the receptor-ligand interactions (Harris et al., 2005; Yeoh et al., 2007).

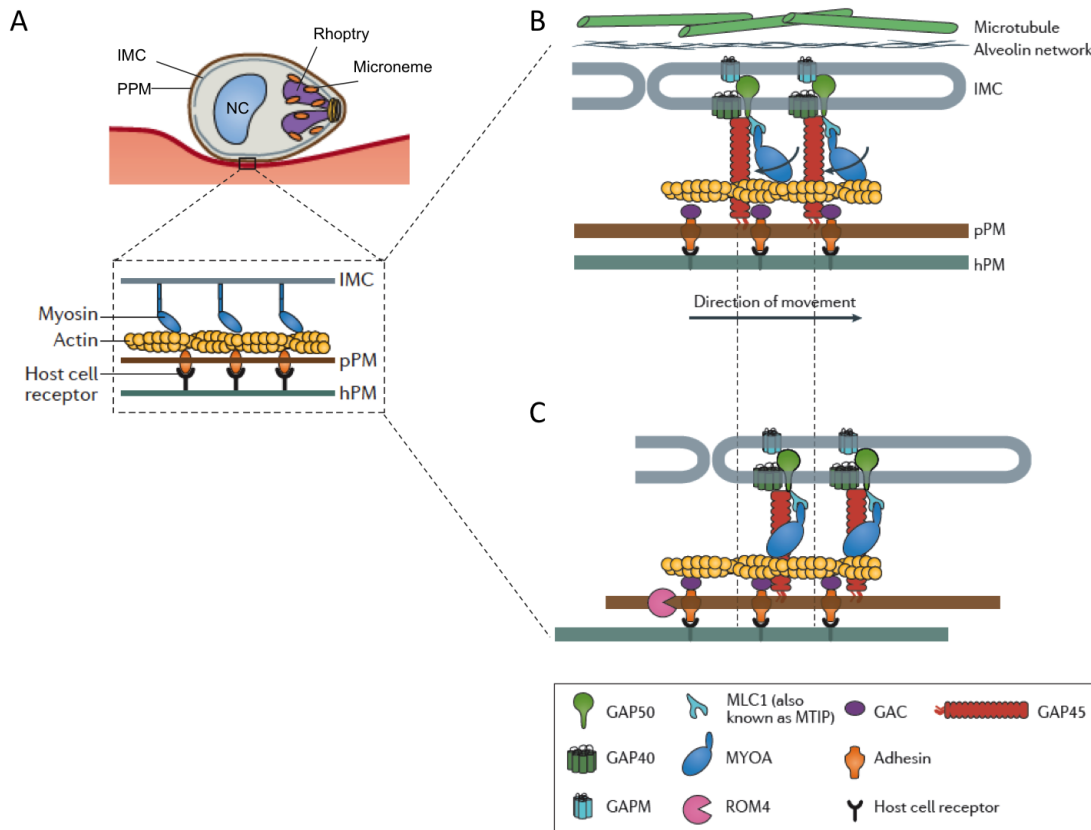


**Figure 9: Gliding motility and the motor complex. A.** Attachment of the merozoite to the host cell surface and generalized gliding motility. Adhesins (orange) inserted in the parasite PM (pPM) are present on the merozoite surface and interact with host cell receptors (black) inserted in the host cell PM (hPM). Gliding motility derives from rearward translocation of adhesion–receptor complexes powered by the myosin motor (blue) anchored to the IMC. Gliding occurs along the actin filaments (yellow). Nucleus, NC. **B and C.** Schematic description of the traction. The core compounds of the motor complex are listed in the grey box. The conformational change of the myosin head on the actin filaments due to ATP hydrolysis drives the forward movement of the parasite. ROM4 separates adhesion–receptor interaction by cleaving the TMs of adhesins and thereby enables movement (adapted from Frénal et al., 2017).

### 1.3.4 Molecular basis for invasion – Receptor-ligand interaction

Already in 1976 the essentiality of a molecular interaction between the merozoite and the RBC could be outlined as *P. vivax* invasion was shown to depend on the Duffy antigen receptor for chemokines (DARC), the Duffy blood group antigen (Miller et al., 1976; Langhi and Orlando, 2006). Since this discovery it was thought that *P. vivax* completely depends on this interaction of DARC with the erythrocyte receptor. However recent studies found Duffy-negative humans in different regions of the world to be



infected with *P. vivax* parasites (Ryan et al., 2006; Cavasini et al., 2007; Ménard et al., 2010; Singh and Chitnis, 2017, review). These findings give important hints for alternative invasion pathways and therefore the implication of different ligands that can be used.

For *P. falciparum* it is known that different strains vary in their use of invasion receptors and thereby on their dependency on sialylated receptors on the erythrocyte surface. While some strains rely on sialic acid-dependent receptor binding, others prefer invasion pathways that are sialic acid-independent. W2mef parasites for example predominantly invade in a sialic acid-dependent manner but are able to alter their invasion pathway upon treatment with neuraminidase. Neuraminidase catalyses the hydrolysis of terminal sialic acid residues thereby cleaving off all sialic acid moieties, which prevents EBA175 from binding to the erythrocytes. A switch to another invasion pathway using *PfRh4* as a ligand allows for reinvasion of W2mef parasites into RBCs. The switching is a reversible process and therefore a helpful tool to face selection pressure (Dolan et al., 1990; Reed et al., 2000; Duraisingh et al., 2003; Gilberger et al., 2003a; Stubbs et al., 2005). Parasites of the 3D7 strain in contrast are not able to switch their invasion pathway but invade erythrocytes in a sialic acid-independent manner.

Most of the parasite proteins that are directly involved in invasion can be subdivided into two groups: adhesins and invasins (Cowman and Crabb, 2006, review; Cowman et al., 2012, review). Proteins of both groups are type I TM proteins, they display an N-terminal signal peptide (SP) and a single TM followed by a short cytoplasmic tail of about 50 amino acids at its N-terminus (Di Christina et al., 2000; Adams et al., 2001). Further both groups display specific binding domains that are essential for receptor-ligand interaction. Invasins do not necessarily bind to host cell receptors but are implicated in the active invasion process. Adhesins mainly function as ligands binding directly to specific receptors present on the RBC surface. They are responsible for the initiation of the first contact to the erythrocyte surface. Two families of important adhesins are known. The Duffy binding-like (DBL) and the reticulocyte binding-like (RBL)

family. The DBL family comprises the Duffy binding proteins of *P. vivax* and *P. knowlesi* as well as the *P. falciparum* EBL proteins. The RBL family includes the *P. yoelii* 234-kDa rhoptry protein, the reticulocyte binding proteins PvRBP-1 and 2 of *P. vivax* as well as several Rh proteins of *P. falciparum* (Gaur et al., 2004; Cowman and Crabb, 2006; Iyer et al., 2007).

### 1.3.4.1 Reticulocyte binding homologue family

The *P. falciparum* Rh family consist of six members: *PfRh1a*, *PfRh1b*, *PfRh2a*, *PfRh2b*, *PfRh3*, *PfRh4*, and *PfRh5*. Besides *PfRh3*, which does not seem to be translated (Taylor et al., 2001), all members are localized in merozoites. Each *Plasmodium* species possesses at least one Rh protein but not all strains display *PfRh* ligands (Duraisingh et al., 2003). Rh family members are well conserved although they significantly differ in sequence and binding manners. Sequence polymorphisms might likely be used to regulate changes in the binding properties of the ligands. A recent study by Lobo and colleagues supposed variations in the ligand sequence to be associated to changes in the invasion pathway that is used by the parasite (Lobo et al., 2006). The binding of *PfRh1* for example is known to depend on sialic acid. *PfRh2b* in contrast could not be proven to directly bind erythrocytes at all but seems to be required for the sialic acid-independent invasion pathway (Rayner et al., 2001; Duraisingh et al., 2003). The so far best characterized Rh-ligand *PfRh4* binds to the complement receptor 1 (CR1) on the host cell surface. This erythrocyte receptor is neuraminidase-resistant. In the *P. falciparum* clone Dd2 the Rh4 gene was shown to be up-regulated when parasites were cultured in neuraminidase-treated erythrocytes. It further could be confirmed that it is essential for switching of the invasion pathway as parasites with a depleted *PfRh4* gene are disabled to change to a sialic acid independent invasion (Kaneko et al., 2002; Gaur et al., 2007; Stubbs et al., 2005; Tham et al., 2010).

Rh members in general are large proteins. *PfRh4* for example is expressed as a 220 kDa protein, displaying a TM. Rh5 in contrast is relatively small (63 kDa) and lacks the

cytosolic region at the C-terminus that is common to all other family members as well as the TM. Instead it was shown to be associated to the membrane via the Rh5 interacting protein (*PfRipr*) (Baum et al., 2009; Rodriguez et al., 2008). *PfRh5* is the only member of both the Rh and the EBL family that seems to be essential for invasion. It binds to the RBC receptor basigin (also called CD174). Basigin is a glycosylated receptor, which is resistant to chymotrypsin, trypsin and neuraminidase. This interaction seems to be essential to form the tight junction and therefore for proceeding of the invasion process (Hayton et al., 2008; Baum et al., 2009; Crosnier et al., 2011).

### 1.3.4.2 The erythrocyte binding like family

The erythrocyte binding ligands are a family of proteins located in the micronemes and known to bind sialoglycoproteins on the RBC surface with high affinity (Sim et al., 1992; Adams et al., 2001; Treeck et al., 2006). In *P. falciparum* this family comprises six members: EBA165, EBA175, EBA181, EBL1, BAEBL, and MAEBL (Thompson et al., 2001; Camus and Hadley, 1985; Sim, 1990; Adams et al., 2001; Mayer et al., 2001; Gilberger et al., 2003a; Blair et al., 2002). Their binding to a number of diverse but specific receptors on the host cell provides a set of different invasion pathways. The identified receptors for the EBL family members are Glycophorin C (GlyC), GlyA, receptor E, and GlyB (Maier et al., 2003; Camus and Hadley, 1985; Gilberger et al., 2003b; Mayer et al., 2009). Most EBL proteins are involved in the invasion of merozoites into RBCs. MAEBL on the other hand could be shown to be essential for sporozoite invasion of salivary glands (Kariu et al., 2002). All members of the EBL family possess a conserved N-terminal cysteine-rich domain for the binding to erythrocytes, the DBL domain. Name giving was the first erythrocyte-binding domain that was ever identified, region II of the *P. vivax* Duffy-binding protein (Chitnis and Miller, 1994). MAEBL in contrast to all other members displays a duplicated MAEBL ligand domain instead of the double DBL domain (Figure 10). This binding domain shows similarities to the AMA1 ectodomain.

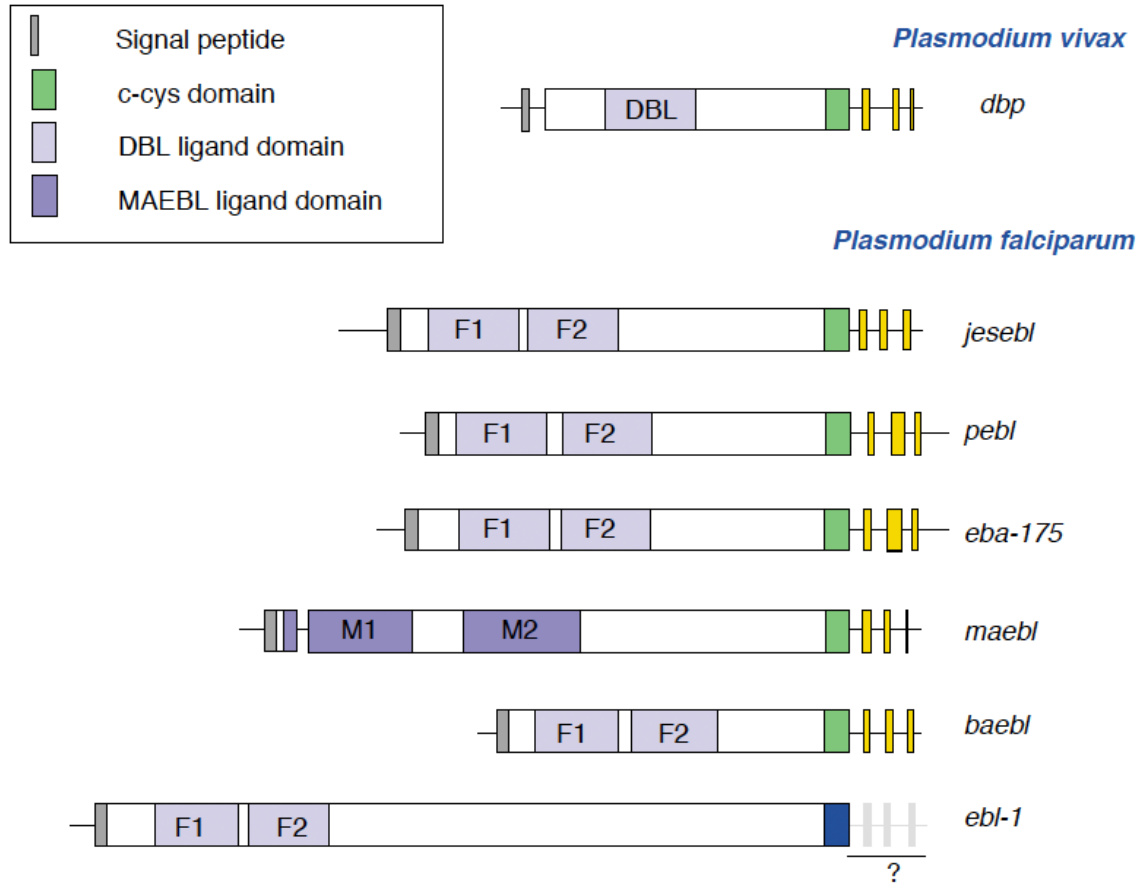


**Figure 10: Schematic representation of the gene structure of EBL family members of *P. falciparum* and *P. vivax* represented by the exon structures.** All members display a double DBL domain (F1 and F2) except for *maeb1*, which displays a duplication of the MAEBL ligand domain. Common features are the signal domain (grey), the ligand domains (light and darker lilac) as well as the carboxyl cysteine-rich (c-cys) domain (green). The yellow boxes represent the putative TM and cytoplasmic domains (Adams et al., 2001).

### 1.3.4.3 Erythrocyte binding antigen 175

The 175-kilodalton EBA was the first ligand identified to bind erythrocytes with high affinity (Camus and Hadely, 1985). EBA175 binds to the integral TM host cell receptor GlyA in a sialic acid dependent manner, which specifically requires the sialic acid moieties of the O-glycans of GlyA (Camus and Hadley, 1985; Orlandi et al., 1992; Sim et al., 1994; Marchesi et al., 1972). It is expressed during late schizogony and secreted from their micronemal localization in the merozoites during invasion (Orlandi et al., 1990; Sim et al., 1990). *PfEBA175* shows a highly conserved gene structure. The N-

terminal SP is followed by a duplicate cysteine-rich region II (F1 and F2), which was shown to be responsible for receptor binding (Mayor et al., 2005; Sim et al., 1994). These region II domains are highly conserved among over 30 laboratory and field isolates and importantly these domains are unique *Plasmodium* features (Aravind et al., 2003; Liang and Sim, 1997). Further their significant homology to the DBL proteins of *P. vivax* and *P. knowlesi* classifies all three proteins as members of the EBL family. The N-terminal single TM domain separates the extracellular cytoplasmic domain (CPD) from a 3'cysteine-rich region, which might function in protein sorting (Figure 11) (Adams et al., 1992, Gilberger et al., 2003b).

EBA175 - 1502 aa



**Figure 11: Schematic structure of the type I transmembrane protein *PfEBA175*.** The N-terminal SP is depicted in red. The duplicate cysteine-rich region II (F1 and F2, green) is responsible for receptor binding. The 3'cysteine-rich region (3'Cys, orange) is followed by a TM (blue) and the CPD (light green).

The cytoplasmic tail plays an essential role during merozoite invasion. Gilberger and colleagues could show that removal of the CPD results in a protein unable to fulfil its function (Gilberger et al., 2003b). Treatment with neuraminidase cleaves off all sialic acid moieties of the O-glycans of the receptor GlyA, which then prevents EBA175 from binding. As described before only sialic acid-independent binding remains possible. Parasites of the W2mef strain predominantly invade in a sialic acid-dependent manner, using EBA175 as preferred ligand. Culturing W2mef parasites in neuraminidase treated erythrocytes interestingly leads to a switch to the earlier mentioned sialic acid-independent Rh4 invasion pathway. The switch even between members of different gene families illustrates the perfect adaptation of the parasite to threatening challenges such as host receptor polymorphisms and the host immune system. Further there seems

to be certain functional overlap between members of the RH and EBL families. (Sim et al., 1992; Dolan et al., 1990; Reed et al., 2000; Duraisingh et al., 2003; Gilberger et al., 2003b; Stubbs et al., 2005).

### 1.4 Post-translational modifications

The parasite travels between many diverse stages and has to adapt to different hosts as well as host cells during his life cycle. Numerous proteins are involved in the different steps, which need to be strictly regulated. The *Plasmodium* blood stage proteome comprises ~5300 proteins and their timing of expression must be strictly adhered to their moment of function (Gardner et al., 2002). One option to control parasite development is the regulation at the epigenetic level by gene silencing, which was initially thought to be the main way of regulation (Le Roch et al., 2003; Bozdech and Llinas et al., 2003). Nevertheless, post-translational regulation is now commonly accepted as crucial regulatory mechanism implicated in controlling protein folding, localization, binding, and activity of enzymes as well as stability. Importantly, failure may lead to diverse pathologies or death of the parasite (Foth et al., 2008; Doerig et al., 2015). Post-translational modification (PTM) in general is understood as covalent alterations of specific functional groups on a polypeptide mediated by enzymes. The fact that many PTMs are reversible enables dynamic regulation. Well-understood modifications in *Plasmodium* include lipidation (myristoylation and palmitoylation), acetylation and methylation, as well as phosphorylation. These alterations are involved in the regulation of host cell invasion, egress, transition, and even virulence (reviewed in Doerig et al., 2015).

Expression of the 60 members of the *var* gene family encoding PfEMP1 for example is tightly regulated by histone acetylation and methylation (Lopez-Rubio et al., 2007; Kyes et al., 2007). Lipidation can mediate membrane-attachment and sub-cellular trafficking

of proteins such as the glideosome associated protein 45 (GAP45) (Maurer-Stroh et al., 2002; Resh, 1999; Rees-Channer et al., 2006).

Probably the most common mechanism to regulate cell physiology is phosphorylation. A phosphate group is transferred mostly from ATP and covalently attached to specific amino acids. This process is mediated by kinases and protein phosphatases. The *P. falciparum* kinome comprises 85-99 genes encoding protein-kinases related enzymes and 30 genes encoding phosphatases (Talevich et al., 2012; Doerig et al., 2015). It is well known, that eukaryotic protein kinases target residues carrying an alcohol group. These are the amino acids serine (S), threonine (T), and tyrosine (Y). Most phosphorylation events occur at serines (89%), followed by T (10.4%) and only 0.5% of the phosphorylated sites were found to be tyrosines (Treeck et al., 2011). This is still astonishing given the fact that no tyrosine specific kinases or phosphatases are known in *P. falciparum* (Ward et al., 2004). Nevertheless, phosphorylated Y are often involved in signalling pathways such as the mitogen-activated protein (MAP) kinase pathway, which is critical for the parasite (Lim and Pawson, 2010; Tan et al., 2009). This phosphorylation is suggested to result from autophosphorylation (which is also known for the glycogen synthase kinase 3 (GSK3)). Interestingly, many phosphorylated proteins were found in the IMC and invasome (Treeck et al., 2011) underlining the importance of PTM of invasion-related proteins, which might – although not proofed yet – be also true for EBA175.

Phosphorylation is not only used for post-translational protein regulation. It also mediates transcriptional regulation such as the eukaryotic translation initiation factor (eIF2). Phosphorylation of the  $\alpha$  subunit eIF2 $\alpha$  was shown to regulate maintenance of dormancy in *Plasmodium* spp. (reviewed in Zhang et al., 2013). Nonetheless, phosphorylation is a well-known PTM, which occurs in diverse life stages of the parasite, including mosquito, liver and – importantly – blood stages. In the late blood stages almost 1700 proteins are predicted to be phosphorylated (Treeck et al., 2012; Pease et al., 2013), comprising many invasion ligands such as AMA1, Rh4 and Rh2b (Treeck et al.,

2009; Tham et al., 2015; Engelberg et al., 2013). Apparently the majority of adhesin CPDs is phosphorylated *in vitro* (Tham et al., 2015).

Phosphorylation of the cytoplasmic domain of AMA1 is essential for host cell invasion and it was shown that phosphorylation of AMA1 CPD by the cyclic AMP-dependent protein kinase A (PKA) relies on a phospho-priming step mediated by GSK3 (Treeck et al., 2009; Leykauf and Treeck et al., 2010; Engelberg et al., 2013; Prinz et al., 2016). This type I TM protein is synthesized during late schizogony and is secreted from the micronemes to the merozoite surface where it interacts with the parasite-derived RON complex (Besteiro et al., 2009). At its C-terminus AMA1 provides a relatively short CPD, which is crucial for the functionality of the protein (Treeck et al., 2009). Six phosphorylation sites are available in the tail and it was shown that phosphorylation of specific amino acid residues in the CPD is essential (Leykauf and Treeck et al., 2010). Interestingly the functionality of AMA1 seems to be dependent on a two-step phosphorylation. The first phosphorylation step is mediated by the protein kinase 2 (PK2), which phosphorylates a serine at position 610 (S610) (Leykauf and Treeck et al., 2010). It is suggested that a resulting conformational change of the protein exposes the second phosphorylation site (T613), which is then accessible for another kinase – GSK3 (Leykauf and Treeck et al., 2010; Engelberg et al., 2013; Prinz et al., 2016). Phosphorylation of the CPD is not required to anchor AMA1 to the actin-myosin motor as aldolase can still bind the tail. However it appears to be essential for the formation of the moving junction (Leykauf and Treeck et al., 2010).

Recently, phosphorylation of the CPD was also demonstrated for *PfRh4* (Tham et al., 2015). *PfRh4* is essential in the sialic acid-independent pathway (Maier et al., 2003; Tham et al., 2009). W2mef parasites were not able to switch invasion pathways to invade neuraminidase-treated RBCs upon disruption of the gene (Maier et al., 2003). During invasion *PfRh4* interacts with CR1 on the RBC surface and it was shown that tyrosine residues within the CPD of *PfRh4* are essential for this invasion pathway (Tham et al., 2010; 2015). Albeit no *P. falciparum* tyrosine kinases are identified to date it was



suggested that this likely involves the phosphorylation of Y residues (Ward et al., 2004; Tham et al., 2015). This suggests the implication of specific amino acids in the CPD in signalling of downstream invasion events and it was shown that these residues are essential for RBC invasion via receptor-ligand interaction of *PfRh4* and CR1 (Tham et al., 2015). It was further demonstrated that mutant *P. falciparum* merozoites without functional Rh4 protein are not able to invade neuraminidase-treated RBCs, though they still attach to the host cell (Tham et al., 2015). Nonetheless, the exact role of this ligand in invasion could not be identified to date.

Another invasion ligand of the Rh family is *PfRh2b*. Deletion of the CPD of the mutation of conserved acidic residues within this domain is not tolerated by *P. falciparum* parasites (DeSimone et al., 2009). Further it was shown that the exchange of the *PfRh2a* CPD with *PfRh2b* CPD activates the otherwise inactive ligand (Dvorin et al., 2010). These findings demonstrate a specific function of the tail of the invasion ligand. Engelberg and collaborators therefore suggested specific phosphorylation of residue S3233 likely mediated by *P. falciparum* casein kinase 2 (*PfCK2*) (Engelberg et al., 2013). Despite late stage phosphorylation of *PfRh2b* CPD, mutation of S3233 did not alter parasite invasion. It therefore was suggested that instead of directly influencing the invasion event phosphorylation of S3233 might trigger a pre-invasive process, which might be connected to translocation or to priming for invasion (Engelberg et al., 2013).

### 1.5 The invadome

Together these findings demonstrate that invasion is a complex process involving a not yet fully understood network of interacting proteins. Most of these proteins are situated either in the apical secretory organelles or on the surface of merozoites (Cowman and Crabb, 2006). Further it is known that many invasion related proteins such as AMA1 or MSP1 share structural and transcriptional features. They all comprise a N-terminal SP,

which enables entry into the secretory pathway and are transcribed during late schizogony (Bozdech et al., 2003; Le Roch et al., 2003). Proteins that are predicted to be involved in invasion are collated as the “invadome”. Different investigations have been carried out to functionally annotate proteins based on primary sequence and expression data (Le Roch et al., 2003; Bozdech et al., 2003; LaCount et al., 2005). Haase and collaborators combined predicted localization with transcriptional and structural features to perform a genome wide search. They could identify 49 hypothetical proteins likely to be involved in invasion (Haase et al., 2008). Hu, Cabrera and collaborators generated a transcriptional data set based on DNA microarray profiling of perturbations that reflects the functional relationships between *P. falciparum* genes (Hu and Cabrera et al., 2009). Based on this data set, a high confidence gene network was generated – called PlamsOINT – which enables functional prediction of almost 90% of the proteome (function of 2545 hypothetical proteins was predicted). Concentrating on late blood stages, a subnetwork of 416 genes likely to be implicated in invasion was generated. By the use of an ectopically GFP (green fluorescent protein)-tagging approach it could be shown that 31 out of 42 expressed and localized proteins actually were associated to invasion-related compartments such as the merozoite surface, the IMC, or apical organelles.

Substantial progress has been achieved during the last decades to unravel the complex network of invasion-related proteins. But an indefinite number of proteins implicated in the multifaceted process of invasion still remains unknown necessitating an update of the invadome.

### 1.6 Aims of this work

Invasion of the obligatory intracellular *Plasmodium* parasite is a process not completely understood to date implicating an unknown number of proteins. The aim of this thesis therefore was to:

I. Investigate the impact of CDP-phosphorylation on EBA175-functionality:

For other invasion proteins it was shown that phosphorylation of their cytoplasmic domain was essential for their function in invasion. For EBA175 it was shown before that deletion of the cytoplasmic domain results in a switch of the invasion pathway of W2mef parasites. To investigate into the role of the phosphorylation sites within the cytoplasmic domain a CPD-phospho-mutant should be generated to assess specific phosphorylation sites within the C-tail using a neuraminidase invasion assay.

II. Identify novel parasite proteins that are secreted and might function as ligands during the invasion process. Using a bioinformatic screen putative candidate genes were identified and endogenous GFP tagging allowed for further localization analysis.

## 2 Material and Methods

### 2.1 Material

#### 2.1.1 Chemicals and biological reagents

Reagents	Manufacturer / Distributor
Acetic acid	Roth, Karlsruhe
Acrylamide/Bisacrylamide solution (40:5)	Roth, Karlsruhe
Agar LB (Lennox)	Roth, Karlsruhe
Agarose	Invitrogen
Albumax II	Gibco, Life Technologies, USA
Albumin bovine fraction V (BSA)	Biomol, Hamburg
Ammonium persulfate (APS)	Applichem, Darmstadt
Ampicillin	Roche, Mannheim
Bacto™ Yeast extract	BD, USA
Bacto™ Peptone	BD, USA
Blasticidin S (BSD)	Invitrogen, Karlsruhe
BODIPY <sup>R</sup> TR Ceramid	Sigma-Aldrich, Steinheim
Bromphenol Blue	Merck, Darmstadt
Calcium chloride (CaCl <sub>2</sub> )	Sigma-Aldrich, Steinheim
Clarity™ Western ECL Substrate	Bio-Rad
Concanavalin A G-250	Sigma-Aldrich, Steinheim
Coomassie Brilliant Blue G-250	Merck, Darmstadt
Dako Fluorescence mounting medium	DAKO, Hamburg
DAPI (4',6-Diamidino-2-phenylindole)	Roche, Mannheim
Deoxynucleoside triphosphate (dNTP)	Thermo Scientific
Dimethyl sulfoxide (DMSO)	Sigma-Aldrich, Steinheim
Disodium phosphate (Na <sub>2</sub> HPO <sub>4</sub> )	Roth, Karlsruhe
Disodium hydrogen phosphate (NaH <sub>2</sub> HPO <sub>4</sub> )	Roth, Karlsruhe
1,4-Dithiothreitol (DTT)	Roche, Mannheim
Dulbecco's Phosphate Buffered Saline (DPBS)	Pan Biotech, Aidenbach
Ethanol	Merck, Darmstadt

## Material and Methods

Ethidium bromide	Sigma-Aldrich, Steinheim
Ethylenediaminetetraacetic acid (EDTA)	Biomol, Hamburg
Ethylene glycol-tetraacetic acid (EGTA)	Biomol, Hamburg
Formaldehyde 10%, methanol free, Ultra Pure	Polysciences
Gentamycin	Ratiopharm, Ulm
Giemsa's azur eosin methylene blue solution	Merck, Darmstadt
D-Glucose	Merck, Darmstadt
Glutaraldehyde (25%)	Roth, Karlsruhe
Glycerol	Merck, Darmstadt
Glycine	Biomol, Hamburg
HEPES (4-(2-hydroxyethyl)-1-piperazineethanesulfonic acid)	Roche, Mannheim
Hoechst33342	Chemodex, Switzerland
Hydrochloric acid (HCl)	Merck, Darmstadt
Hypoxanthine	Biomol, Hamburg
Isopropanol	Roth, Karlsruhe
Magnesium chloride (MgCl <sub>2</sub> )	Merck, Darmstadt
Manganese(II) chloride (MnCl <sub>2</sub> )	Merck, Darmstadt
β-Mercaptoethanol	Merck, Darmstadt
Methanol	Roth, Karlsruhe
Milk powder	Roth, Karlsruhe
3-(N-morpholino)propansulfonic acid (MOPS)	Sigma-Aldrich, Steinheim
Neomycin, G418	Sigma-Aldrich, Steinheim
Neuraminidase [1.5 U/ml]	Sigma-Aldrich, Steinheim
Percoll	GE Healthcare, Sweden
Potassium chloride (KCl)	Merck, Darmstadt
Potassium dihydrogen phosphate (KH <sub>2</sub> PO <sub>4</sub> )	Merck, Darmstadt
Protease inhibitor cocktail	Roche, Mannheim
RPMI (Roswell Park Memorial Institute) Medium	Applichem, Darmstadt
Rubidium chloride (RbCl)	Sigma-Aldrich, Steinheim
Saponin	Sigma-Aldrich, Steinheim

SimplyBlue™ Safestain Coomassie	
Sodium acetate (C <sub>2</sub> H <sub>3</sub> NaO <sub>2</sub> )	Merck, Darmstadt
Sodium bicarbonate (NaHCO <sub>3</sub> )	Sigma-Aldrich, Steinheim
Sodium chloride (NaCl)	Gerbu, Gaiberg
Sodium dihydrogen phosphate (NaH <sub>2</sub> PO <sub>4</sub> )	Roth, Karlsruhe
Sodium dodecyl sulfate (SDS)	Applichem, Darmstadt
Sodium hydroxide	Merck, Darmstadt
Sorbitol	Sigma-Aldrich, Steinheim
TEMED (N,N,N,N-Tetramethylethylenediamine)	Merck, Darmstadt
Tris-Base	Roth, Karlsruhe
Tris-EDTA (TE)	Invitrogen, Karlsruhe
Triton X-100	Biomol, Hamburg
Tween 20	Merck, Darmstadt
Water for molecular biology (Ampuwa)	Fresenius Kabi, Bad Homburg
WR 99210	Jacobus Pharmaceuticals, Washington, USA
Xylencyanol	

---

### 2.1.2 Labware and Disposables:

<b>Labware / Disposables</b>	<b>Specification</b>	<b>Manufacturer / Distributor</b>
Cryotubes	(1.6 ml)	Sarstedt, Nümbrecht
Culture bottles	(50 ml)	Sarstedt, Nümbrecht
Dako pen		DAKO, Hamburg
Disposable pipette tips	(1-10, 20-200, 100-1000 µl)	Sarstedt, Nümbrecht
Eppendorf reaction tubes	(1,5 and 2 ml)	Sarstedt, Nümbrecht
Falcon tubes, conical	(15 and 50 ml)	Sarstedt, Nümbrecht
Filter tips	(1-10, 2-20, 20-200, 100-1000 µl)	Sarstedt, Nümbrecht
Flow cytometry tubes	55.1579	Sarstedt, Nümbrecht
Glass cover slips	(24x65 mm thickness) (0.13-0.16 mm)	R. Langenbrinck, Emmendingen

## Material and Methods

Glass slides		Engelbrecht, Edermünde
Gloves, latex		SHIELD scientific, Bennekom, Netherlands
Leukosilk tape		BSN medical, Hamburg
Microscopy dishes, uncoated	60 µl	Ibidi, Martinsried
Multiply-µ Strip Pro 8-Strip		Sarstedt, Nümbrecht
PCR reaction tube		
Nitrocellulose blotting membrane Protran™	Amersham 0.45 µm	GE Healthcare
One way cannulas		Braun, Melsungen
One way syringe		Braun, Melsungen
Parafilm		Bemis, USA
Pasteur pipettes		Brand, Wertheim
Petri dishes	15x60mm, 14x90 mm	Sarstedt, Nümbrecht
Plastic pipettes	(5, 10, 25 ml)	Sarstedt, Nümbrecht
Sterile filter	0.22 µm	Sarstedt, Nümbrecht
Transfection cuvettes	0.2 cm	Bio-Rad, Munich
Whatman™ Chromatography Paper	3 MM Chr	GE Healthcare UK Limited

### 2.1.3 Technical and mechanical devices

Devices	Specification	Manufacturer / Distributor
Acylamide gel chamber	Protean	
Agarose gel chamber	Wide Mini-Sub® Cell GT basic	Bio-Rad, Munich
Analytical balance	572	Kern, Balingen
Casting stand	Mini-PRPTEAN®	Bio-Rad, Munich
Casting plates	Mini-PRPTEAN®	Bio-Rad, Munich
Casting frames	Mini-PRPTEAN®	Bio-Rad, Munich
Centrifuges:	Megafuge 1.0R	Heraeus, Hannover

## Material and Methods

	J2 HS Ultracentrifuge	Beckmann Coulter, Krefeld
	Rotor JA-12	
	Avanti J-26S Xp	Beckmann Coulter, Krefeld
	Rotor Ja-14	
Tabletop centrifuge	5424	Eppendorf, Hamburg
Developer	ChemiDoc XRS+	Bio-Rad, Munich
Electrophoresis chamber	Mini-PRPTEAN®	Bio-Rad, Munich
Electroporator	Gene Pulser XCell	Bio-Rad, Munich
	Nucleofector II AAD-1001N	Amaxa Biosystems, Germany
Flow cytometer	LSR II	BD Instruments, USA
Gel documentation		
Gel doc cam.		
Ice machine	EF 156 easy-fit	Scotsman
Incubator:		
Bacterial incubator	CO-150, CO <sub>2</sub> Incubator	New Brunswick Scientific
<i>P.f.</i> culture incubator	Heratherm IGS400	Thermo Scientific, Langenselbold
Shaking incubator	innova 40	New Brunswick Scientific
Laboratory scale	Kern 572	Kern & Sohn, Balingen
Magnetic stirrer	RSM-10HP	PHOENIX Instrument
Microscopes:		
Confocal microscope	Olympus FV1000	Olympus, Hamburg
Fluorescence microscope	Axioscope 1	Zeiss, Jena
Light microscope	Axio Lab.A1	Zeiss, Jena
Microscope Hamamatsu digital camera	Ocra C4742-95	Hamamatsu Photonics K.K., Japan
Microwave	micromaxx	
PCR cycler	C1000 Touch Thermo Cycler	Bio-Rad, Munich
pH-meter	SevenEasy	Mettler-Toledo, Gießen
Pipettes	10, 20, 200, 1000 µl	Gilson, Middleton, USA
Pipettor	Matrix CellMate II	Thermo Scientific, Langenselbold



## Material and Methods

Power-supply	Consort EV231	Merck, Darmstadt
	PowerPac basic	Bio-Rad, Munich
Roller mixer	SRT 6D	Stuart
Safety cabinet		Düperthal
Spectrophotometer	NanoDrop 2000c	Thermo Fisher Scientific
Sterile laminar flow bench	Sterile Gard III Advance	Baker, Stanford, USA
	Safe 2020	Thermo Scientific, Pinneberg
Thermoblock	Thermomixer F1.5	Eppendorf, Hamburg
Ultrapure water purification system	Milli Q	Millipore
UV-transilluminator	PHER Olum 289	Biotech Fischer, Reiskirchen
Vacuum pump	BVC Control	Vacuunbrand, Deutschland
		Janke & Kunkel IKA
Vortexer	Vortex-Genie 2	Scientific Industries
Waterbath	1083	GFL, Burgwedel

### 2.1.4 Kits and standards

Designation	Manufacturer / Distributor
NucleoSpin® Plasmid Kit	Macherey-Nagel, Düren
NucleoSpin® Gel and PCR Clean-up	Macherey-Nagel, Düren
QIAam® DNA Mini Kit	Qiagen, Hilden
QIAGEN® Plasmid Midi Kit	Qiagen, Hilden
Western Blot ECL-Clarity™ Detection Kit	Bio-Rad, USA
GeneRuler™ 1 kb DNA Ladder	Thermo Scientific, Schwerte
PageRuler™ Prestained Protein Ladder	Thermo Scientific, Schwerte
PageRuler™ (Plus) Prestained Protein Ladder	Thermo Scientific, Schwerte

### 2.1.5 Software, data bases and bioinformatical tools

Adobe PhotoShop CS5

Adobe Illustrator CS5

AxioVision v 4.7	Carl Zeiss Microscopy
BLAST	<a href="https://blast.ncbi.nlm.nih.gov/Blast.cgi">https://blast.ncbi.nlm.nih.gov/Blast.cgi</a>
Clustal W2	
ExPASy Proteomic Tools	
FACS Diva v 6.1.3	BD Bioscience
MS Office	Microsoft Corporation
NanoDrop 2000	Thermo Fisher Scientific
NetPhos 3.1	<a href="http://www.cbs.dtu.dk">http://www.cbs.dtu.dk</a>
PlasmoDB	Plasmodb.org
SnapGene Viewer 2.5.0	GSL Biotech

### 2.1.6 Stock solutions, buffers and media

#### 2.1.6.1 Cell biological work

##### *P. falciparum* cell culture (*in vitro*)

RPMI-complete medium	15.87 g RPMI 1640 1 g NaH <sub>2</sub> CO <sub>3</sub> 2 g Glucose 0.5% Albumax II 0.0272 g Hypoxanthine 0.5 ml Gentamycin (40 mg/ml) Fill up to 1 l with ddH <sub>2</sub> O pH 7.2, sterile filter
10xPBS	5.7 g Na <sub>2</sub> HPO <sub>4</sub> 1.25 g NaH <sub>2</sub> PO <sub>4</sub> 15.2 g NaCl Fill up to 1 l with ddH <sub>2</sub> O pH 7.4

## Material and Methods

Sorbitol-synchronization solution	5% (w/v) D-Sorbitol in ddH <sub>2</sub> O, sterile filter
Cryo-Freezing solution (MFS)	38.8 g Sorbitol 8.1 g NaCl 350 ml Glycerol in dH <sub>2</sub> O, sterile filtered
Thawing solution (MTS)	3.5 % (w/v) NaCl in ddH <sub>2</sub> O, sterile filter
Transfection buffer – Cytomix	120 mM KCl 0.15 mM CaCl <sub>2</sub> 2 mM EGTA 5 mM MgCl <sub>2</sub> 10 mM K <sub>2</sub> HPO <sub>4</sub> 10 mM KH <sub>2</sub> PO <sub>2</sub> 25 mM HEPES, pH 7.6, in dH <sub>2</sub> O, sterile filter
Amaza transfection buffer	90 mM NaPO <sub>4</sub> 5 mM KCL 0.15 mM CaCl <sub>2</sub> 50 mM HEPES pH 7.3, in dH <sub>2</sub> O, sterile filter
Saponin lysis buffer	0.03 % Saponin in 1xPBS
Fixing solution	4 % Formaldehyde 0.0075 % Glutaraldehyde (25 %) 500 µl 10xPBS fill up to 5 ml with dH <sub>2</sub> O
Permeabilization buffer	0.1 % Triton X-100 in 1xPBS

## Material and Methods

Blocking buffer	3 % BSA in 1xPBS
Blood	Sterile human erythrocyte concentrate, blood group O <sup>+</sup> (Blutbank UKE, Hamburg, Germany)
Selection drugs:	
WR99210 - Stock solution	20 mM WR99210, in DMSO
- Working solution	20 $\mu$ M WR99210 (stock solution 1:1000), in fresh RPMI complete medium, sterile filter
Blasticidin S (BSD) working solution	5 mg/ml in RPMI complete medium, sterile filter
G418 (neomycin) working solution	50 mg/ml G418 in RPMI complete medium, sterile filter
10% Giemsa	10 ml Giemsa solution 90 ml dH <sub>2</sub> O
Percoll stock solution (90 %)	90 % (v/v) Percoll 10 % (v/v) 10xPBS
60 % Percoll solution	6.7 ml Percoll stock solution 3.3 ml RPMI complete medium
Lysis buffer	4 % SDS 0.5 % Triton X-100 0.5xPBS in dH <sub>2</sub> O
Ho33342 stock solution (10x)	4.5 mg Ho33342, in 1ml DMSO
Ho33342 working solution (1x)	0.45 mg Ho33342, in 1ml DMSO
FC stop solution	0.5 $\mu$ l Glutaraldehyde (25%), in 40ml RPMI complete medium

**2.1.6.2 Microbiological work**

*E. coli* culture:

Ampicillin stock solution	100 mg/ml Ampicillin in 70% ethanol
10x LB-Medium – Stock solution	10 % yeast extract 5 % Peptone 10 % NaCl in ddH <sub>2</sub> O, autoclave
LB-Agar	1.5 % Agar-Agar in 1x LB-medium, autoclave
LB+AMP selection medium	1x LB-medium (autoclaved) 100 µg/ml Ampicillin
Glycerol stabilate solution	50 % (v/v) Glycerol in 1x LB medium

Chemical competent cells:

TFBI solution	30 mM sodium acetate 50 mM MnCl <sub>2</sub> 100 mM RbCl 10 mM CaCl <sub>2</sub> 15 % (v/v) Glycerol pH 5.8 (using 0.2 N sodium acetate), in dH <sub>2</sub> O, sterile filter
TFBII solution	10 mM MOPS 75 mM CaCl <sub>2</sub> 10 mM RbCl 15 % (v/v) Glycerol pH 7.0 (using NaOH), in dH <sub>2</sub> O, sterile filter

### 2.1.6.3 Molecular biological work

#### Gibson assembly

5x isothermal reaction buffer

3 ml Tris-HCl, pH 7.5  
150  $\mu$ l 2 M MgCl<sub>2</sub>  
60  $\mu$ l 100 mM dGTP, dATP, dTTP, dCTP  
300  $\mu$ l 1 M DTT  
1.5 g PEG-8000  
300  $\mu$ l 100 nM NAD  
add to 6 ml dH<sub>2</sub>O

Assembly master mixture (1.2 ml)

320  $\mu$ l 5x isothermal reaction buffer  
0.64  $\mu$ l 10 U /  $\mu$ l T5 exonuclease  
20  $\mu$ l 2 U /  $\mu$ l Phusion DNA polymerase  
160  $\mu$ l 40 U /  $\mu$ l Taq DNA ligase  
add to 1.2 ml H<sub>2</sub>O

#### DNA precipitation

Sodium acetate

3 M NaAc, pH 5.2

Ethanol

100 %

70 %

TE buffer (Tris-EDTA)

10 mM Tris-HCl, pH 8.0

1 mM EDTA, pH 8.0

#### DNA separation

50x TAE buffer

2 M Tris-Base

1 M Glacial acetic acid

0.5 M EDTA,

pH 8.5, add to 1 l with ddH<sub>2</sub>O, autoclave

Agarose gel

1 - 2 % Agarose in 1x TAE buffer

6x DNA loading dye  
40 % (w/v) Glycerol  
2.5 % (w/v) Xylene cyanol  
2.5 % (w/v) Bromphenol blue  
in dH<sub>2</sub>O

## **2.1.7 Biochemical work**

### **2.1.7.1 Protein separation via SDS-PAGE**

10x Electrophoresis buffer – stock solution  
1 % (w/v) SDS  
1.92 M Glycine  
250 mM Tris-HCl,  
in dH<sub>2</sub>O

1x Electrophoresis buffer – working solution  
1:10 dilution of stock solution in dH<sub>2</sub>O

Stacking gel buffer  
1 m Tris-HCl, pH 6.8

Separating gel buffer  
1.5 M Tris-HCL, pH 8.8

Stacking gel (4 %) 5 ml, 2 gels  
4.35 ml dH<sub>2</sub>O  
0.75 ml stacking gel buffer  
0.75 ml Acryl amide (40 %)  
6 µl TEMED  
60 µl SDS (10 %)  
60 µl APS (10 %)

Separating gel (8 %) 10 ml  
5.2 ml dH<sub>2</sub>O  
2.5 ml separating gel buffer  
2 ml Acryl amide (40 %)  
4 µl TEMED  
100 µl SDS (10 %)  
100 µl APS (10 %)

Separating gel (12 %) 10 ml, 2 gels  
4.2 ml dH<sub>2</sub>O  
2.5 ml separating gel buffer

	3 ml Acryl amide (40 %)
	4 µl TEMED
	100 µl SDS (10 %)
	100 µl APS (10 %)
5x SDS loading dye	12 % SDS (w/v)
	300 mM Tris, pH 6.8
	60 % (v/v) Glycerol
	0.05 % (w/v) Brophenol blue
	600 mM DTT
Ammonium persulfate (APS)	10 % (w/v) APS in dH <sub>2</sub> O

### 2.1.7.2 Protein transfer – Western blotting

10x Transfer buffer – stock solution	250 mM Tris-HCl
	1.92 M Glycine
	0.37 % (w/v) SDS, in dH <sub>2</sub> O
1x Transfer buffer – working solution	25 mM Tris-HCl
	192 mM Glycine
	0.037 % (w/v) SDS
	20 % (v/v) Methanol, in dH <sub>2</sub> O
Blocking buffer	5 % milk powder in 1xPBS
Wash buffer (PBS-Tween)	1xPBS
	0.05 % Tween-20

### 2.1.8 Bacterial and parasite strains

Bacterial strains:

<i>E. coli</i> XL-10 gold	Tet <sup>r</sup> Δ(mcrA)183Δ(mcrCB-hsdSMRmrr)173 endA1 supE44 thi-1 recA1 gyrA96 relA1 lac Hte [F' proAB lacI <sup>q</sup> Z ΔM15 Tn10(Tet <sup>r</sup> ) Amy Cam <sup>r</sup> ]
---------------------------	--



Parasite strains:

<i>Plasmodium falciparum</i> 3D7	Clone of the NF54 isolate (MR4-1000) due to limiting dilution cloning, (Walliker et al., 1987) Manasses/USA, origin Africa
<i>Plasmodium falciparum</i> W2mef	Derived from the Indochina III/CDC strain

## 2.1.9 Antibodies

### 2.1.9.1 Primary antibodies

Atnigen	Organism	Dilution	Application	Source
Aldolase	rabbit	1:2000	Western blot	
GFP	mouse	1:1000 1:500	Western blot IFA	Roche (Mannheim, Germany)
EBA175	rabbit	1:2000	Western blot	
EBA181	rabbit	1:2000	IFA	

### 2.1.9.2 Secondary antibodies

Atnigen	Organism	Conjugation	Dilution	Application	Source
Mouse	Rabbit	HRP	1:3000	Western blot	Dianova, Hamburg, Sigma, Steinheim
Rabbit	Goat	HRP	1:3000	Western blot	Dianova, Hamburg, Sigma, Steinheim
Mouse	Goat	Alexa Fluor® 488	1:2000	IFA	
Mouse	Goat	Alexa Fluor® 594	1:2000	IFA	

### 2.1.10 Fluorescence dyes

Hoechst 33342	Chemodex
Dihydroethidium	Cayman
DAPI	Roche

### 2.1.11 Enzymes and Polymerases

#### Enzymes

Restriction enzyme	Concentration [U/ml]	Manufacturer/Distributor
AvrII (G <sup>^</sup> GTACC)	5	NEB, Ipswich, USA
DpnI (GA(CH <sub>3</sub> ) <sup>^</sup> TC)	20	NEB, Ipswich, USA
KpnI-HF (CCTAGG)	20	NEB, Ipswich, USA
MluI-HF (A <sup>^</sup> CGCGT)	20	NEB, Ipswich, USA
NotI-HF (GC <sup>^</sup> GGCCGC)	20	NEB, Ipswich, USA
T4 DNA-Ligase	[4 U/μl]	NEB, Ipswich, USA
Neuraminidase	1.5	Sigma Aldrich

#### Polymerases

DNA-Polymerase	Concentration [U/μl]	Manufacturer/Distributor
FirePol® DNA Polymerase	5	Solis BioDyne, Estland
Phusion® High-Fidelity DNA Polymerase	2	NEB, Ipswich, USA
Taq DNA Polymerase	5	NEB, Ipswich, USA

### 2.1.12 Plasmids

**pARL1a- (Crabb et al., 2004):** pARL1a- vector is a shuttle plasmid allowing selection in bacteria as well as in *Plasmodium*. After transformation into *E. coli* the encoded β-

lactamase gene confers resistance against ampicillin. When transfected in *P. falciparum* the plasmid encodes the human dihydrofolate reductase (hDHFR), which confers resistance against the selection drug WR99210. For the integration of genes the *ama1* promoter was removed by *NotI/AvrII* or *NotI/MluI* digest. Insertion of correspondingly digested fragments allows C-terminal tagging of the genes.

**SLI-vector (for Selection linked integration):** the SLI-vector is used for endogenous GFP tagging of genes of interest (GOI) via homologous recombination. Insertion of the GOI is achieved via *NotI/MluI* digestion. The encoded  $\beta$ -lactamase gene confers resistance against ampicillin after transformation into *E. coli*. After transfection into *P. falciparum* the plasmid encodes the human dihydrofolate reductase (hDHFR), which confers resistance against the selection drug WR99210. Additionally the plasmid encodes for an additional positive selection marker, namely neomycin phosphotransferase II gene, which is expressed after correct integration of the GOI under the endogenous promoter, but is separated by a skip peptide. Selection of parasites with integrated plasmid can be achieved due to addition of the selection drug neomycin.

### 2.1.13 Oligonucleotides

A full complete list of oligonucleotides that were used for this study is provided in the appendix.

## 2.2 Methods

### 2.2.1 Molecular biological methods

#### 2.2.1.1 Polymerase chain reaction (PCR) for DNA amplification

Polymerase chain reaction (PCR) (Mullis and Faloona, 1987) was used to specifically amplify DNA fragments from DNA templates. For preparative PCRs Phusion polymerase with proofreading function was used. FirePol polymerase was used for colony screen and analytical PCR control (see next section). Specific oligonucleotides (primer pairs, forward and reverse flanking the 5' and 3' regions) were used from a 100  $\mu$ M stock solution. Primers were designed using sequence information given on PlasmODB ([www.plasmodb.org](http://www.plasmodb.org)). Typical PCR-reactions were prepared as follows:

#### Preparative PCR:

5x Phusion buffer	10 $\mu$ l
dNTPs (2.5 mM)	5 $\mu$ l
Primer sense	1 $\mu$ l
Primer reverse	1 $\mu$ l
Template DNA	0.3 – 0.5 $\mu$ l
Phusion polymerase	0.3 $\mu$ l
dH <sub>2</sub> O	to 50 $\mu$ l

#### PCR program:

Phase	Temperature	Time
Denaturation	95 °C	4 min
30 cycles	Denaturation	95 °C 15 s
	Annealing	42 °C 30 s
	Elongation	62 °C x min
Storage	4 °C	$\infty$

x depends on the length of the PCR product and was usually set to 1 min / 1000 bp. PCR settings were adjusted depending on the PCR product and primer-sequence.

**2.2.1.2 Analytical PCR control and colony screen**

Analytical PCR was performed to screen for positive clones after transformation into *E.coli* bacteria (colony PCR) or to check for correct integration. For the colony screen single colonies were picked from agar plates (over night cultured *E.coli* cultures after transformation) and used as template in a typical PCR-reaction as follows:

**Analytical PCR:**

10x FirePol buffer	1 µl
MgCl <sub>2</sub>	1µl
dNTPs (2.5 mM)	1µl
Primer sense	0.4 µl
Primer reverse	0.4 µl
Template DNA	0.3 µl
/ bacterial colony	
Phusion polymerase	0.1 µl
dH <sub>2</sub> O	to 10 µl

**PCR program:**

Phase	Temperature	Time
Denaturation	95 °C	4 min
25 cycles	Denaturation	95 °C 30 s
	Annealing	45 °C 30 s
	Elongation	64 °C x min
Storage	4 °C	∞

x depends on the length of the PCR product and was usually set to 1 min / 1000 bp. PCR settings were adjusted depending on the PCR product and primer-sequence.

**2.2.1.3 Agarose gel electrophoresis**

According to their length DNA fragments can be separated by agarose gel electrophoresis as based on their negatively charged phosphate backbone they will move toward the anode in an electric field. Samples were loaded onto 1 % agarose gels. Agarose was mixed with 1x TAE buffer and dissolved by boiling. After cooling down, the agarose solution was transferred into a gel tray and Ethidiumbromide was added to a final concentration of 1 µg/ml. To generate pockets for DNA loading combs were placed into the gel tray right after. The hardened gel then was transferred into an electrophoresis chamber filled with 1x TAE. Samples were mixed with 6x DNA loading dye and loaded into the pockets. Electrophoresis was performed at 120 V for 20 minutes. 1kb GeneRuler was used as a DNA ladder and separated bands were visualized via UV light using the ChemiDoc XRS+ system.

**2.2.1.4 PCR-product purification**

Obtained PCR-products and digested DNA fragments as well as vectors were purified using the NucleoSpin® Gel and PCR Clean-up kit according to the manufacturer's protocol and eluted in 20 - 40 µl dH<sub>2</sub>O.

**2.2.1.5 "Preparative" DNA digestion**

Purified DNA fragments and plasmids were digested to create "sticky ends" for subsequent ligation. Depending on the used vector different restriction enzymes were used. DpnI was used if PCR-products were amplified from methylated template DNA. The incubation time for preparative restriction was 2.5 - 3 h at 37 °C.

<b>Reagents</b>	<b>Volume</b>
10x NEB cut smart buffer	5 µl
Each restriction enzyme	0.5 µl
DpnI (for PCR-products only)	1 µl

DNA (plasmid / PCR)	2 $\mu$ l / whole volume
dH <sub>2</sub> O	ad 50 $\mu$ l

**2.2.1.6 Analytical DNA digestion (test digest)**

Plasmids were analytically digested using 2  $\mu$ l of purified DNA (mini or midi DNA) in a total reaction volume of 10  $\mu$ l. 1  $\mu$ l of 10x cut smart buffer and 0.2  $\mu$ l of diluted enzymes were added and adjusted to the final volume by addition of dH<sub>2</sub>O. After 1 h incubation at 37 °C the fragments were visualized by gel electrophoresis.

**2.2.1.7 Ligation**

Digested vector DNA and PCR-fragments were ligated using T4 ligase. Ligation was used to produce plasmids that can be transformed into *E. coli* for multiplication on LB-agar-plates. The ligation reaction mix was incubated for 20 minutes at room temperature.

<b>Reagents</b>	<b>Volume</b>
10x T4 ligase buffer	1 $\mu$ l
PCR product	7 $\mu$ l
Vector DNA	1 $\mu$ l
T4 ligase	1 $\mu$ l

**2.2.1.8 DNA ligation via Gibson assembly**

Alternatively DNA ligation can be performed via Gibson DNA assembly (Gibson et al., 2009). This method allows the ligation of up to 6 inserts into one vector. This protocol does not need sticky ends but needs to overlap with the vector sequence in 15 - 35 bp. Therefore only DpnI digestion is necessary. The ligation reaction was incubated for 60 minutes at 50 °C. A typical reaction is shown below:

Reagents	Volume
Assembly master mixture	7.5 $\mu$ l
PCR product	1 $\mu$ l
Vector DNA	1 $\mu$ l
dH <sub>2</sub> O	ad 10 $\mu$ l

### 2.2.1.9 Production of chemically competent *E. coli*

The rubidium chloride method was used to render *E. coli* bacteria chemo-competent (Hanahan, 1983). This treatment leads to a decreased stability of the bacterial cell wall resulting in an increased plasmid uptake. Therefore 20 ml LB medium were inoculated with a glycerol stabulate of the *E. coli* XL Gold strain and incubated at 37°C, overnight, shaking. 10 ml of the culture were transferred into an 200 ml LB-holding Erlenmeyer flask and incubated at 37°C, shaking, until an OD<sub>600</sub> of 0.5-0.6. The bacteria were harvested by centrifugation af 2400 x g for 20 minutes at 4°C. Subsequently the pellet was re-suspended in 60 ml TFBI buffer and incubated on ice for 10 minutes. After another centrifugation step at same conditions the pellet was re-suspended in 8 ml TFBII buffer and 100  $\mu$ l aliquots were prepared in 1.5 ml reaction tubes and stored at -80°C until further use.

### 2.2.1.10 Transformation into chemically competent *E. coli* cells

For the transformation of the ligation reaction mix into chemically competent cells 50  $\mu$ l aliquots of *E.coli* cells were thawed on ice for 5 - 10 minutes. The ligation mix (or 2  $\mu$ l of a sequenced plasmid) was added and incubated on ice for 10 minutes. After a 40 second heat shock at 42°C and following cool down on ice for 1 minute, 1 ml of LB medium (without ampicillin) was added and incubated at 37°C for 30 minutes, shaking, 750 rpm. The suspension subsequently was evenly distributed on ampicillin containing LB-agar plates using sterile glass beads and cultured over night at 37 °C.



#### **2.2.1.11 Overnight culture of *E. coli* for subsequent plasmid DNA preparation**

For plasmid preparations bacteria from an agar plate (or from a glycerol stock) were inoculated in LB medium at 37 °C overnight with vigorous shaking. Volume was dependent on mini or midi preparation. For plasmid mini preparation 2 ml LB medium was used in a 2 ml reaction tube, plasmid midi preparation were inoculated in 150 - 200 ml LB medium using an 1 l Erlenmeyer flask.

#### **2.2.1.12 Freezin of *E. coli***

For long term storage 500 µl overnight *E. coli* culture were resuspended in 500 µl of glycerol in a 2 ml reaction tube and stored at -80 °C.

#### **2.2.1.13 Plasmid-DNA isolation (mini and midi preparation)**

Plasmid-DNA was extracted from 2 ml overnight cultures using the NucleoSpin® Plasmid Kit for mini preparation according to the manufacturer's protocol. Midi preparations were purified from 150 ml overnight cultures using the QUIAGEN®Plasmid Midi Kit. In brief, these preparations are based on the principle of alkaline lysis of cells and subsequent binding of the DNA to a silica membrane under physiological conditions. Mini preparation was eluted in 50 µl dH<sub>2</sub>O and midi preparations in 200 µl TE buffer. Eluted DNA was used for restriction digest (mini preparation) or for transfection of *P. falciparum* (midi preparation).

#### **2.2.1.14 Determination of DNA concentration via Nanodrop**

DNA concentration was determined using Thermo Scientific NanoDrop 2000c Spectrophotometer measuring the absorbance at 260/280 nm ( $A_{260/280}$ ). Hereby 260 nm is the absorbance maximum of nucleic acids, 280 nm the maximum of proteins. The

optimum  $A_{260/280}$  value for pure DNA is considered about 1.8. dH<sub>2</sub>O or TE buffer were used as blank depending on the elution solution. Software: NanoDrop 2000.

### **2.2.1.15 Sequencing of plasmid DNA**

To verify correct integration of the PCR fragment into the vector and to exclude mutations of the insert purified plasmids were sent for sequencing. A sequencing primers (2 µl) that binds the vector in front of the insert was mixed with 5 µl of the plasmid DNA and dH<sub>2</sub>O was added to a reaction volume of 15 µl. Sequencing was performed by Sequence Laboratories (Seqlab, Göttingen).

### **2.2.1.16 DNA precipitation**

For DNA precipitation 100 µg of purified plasmid DNA was mixed with 0.1 volume of sodium acetate 3 M pH 5.6 in a 1.5 reaction tube. Three volumes of 100 % ethanol was added, mixed by vortexing and stored at -20 °C overnight or at least for 20 minutes. The solution was centrifuged at maximum speed for 15 minutes. After removing the supernatant the DNA pellet was washed with 70 % ethanol. Following a subsequent centrifugation step the supernatant was removed and the pellet air-dried under sterile culture conditions and solved in sterile TE buffer (the volume was depend on the transfection method).

## **2.2.2 Biochemical technics**

### **2.2.2.1 Discontinuous SDS-Polyacrylamide gel electrophoresis (SDS-PAGE)**

According to their molecular weight proteins can be separated via discontinuous SDS-PAGE (Laemmli, 1970). To enable a charge-independent separation in an electric field SDS-PAGE is performed under denaturing conditions. SDS, a strongly negatively charged detergent, binds and unfolds the proteins leading to negatively charged samples and

thus preventing protein-protein-interactions. DTT (a detergent of the SDS buffer) leads to a reduction of disulfide bonds, which contributes to denaturation of the protein. To separate the proteins 8 % and 12 % polyacrylamide gels were used in this study. SDS-PAGE was performed at 200 V for 1 - 1.5 h according to the size of the proteins.

### **2.2.2.2 Western blot**

Proteins that were separated via SDS-PAGE were blotted onto a nitrocellulose membrane and immobilized using a wet transfer system. Therefore the membrane was layered on the polyacrylamide gel and sandwiched between 6 Whatman filter papers as well as 2 sponges all soaked in WB transfer buffer. The sandwich was placed into the blotting chamber letting the gel face the cathode with the membrane facing the anode. After filling the chamber with WB transfer buffer, the transfer was performed by 100 V for 1 h and a cooling unit placed into the tank (or alternatively in a fridge at 4 °C).

### **2.2.2.3 Immunodetection of proteins**

Proteins that were immobilized via western blot can be detected using specific antibodies. Therefore the nitrocellulose membrane was incubated with 5 % milk powder in 1xPBS for 1 h at room temperature to block all unspecific binding sites. Subsequently incubation with the primary antibody diluted in 2.5 % milk powder in 1xPBS followed overnight at 4 °C. The membrane was washed 3 times with 1xPBS-Tween and subsequently incubated with the secondary antibody conjugated to hoarse radish peroxidase (HRP), diluted in 2.5 % milk powder in 1xPBS, 1 h at room temperature. The membrane was washed 3 times with 1xPBS-Tween and developed using the Western Blot ECL-Clarity™ Detection Kit with an incubation time of 1 minute. Hereby the oxidation of luminol leads to chemiluminescence, which can be detected by x-ray screen. The exposure times ranged from 1 - 20 minutes.

### **2.2.3 Cell cultures technics for *Plasmodium falciparum***

#### **2.2.3.1 *P. falciparum* in continuous cell culture (Trager and Jensen, 1976)**

The *P. falciparum* parasites were kept in continuous cell culture. The parasites were cultured in 5 ml (15x60 mm) or 10 ml (14x90 mm) petri dishes with RPMI complete medium and 5 % human O<sup>+</sup> erythrocytes at 37 °C. The dishes were kept in a gas tight chamber in which the the atmosphere was adjusted to high carbon dioxide and low oxygen levels: 5 % O<sub>2</sub>, 5 % CO<sub>2</sub>, 90 % N<sub>2</sub>. Depending on experiments parasitemia was kept at 0.1 - 5 % by dilution and medium was changed every second day. Transgenic parasites were selected with 4 nM WR99210 (1.5 µl / 10 ml medium).

#### **2.2.3.2 Giemsa staining of blood smears**

Parasitemia was monitored by Giemsa staining of thin blood smears, which results in a purple colored parasite DNA and a light blue staining of the RBC cytoplasm. Therefore 0.5 µl of parasite culture were transferred to a glass slide and smeared using a second glass slide resulting in a thin monolayer of blood. This smear was fixated to the slide due to incubation in methanol for 30 seconds and subsequently stained with Giemsa staining solution for 5 - 10 minutes. After incubation the staining solution was rinsed off by water and the smear was analyzed by an optical light microscope (Zeiss Axio Lab.A1).

#### **2.2.3.3 Long term storage of *P.falciparum* – freezing and thawing**

*P. falciparum* parasites can be long-term stored as cryo-stabilates in liquid nitrogen. Ring stage parasites with a parasitemia of > 5 % were harvested in a 15 ml falcon tube and centrifuged at 1800 x g for 3 minutes. The pellet was resuspended in 1 ml parasite freezing solution (MFS), transferred into a cryo tube and frozen immediately.

Thawing of the cryo-stabilates was performed at 37 °C for 5 minutes. After centrifugation at 1800 x g for 3 minutes the pellet was resuspended in 1 ml parasite

thawing solution (MTS). After another centrifugation step the pellet was washed in 1 ml RPMI complete medium and transferred into a 5 ml culture dish containing fresh RPMI complete medium and 5 % hematocrit. The selection drug was added 24 h later after the medium was exchanged.

### 2.2.3.4 Synchronization

**Sorbitol synchronization (Lambros and Vanderberg, 1979):** to synchronize a parasite culture the culture was transferred into a 15 ml falcon tube and spun down at 1800 x g for 3 minutes. The supernatant was discarded and the pellet was resuspended in pre-warmed 5 % D-sorbitol solution. After incubation for 10 minutes at 37 °C the falcon tube was centrifuged by 1800 x g for 3 minutes. The pellet was washed with RPMI complete medium and re-cultured in fresh RPMI complete medium. The hematocrit was adjusted to 5 %. Sorbitol synchronization leads to a culture holding only parasites of 0 - 12 hours post invasion stage.

**Synchronization via Percoll gradient:** a Percoll gradient was used to separate schizonts from trophozoites, ring stages and uninfected erythrocytes either to synchronize a culture to late stages or for the preparation of late-stage-western blot pellets. 4 ml of 60 % Percoll solution was provided in a 15 ml falcon tube. 8 ml parasite culture was slowly layered on top of the Percoll solution and centrifuged at 2000 x g for 6 minutes. The top layer now is medium followed by the schizont layer which was transferred into another 15 ml falcon tube, washed with RPMI complete medium and re-cultured in fresh RPMI complete medium or prepared for further use.

### 2.2.3.5 Transfection of *P. falciparum*

(Wu et al., 1995; Crabb and Cowman, 1996; Fidock and Wellems, 1997)

**Transfection using the BioRad system:** Plasmid DNA can be transfected into *P. falciparum* parasites via electroporation. 100 µg of purified plasmid DNA (from a midi preparation) was precipitated in a 1.5 reaction tube (DNA precipitation). 0.1 volume of sodium acetate 3 M pH 5.6 and three volumes of 100 % ethanol was added, mixed by vortexing and stored at -20 °C overnight or at least for 20 minutes. The solution was centrifuged at maximum speed for 15 minutes. After removing the supernatant the DNA pellet was washed with 70 % ethanol. After a subsequent centrifugation step the supernatant was removed and the pellet air-dried under sterile culture conditions, dissolved in 15 µl sterile TE buffer and mixed with 385 µl cytomix. In the meantime, 5-10 ml of parasite culture containing 5-10 % synchronized ring stage parasites was centrifuged 3 minutes at 1800 x g. The pellet was mixed with the cytomix/DNA solution and transferred into an electroporation cuvette (2 mm, BioRad). Electroporation was performed using the Gene Pulser Xcell (310 V, 950 µF,  $\infty \Omega$ ). The parasites were transferred into a 14x90 petri dish containing 10 ml fresh RPMI complete medium and hematocrit was adjusted to 5 %. After 24 hours the selection drug was added and medium was changed daily for the first 5 days and every second day from that day onwards. In this study parasites of the W2mef *Plasmodium* strain, which were used for the EBA175-project were transfected via the BioRad system.

**Transfection using the Amaxa system:** For transfection using the Amaxa system, 50 µg of purified plasmid DNA was precipitated (see DNA precipitation), dissolved in 10 µl sterile TE and mixed with 90 µl Amaxa transfection buffer. Late schizonts were harvested with 60 % Percoll solution (see synchronization using Percoll). 10-15 µl of the schizont pellet were mixed with the DNA/Amaxa transfection solution and transferred into an electroporation cuvette (2 mm, BioRad). Electroporation was performed using the Nucleofector II AAD-100N (program: U-033). Transfected parasites were transferred into a 1.5 ml reaction tube containing 300 µl erythrocytes and 200 µl RPMI complete medium pre-warmed to 37 °C. Under rigorous shaking the reaction tube was incubated for 15-60 minutes at 37 °C. Parasites then were transferred into a 15x60 mm petri dish containing fresh RPMI complete medium. After 24 h the medium was changed and the

selection drug was added. For the first 5 days the medium was changed every 24 hours, then every second day. In this study parasites from the 3D7 *Plasmodium* strain, which were used for the bioinformatic screen were transfected using the Amaxa system.

### **2.2.3.6 Selection for transgenic parasites using SLI**

For integrant selection via SLI (selection linked integration), transfected cultures containing an episomal plasmid selected with WR99210 were adjusted to a parasitemia of 2-5 %, G418 (neomycin) was added to a final concentration of 400 µg/ml (Birnbaum and Flemming et al., 2017) and WR99210 selection pressure was discarded. Until day 7 after starting G418 (neomycin) selection pressure the cultures were fed every day, then every other day. On day 16 parasites were taken off drug. If no parasites were obtained until day 60 the culture was discarded. DNA of reappearing parasites was isolated using the QIAamp® DNA Mini Kit and used for integration check PCRs.

For essentiality checks with SLI-TGD, a culture containing the episomal plasmid after WR-selection was split into three 5-ml cultures and placed under G418 selection (400 µg/ml). If no correct integration event occurred on two occasions (with a total of six cultures), the target gen was assumed to be essential (Birnbaum and Flemming et al., 2017). If no parasites were obtained until day 60 the culture was discarded.

### **2.2.3.7 Selection for transgenic parasites via “on/off cycling”**

For selection of integrands using the “on/off” cycling method, transfected cultures were kept on selection pressure until parasites were obtained. Then the selection drug was discarded and the culture was held off drug for 14 days. On day 15 the parasites were set under selection pressure again until reappearance. This cycling went on until a GFP signal was obtained in the selected parasite cultures. Genomic DNA was isolated and tested for correct integration of the gene via PCR.

#### 2.2.3.8 Isolation of genomic DNA

To verify the correct integration of a plasmid into the parasite genome, genomic DNA (gDNA) of transgenic and wild type *P. falciparum* parasites was isolated and used for PCR analysis. 5 ml of parasite culture were transferred into a 15 ml falcon tube and centrifuged at 1800 x g for 3 minutes. Genomic DNA was purified from the pellet using the QIAamp® DNA Mini Kit according to the manufacturer's protocol and eluted in 40 µl dH<sub>2</sub>O.

#### 2.2.3.9 Isolation of parasites by (restricted) saponin lysis

Parasites can be isolated from a blood culture using saponin in low concentration (Umlas and Fallon, 1971). Saponin shows a hemolytic activity leading to lysis of the erythrocyte membrane as well as the parasitophorous vacuole membrane while the parasite plasma membrane stays intact. The resulting parasite material can be further used for protein preparation. 5-10 ml of parasite culture were harvested in a 15 ml falcon tube (1800 x g, 3 minutes) and incubated in 3 ml of 0.03 % saponin solution in 1xPBS for 10 minutes on ice. After incubation the lysate was transferred in to a 2 ml reaction tube and centrifuged at maximum speed (16000 x g) for 5 minutes. The pellet was washed with ice-cold 1xPBS until the supernatant remained clear from haemoglobin. The pellet was transferred into a 1.5 ml reaction tube and resuspended in 20-80 µl of dH<sub>2</sub>O and mixed with the appropriate amount of 4x SDS lysis buffer. The solution was heated at 85 °C for 5 minutes and centrifuged for 5 minutes at maximum speed. For SDS-PAGE 5-15 µl per sample were used.

#### 2.2.3.10 Fixation of parasite material for Immunofluorescence assays (IFAs)

**Methanol- and acetone-fixation:** For immunofluorescence assays parasites can be fixed to a glass slide by methanol or acetone. A thin blood smear was incubated for 4 minutes in ice-cold methanol or RT acetone for 30 minutes and dried on air afterwards. For further preparation a region of interest (ca. 0.5x0.5 cm square) was marked with a



DAKO pen and rehydrated with 1xPBS for 5 minutes. The 1xPBS was removed and all further steps were performed in a humid chamber. The marked square was incubated with the primary antibody in 3 % BSA in 1xPBS for 1-2 hours at RT. The region was washed three times with 1xPBS and subsequently incubated with the secondary antibody in 3 % BSA in 1xPBS in the dark for 1 hour. After incubation the antibody solution was washed off three times with 1xPBS (5 minutes incubation per wash step) whereby for the last wash step DAPI is diluted 1:1000 in 1xPBS and incubated for 5 minutes. DAKO mounting medium was added, covered with a cover slide and sealed with nail polish. The IFAs could be imaged by fluorescence microscopy a few hours later after the mounting medium had dried.

**Formaldehyde/Glutaraldehyde-fixation:** 10 ml parasite culture were harvested in a 15 ml falcon tube, 1800 x g for 3 minutes, and the pellet was resuspended in 1 ml of fixing solution for 30 minutes at RT. After three wash steps with 1xPBS 1 ml 0.1 % Triton X-100 in 1xPBS was used to permeabilize the parasite membranes for two minutes at room TR. The fixed parasites were washed three times and subsequently incubated with 3 % BSA in 1xPBS to block unspecific binding sites for 1 h at RT. The pellet was incubated with the primary antibody diluted in 3 % BSA in 1xPBS under rolling conditions for 1-2 h at RT, or overnight at 4 °C. The secondary antibody, diluted in 3 % BSA in 1xPBS was added after three washing steps and incubated for 1 h at room temperature, rolling. The antibody was washed off three times with 1xPBS, 10 minutes each, whereby for the last washing step DAPI was added in a 1:1000 dilution and incubated for 10 more minutes rolling in the dark. The pellet was resuspended in 50-100 µl 1xPBS and stored at 4 °C for further analysis. All centrifugation steps were performed at 2000 x g for 3 minutes. The IFAs could be imaged by fluorescence microscopy using 2-4 µl parasite material on a glass slide covered with a coverslip.

### 2.2.4 Live cell and fluorescence imaging

For localization of GFP-tagged proteins fluorescence microscopy was performed using a Zeiss Axioscope M1, equipped with a 100x/1.4- and 63x/1.4-numerical aperture oil objectives. The pictures were acquired using a Hamamatsu Orca C4742-95 camera and the Zeiss Axiovision software (version 4.7) and further processed using Adobe PhotoShop CS5. For sample preparation 500-1000  $\mu$ l parasite culture were transferred into a 1.5 ml reaction tube and incubated with DAPI in a final concentration of 1  $\mu$ g/ml for 5 minutes at room temperature. The parasites were centrifuged at 1800 x g for 1 minute and the supernatant was exchanged for 1 pellet volume of fresh RPMI complete medium. After resuspending, 4-5  $\mu$ l were transferred to a glass slide, covered with a coverslip and imaged immediately.

### 2.2.5 Neuraminidase invasion assay

For characterizing the invasion phenotype of EBA175-wt and -P0 parasites erythrocyte invasion assays were performed (Dolan et al., 1994; Engelberg et al., 2013; Reed et al., 2000). 500  $\mu$ l of erythrocytes were incubated with 75 mU neuraminidase in RPMI complete medium. Parasite cultures were diluted to 0.5 % start parasitemia and likewise incubated with neuraminidase working solution in a final concentration of 75 mU. After incubation for 1 h at 37 °C under rolling conditions parasites and RBCs were washed twice with RPMI complete medium and kept in culture under standard conditions. Parasitemia was counted using the LSRII.

### 2.2.6 Flow cytometry FACS

Parasitemia of the neuraminidase invasion assays was analyzed via flow cytometry. For staining of the parasites 20  $\mu$ l thoroughly resuspended parasite culture was transferred into a flow cytometry tube. 80  $\mu$ l RPMI complete medium were mixed with 1  $\mu$ l of HO33342 working solution and 1  $\mu$ l of DHE. The mixture was added to the parasites

containing flow cytometry tube and incubated for 20 minutes in the dark. Thereafter 400 µl FC stop solution was added and parasitemia was measured using LSRII with the gating as described elsewhere (Malleret et al., 2011).

### 2.2.7 Gene identification

Primary sequence data and gene expression profiles were analysed using resources implemented at the PlasmoDB data base (<http://plasmoDB.org>, release 33). To search the data base for putative candidates following query parameters were used: a) predicted signal peptide and b) late transcription. Following data sets were used to search for late transcribed genes: Le Roch et al. (2003) and Bozdech and Llinas et al. (2003) were used for microarray evidence. Settings for query parameters: temperature synchronized parasites from late rings to schizont stages and merozoites (Le Roch et al, 2003) and min. expression at 16 h +/- 8 h and a max. expression at 42 h +/- 6 h (Bozdech and Llinas et al., 2003). For RNA sequencing evidence Bartfai et al. (2010) was used. Settings: minimum transcription: 25 hpi; maximum transcription: 40 hpi. Genes were returned upon  $\geq 3$ - fold change induction.

### 3 Results

#### 3.1 Regulatory steps in invasion – phosphorylation of EBA175 CPD

##### 3.1.1 Generation of EBA175 mutants

Previous results showed that the deletion of the CPD of EBA175 results in a switch of the invasion pathway of W2mef parasites (Gilberger et al., 2003). Additionally, work on other adhesins such as AMA1 (Treeck et al., 2009) and Rh4 (Tham et al., 2015) indicated that the phosphorylation of residues within the CPD is essential for their function during the invasion process with the exception of Rh2b (Engelberg et al., 2013; please see introduction xx). Therefore, the function of the putative phosphorylation sites in the CPD of EBA175 should be assessed.

The cytoplasmic domain of EBA175 consists of 61 amino acids with 9 putative phosphorylation sites. These are S1442, Y1446, S1448, S1449, T1466, S1473, T1483, S1489, and Y1491 (Figure 12). NetPhos 3.1 (<http://www.cbs.dtu.dk>) is a software, that pre-estimates phosphorylation in eukaryotic proteins using ensembles of neural networks. It predicts the phosphorylation of 4 residues (S1442, Y1446, T1466, and S1489) with a score of 0.630, 0.840, 0.601, and 0.614 (respectively; cut off score at 0.5) within the cytoplasmic domain with functional implication for erythrocyte invasion.

In order to test this hypothesis, a phospho-mutant (EBA175<sub>phospho</sub>) was generated comprising following alanine substitutions: S1448, S1449, T1466, S1473, T1483, and S1489 (Fig. 2). The rationale to exclude the two predicted amino acids is i) the absence of tyrosine kinases in the kinome of the parasite (Y1446 and Y1491) and ii) the direct positioning of S1442 after the transmembrane domain. The rationale for including the additional amino acids were their borderline prediction score with 0.464 (S1448), 0.461 (S1449), 0.451 (S1473), and 0.483 (T1483).

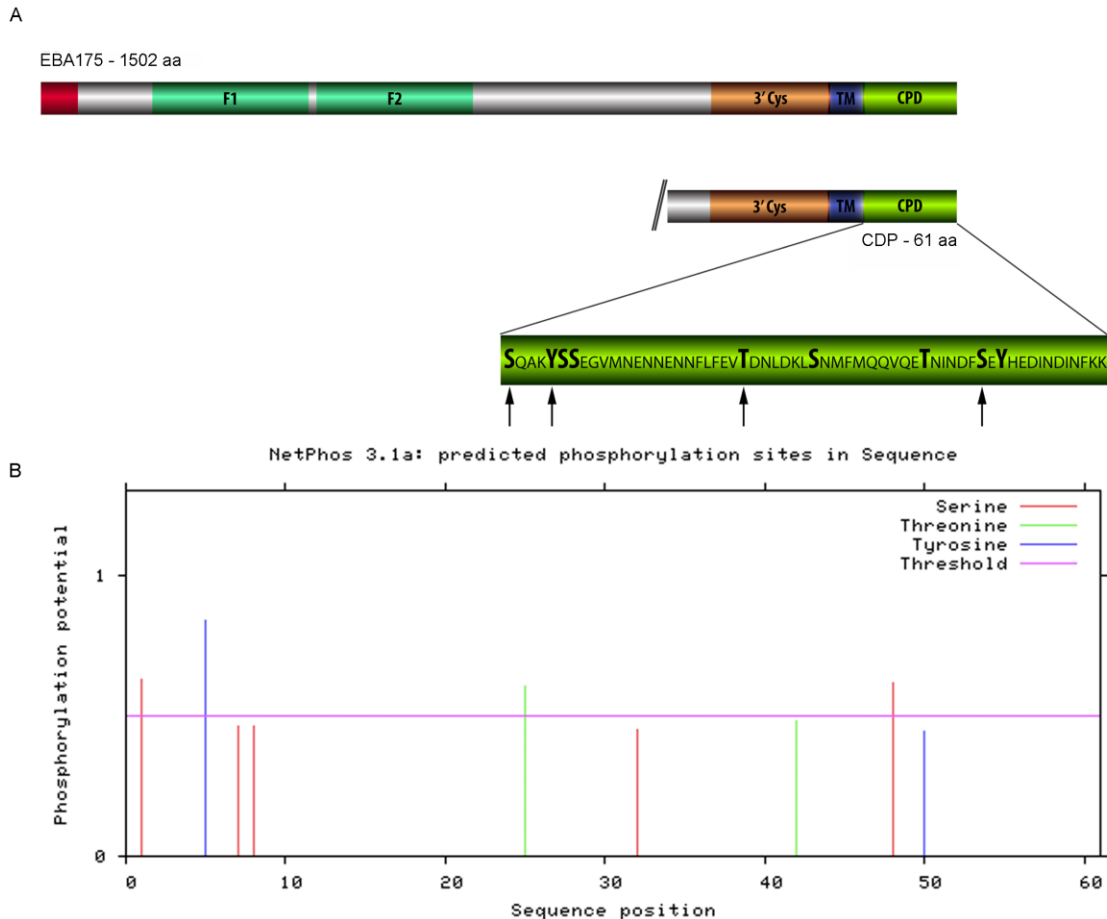


**Figure 12: Putative phosphorylation sites of EBA175.** **A.** Schematic representation of the protein structure of EBA175, its cytoplasmic domain (consisting of 61 amino acids) and the predicted phosphorylation sites. Arrows indicate amino acids that were predicted by NetPhos 3.1 to be phosphorylated with a score  $> 0.5$ . (3'Cys, cysteine rich domain at the 3' end; TM, transmembrane domain; CPD, cytoplasmic domain). **B.** Graphic representation of the NetPhos 3.1 prediction, threshold of 0.500.

Mutations leading to the amino acid substitutions in the coding region of EBA175 were introduced by overlap PCR using appropriate primer combinations (Figure 13A). Genomic DNA from *P. falciparum* 3D7 parasites was used as a template. First, the 795 bp of the 3' end of *eba175* were cloned into the *NotI/AvrII* site of the vector pARL-GFP (Crabb et al., 2004; primer combination P1+P2, 795 bp), releasing the promoter of the vector and resulting in the vector pARL\_EBA175GFP<sub>int</sub>. This vector subsequently was used as template to generate pARL\_EBA175<sub>phospho</sub>GFP<sub>int</sub>. To achieve this, the fragments were generated stepwise by the use of different primer combinations (appendix, tab. X). In the first step mutation S1448 and S1449A were introduced via overlap PCR. The first

fragment was amplified using primer P1 and P5 (Figure 13A) and the second fragment with primers P6 and P2. Both fragments were used as template (1:1 ratio) for a subsequent PCR using the primers P1 and P2. Of note, an intron of 125 bp separating S1448 from S1449 was deleted, using primer P5 and P6, given that attempts to amplify the mutated sequence failed when the intron was present. The resulting amplicon was used as template for the subsequent overlap PCR introducing T1466A and S1473A (primer combination P1+P7 was used for the first fragment, and P8+P2 for the second fragment). The resulting fragments (ratio 1:1) were amplified with the primers P1+P2. Finally, this PCR fragment comprising S1448, S1449A, T1466A, and S1473A served as template to mutate T1483 and S1489 into alanines (primer combination P1+P9). The product was digested with *NotI* and *AvrII* and cloned into the pARL\_GFP vector resulting in the vector pARL\_EBA175<sub>phospho</sub>GFP<sub>int</sub>. Both plasmids (pARL\_EBA175GFP<sub>int</sub> and pARL\_EBA175<sub>phospho</sub>GFP<sub>int</sub>, Figure 13B) were sequenced to ensure that the coding region of the eba175 fragment is in frame with the GFP and displays all desired amino acid exchanges in the absence of other mutations (data not shown).

The generated plasmids (pARL\_EBA175GFP<sub>int</sub> and pARL\_EBA175<sub>phospho</sub>GFP<sub>int</sub>) were transfected into the W2mef parasites. Integration of the plasmids occurs due to spontaneous homologous recombination. Using the selection drug WR99210 for *on/off cycles* the parasites were selected for integrands (see methods 2.3.5). Parasites with integrated plasmids could be proliferated and correct integration was confirmed via PCR with appropriate oligomers (Figure 14A), western blot and microscopy (Figure 3B-5). EBA175 has a theoretical molecular weight of 175 kDa and as a GFP fusion of about 202 kDa. Using anti-GFP and anti-EBA175 specific antibodies a single band can be detected running above 200 kDa (Figure 14B). In the parental W2mef cell line no GFP signal was detectable. As expected, the smaller wild type EBA175 protein migrates faster in the SDS-PAGE due to the lack of GFP.

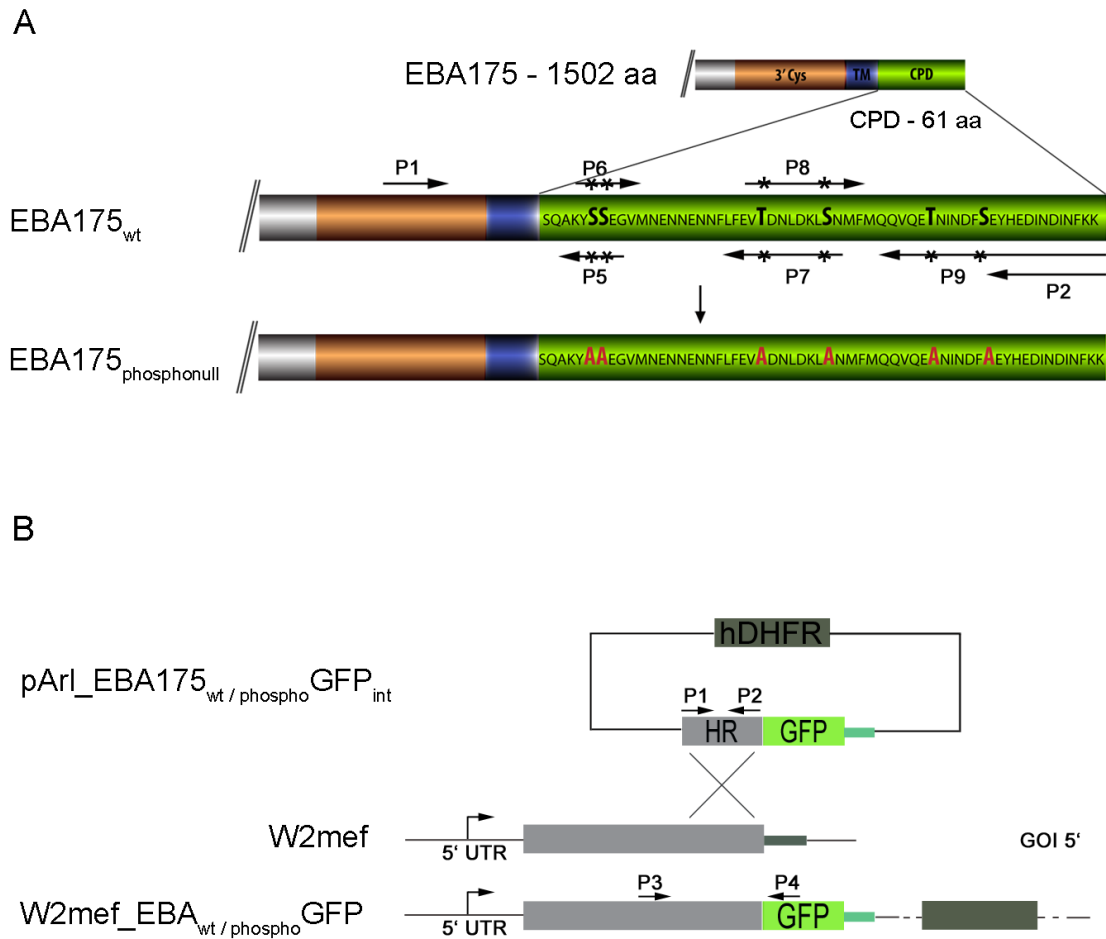


**Figure 13: Schematic representation of the PCR-based mutation strategy and integration of the plasmids into the endogenous *eba175* locus.** **A.** PCR strategy of the EBA175<sub>phospho</sub>GFP construct. Arrows indicate primers, asterisk indicate sequence mutations in the primer to introduce point mutations. The mutant sequence coding the multiple amino acid substitutions was generated stepwise as described above. (3' Cys, cysteine rich domain at the 3' end; TM, transmembrane domain; CPD, cytoplasmic domain). **B.** Schematic representation of the homologues recombination of pArl\_EBA175<sub>wt</sub>GFP and pArl\_EBA175<sub>phospho</sub>GFP into the endogenous *eba175* locus. Homology region, HR, is depicted as grey box. The pArl-vector also encodes the green fluorescent protein (GFP, green box) and the human dihydrofolate reductase (hDHFR, dark green box). The primer combination P1+P2 indicates amplification of the 0.8 / 0.67 kb-fragment that was cloned into the vector. P3+P4 represents the primer combination that was used to confirm correct integration of the plasmid.

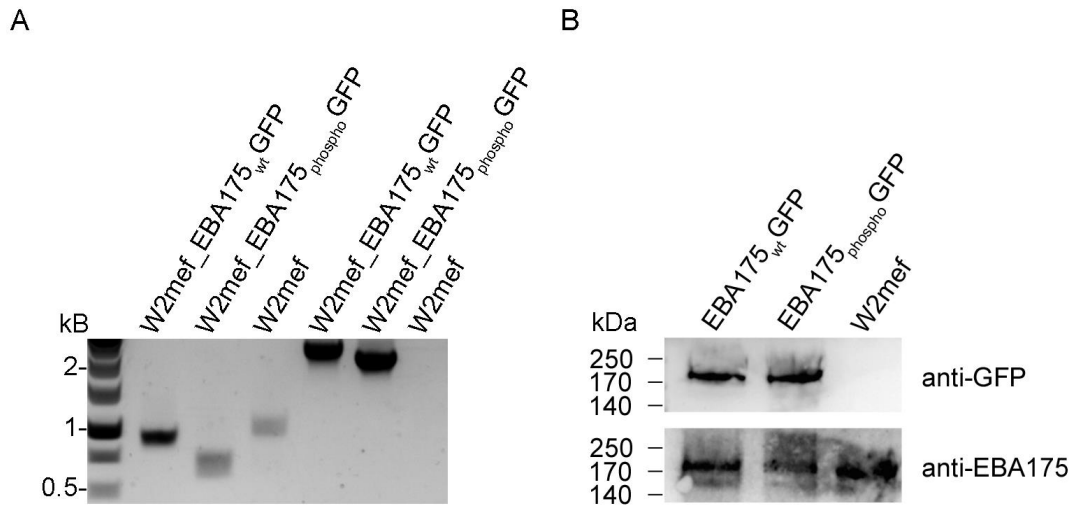


**Figure 14: Evidence for correct integration and expression of the EBA175 wild type and phospho-mutant.** **A.** PCR analysis of the specific integration of plasmids into the endogenous *eba175* locus. Primer combination P1+P2 (please refer to Fig. 1) amplified a 0.8 kb fragment in the transgenic as well as in the parental W2mef cell lines. The primer combination P3+P4 resulted in a 2.2 kb (2161 bp, wild type) and 2 kb (2036 bp, phospho-mutant) fragment in both transgenic cell lines but not in the parental W2mef cell line. **B.** Western blot analysis to confirm expression of the fusion proteins. Anti-GFP specific antibodies were used to detect the wild type- as well as the mutant-fusion protein at a size of about 200 kDa (calculated size: 202 kDa; upper panel). Anti-EBA175 specific antibodies were used as a loading control (lower panel).

### 3.1.2 Localization of EBA175<sub>wt</sub>GFP and EBA175<sub>phospho</sub>GFP

To date, EBA175 was never endogenously tagged with GFP. To assess if C-terminal GFP is interfering with micronemal localization of EBA175 the fusion protein was localized in unfixed and fixed W2mef parasites expressing EBA175<sub>wt</sub>GFP. Using unfixed parasites EBA175<sub>wt</sub>GFP expression could be detected at the apical pole in late schizonts as well as in free merozoites (Figure 15A), as previously reported (Orlandi et al., 1990; Sim et al., 1990; Sim et al., 1992). In early stages, such as trophozoites, no expression was detectable. Additionally, EBA175<sub>wt</sub>GFP was co-localized in glutaraldehyde-fixed parasites with the microneme protein EBA181. Both proteins co-localized (Pearson coefficient  $r=0.93$ ), which confirmed the expected micronemal localization of EBA175<sub>wt</sub>GFP (Figure 15B).



After having established correct localization of the wild-type EBA175<sub>wt</sub>GFP, the localization of the mutant EBA175<sub>phospho</sub>GFP was examined to test putative function of phosphorylation on microneme trafficking of EBA175. Like the wild-type protein, the GFP-fusion localized to the apical pole of merozoites and nascent parasites in the schizont stages (Figure 16A). Again, microneme localization was confirmed by co-localization with antibodies directed against EBA181 (Figure 16B, Pearson coefficient  $r=0.867$ ).

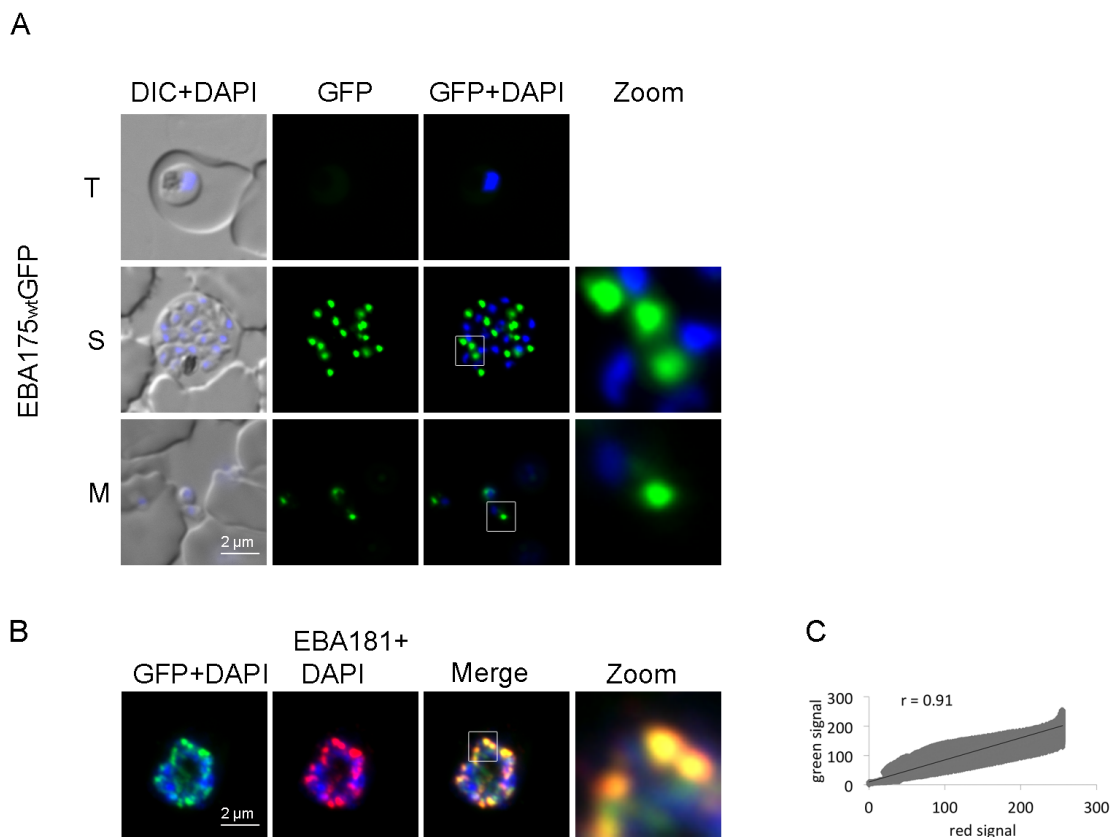


**Figure 15: Localization of EBA175<sub>wt</sub>GFP.** **A.** Localization of EBA175<sub>wt</sub>GFP (green) in unfixed parasites using fluorescence microscopy in trophozoites (T), schizonts (S), and free merozoites (M). Nuclei are stained with DAPI in blue. **B.** Co-localization of EBA175<sub>wt</sub>GFP with the microneme marker EBA181 (red) in fixed parasites. Nuclei are stained with DAPI (blue). 5x zoom area is indicated by a white box, scale bar 2  $\mu$ m. **C.** Co-localization was quantified by calculating the intensity correlation of the red and the green signals (x-/y-axis) within the zoom area (the average was calculated from five different areas). The Pearson coefficient ( $r$ ) is indicated in the scatter plot.

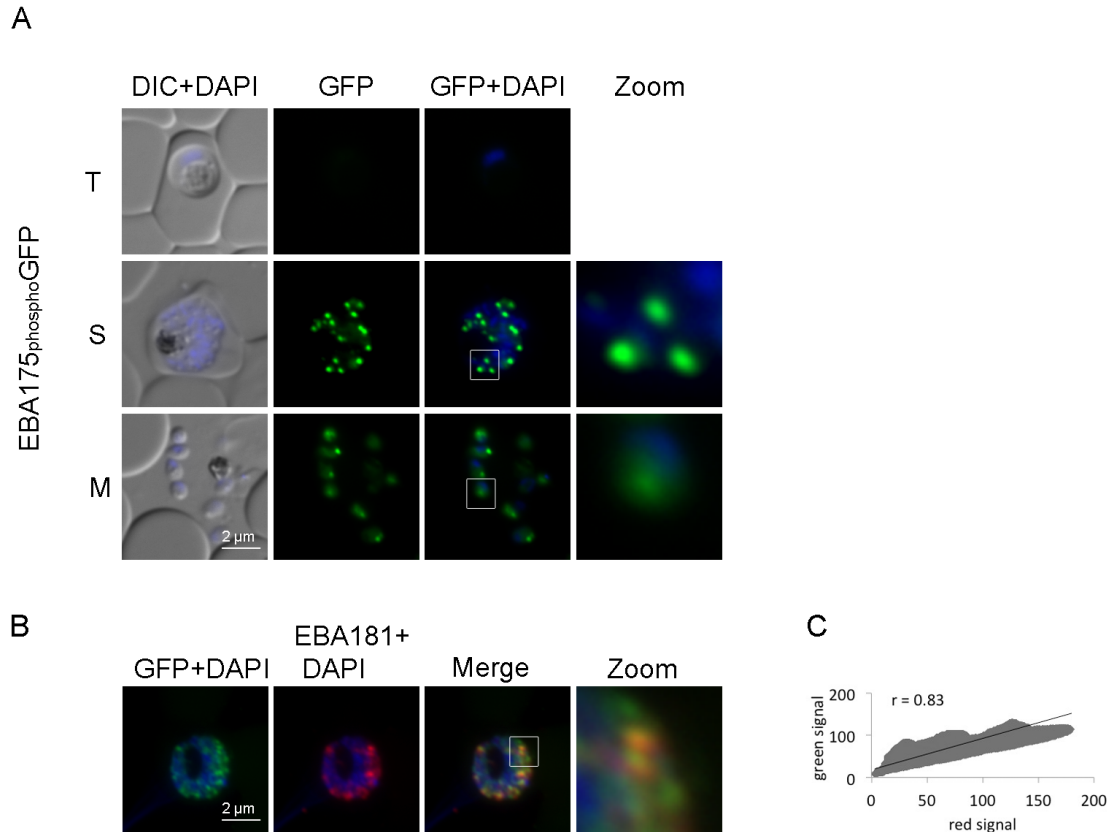


**Figure 16: Localization of EBA175<sub>phospho</sub>GFP.** **A.** Localization of EBA175<sub>phospho</sub>GFP (green) in unfixed parasites using fluorescence microscopy in trophozoites (T), schizonts (S), and free merozoites (M). Nuclei are stained with DAPI in blue. **B.** Co-localization of EBA175<sub>phospho</sub>GFP with the microneme marker EBA181 (red) in fixed parasites. Nuclei are stained with DAPI (blue). 5x zoom area is indicated by a white box, scale bar 2  $\mu$ m. **C.** Co-localization was quantified by calculating the intensity correlation of the red and the green signals (x-/y-axis) within the zoom area (the average was calculated from five different areas). The Pearson coefficient (r) is indicated in the scatter plot.

### 3.1.3 Functional analysis of EBA175<sub>wt</sub>GFP and EBA175<sub>phospho</sub>GFP

EBA175 is the major parasite ligand in the parasite strain W2mef and these parasites mainly rely on the EBA175-Glyphorin A interaction. Functional inactivation of EBA175 in this parasite line leads to a switch in the invasion pathway (Dolan et al., 1990; Reed et al., 2000; Stubbs et al., 2005). This switch can be measured by using erythrocytes treated with the glycoside hydrolase neuraminidase. Due to the enzymatic activity, these treated erythrocytes lack the terminal sialic acid moieties of the glycoprotein A, which is needed for the binding of EBA175. Therefore W2mef parasites cannot invade

neuraminidase treated erythrocytes – except EBA175 is not functional and the mutant parasites had switched to a different invasion pathway (see introduction 1.2.8).

First, to assess the influence of the GFP tag at the C-terminal end of EBA175 on the invasion phenotype, EBA175<sub>wt</sub>GFP along with parental W2mef and 3D7 parasites (as an additional control) were used in an 72h-invasion assay as described (see methods 2.2.5).

As expected, in the control cell line 3D7 there was no difference in parasitemia for treated or untreated erythrocytes. The parental W2mef cell line showed a clear reduction of 56.3% parasitemia with neuraminidase-treated RBCs (Figure 17A). This is lower than the previously published results, which show a reduction of invasion between 84% and 94% (Gilberger et al., 2003; Duraisingh et al., 2003; respectively), but a clear and reduction compared to the controls. Importantly, EBA175<sub>wt</sub>GFP expressing parasites showed, like the parental W2mef cell line, a similar reduction (52.8% vs. 56.3%; Figure 17A), revealing that the GFP-tag on EBA175 has no detrimental effect on EBA175 function. Hindered invasion was also seen in light microscopy showing free merozoites of W2mef and EBA175<sub>wt</sub>GFP that are not able to invade neuraminidase-treated erythrocytes (**Fehler! Verweisquelle konnte nicht gefunden werden.**B). This result validated the experimental set-up and allows the functional investigation of amino acids within the cytoplasmic domain of EBA175.

Second, the functional implication of the inserted point mutations – deleting 6 putative phosphorylation sites within the EBA175 cytoplasmic domain – was tested. Applying the same experimental set up in a 48h-invasion assay, EBA175<sub>phospho</sub>GFP proliferation in neuraminidase-treated erythrocytes was compared to EBA175<sub>wt</sub>GFP. With 80.3% (phospho-mutant) versus 76.68% (wild type parasites) reduced proliferation the mutant EBA175 shows no substantial change and is comparable with the parental W2mef cell line (84.27%), which was used as control (Figure 18A and B). Therefore, it can be concluded that none of the putative phosphorylation sites (S1448, S1449, T1466, S1473, T1483, S1489) are essential residues for EBA175 function.

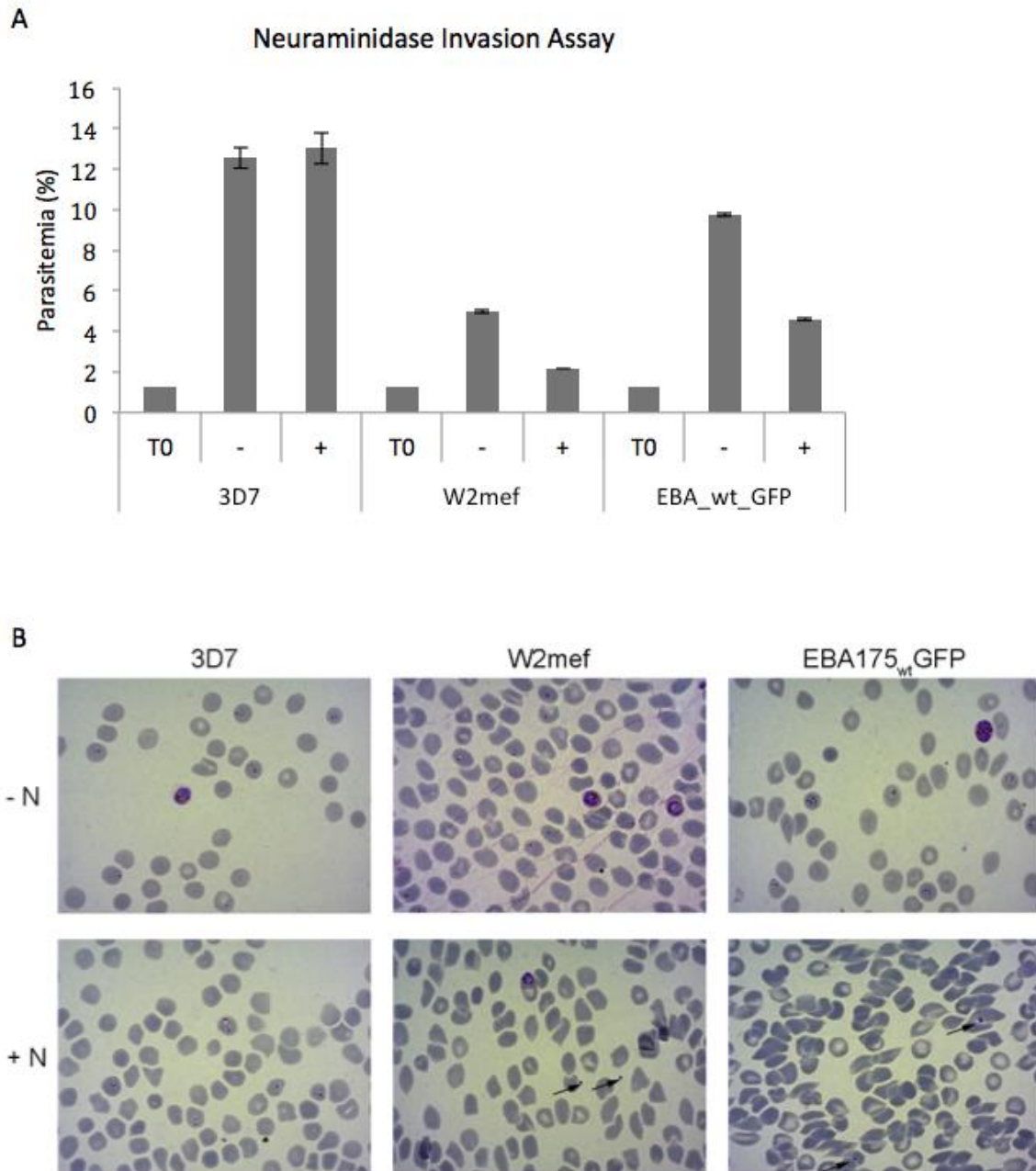


**Figure 17: Neuraminidase Invasion assay comparing parental 3D7, W2mef and transgenic W2mef-EBA175<sub>wt</sub>GFP parasitemia after 72 h. A.** Comparison of the parasitemia 72 hours after neuraminidase treatment. Start parasitemia (T0) was measured before neuraminidase treatment. Parasitemia shown is normalized to 3D7 control (1.24 % start parasitemia). 3D7 parasites show no reduction of proliferation in treated versus untreated parasites. W2mef parasites show a reduced parasitemia in the treated compared to untreated parasites after 72 hours of proliferation. A comparable reduction of parasitemia was observed for W2mef-EBA175<sub>wt</sub>GFP parasites. Error bars correspond to standard deviation. The data were obtained from two independent experiments that were performed in duplicates. **B.** Light microscopy of untreated (-N, upper panel) and treated (+N, lower panel) 3D7, W2mef and W2mef-EBA175<sub>wt</sub>GFP parasites 72 hours after treatment with neuraminidase. Arrows indicate not invading merozoites.

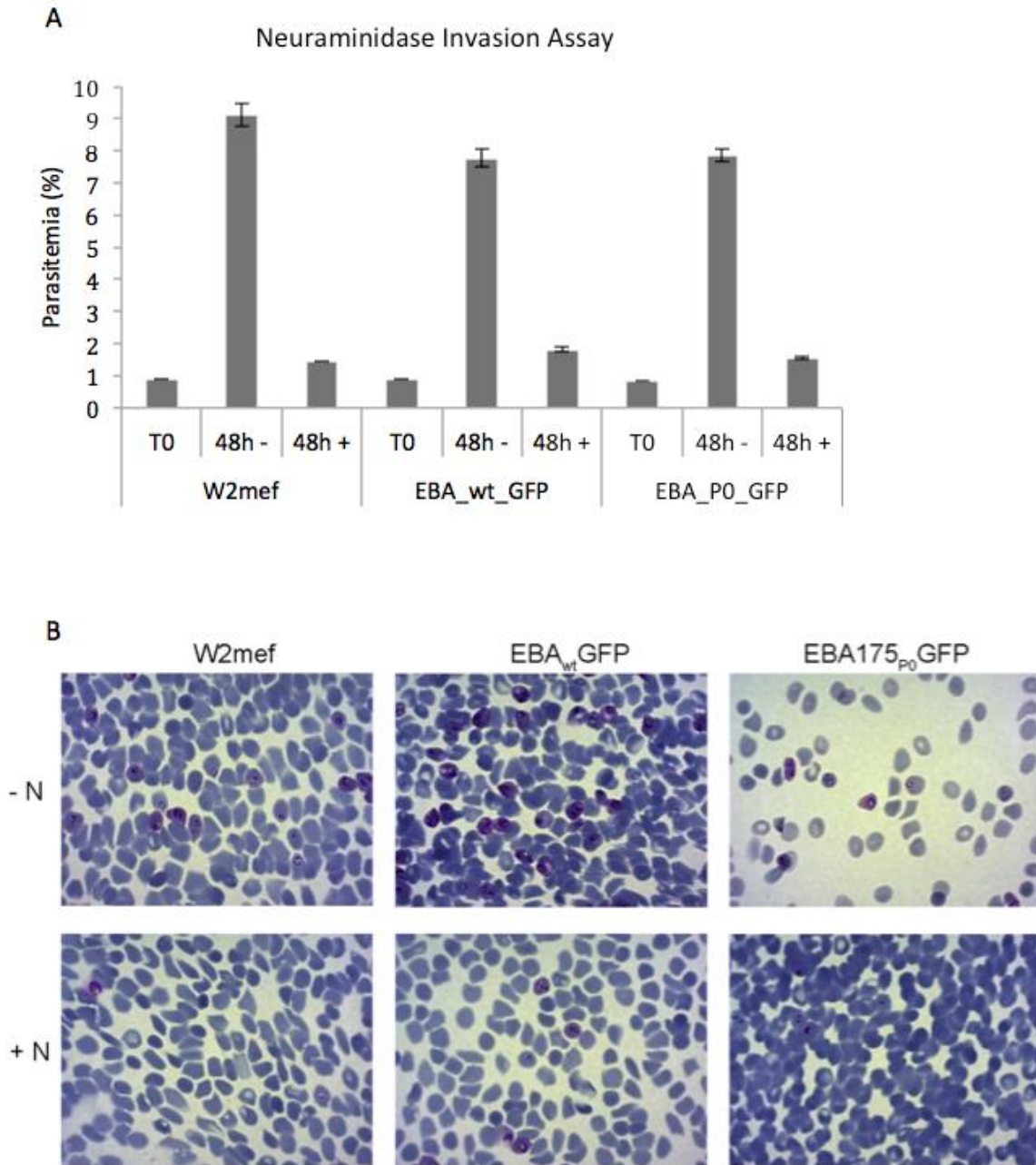


**Figure 18: Neuraminidase invasion assay comparing the parasitemia of parental W2mef, transgenic W2mef-EBA175<sub>wt</sub>GFP and -EBA175<sub>P0</sub>GFP parasites after 48 hours.** **A.** Comparison of the parasitemia 48 hours after neuraminidase treatment. Start parasitemia (T0) was measured before neuraminidase treatment and set to 0.8 %. The parental W2mef cell line was used as control. The neuraminidase treated samples show a significantly reduced parasitemia (48 h +, 1.435 %) compared to the untreated samples (48 h -, 9.12 %). The same was observed for W2mef-EBA<sub>wt</sub>GFP parasites (7.76 % in untreated (48h-), versus 1.81 % in neuraminidase treated samples (48h+)). The phospho-mutant (W2mef-EBA<sub>P0</sub>GFP) cell line displayed a comparable reduction of invasion (untreated (48h-), 7.87 % parasitemia; 48h+, 1.55 % parasitemia). Error bars correspond to standard deviation. The data were obtained from two independent experiments that were performed in duplicates. **B.** Light microscopy of untreated (-N, upper panel) and treated (+N, lower panel) parental W2mef, W2mef-EBA175<sub>wt</sub>GFP and W2mef-EBA175<sub>P0</sub>GFP parasites 48 hours after treatment with neuraminidase.

### 3.2 Bioinformatic screen for novel, secreted proteins implicated in erythrocyte invasion

To expand the list of secreted proteins playing a role in invasion we searched for novel candidates using published data sets and initiated their experimental validation. Two criteria were defined as essential:

- The presence of a predicted signal peptide (SP)
- A late expression profile, similar to well established and documented invasins and adhesins such as EBA175, Rh2b or AMA1 (Camus and Hadley, 1985; Orlandi et al., 1990; Duraisingh et al., 2003; Srinivasa et al., 2011).

The expression profiles of these genes and 11 others (RopH3, SERA5, RH5, EBA181, MSP7, MTRAP, EBL1, RH4, MSP1, RAP2, and MSP9) are depicted in Figure 19A. These genes were used as a control group to validate the individual output data sets. To identify putative candidates following data sets and parameters were used ([www.plasmodb.org](http://www.plasmodb.org)):

#### I. Microarray evidence:

- 3D7 life cycle expression data, Le Roch et al. (2003) : using data from temperature synchronized parasites from late rings to schizont stages and merozoites provided a list of 113 genes.
- 3D7 expression data during the erythrocytic stage, Bozdech and Llinas et al. (2003): a minimum expression at 16 h +/- 8 h and a maximum expression at 42 h +/- 6 h provided 132 hits.

Combining both data sets resulted in a list of 164 genes. Both output data sets contained the complete group of control genes (Figure 19B).

II. RNA sequencing evidence based on data from the transcriptome during intraerythrocytic development published by Bartfai et al. (2010). Settings: minimum

transcription: 25 hpi; maximum transcription: 40 hpi. These settings provided a list of 243 genes, which was also validated by the control group (Figure 19B).

Combining the data sets resulted in a preliminary list of 287 candidates. Already characterized genes were excluded, which resulted in a list of 156 putative candidates or candidates of unknown function that were not characterized in *P.falciparum* (at the time of analysis). Out of these 38 candidates were chosen for further analysis. A schematic description of the search strategy is depicted in Figure 19B. Table 1 provides a list of all 38 candidates.

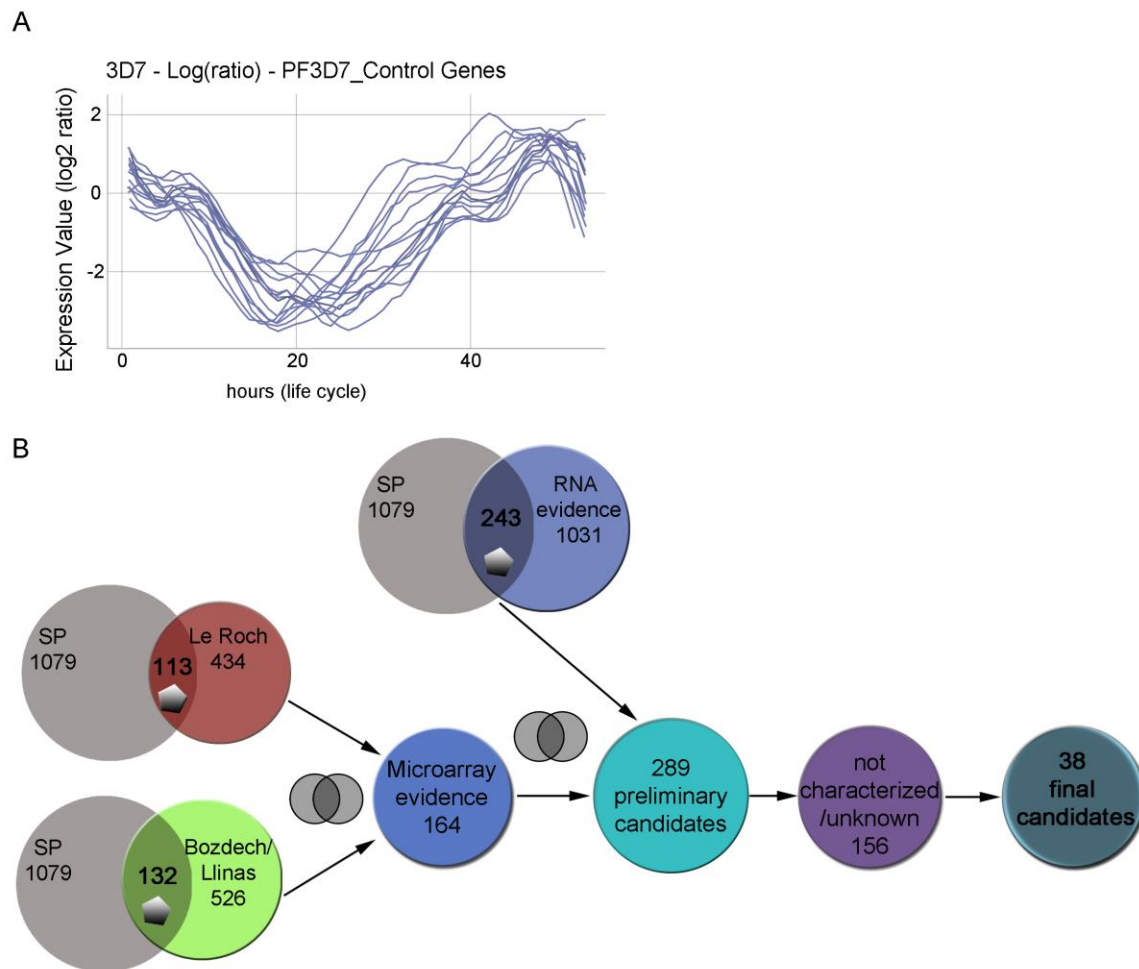


**Figure 19: Schematic description of the search strategy for novel invasion associated candidates and expression profiles. A.** Expression values of the control genes. Expression values (log<sub>2</sub> ratio) of 13 selected control genes representing the common profiles of late transcribed genes known to be implicated in invasion (RopH3, EBA175, SERA5,

RH5, EBA181, AMA1, MSP7, MTRAP, EBL1, RH4, MSP1, RAP2, and MSP9). All of the representatives show an upregulation in late stages during the parasite blood cycle. Expression values are available on PlasmoDB (PlasmoDB.org). Represented expression profiles are solely based on micro array analysis published by Bozdech et al. (2003) and Llinás et al. (2006). **B.** Schematic representation of the search strategy. The final candidate list was obtained from different data sets. I. Two studies were chosen for microarray evidence: 1. Le Roch et al. (2003) (434 hits, out of which 113 contained a predicted SP) and 2. Bozdech et al., and Llinas et al. (2003 and 2006, respectively) (526 genes in total with 132 containing a predicted SP). Genes containing a SP were pooled, resulting in a list of 164 hits. II. RNA evidence was obtained from Bartfai et al. (2010) (1031 genes, 243 comprise a predicted SP). All control genes were covered by the chosen criteria (gradient pentagon). Both data sets were pooled, already characterized genes were excluded and a final list of 38 candidates was selected for further experimental validation. Gradient pentagon: set of control genes; interlocked grey rings: union of output data; SP: signal peptide.

### 3.2.1 Experimental validation of candidate genes

#### 3.2.1.1 3'GFP-tagging of 38 candidate genes

To investigate the expression and localization of the 38 candidate genes we initiated their endogenous tagging with the green fluorescent protein (GFP). The 3' end of the genes was cloned into the pSLI-GFP vector system (Birnbaum and Flemming et al., 2017), which allows endogenous GFP-tagging using selection-linked integration (SLI). This innovative method allows fast integration into the genome via neomycin-dependent selection (Figure 20, and methods 2.3.4).

Gene specific oligonucleotides that were used for the cloning are listed in the appendix. 3D7 parasites were transfected with the 38 generated gene specific pSLI-GFP plasmids and first selected on WR99210. Next, parasites were selected for integrated pSLI plasmid via neomycin selection. Despite using a very reliable and effective integration method it was not possible to endogenously tag all candidates with GFP. For 2 pSLI constructs no parasites were re-obtained after neomycin selection and 7 pSLI constructs could not be integrated correctly into the endogenous locus even after 6 to 9 independent attempts using neomycin selection (Figure 22A). The remaining stable transgenic cell lines were further analysed. Correct, gene specific integration and 3'GFP-tagging of the targeted candidate was confirmed by PCR analysis. Appropriate oligonucleotides were used as indicated in Figure 20. Correct integration of the pSLI plasmid could be shown for 29 candidate genes (Figure 21).



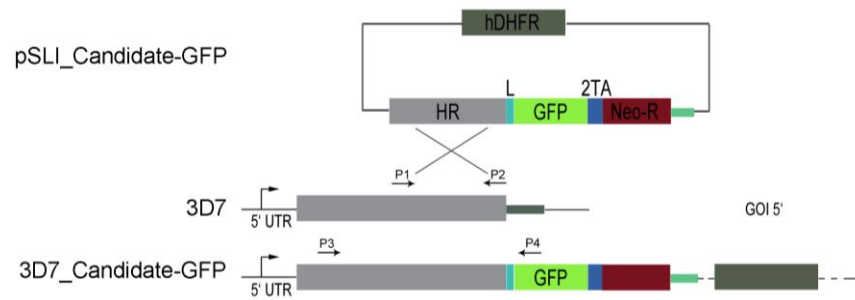


**Figure 20: Schematic description of the integration strategy for novel invasion associated candidates.** Representation of the homologue recombination of candidate genes into the endogenous locus (homology region, HR, grey box). The SLI vector also encodes additional open reading frame (ORF) coding for i) a linker (L, light blue box), separating the gene fragment from the ORF coding for the green fluorescent protein (GFP, light green box), ii) a skip peptide (2TA, dark blue box) leading to skipping of translation, iii) neomycin phosphotransferase II gene (Neo-R, red box), and human dehydrofolate reductase (hDHFR, dark green box). Two gene specific oligonucleotide pairs were designed in order to 1) amplify a 3' fragment in the parental as well as in the transgenic cell line (P1+P2) and 2) amplify a fragment only if the pSLI vector is correctly integrated (P3+P4, sequences of all oligonucleotides are listed in tab. Xx in the appendix). Primer combination P1+P2 indicates amplification of the fragment that was cloned into the vector. Primer combination P3+P4 was used to confirm correct integration, indicated by straight arrows. Flexed arrows indicate the endogenous promoter. (Adapted from Birnbaum and Flemming et al., 2017).

## Results

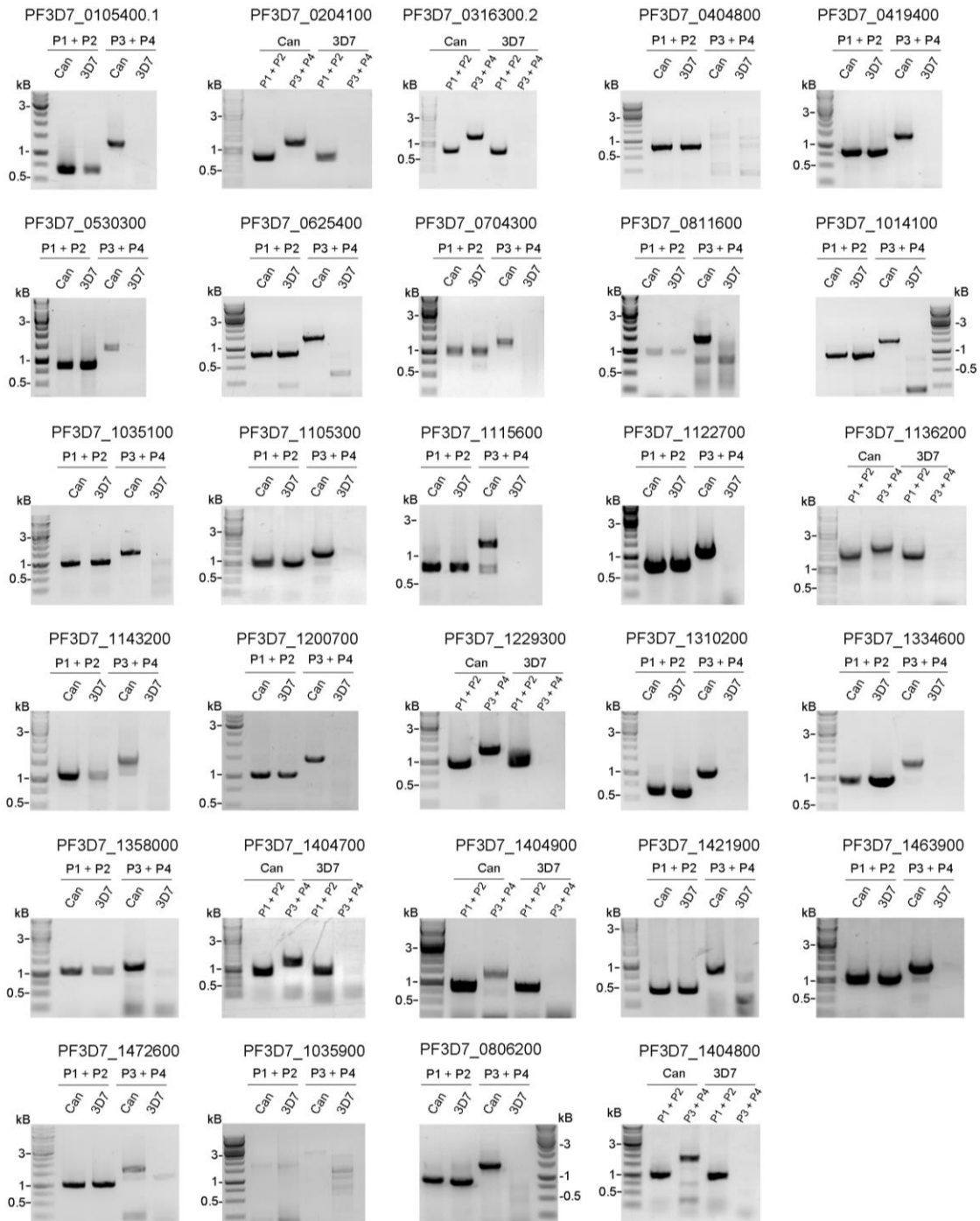


**Figure 21: PCR analysis of correctly integrated candidates.** P1+P2: oligonucleotide pair that was used for amplification of the gene specific fragment. P3+P4: oligonucleotide pair that was used for amplification of a fragment after correct integration of the pSLI vector into the appropriate gene locus. P4 was designed to bind the 5' region of the GFP-tag. The oligonucleotides that were used are schematically depicted in **Figure 20** and sequences of all primers that were used are listed in the appendix.

### 3.2.2 Candidate expression and localization

First, expression and localization of the GFP fusion proteins within the 29 transgenic cell lines were investigated in live parasites using fluorescence microscopy. Depending on expression level and putative cellular localization the candidates were subdivided into the following 5 categories: proteins with 1) surface localization, 2) inner membrane or basal complex localization, 3) apical localization, 4) other localization, and 5) proteins with low or no detectable GFP signal.

Four candidates could be localized to the surface, two candidates to the inner membrane complex or the basal complex (IMC/BC), and nine candidates localized to the apical organelles (Figure 22B and C). An overview of annotation and localization for all candidates is provided in Table 1. In the following section the different candidate groups will be introduced in detail. A symbolic description of candidate localization of group 1, 2 and 3 is provided in Figure 22C.

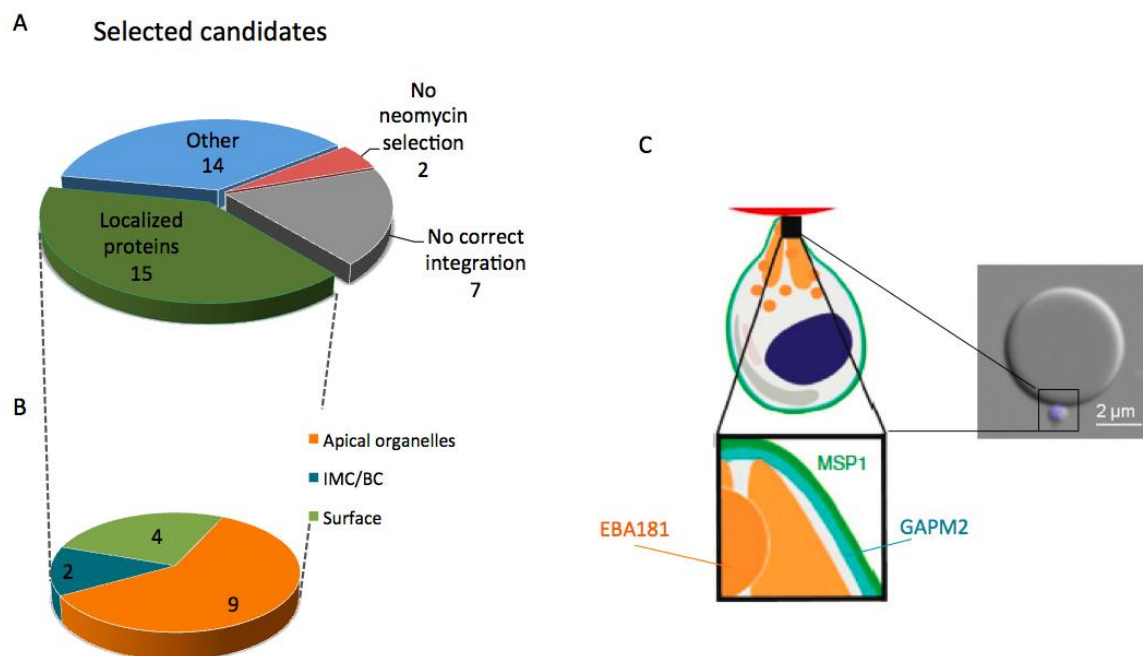


**Figure 22: Representation of selected and localized Candidates.** **A.** Out of a total of 38 candidates 15 GFP-fusion proteins could be localized to invasion related organelles (referred to as “localized proteins”, green), 14 proteins were identified in other localizations or could not be determined due to low expression (grouped as “other”, blue), 7 candidate genes could not be integrated using the SLI method (red), and for 2 pSLI plasmids no parasites were obtained on neomycin selection. **B.** Sectioning of candidate localization to the different organelles. Six candidates could be shown to localize to apical organelles (orange), three candidates referred to the IMC or BC (blue), and three

candidates displayed a surface localization (depicted in green). **C.** Schematic representation and microscopy of a free and invasive merozoite, attaching to the erythrocyte membrane. Apical organelles are depicted in orange, IMC in turquoise, the surface is colored in green. Examples for common compartment specific marker proteins are provided in corresponding colours (processed from Hu et al., 2009). Nucleus is stained with DAPI in blue, scale bar 2  $\mu$ m.

Gene ID	Annotation	Localization
PF3D7_1136200	conserved Plasmodium protein, unknown function	surface
PF3D7_1143200	DnaJ protein, putative	surface
PF3D7_1229300	conserved Plasmodium protein, unknown function	surface
PF3D7_1421900	copper transporter, putative	surface
PF3D7_0530300	conserved Plasmodium membrane protein, unknown function	IMC/BC
PF3D7_0704300	conserved Plasmodium membrane protein, unknown function	IMC/BC
PF3D7_0105400.1	conserved Plasmodium protein, unknown function	apical
PF3D7_0811600	conserved Plasmodium protein, unknown function	apical
PF3D7_1014100	merozoite surface protein MSA180, putative	apical
PF3D7_1115600	peptidyl-prolyl cis-trans isomerase (CYP19B)	apical
PF3D7_1310200	conserved Plasmodium protein, unknown function	apical
PF3D7_1404700	conserved Plasmodium protein, unknown function	apical
PF3D7_1404900	conserved Plasmodium protein, unknown function	apical
PF3D7_1463900	conserved Plasmodium membrane protein, unknown function	apical
PF3D7_1035900	probable protein, unknown function(M566)	apical
PF3D7_0204100	conserved Plasmodium protein, unknown function	low expression
PF3D7_0316300.2	inorganic pyrophosphatase, putative	cytosolic
PF3D7_0404800	conserved Plasmodium protein, unknown function	cytosolic
PF3D7_0419400	conserved Plasmodium protein, unknown function	cytosolic
PF3D7_0625400	conserved Plasmodium protein, unknown function	exported/ cytosolic
PF3D7_0806200	C-mannosyltransferase, putative	under progress
PF3D7_1035100	probable protein, unknown function	low expression
PF3D7_1105300	conserved Plasmodium protein, unknown function	PV
PF3D7_1122700	conserved Plasmodium protein, unknown function	low expression
PF3D7_1200700	acyl-CoA synthetase (ACS7)	Low expression
PF3D7_1334600	MSP7-like protein (MSRP3)	PV
PF3D7_1358000	patatin-like phospholipase, putative	low expression
PF3D7_1404800	conserved Plasmodium protein, unknown function	low expression
PF3D7_1472600	protein disulfide-isomerase (PDI-14)	PV
PF3D7_0210800	conserved Plasmodium protein, unknown function	N.I.
PF3D7_0410700	Ribosome biogenesis GTPase A, putative	no selection
PF3D7_0423300	conserved Plasmodium protein, unknown function	N.I.
PF3D7_0716300	conserved Plasmodium protein, unknown function	N.I.
PF3D7_0721100	conserved Plasmodium protein, unknown function	N.I.
PF3D7_0725400	conserved Plasmodium protein, unknown function	N.I.
PF3D7_0730800.1	Plasmodium exported protein, unknown functions	N.I.
PF3D7_1030200	conserved Plasmodium protein, unknown function	no selection
PF3D7_1352500	thioredoxin-related protein, putative	N.I.

**Table 1: Localized candidates.** Colour code refers to localization of the proteins: surface localization: turquoise, IMC/BC localization: green, apical localization: orange, other localization: dark grey. Shading in light grey refers to candidates that could not be integrated via SLI: N.I., no correct integration upon neomycin selection could be achieved; no selection: no parasites were obtained upon neomycin selection.

### Group 1: Candidates with a surface localization

Surface located proteins such as MSP1 are involved in primary contact formation of the parasite to red blood cells, which is essential to initiate the invasion process and therefore crucial for parasite survival (Tanabe et al., 1987). Among the 15 putative hits the search for novel invasion related candidates revealed four surface located proteins. A schematic representation of surface localization is depicted in Figure 23.

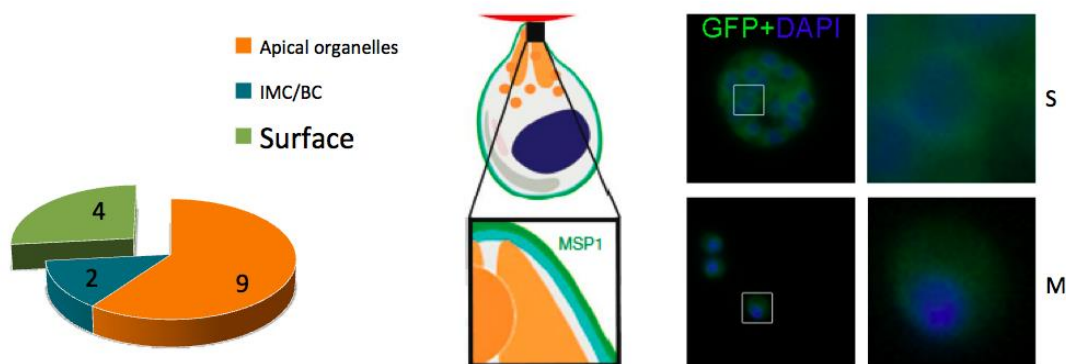


**Figure 23: Schematic representation of surface localized proteins in late schizonts and free merozoites.** Four out of 15 candidates were identified to localize to the surface (left panel). MSP1 is given as representative surface specific marker in green (schematic, middle panel; processed from Hu et al., 2010); right panel: exemplary GFP-tagged surface protein in green in schizonts (S, upper panel) and free merozoites (M, lower panel), nuclei are stained with DAPI in blue, 5x zoom area is indicated with a white box.

**Candidate PF3D7\_1136200** is a conserved *Plasmodium* protein of unknown function. RNA seq as well as microarray data report slightly increased expression values in late schizont stages. The protein of 679 aa does not comprise any transmembrane domains (Figure 24A). Correct integration leading to a GFP fusion protein was confirmed by PCR (P1+P2, 1615 bp; P3+P4, 2032 bp; Figure 21). Performing fluorescence microscopy the GFP signal of the fusion protein a surface-like staining was detectable starting in late schizonts until merozoites were released from the blood cell (Figure 24B, middle and lower panel). In trophozoites no fluorescence signal was detectable (Figure 24B, upper panel). This observation suggests candidate PF3D7\_1136200 as a novel surface protein.

Expression was also investigated by western blot analysis. Using GFP-specific antibodies the fusion protein was detected at approximately 120 kDa (Figure 24C), which is a bit higher than expected (103.6 kDa). This might result from post-translational modification such as phosphorylation.

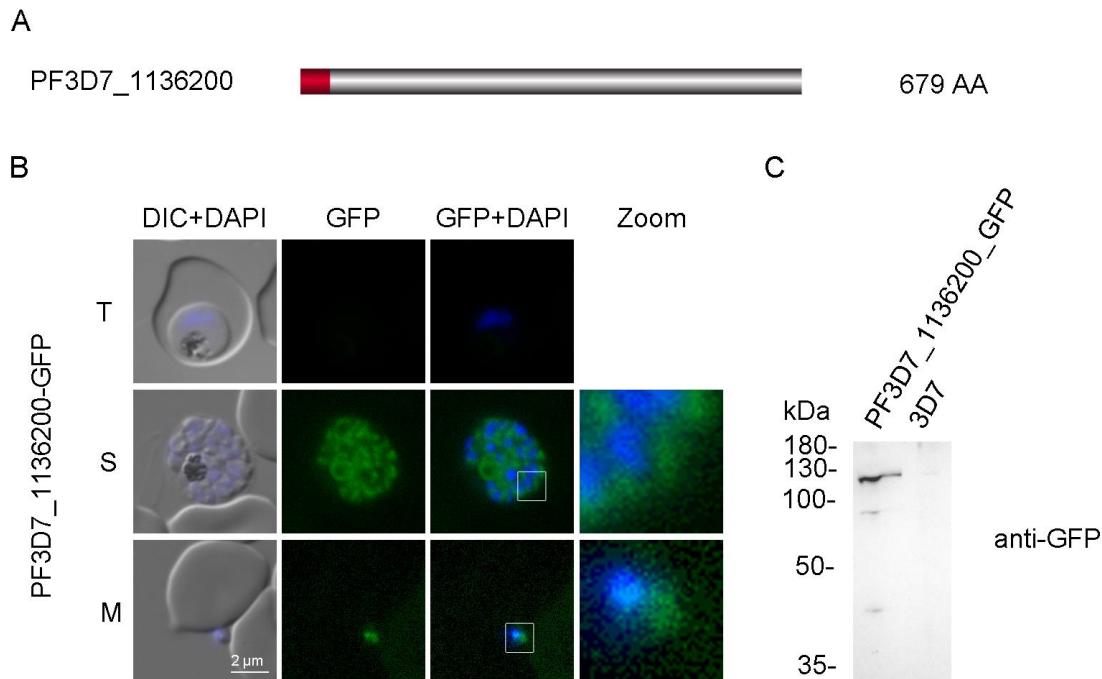


**Figure 24: Analysis of PF3D7\_1136200 localization.** **A.** Schematic protein structure of PF3D7\_1136200. Protein length, 679 aa; signal peptide, red box. **B.** Localization of 1136200-GFP (green) via fluorescence microscopy of unfixed parasites in trophozoites (T), schizonts (S) and free merozoites (M). Nuclei are stained with DAPI in blue, 5x zoom area is indicated with a white box, scale bar 2  $\mu$ m. **C.** Western blot analysis of PF3D7\_1136200-GFP. GFP specific antibodies were used to detect the fusion protein at 120 kDa (expected size 103.6 kDa).

**Candidate PF3D7\_1143200** is an annotated, putative DnaJ protein (Hiller et al., 2004; LaCount et al., 2005). It comprises two transmembrane domains spanning aa 110-132 and 11 203-225 (depicted in Figure 25A) as well as a predicted DnaJ DnaJ domain (not depicted). Transcriptomic data provide a profile with transcriptional up-regulation in late stages starting at around 38 hours post infection (hpi). This was confirmed by microarray as well as RNA evidence. Correct integration was confirmed by PCR analysis (P1+P2, 1118 bp; P3+P4, 1655 bp; Figure 21). Late expression was determined by

fluorescence microscopy. As expected no signal was detected in early stages (Figure 25, upper panel, trophozoites) but a clear signal was visual in late schizonts (S) and free merozoites (M; Figure 25B, middle and lower panel, respectively). Fluorescence microscopy revealed a surface-like localization of PF3D7\_1143200-GFP. Expression of the fusion protein was confirmed by western blot analysis. Using GFP specific antibodies a protein of approximately 70 kDa (predicted size 66.36 kDa) was visualized (Figure 25C). The second band might result from processing of the fusion protein.

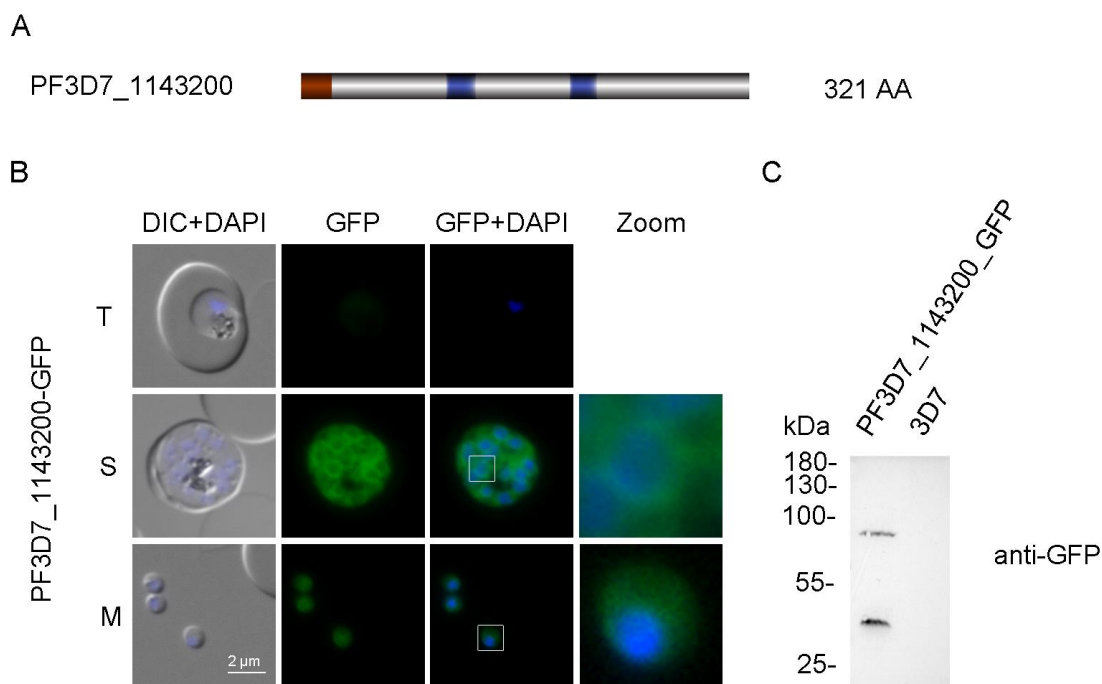


**Figure 25: Analysis of PF3D7\_1143200 localization.** **A.** Schematic protein structure of PF3D7\_1143200. The signal peptide (SP) is depicted as a red box, transmembrane domains (TM) are indicated as blue boxes. **B.** Localization of 1143200-GFP (green) in unfixed parasites using fluorescence microscopy in trophozoites (T), schizonts (S) and free merozoites (M). Nuclei are stained with DAPI in blue. 5x zoom area is indicated by a white box, scale bar 2  $\mu$ m. **C.** Western Blot analysis of late stage 3D7\_1143200-GFP parasite material was performed to confirm protein expression. The GFP fusion protein was detected with an anti-GFP antibody at the expected size of about 70 kDa (calculated 66.36 kDa, upper panel). Material from parental 3D7 parasites was used as a control.

**Candidate PF3D7\_1229300** is a 990 aa protein of unknown function, which is conserved among *Plasmodium*. Its C-terminus comprises one predicted transmembrane domain spanning aa 891-913 (Figure 26A). Transcriptomics provide a minimum expression value

at around 15 hpi and maximum expression at around 40 hpi. Correct integration of the generated pSLI-1229300-GFP vector was verified by PCR analysis (P1+P2, 1022 bp; P3+P4, 1489 bp; Figure 21). Stage specific expression and localization was determined by fluorescence microscopy. No fluorescence signal was obtained in trophozoites (T; Figure 26B, upper panel). In schizonts (S) an slightly cytosolic and surface-like signal emerged around the nascent daughter cells and was still detectable on the surface of free merozoites (M; Figure 26B, middle and lower panel, respectively). This observation suggests PF3D7\_1229300 as a novel surface protein. Expression of the endogenously tagged protein was further determined by western blot analysis using anti-GFP specific antibodies (predicted size: 144.4 kDa; Figure 26C). Parental 3D7 served as control for antibody specificity of anti-GFP.

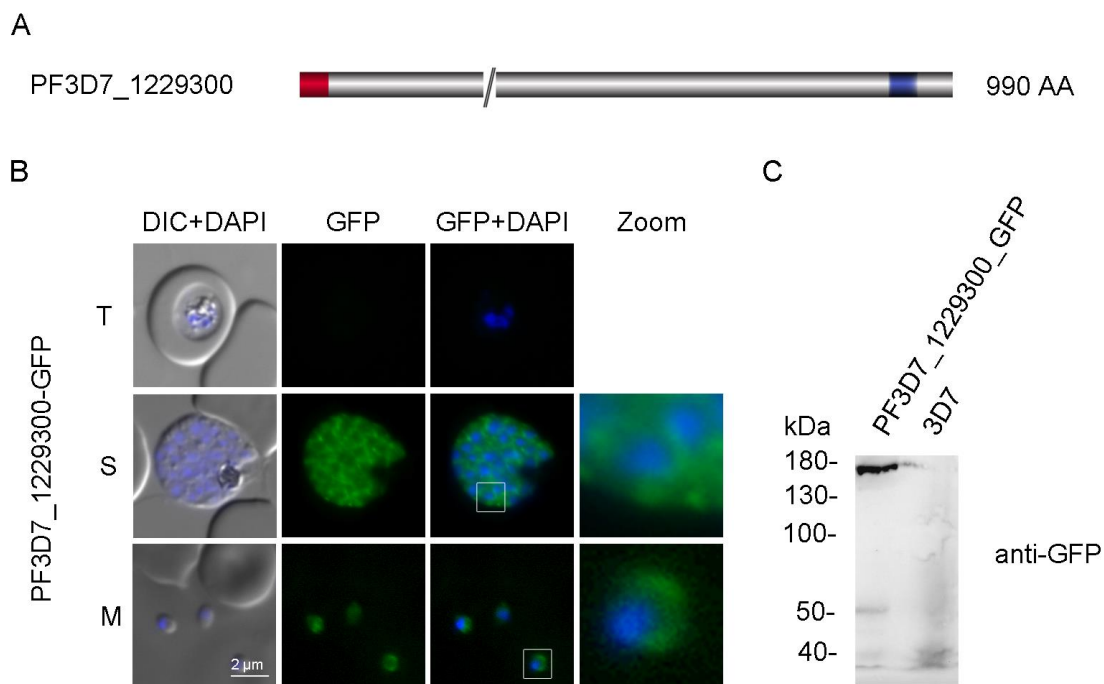


**Figure 26: Analysis of PF3D7\_1229300 localization.** **A.** Schematic protein structure of PF3D7\_1229300. 298 aa; SP, red box; TM, blue box; “//”, part of the protein that is not depicted here. **B.** Localization studies of 1229300-GFP (green) in unfixed parasites via fluorescence microscopy in trophozoites (T), schizonts (S) and free merozoites (M). Nuclei are stained with DAPI in blue. **C.** Western blot analysis of 3D7\_1229300-GFP using GFP specific antibodies and parental 3D7 as control. Calculated size: 144.4 kDa.



**Candidate PF3D7\_1421900** is annotated as putative copper transporter (CTR2) (Kenthirapalan et al., 2016; Zuegge et al., 2001). The gene encodes for a protein of 160 aa, which comprises 3 TMs spanning 64-86 aa, 114-136 aa, and 140-159 aa (Figure 27A). Transcription data confirm a late, but weak up-regulation of expression during late schizogony. Correct integration into the genomic locus was certified by PCR analysis (P1+P2, 508 bp; P3+P4, 943 bp; Figure 21). Fluorescence microscopy revealed a cytosolic and surface-like localization of the GFP-fusion protein in schizonts, which was still visible in free merozoites. This suggests PF3D7\_1421900 as a surface protein (Figure 27B).

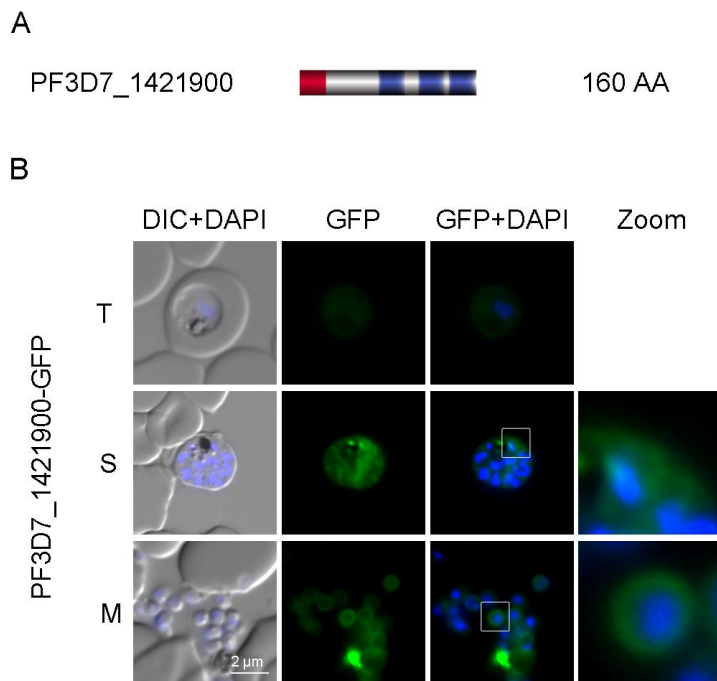


**Figure 27: Analysis of PF3D7\_1421900-GFP localization.** **A.** Schematic protein structure of PF3D7\_1421900. Protein length, 160 aa; SP, red box; TM, blue box. **B.** Localization of 1421900-GFP (green) in unfixed parasites by fluorescence microscopy in trophozoites (T), schizonts (S) and merozoites (M). Nuclei are stained with DAPI (blue), nuclei are stained with DAPI (blue), scale bar 2  $\mu$ m.

### Group 2: Candidates localizing to the inner membrane complex and basal complex

The inner membrane complex (IMC) is a unifying and common feature of all Alveolata (Cavalier-Smith, 1993). Three candidates were found to localize to the IMC or the BC, which are involved in motility and cytokinesis. Further, the IMC drives the morphological changes of the parasite during sexual differentiation (Meszoely et al., 1987; Kono et al., 2012). It emerges as cramp-like structures (in T1 stages) to expand during schizogony and finally completely surrounds the nascent daughter cells (T3, Figure 28).

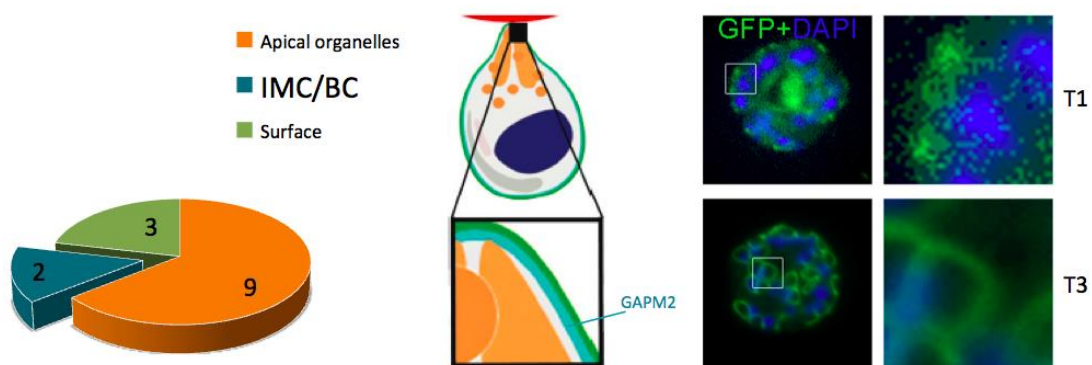


**Figure 28: Schematic representation of IMC or BC localized proteins in T1 and T3 phase of late schizonts.** Two candidates were identified to localize to the inner membrane complex (IMC) or to the basal complex (BC, left panel). GAPM2 is illustrated as representative IMC specific marker in turquoise (schematic, processed from Hu et al., 2010), exemplary GFP-tagged surface candidates are depicted in the right panel in green, T1 and T3, nuclei are stained with DAPI in blue, 5x zoom area is indicated with a white box.

**Candidate PF3D7\_0530300** is a 1446 aa long protein. It is a conserved *Plasmodium* membrane protein of unknown function displaying 10 predicted TMs (aa 89-111, 779-801, 852-874, 884-906, 1254-1276, 1296-1318, 1325-1344, 1354-1376, 1389-1411, and 1421-1440; Figure 29A). Transcriptomic data provide an expression profile with a minimum expression at around 20 hpi and a maximum in during schizogony around 40-48 hpi. Correct integration into the genomic locus was verified by PCR analysis (P1+P2, 884 bp; P3+P4, 1387 bp; Figure 21). Fluorescence microscopy determined late expression as no GFP signal was obtainable in early stages but became visible in

schizonts and free merozoites (Figure 29B). The localization was further examined by stage specific fluorescence microscopy (data not shown). The detected signal suggests an IMC-like localization for candidate PF3D7\_0530300. Expression of the fusion protein was further validated by western blot analysis. Using GFP specific antibodies the protein was detected at the expected size of 200 kDa (Figure 29C).

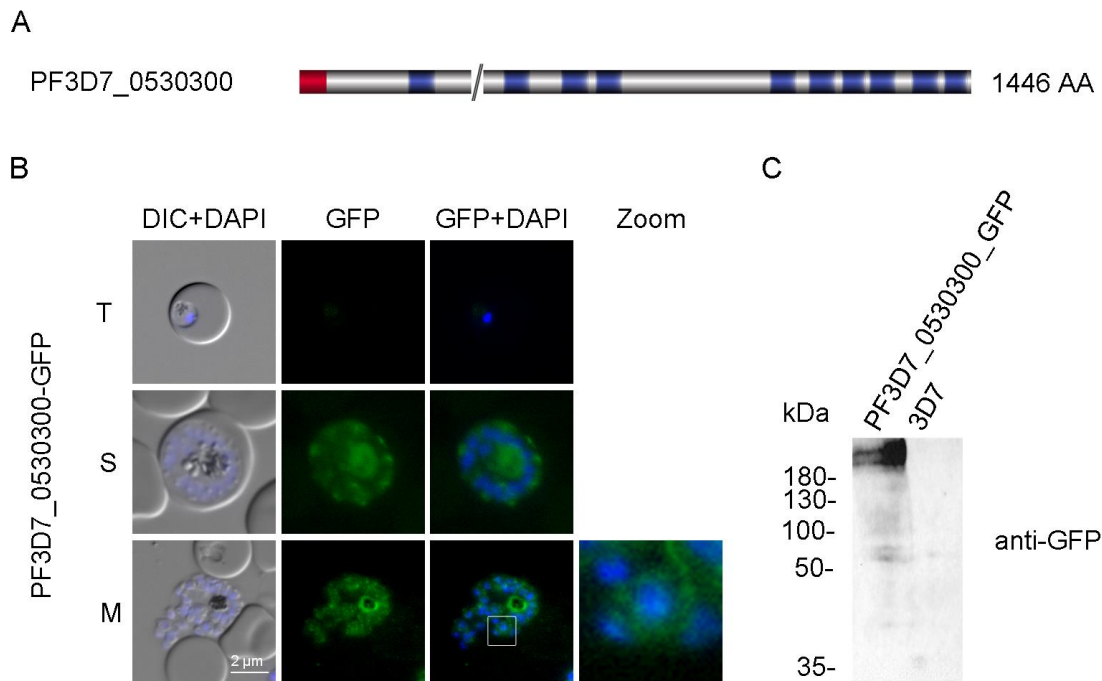


**Figure 29: Analysis of PF3D7\_0530300 localization.** **A.** Schematic presentation of the protein structure of PF3D7\_0530300. Protein length, 1446 aa; SP, red box; TM, blue boxes; “//” indicates part of the protein structure that is not depicted here to shorten the schematic structure. **B.** Fluorescence microscopy of 0530300-GFP (green) in unfixed parasites in trophozoites stages (T, upper panel), schizont stages (S, middle panel) and free merozoites (M, lower panel). DAPI staining of nuclei in blue, 5x zoom is indicated by a white square, scale bar 2  $\mu$ m. **C.** Western blot analysis of PF3D7\_0530300-GFP. Using GFP specific antibodies the protein was detected at the expected size (calculated 200.3 kDa) in the transgenic but not the parental 3D7 cell line.

**Candidate PF3D7\_0704300** is a conserved *Plasmodium* membrane protein of unknown function. The gene encodes for 1852 aa comprising three predicted transmembrane domains in close proximity to its N-terminal signal peptide (aa 52-74, 78-100, and 112-134; Figure 30A). An expression minimum is reported at around 12-15 hpi. The maximum expression value was reported during schizogony at around 40-48 hpi, which

was confirmed by microarray as well as RNA evidence. PCR analysis confirmed correct integration of the pSLI\_0704300-GFP plasmid into the endogenous locus (P1+P2, 1069; P3+P4, 1483; Figure 21). Using fluorescence microscopy no fluorescence signal was obtained in early stages until trophozoites (T, Figure 30B, upper panel). Ring-like structures were detectable in late schizonts (S, Figure 30B, middle panel) marking a ring-like structure. In free merozoites the GFP signal was not visible anymore except for a GFP signal in close proximity to the food vacuole (M, Figure 30B, lower panel). During schizogony this structure was observed to move from the apical to the basal pole (not shown) suggesting a BC-associated localization for PF3D7\_0704300.

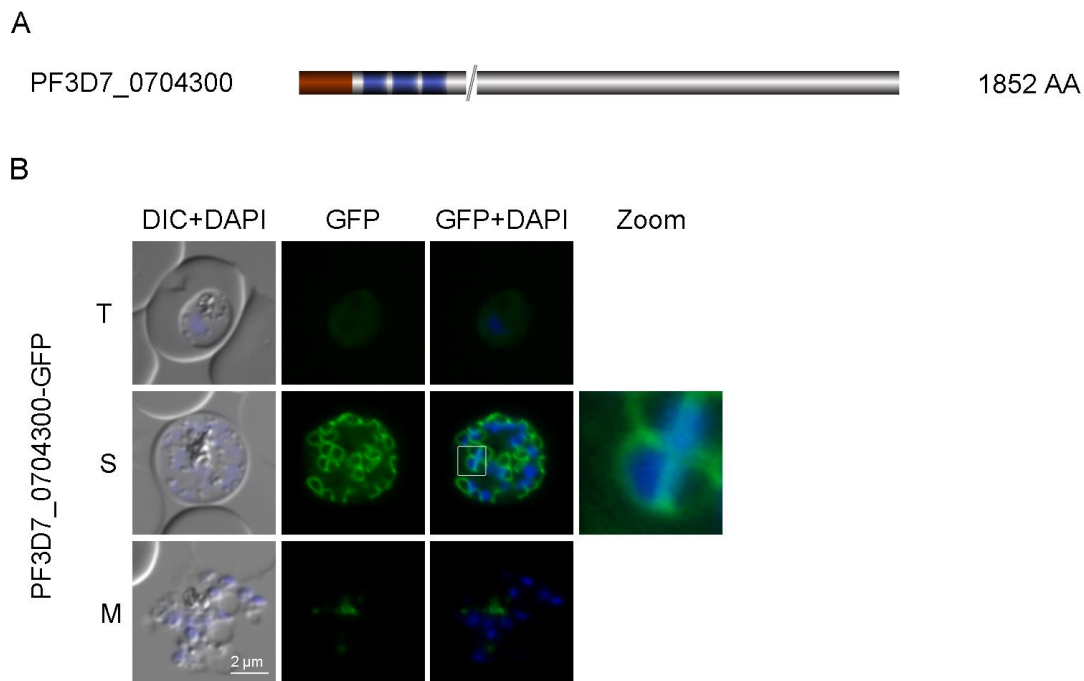


**Figure 30: Analysis of PF3D7\_ localization.** **A.** Schematic protein structure of PF3D7\_0704300; protein length, 1852 aa; SP, red box; TM, blue boxes; “//”, the middle part of the protein is not depicted. **B.** Fluorescence microscopy of 0704300-GFP (green) in unfixed parasites in trophozoites stages (T, upper panel), schizont stages (S, middle panel) and free merozoites (M, lower panel), DAPI staining of nuclei in blue.

### Group 3: Candidates with apical localization

Six of the candidates were identified to localize to organelles of the apical pole such as the micronemes and the rhoptries as schematically depicted in Figure 31. Known apical proteins such as AMA1 and EBA175 were shown to be implicated in tight junction and moving junction formation during the active process of ongoing invasion (Singh et al., 2005; Besteiro et al., 2009; Riglar et al., 2011).

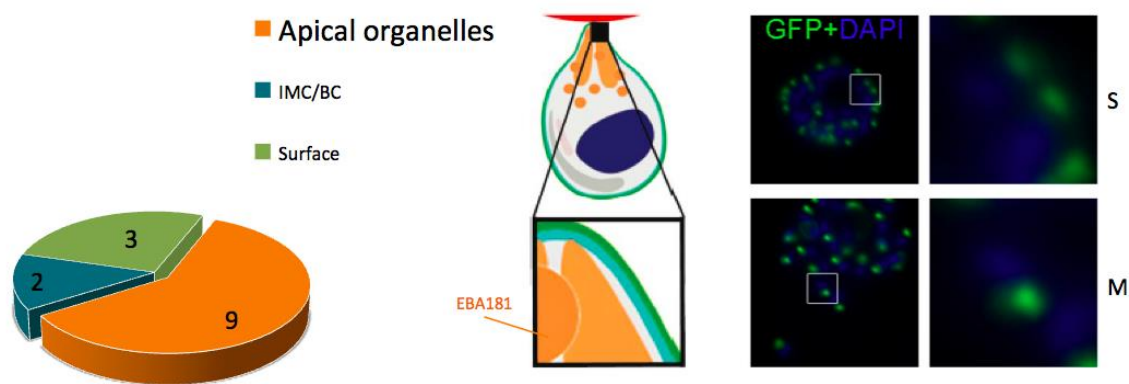


**Figure 31: Schematic representation of proteins with apical localization.** Nine candidates were identified to localize to the apical end (left panel). EBA181 is given as representative marker for apical proteins in orange (schematic, processed from Hu et al., 2010), fluorescence microscopy of an exemplary GFP-tagged apical protein in late schizonts (S) and free erozoites (M) is depicted in green in the right panel, nuclei are stained with DAPI in blue, 5x zoom area is indicated with a white box.

**Candidate PF3D7\_0105400.1** is a conserved *Plasmodium* protein of unknown function. It consists of 140 aa comprising one single predicted transmembrane domain (aa 88-110; Figure 32A). Transcription data show an expression minimum at around 20 hpi, and a maximum at 40-5 hpi. Correct integration was confirmed by PCR analysis (P1+P2, 672 bp; P3+P4, 1345 bp; Figure 21). The late expression profile was further validated via fluorescence microscopy. A GFP signal could not be visualized in early stages (Figure 32B, upper panel, T) but became detectable in schizonts (S) as well as in free merozoites (M) (Figure 32B, middle and lower panel, respectively). Microscopy displayed an apical localization of PF3D7\_0105400.1 in late stages. Expression of the GFP fusion protein was

also confirmed by western blot analysis using parasite material from a synchronized 3D7\_0105400.1 culture harvested from late stages. The protein was detected at the expected size of 44 kDa (43.85 kDa) using anti-GFP specific antibodies (Figure 32C). Parental 3D7 material was used as a control.

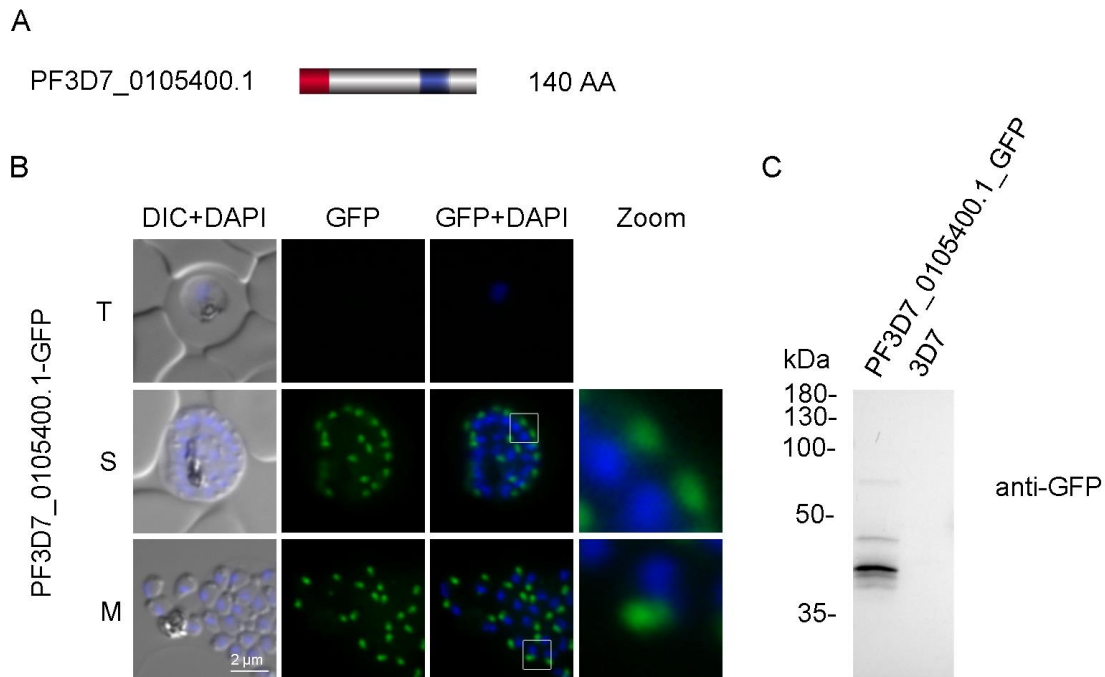


**Figure 32: Analysis of PF3D7\_0105400.1 localization.** **A.** Schematic representation of the protein structure of PF3D7\_010540.1. Protein length, 140 aa; SP, red box; TM, blue box. **B.** Localization of 0105400.1-GFP (green) via fluorescence microscopy of unfixed parasites, (T, trophozoite stages, upper panel; S, schizont stage, middle panel; M, free merozoites, lower panel). Nuclei stained with DAPI, blue. **C.** Western blot analysis of synchronized 3D7\_0105400.1-3D7 parasite culture harvested at late stages. GFP specific antibodies were used to detect the fusion protein at 44 kDa protein (expected size 43.85 kDa). Parental 3D7 material was added as a negative control.

**Candidate PF3D7\_0811600** is a conserved *Plasmodium* protein of unknown function. It is 1210 aa long and does not comprise any predicted transmembrane domains (Figure 33A). Transcriptomics reveal minimum expression at around 10 hpi and a maximum expression during schizogony at around 40 hpi, which was confirmed by RNA as well as for microarray evidence. Correct integration of pSLI-0811600-GFP into the appropriate gene locus was confirmed by PCR analysis (P1+P2, 981 bp; P3+P4, 1530 bp; Figure 21). Fluorescence analysis revealed a membrane-associated signal in trophozoites and early

schizonts that changed to a distinct apical localization in late schizonts (Figure 33B). In free merozoites the GFP signal was still detectable at the apical pole of every mature daughter cell (Figure 33B, lower panel). Expression of the protein was confirmed via western blot analysis using material harvested from late stage parasites and parental 3D7 material as a control. Probing with anti-GFP specific antibodies revealed a protein of 171 kDa corresponding to the expected size (Figure 33C).

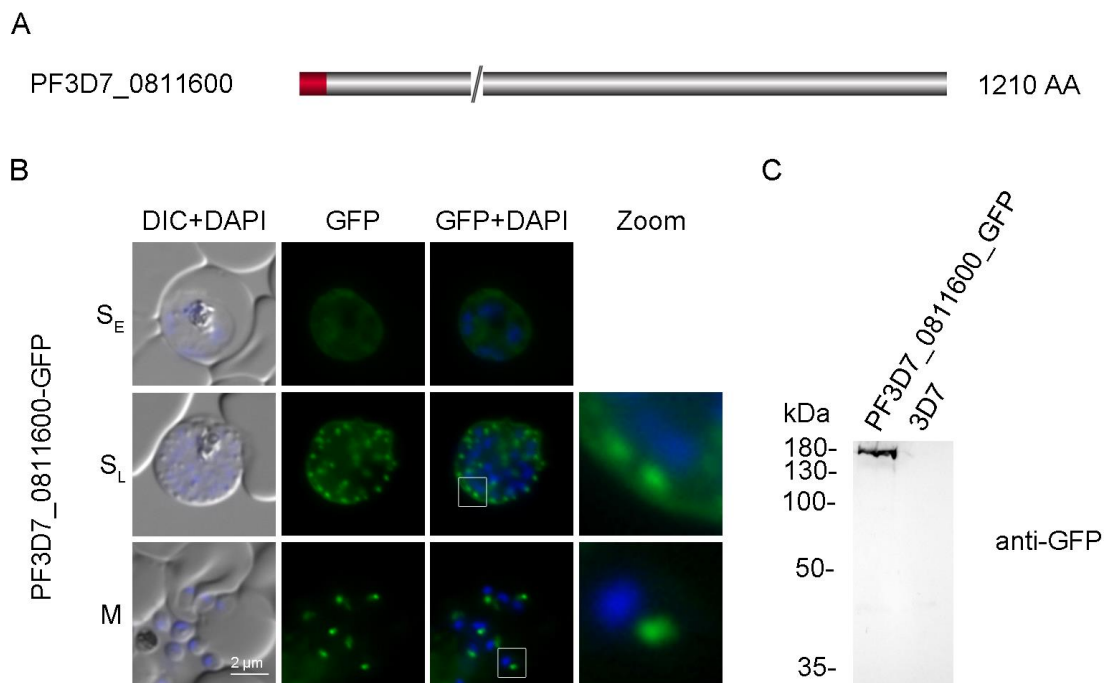


**Figure 33: Analysis of PF3D7\_0811600 localization.** **A.** Schematic protein structure of PF3D7\_0811600. Protein length, 1210 aa; SP, red box; “//”, part of the protein that is not depicted. **B.** Stage specific fluorescence microscopy analysis to reveal localization of 0811600-GFP (green) in unfixed parasites. Nuclei stained with DAPI (blue) ( $S_E$  and  $S_L$ : early and late schizont; M: free merozoites). **C.** Western Blot analysis to verify specific expression 0811600-GFP. Parasite material from a synchronized 0811600-GFP culture was harvested at late stages and probed with anti-GFP antibodies. The GFP fusion protein was detected at the calculated size of about 170 kDa (calculated 171 kDa). Parental 3D7 parasite material was harvested as a control.

**Candidate PF3D7\_1014100** was recently annotated as a putative merozoite surface protein MSA180 (Muh et al., 2017). The candidate gene encodes a protein of 1455 aa, which does not display a transmembrane domain (Figure 34A). Microarray as well as RNA seq evidence confirm a transcription maximum during late schizogony and merozoites.

Correct integration into the endogenous locus was proofed by PCR analysis (P1+P2, 966 bp; P3+P4, 1503 bp; Figure 21). Fluorescence microscopy analysis displayed an exported phenotype in early stages (T, Figure 34B, upper panel). During schizogony the GFP signal was detectable in a nuclear and perinuclear localization. In free merozoites protein was visual in every nascent daughter cell forming distinct foci at the morzoite pole suggesting PF3D7\_1014100 as a novel apical protein (Figure 34B, middle and lower panel).

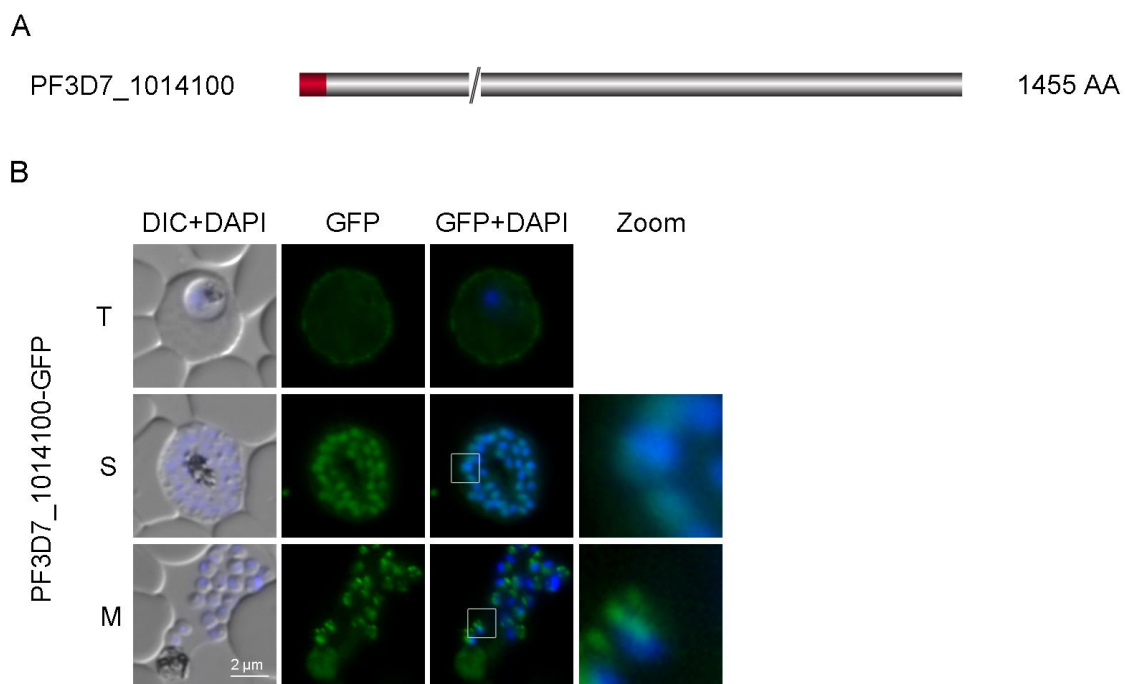


**Figure 34: Analysis of PF3D7\_1014100-GFP localization.** **A.** Schematic protein structure of PF3D7\_1014100. Protein length, 1455 aa; SP, red box; “//”, part of the protein that is not depicted. **B.** Localization of 1014100-GFP (green) in unfixed parasites by fluorescence microscopy in trophozoites (T), schizonts (S) and merozoites (M). Nuclei are stained with DAPI (blue), nuclei are stained with DAPI (blue), scale bar 2  $\mu$ m.

**Candidate PF3D7\_1115600** is an annotated peptidyl-prolyl cis-trans isomerase, termed CYP19B (Hirtzlin et al., 1995; Marín-Menéndez et al., 2012). It is a relatively small protein of 195 aa without any predicted transmembrane domains (Figure 35A). Transcription data provide an expression profile with minimum expression at around 10 hpi and a maximum expression during schizogony around 40 hpi. Correct integration



was confirmed by PCR analysis (P1+P2, 779 bp; P3+P4, 1763 bp; Figure 21) and fluorescence microscopy was performed to investigate into stage specific localization of 3D7\_1115600-GFP. No signal was obtained in trophozoite stages (T) but in late schizont (S) as well as in free merozoites (M) a fluorescence signal was clearly visible revealing an apical localization (Figure 35B). Expression of the GFP fusion protein was validated via western blotting. The protein was visualized at a size of about 50 kDa in the transgenic but not the parental 3D7 cell line (expected size 48.73 kDa; Figure 35C). However, the protein was described previously and therefore mistakenly selected for localization analysis (Hirtzlin et al., 1995; Marín-Menéndez et al., 2012). However, in contrast to previous findings, which demonstrated a cytosolic localization of the protein, our analysis revealed a distinct apical localization of the candidate.

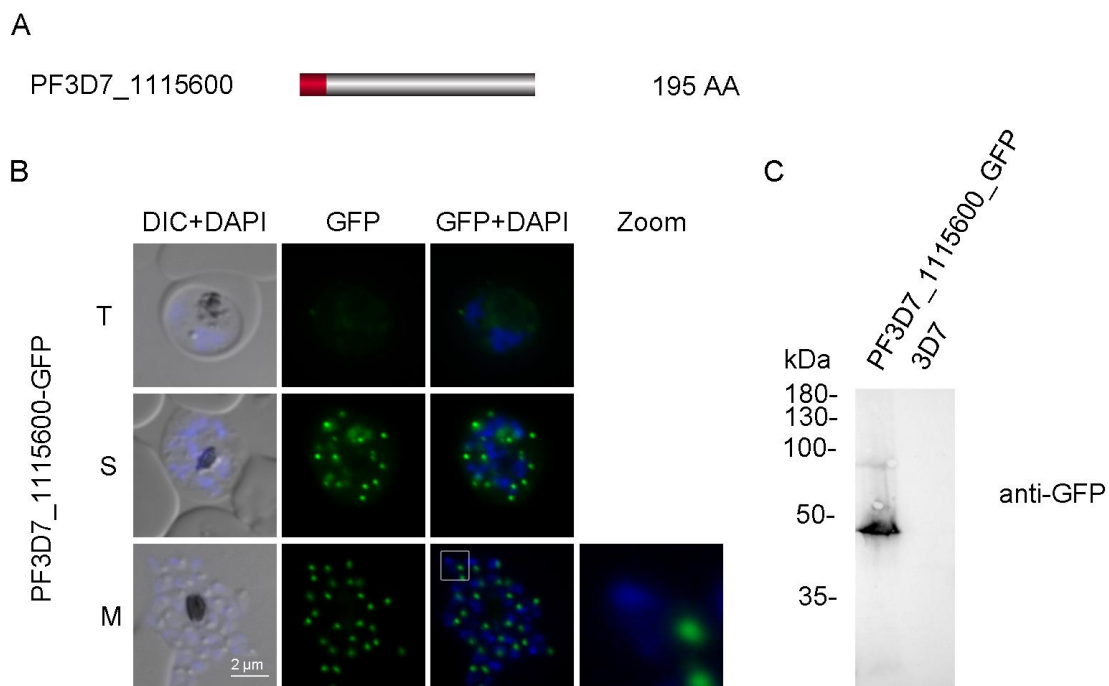


**Figure 35: Analysis of PF3D7\_1115600 localization** **A.** Schematic protein structure of PF3D7\_1115600. Protein length, 195 aa; SP, red box. **B.** Fluorescence microscopy of unfixed parasites for localization of 1115600-GFP (green) in trophozoites (T), schizonts (S), free merozoites (M). Nuclei are stained with DAPI (blue). **C.** Western blot analysis to confirm correct expression of 1115600-GFP. Anti-GFP antibodies were used to detect the GFP fusion protein, 48.73 kDa in the transgenic but not the parental 3D7 cell line.

**Candidate PF3D7\_1310200** is a *Plasmodium* conserved protein of unknown function. This protein consists of 144 aa and is predicted to display one single transmembrane domain in close proximity to its C-terminus (aa 100-132; Figure 36A). Minimum expression was detected at around 20 hpi and maximum expression was shown for late schizonts and merozoites at around 40-5 hpi. Correct integration was confirmed by PCR analysis (P1+P2, 640 bp; P3+P4, 1092 bp; Figure 21). Late expression was confirmed via fluorescence microscopy. No signal was visible in trophozoites but was detected in schizonts (Figure 36B, upper and middle panel, respectively). The GFP signal was enduring until merozoites were formed suggesting a rather apical localization (Figure 36B, lower panel).

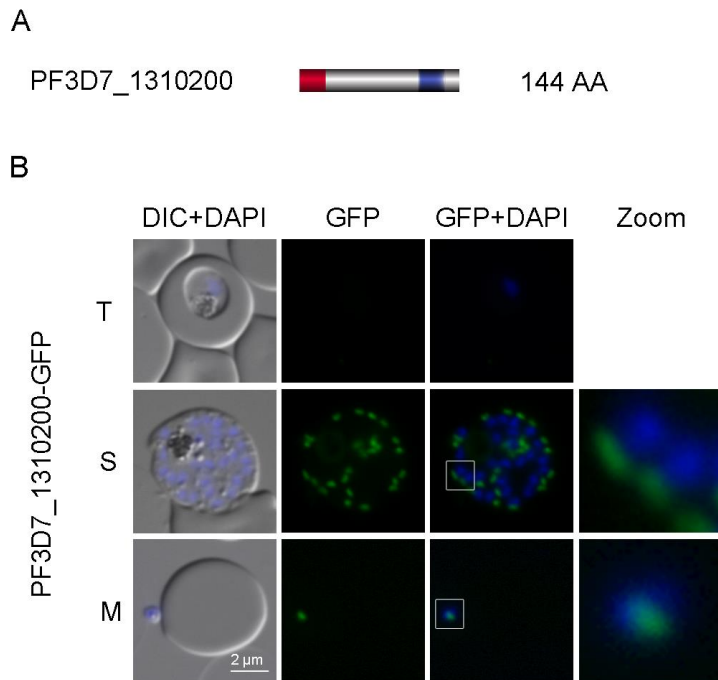


**Figure 36: Analysis of PF3D7\_1310200-GFP localization.** **A.** Schematic protein structure of PF3D7\_1310200. Protein length, 144 aa; SP, red box; TM, blue box. **B.** Localization of 1310200-GFP (green) in unfixed parasites by fluorescence microscopy in trophozoites (T), schizonts (S) and merozoites (M). Nuclei are stained with DAPI (blue).

**Candidate PF3D7\_1404700** is a conserved *Plasmodium* protein of unknown function. The candidate gene encodes for 290 aa (Figure 37A). RNA seq as well as microarray data confirmed increased expression values in late schizont stages. PCR analysis could confirm correct integration into the genomic locus (P1+P2, 872 bp; P3+P4, 1292 bp; Figure 21) leading to the GFP-fusion protein. Performing fluorescence microscopy of unfixed parasites no GFP signal was detectable until late schizont stages. In merozoites a strong, rather polar signal was detectable which might be located at the apical pole (Figure 37B). To clearly localize the GFP signal co-localization studies need to be performed.

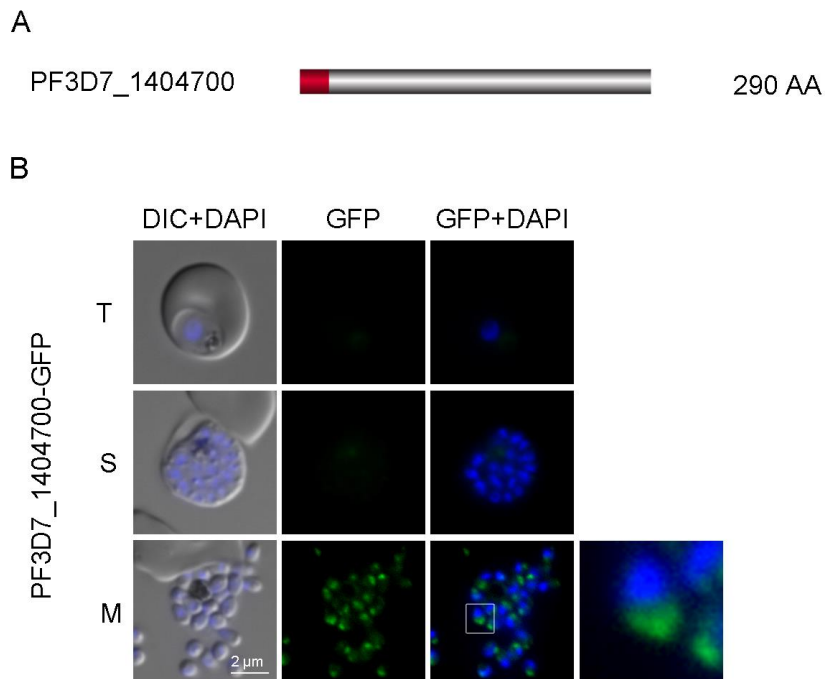


**Figure 37: Analysis of PF3D7\_1404700-GFP localization.** **A.** Schematic protein structure of PF3D7\_1404700. Protein length, 144 aa; SP, red box; TM, blue box. **B.** Localization of 1404700-GFP (green) in unfixed parasites by fluorescence microscopy in trophozoites (T), schizonts (S) and merozoites (M). Nuclei are stained with DAPI (blue), nuclei are stained with DAPI (blue), 5x zoom area is indicated with a white box, scale bar 2  $\mu$ m.

**Canidate PF3D7\_1404900** consists of 297 aa and is a conserved *Plasmodium* protein of unknown function (Figure 38A). Transcriptomics reveal slightly up-regulated expression values during very late schizogony and in merozoites. Correct integration could be

confirmed by PCR analysis (P1+P2, 959 bp; P3+P4, 1612 bp; Figure 21). Fluorescence microscopy analysis of unfixed parasites showed a weak, rather cytosolic GFP signal in trophozoites. This signal seemed to vanish in schizonts but reappeared in merozoites revealing a cytosolic localization with accumulation at the apical pole (Figure 38B). However a clear localization could not be determined.

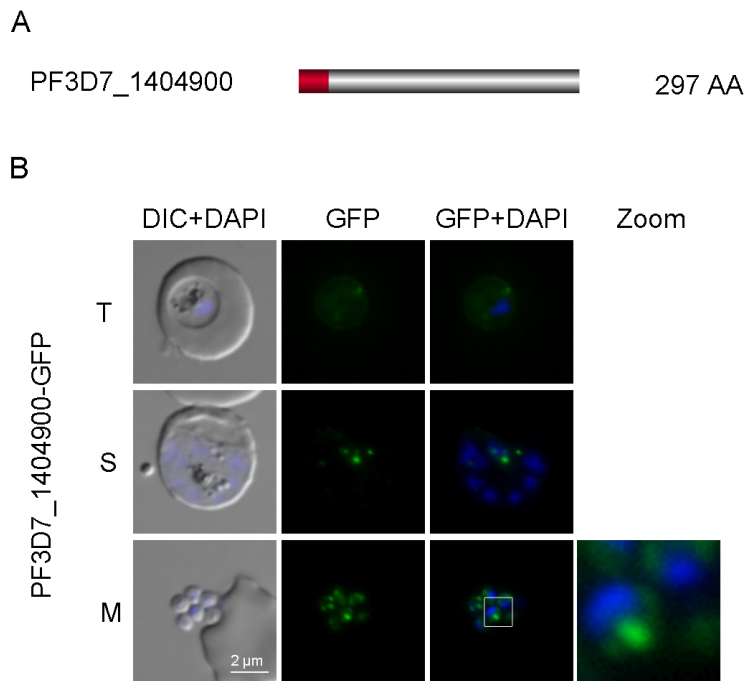


**Figure 38: Analysis of PF3D7\_1404900 expression and localization.** **A.** Schematic protein structure of PF3D7\_1404900. Protein length, 297 aa; SP, red box. **B.** Localization of 1404900-GFP (green) via fluorescence microscopy of unfixed parasites in trophozoites (T), schizonts (S) and free merozoites (M). Nuclei are stained with DAPI in blue, 5x zoom area is indicated with a white box, scale bar 2 µm.

**Candidate PF3D7\_1463900** is a 1071 aa long putative EF-hand calcium-binding domain-containing protein (Treeck et al., 2009) with seven predicted transmembrane domains (Figure 39A). Minimal expression values were reported around 15 hpi and maximal expression around 40-5 hpi during late schizogony. Correct integration of the pSLI-1463900-GFP plasmid leading to 1463900-GFP fusion protein was confirmed by PCR analysis (P1+P2, 989 bp; P3+P4, 1513 bp; Figure 21). Late stage expression was examined and confirmed by fluorescence microscopy. As expected a GFP signal was not

detectable in trophozoite stage parasites (Figure 39B, upper panel) but became clearly visible in schizonts (Figure 39B, middle panel) and lasted until the release of merozoites (Figure 39B, lower panel). The microscopy analysis revealed an apical localization of PF3D7\_1463900. Expression of the fusion protein was confirmed by western blot analysis using parasite material derived from a synchronized late-stage 3D7\_1463900-GFP parasite culture. GFP specific antibodies visualized a protein of about 150 kDa in the transgenic but not the parental 3D7 cell line (predicted size 154 kDa; Figure 39C).

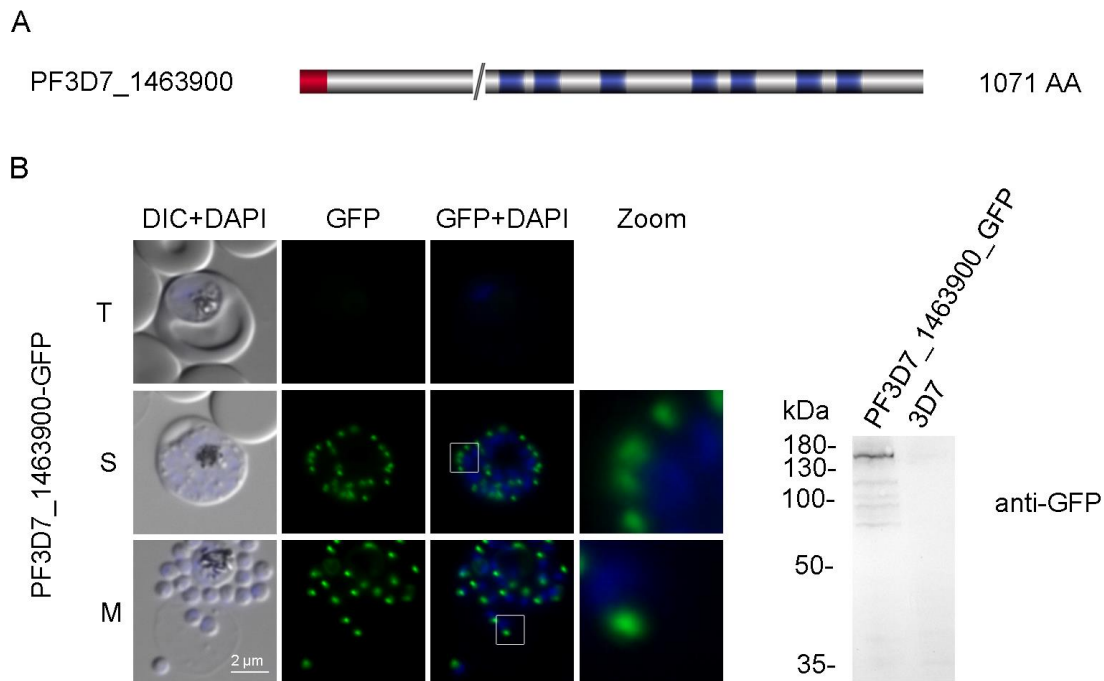


**Figure 39: Analysis of PF3D7\_1463900 localization.** **A.** Schematic representation of the protein structure of PF3D7\_1463900. **B.** Localization of 1463900-GFP (green) using fluorescence microscopy and unfixed parasites in trophozoite stage (T, upper panel), schizont stage (S, middle panel) and free merozoites (M, lower panel). Nuclei stained with DAPI in blue. **C.** Western blot analysis of synchronized late-stage 3D7\_1463900-GFP parasite material. The GFP fusion protein was detected with an anti-GFP antibody (upper panel, indicated by the arrow) at the expected size of about 150 kDa (calculated size 154 kDa). Parental 3D7 parasite material was added as control.

**Candidate PF3D7\_1035900** was annotated as M556, a probable protein of unknown function (566 aa; Figure 40) (LaCount et al., 2005). This candidate gene does not encode for any TM but for a predicted pumillo homology domain, which is a sequence-specific

RNA binding domain. Members of the pumillo family (Puf) are known to bind RNA sequences in 3'UTR regions of mRNA and thereby regulating translation. Puf proteins often function in asymmetric cell division and regulation of cell fate specification (Barker et al., 1992; Spassov and Jurecic, 2003). Transcription data affirmed maximal expression in late schizonts and merozoites. Correct integration of pSLI\_1035900-GFP into the genomic locus was confirmed by PCR analysis (P1+P2, 1710 bp; P3+P4, 2577; Figure 21) and expression of the GFP-fusion protein was investigated using fluorescence microscopy (Figure 40B). No signal was detectable in trophozoite stages and early schizonts but became visible in late schizonts (Figure 40B). Investigation of free merozoites revealed a GFP signal at the pole of nascent daughter merozoites displaying two distinct foci at the pole of every parasite as was also seen for candidate PF3D7\_1014100 (Figure 34). This suggests PF3D7\_1035900 as a protein of the secretory organelles.

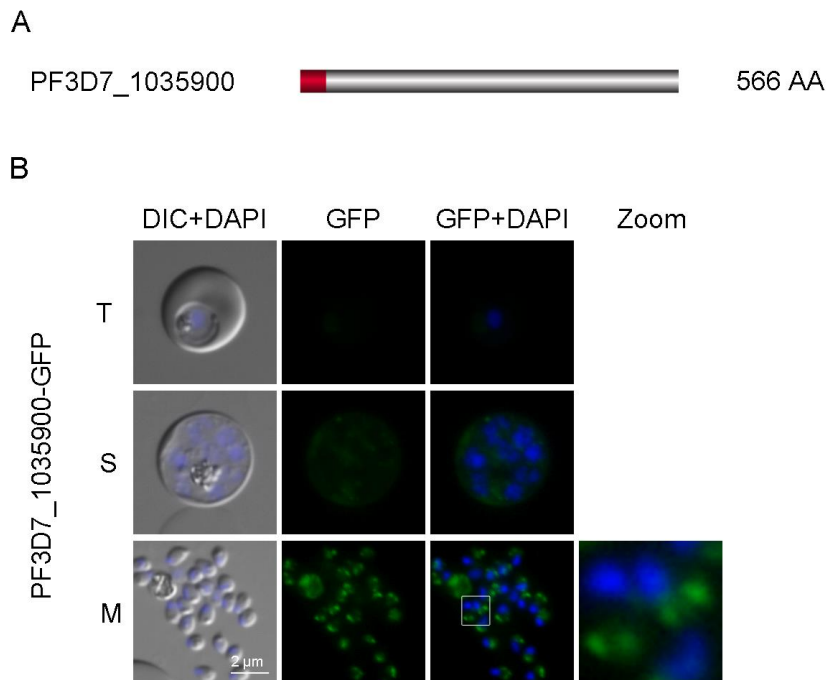


**Figure 40: Analysis of PF3D7\_1035900-GFP expression and localization.** **A.** Schematic protein structure of PF3D7\_1035900. Protein length, 566 aa; SP, red box. **B.** Localization of 1035900-GFP (green) in unfixed parasites by fluorescence microscopy in trophozoites (T), schizonts (S) and merozoites (M). Nuclei are stained with DAPI (blue), nuclei are stained with DAPI (blue), scale bar 2  $\mu$ m.

#### Group 4: Candidates with other localization

Not all candidates could be localized to distinct invasion related compartments of the parasite. Provided here is an overview of candidates that either showed localization to compartments not directly connected to invasion or candidates with an expression too low for fluorescence microscope analysis. Cloning and SLI-integration was performed as described previously. For every candidate correct integration was confirmed by PCR analysis (Figure 21).

**Candidate PF3D7\_0316300.2** was recently annotated as a conserved inorganic pyrophosphatase of 431 aa without any transmembrane domain (Figure 41A) (Jamwal et al., 2017). Transcriptomics show an up-regulated expression during schizogony. Correct integration was validated by PCR analysis (P1+P2, 739 bp; P3+P4, 1375 bp; Figure 21). Fluorescence microscopy revealed a cytosolic localization with distinct foci in late stages, which was still detectable in free merozoites (Figure 41B).

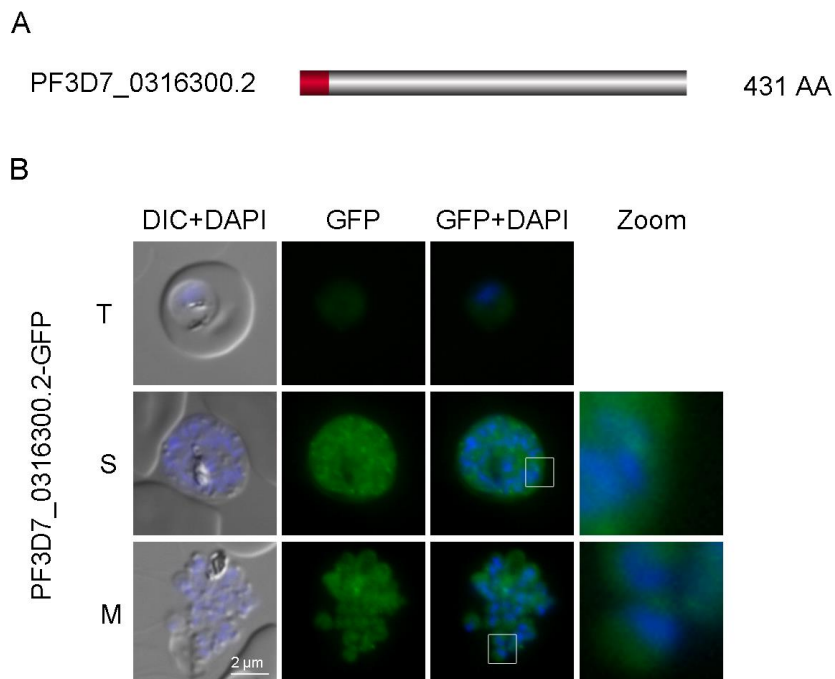


**Figure 41: Analysis of PF3D7\_0316300.2 localization.** **A.** Schematic protein structure of PF3D7\_0316200.2. Protein length, 431 aa; signal peptide, red box. **B.** Localization of 0316200.2-GFP (green) via fluorescence microscopy of unfixed parasites in trophozoites (T), schizonts (S) and free merozoites (M). Nuclei are stained with DAPI in blue, 5x zoom area is indicated with a white box, scale bar 2  $\mu$ m.

**PF3D7\_0404800** is a conserved protein of unknown function. The candidate gene consists of 1866 bp, encoding for a protein of 576 aa, which does not display any transmembrane domain (Figure 42A). Array data show a rather weak up-regulation of expression values in late stages, which was also true for RNA seq data, although RNA evidence report a higher transcription in early ring stages. Correct integration of pSLI\_0404800-GFP into the appropriate gene locus as validated by PCR analysis (P1+P2, 815 bp; P3+P4, 1212 bp; Figure 21). Fluorescence microscopy of unfixed parasites revealed a rather cytosolic localization in late schizonts. After RBC rupture the GFP-signal was still detectable in released merozoites (Figure 42B).

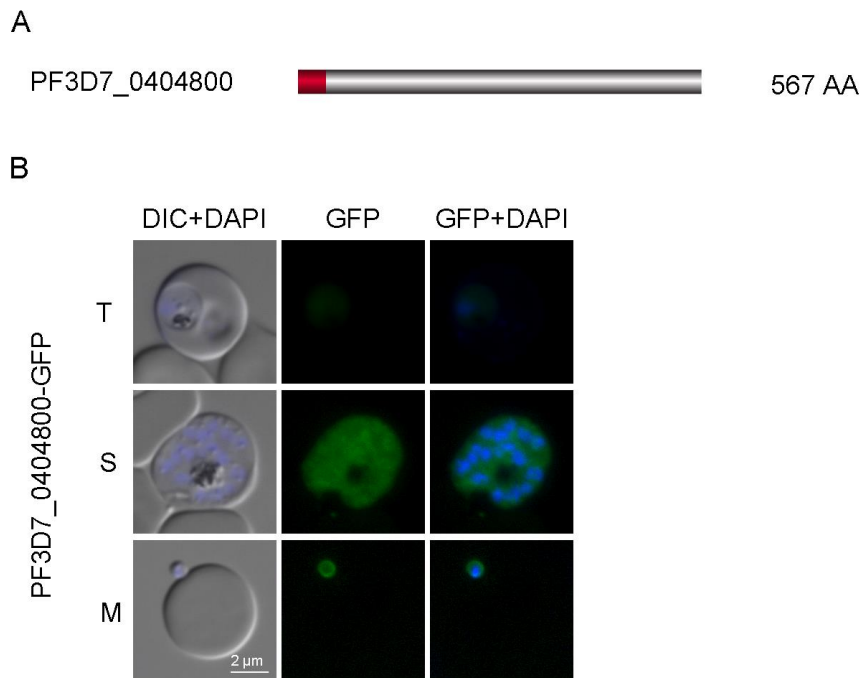


**Figure 42: Analysis of PF3D7\_0404800-GFP localization.** **A.** Schematic protein structure of PF3D7\_0404800. Protein length, 567 aa; SP, red box. **B.** Localization of 0404800-GFP (green) in unfixed parasites by fluorescence microscopy in trophozoites (T), schizonts (S) and merozoites (M). Nuclei are stained with DAPI (blue), nuclei are stained with DAPI (blue), scale bar 2  $\mu$ m.



**PF3D7\_0625400** is a conserved *Plasmodium* protein of unknown function. Transcriptomic data show up-regulated expression values from very late schizont stages to very early rings up to 8 hpi. The candidate gene encodes a protein of 412 aa not displaying and transmembrane domain (Figure 43A). Correct integration into the genomic locus was confirmed by PCR analysis (P1+P2, 837; P3+P4, 1357 bp; Figure 21). Fluorescence analysis revealed an exported phenotype during early trophozoite stages until late schizont stages (Figure 43B; even though no export sequence was predicted). After egress from the erythrocytes the fluorescence signal was detectable in the cytosol of the free merozoites (Figure 43B).

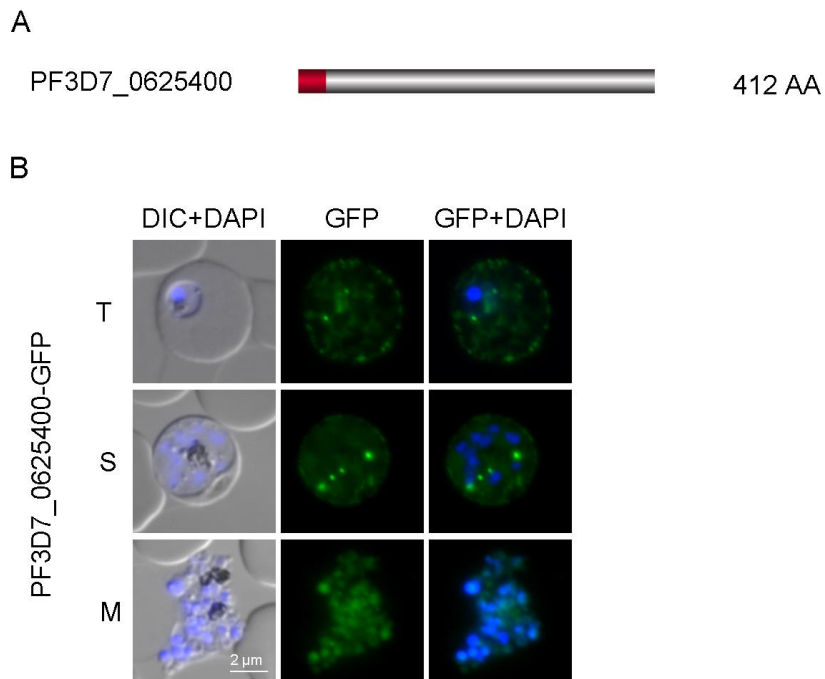


**Figure 43: Analysis of PF3D7\_0625400-GFP localization.** **A.** Schematic protein structure of PF3D7\_0625400. Protein length, 412 aa; SP, red box. **B.** Localization of 0625400-GFP (green) in unfixed parasites by fluorescence microscopy in trophozoites (T), schizonts (S) and merozoites (M). Nuclei are stained with DAPI (blue), nuclei are stained with DAPI (blue), scale bar 2  $\mu$ m.

**Candidate PF3D7\_1105300** is a conserved *Plasmodium* protein of unknown function. RNA seq as well as microarray data show an up-regulation in late schizonts. The protein consists of 730 aa and displays one single TM at its C-terminal end spanning aa 681-703 (Figure 44A). Correct integration into the endogenous locus was confirmed by PCR analysis (P1+P2, 1044 bp; P3+P4, 1466 bp; Figure 21). Fluorescence analysis of unfixed parasites showed a membrane-associated signal in trophozoites, which might be located in the PPM or PV. Despite transcriptomics evidenced maximal expression during late schizogony the signal was not detectable in late schizonts or merozoites (Figure 44B). Expression of the protein was confirmed by western blot analysis using GFP specific antibodies. The GFP fusion protein was detected at the expected size of 117 kDa (Figure 44C).

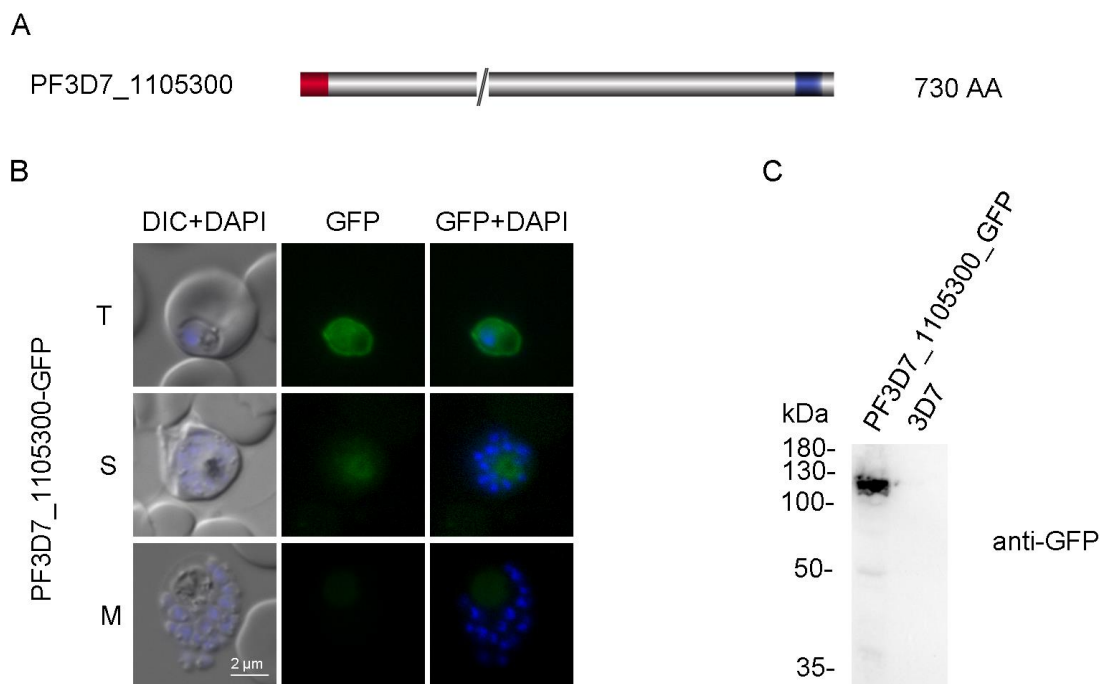


**Figure 44: Analysis of PF3D7\_1105300 localization.** **A.** Schematic protein structure of PF3D7\_1105300. Protein length, 730 aa; SP, red box; TM, blue box, “//” indicates part of the protein that is not depicted in the schematic. **B.** Localization of 1105300-GFP (green) via fluorescence microscopy of unfixed parasites in trophozoites (T), schizonts (S) and free merozoites (M). Nuclei are stained with DAPI in blue, scale bar 2  $\mu$ m. **C.** Western blot analysis of PF3D7\_1105300-GFP. The GFP fusion protein was detected with an anti-GFP antibody at the expected size of about 117 kDa. Material from parental 3D7 parasites was used as a control.

**Candidate PF3D7\_1334600** is a protein of 298 aa termed MSRP3 (Mello et al., 2002). It does not have any predicted transmembrane domains but a predicted C-terminal MSP7-like domain (not shown; aa 202-298; Figure 45A). This gene was identified earlier and supposed to interact with the amino-terminal proteolytic fragment of MSP1 (Mello et al., 2002) but no protein-based analysis has been performed in previous studies. Microarray and RNA evidence confirm an up-regulated expression during schizogony starting at around 40 hpi. Correct integration was confirmed by PCR (P1+P2, 953 bp; P3+P4, 1524 bp; Figure 21). Fluorescence microscopy corroborated a constant expression during late schizont stages. The GFP signal was detectable around every newly forming daughter cell in a “waggon-wheel”-like manner, while no signal was visible around free merozoites, suggesting a PV-associated localization for candidate PF3D7\_1334600 (Figure 45B). Expression of the GFP-tagged protein was analyzed via western blot. Using GFP specific antibodies the fusion protein was detected at the expected size (calculated size 61.5 kDa, Figure 45C).

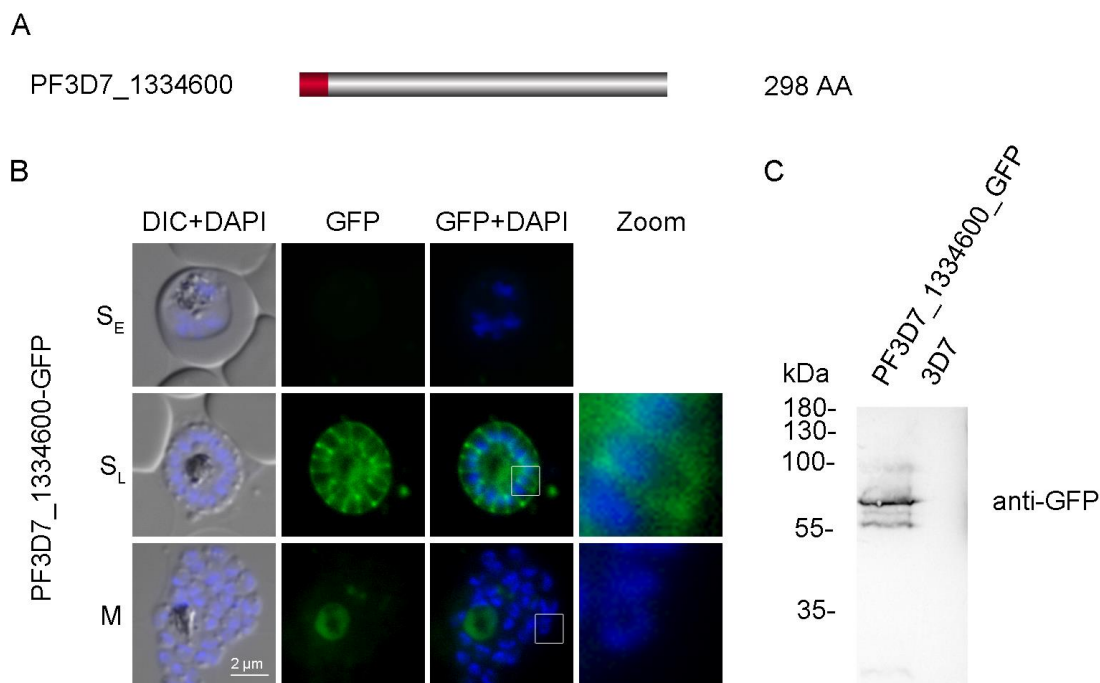


**Figure 45: Analysis of PF3D7\_1334600 localization.** A. Schematic protein structure of PF3D7\_1334600; protein length, 298 aa; SP, red box. B. Localization of 1334600-GFP (green) via fluorescence microscopy of unfixed parasites in early

and late schizonts ( $S_E$  and  $S_L$ ) and free merozoites (M). Nuclei are stained with DAPI in blue. **C.** Western blot analysis of PF3D7\_1334600-GFP. Anti-GFP antibodies were used to detect the fusion protein at a calculated size of 61.5 kDa. Material harvested from a parental 3D7 parasites was used as a control.

**Candidate PF3D7\_1472600** encodes for a protein of 553 aa (Figure 46) and was identified earlier as protein disulfide-isomerase (PDI-14) (Mahajan et al., 2006). No characterization studies were done for this candidate in the named approach. But another candidate of the study, *PfPDI* was biochemically characterized and suggested to function in correct folding of EBA175. PF3D7\_1472600 (PDI-14) however was not deeper investigated and transcription data verify a constant expression with a climax in late schizogony. Therefore this candidate was endogenously fused to GFP and PCR analysis confirmed correct integration (P1+P2, 1037 bp; P3+P4, 1442 bp; Figure 21). Fluorescence analysis revealed a wagon wheel-like localization during late schizogony, which was not detectable in early stages (Figure 46B). This suggests PF2D7\_1472600 as a PV-associated protein. Nevertheless, further localization studies of free merozoite stages have to be performed, which are not provided here.

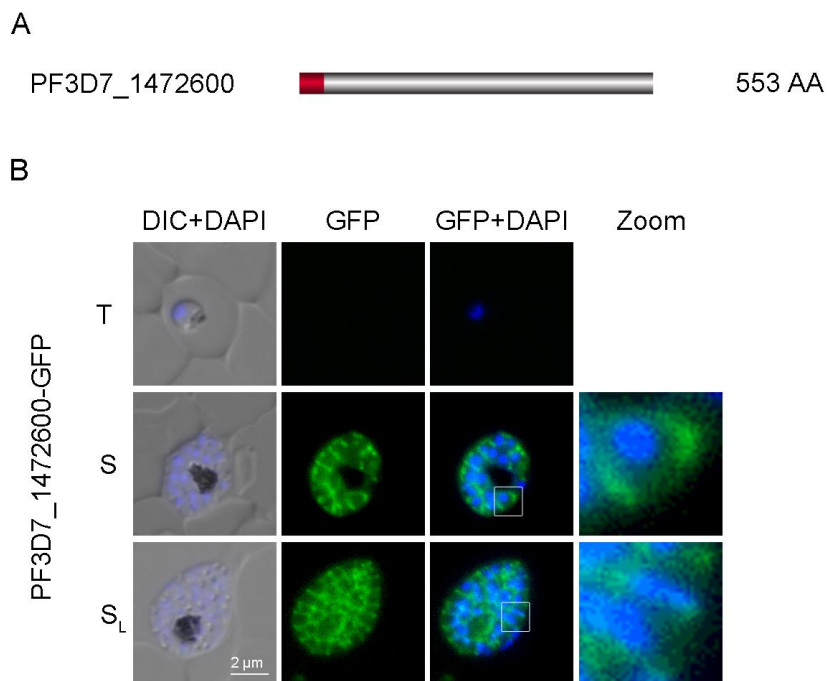


**Figure 46: Analysis of PF3D7\_1472600-GFP localization.** **A.** Schematic protein structure of PF3D7\_1472600. Protein length, 553 aa; SP, red box. **B.** Localization of 1472600-GFP (green) in unfixed parasites by fluorescence microscopy in trophozoites (T), schizonts (S) and late schizonts (S<sub>L</sub>). Nuclei are stained with DAPI (blue), nuclei are stained with DAPI (blue), scale bar 2  $\mu$ m.

**Candidate PF3D7\_0419400** is a conserved *Plasmodium* protein of unknown function. The protein consists of 2472 aa (7960 bp) and comprises one predicted transmembrane domain at its very C-terminal end (aa 2420 – 2440, Figure 47A). RNA seq evidence as well as microarray data confirmed late expression during schizogony with a peak around 40 hpi. Correct integration of the pSLI\_0419400-GFP plasmid into the endogenous locus was confirmed by PCR analysis (P1+P2, 862 bp; P3+P4, 1357 bp; Figure 21). Fluorescence analysis revealed a weak expression in late stages with a rather cytosolic localization in schizonts as well as in merozoites (Figure 47B). However, microscopy was not sufficient to specify the localization of the protein.

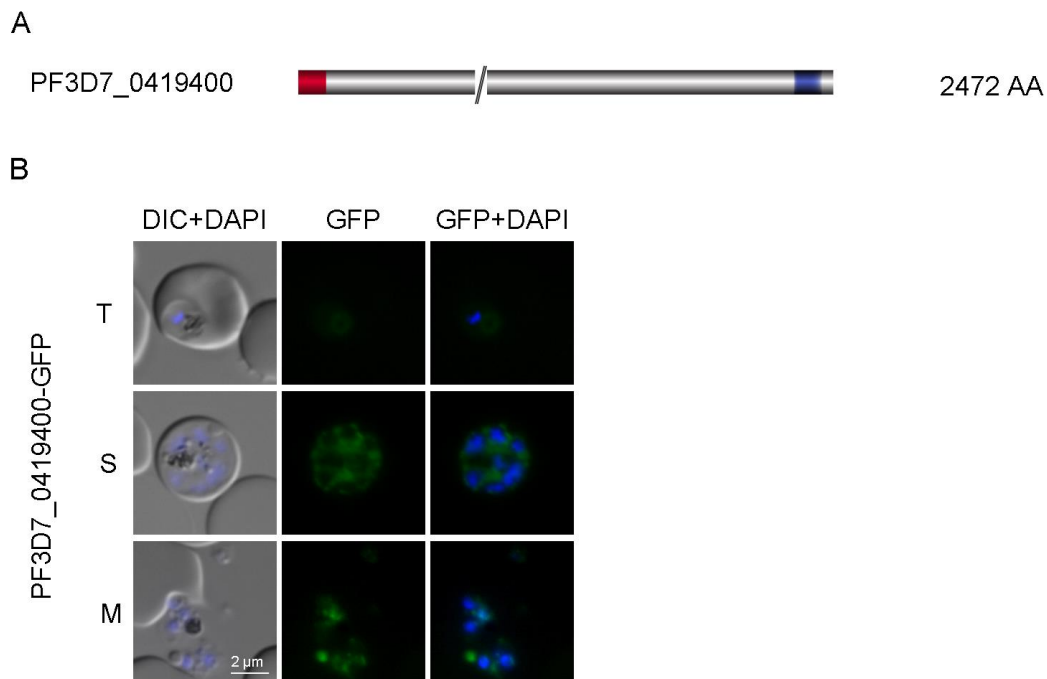


**Figure 47: Analysis of PF3D7\_0419400-GFP expression and localization.** **A.** Schematic protein structure of PF3D7\_0419400. Protein length, 2472 aa; SP, red box; TM, blue box; “//”, part of the protein that is not depicted. **B.** Localization of 0419400-GFP (green) in unfixed parasites by fluorescence microscopy in trophozoites (T), schizonts (S) and merozoites (M). Nuclei are stained with DAPI (blue), nuclei are stained with DAPI (blue), scale bar 2  $\mu$ m.

**Group 5: Candidates that were expressed too low for localization**

**Candidate PF3D7\_0204100** is a conserved *Plasmodium* protein of unknown function. RNA seq as well as micro array data confirm a transcription and late expression with a peak in late schizogony. The candidate gene encodes for a protein of 2296 aa without TMs. Correct integration into the appropriate gene locus was confirmed by PCR analysis (P1+P2, 834 bp; P3+P4, 1375 bp; Figure 21). The expression of the GFP-fusion protein was too low to be detected in fluorescence microscopy of live parasites.

**Candidate PF3D7\_0806200** is a putative C-mannosyltransferase, which has not been functionally characterized to date (Cova et al., 2015). Transcription data from microarray and RNA sequencing evidence revealed minimum expression values around 20 hpi and a maximum at around 40 hpi during schizogony. The candidate gene encodes for 1018 aa comprising 8 predicted TMs. Correct integration into the endogenous locus was confirmed by PCR analysis. However, expression of the GFP fusion protein could not be confirmed by fluorescence analysis to date.

**Candidate PF3D7\_1404800** is a conserved *Plasmodium* protein of unknown function consisting of 954 aa without TMs. Microarray data report an expression peak during late schizogony. RNA seq evidence in contrast present expression peaks in very early stages. PCR analysis confirmed correct integration into the genomic locus (P1+P2, 1063 bp; P3+P4, 1955 bp; Figure 21). An informative GFP signal could not be detected in any stages when fluorescence microscopy was performed.

**Candidate PF3D7\_1035100** is a probable protein (putative) of unknown function (LaCount et al., 2005). RNA and microarray evidence certify late transcription with a maximal peak in late schizogony. The candidate gene encodes for a protein of 561 aa without TMs (**Fehler! Verweisquelle konnte nicht gefunden werden.**A). Correct integration into the endogenous locus was confirmed by PCR analysis (P1+P2, 1016 bp; P3+P4, 1591 bp; Figure 21) and fluorescence analysis revealed a weak expression of the fusion protein in late stages (data not shown). Microscopy data were obtained only for schizont stages, which impedes a clear statement regarding the localization. The

detectable GFP signal may suggest a localization in close proximity to the BC or IMC. But this remains uncertified until further microscopy is done.

**Candidate PF3D7\_1122700** is a conserved protein of unknown function. The gene encodes for 254 aa, displaying 2 TMs spanning aa 118-140 and aa 180-202. Transcription data affirm an up-regulation of expression during schizogony. Correct integration was confirmed by PCR analysis (P1+P2, 790 bp; P3+P4, 1242; Figure 21). The fluorescence signal of PF3D7\_1122700-GFP was too low for detection when fluorescence microscopy was performed.

**Candidate PF3D7\_1200700** was identified as acyl-CoA synthetase (ACS7) (Bethke et al., 2006; Matesanz et al., 2003). Localization studies have not been performed before and late transcription was confirmed for merozoites and early rings by transcriptomics data. The candidate gene encodes for a protein of 926 aa without TMs. Integration of pSLI\_1200700-GFP into the genomic locus was verified by PCR analysis (P1+P2, 1030 bp; P3+P4, 1431 bp; Figure 21) and localization was examined by fluorescence microscopy. However, the signal of the fusion protein was too weak for detection, in trophozoites as well as in later stages.

**Candidate PF3D7\_1358000** was recently annotated as putative patatin-like phospholipase and its homologue in *T. gondii* was found to be involved in the maintenance of apicoplast lipid homeostasis (Lévêque et al., 2017). The gene encodes for a protein of 2012 aa. Correct genome integration was confirmed by PCR analysis (P1+P2, 1091 bp; P3+P4, 1483 bp; Figure 21). For PF3D7\_1358000 no fluorescence microscopy could be performed to further investigate the expression and localization of the candidate protein as the fluorescence signal was too low for detection.

### 3.2.3 Candidate essentiality in the blood stages

To further characterize the candidates, their essentiality was investigated using a targeted gene disruption (TGD) strategy to generate gene truncations (Birnbaum and Flemming et al., 2017). Therefore 300-600 bp of the 5' coding region were cloned into the previously introduced SLI vector and integrated via homologues recombination resulting in a disrupted gene and presumably not functional protein (Figure 48). The parasite cultures were kept on neomycin for six weeks. If truncated constructs could not be integrated correctly in six to nine attempts the gene was considered to be essential. On the other hand if parasites were selectable despite the truncation the gene was considered as dispensable or "not essential". To confirm specific disruption of the candidate genes PCR analysis was performed for every TGD construct. Therefore oligonucleotides were designed to bind the 5'UTR of the appropriate gene and the 5' region of the GFP tag as described previously. Correct integration of the truncated gene and therefore no essential function for blood stage parasites could be achieved for 6 candidates (Figure 49). However, yet no PCR analysis was performed using oligonucleotides the bind the wild type locus of the genes. Therefore it cannot be excluded that the parasites are still holding a functional version of the truncated genes, which will be tested in near future. Despite several attempts no parasites holding a truncated version of the appropriate gene could be obtained for candidates PF3D7\_0530300, PF3D7\_1143200, PF3D7\_1115600, and PF3D7\_1463900. These candidates therefore are considered to be likely essential for blood stage parasites. Further investigations using inducible gene knockout systems will be performed to deeper investigate into the functionality and essentiality of these candidate genes. For all remaining candidates selection for gene truncations were currently under progress (to date of submission). Therefore, no declaration for essentiality could be predicted yet. Data that could be obtained until submission date are listed in Table 2.



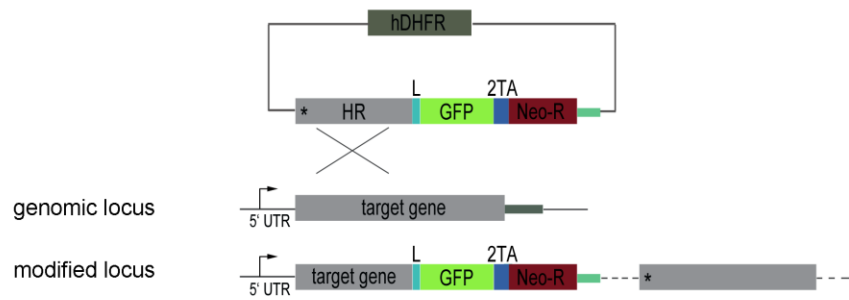


**Figure 48: Schematic of targeted gene disruption strategy using SLI (SLI-TGD).** The N-terminal region of the gene is targeted. Selection can be achieved via SLI. Homology region, HR; L, linker; GFP, light green box; 2TA, skip peptide; Neo-R, neomycin phosphotransferase II gene; hDHFR, human dehydrofolate reductase. Asterisk indicates stop codon, and flexed arrows indicate the endogenous promoter. (Adapted from Birnbaum and Flemming et al., 2017). Two gene specific oligonucleotide pairs were designed to amplify 1) a 5' fragment in the parental as well as in the transgenic cell line and 2) a fragment only if the pSLI-TGD vector is correctly integrated and the gene was disrupted as (sequences of all nucleotides are listed in tab. Xx in the appendix).

Gene ID	Annotation	Localization	Blood stage essentiality
PF3D7_1143200	DnaJ protein, putative	surface	yes
PF3D7_1229300	conserved Plasmodium protein, unknown function	surface	no
PF3D7_0530300	conserved Plasmodium membrane protein, unknown function	IMC/BC	yes
PF3D7_0704300	conserved Plasmodium membrane protein, unknown function	IMC/BC	no
PF3D7_0105400.1	conserved Plasmodium protein, unknown function	apical	no
PF3D7_1115600	peptidyl-prolyl cis-trans isomerase (CYP19B)	apical	yes
PF3D7_1310200	conserved Plasmodium protein, unknown function	apical	no
PF3D7_1463900	conserved Plasmodium membrane protein, unknown function	apical	yes
PF3D7_0419400	conserved Plasmodium protein, unknown function	cytosolic	no
PF3D7_1334600	MSP7-like protein (MSRP3)	PV	no

**Table 2: Blood stage essentiality of localized candidates.** Colour code refers to localization of the proteins: surface localization: turquoise, IMC/BC localization: green, and apical localization: orange. The blood stage essentiality refers to a successful TGD approach (essentiality: yes). If the gene disruption did not affect parasite growth, genes are designated as not essential for blood stages (essentiality: no). The blood stage essentiality refers to a successful TGD approach: gene could be knocked out = not essential. If no parasites could be obtained upon truncation of the gene = likely essential (yes).

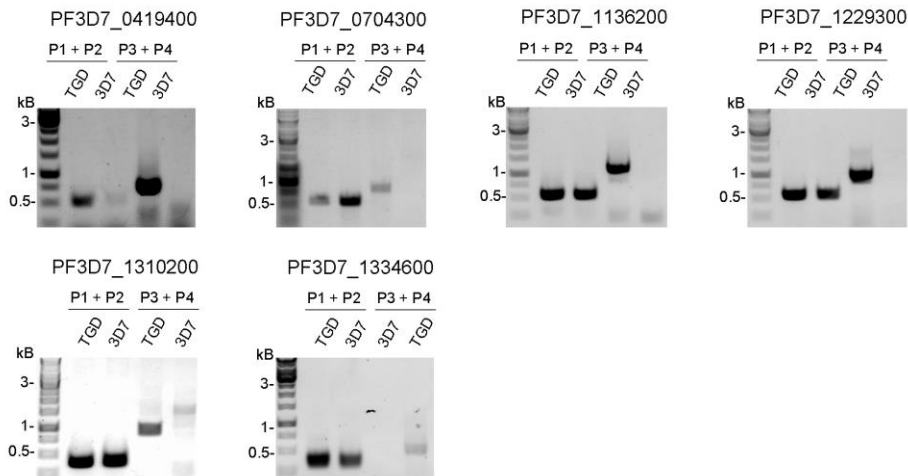


**Figure 49: PCR analysis of correctly integrated TGD constructs.** P1+P2: oligonucleotide pair that was used for amplification of the gene specific 5'TGD fragment. P3+P4: oligonucleotide pair that was used for amplification of a fragment after correct integration of the pSLI vector into the appropriate gene locus. P3 was designed to bind in the 5'UTR of the gene and P4 was designed to bind the 5'region of the GFP-tag. Sequences of all primers that were used are listed in the appendix.

## 4 Discussion

Merozoite invasion into human erythrocytes is a fast and crucial event. The parasite cannot survive outside a host cell and therefore depends on a fast and effective invasion mechanism and machinery. This obliges sequential steps that involve an unidentified number of proteins (LaCount et al., 2005; Tardieux and Baum, 2016) and needs to be tightly organized. All of them – whether known or not – are subject to regulatory mechanisms. Expression can be regulated at the epigenetic level by gene silencing and activation (Le Roch et al., 2003; Bozdech and Llinas et al., 2003) . Nonetheless, regulation also occurs at post-translational level and controls folding, localization, binding, and therefore functionality of proteins (Foth et al., 2008; Doerig et al., 2015).

### 4.1 Regulatory steps in invasion – phosphorylation of EBA175 CPD

For invasion-related proteins such as AMA1 and Rh2b it was shown that phosphorylation of the cytoplasmic tail is mandatory for protein functionality (Treeck et al., 2009; Leykauf et al., 2010; Engelberg et al., 2013; Tham et al., 2014). EBA175 is an important ligand linking the parasite to the erythrocyte surface. It was shown before that removal of the cytoplasmic domain leads to a loss of protein function and to a switch of the invasion pathway in W2mef parasites (Gilberger et al., 2003, Stubbs et al., 2005). Here we investigated the potential impact of phosphorylation on protein functionality. To assess the putative phosphorylation sites in the CPD of EBA175 a phospho-mutant containing six alanine substitutions (S1448, S1449, T1466, S1473, T1483, and S1489) was generated. EBA175<sub>wt</sub>GFP was generated as a wild type control. The expression of the GFP fusion proteins was validated via western blotting. Using GFP-specific antibodies EBA175<sub>phospho</sub>GFP could be detected at a size of about 200 kDa. This is consistent with the wild type protein EBA175<sub>wt</sub>GFP. As the wild type peptide comprises all phosphorylation sites it would be expected to run a bit higher compared

to EBA175<sub>phospho</sub>GFP lacking six putative sites of action. Interestingly both proteins could be detected at a size of about 200 kDa. This result matches the expected size of the wild type GFP fusion protein. However, it suggests that the putative phosphorylation sites might not actually be phosphorylated *in vivo*. Further EBA175 is a microneme protein (Orlandi et al., 1990; Sim et al., 1990; Sim et al., 1992). It was shown before that correct sorting, in contrast to other microneme proteins, is not dependent on the CPD (Gilberger et al., 2003; Di Christina et al., 2000). Here, fluorescence analysis localized both, the wild type and the phospho-mutant protein, to the micronemes, which was confirmed by IFA. This microneme localization confirms that neither the GFP-tag nor the putative phosphorylation of the cytoplasmic domain do have any influence on the apical localization of EBA175.

W2mef parasites use EBA175 as their main invasion ligand, which binds its receptor in a sialic acid-dependent manner. Therefore the effect of the phosphorylation sites on the functionality of the protein was tested by the use of a neuraminidase-based invasion assay. Neuraminidase-treated erythrocytes lack the sialic acid moieties of glycophorin A, preventing EBA175 from binding. Only a switch to another invasion pathway, explicitly *PfRh4*-CR1 interaction, would allow the W2mef parasites to invade into neuraminidase-treated red blood cells. It is known that in W2mef parasites expressing a functional EBA175 ligand, the *PfRh4* gene is silent. Upon loss of EBA175 function *PfRh4* is expressed (Dolan et al., 1990; Reed et al., 2000; Duraisingh et al., 2003; Gilberger et al., 2003a; Stubbs et al., 2005). For *PfRh4* as well as for *PfRh2b* and AMA1 it was recently shown that phosphorylation of the cytoplasmic domain is essential for protein functionality (Tham et al., 2015; Engelberg et al., 2013; Treeck et al., 2009). Depletion of *PfCK2*, the kinase predicted to phosphorylate the cytoplasmic tails of type I transmembrane proteins, blocked parasite invasion into red blood cells. Likewise, for two residues within the cytoplasmic domain of EBA175 (T1466 and S1489) *PfCK2* is the predicted kinase (NetPhosK; Tham et al., 2015). It was shown that mutation of both amino acids to alanine results in a reduced phosphorylation relative to the wild type. But no effect on invasion could be observed. Here, we included 4 other potential phosphorylation sites

to test the effect on invasion into red blood cells. If phosphorylation would be essential for EBA175 functionality, for EBA175<sub>phospho</sub>-parasites no obvious reduction of proliferation would be expected when cultured in neuraminidase-treated RBCs. Mutation of the essential phosphorylation sites presumably would have led to a switch of the invasion pathway resulting in an up-regulated expression of PfRh4. Interestingly the phospho-mutant parasites EBA175<sub>phospho</sub>GFP show a reduced proliferation comparable to wild type EBA175<sub>wt</sub>GFP parasites (80.3% and 76.68%, respectively) when cultured in neuraminidase-treated erythrocytes. These values are comparable with the parental W2mef strain demonstrating that even 6 silenced putative phosphorylation sites do not have any effect on parasite growth. It can be concluded that no switch had occurred in the EBA175<sub>phospho</sub>-parasites. Nevertheless, the actual status of phosphorylation was not tested in this study. The missing effect of the established mutation sites might also indicate that the predicted phospho-sites are not actually phosphorylated. Also, in western blot analysis one would expect the GFP signal of the wild type protein to be detected a bit higher resulting from effective phosphorylation compared to the phospho-mutant. Analysis via a phosphatase assay would be reasonable to test the real status of phosphorylation. Still, Tham and colleagues observed a reduced phosphorylation upon mutation of T1466 and S1489, the two potential target sites for PfCK2, which did not affect invasion as mentioned before (Tham et al., 2015).

To date no tyrosine kinases are confirmed in *P. falciparum* (Ward et al., 2004). However, it could be shown that phosphorylation of PfRh4 was significantly reduced when tyrosine residues were included into the mutation cell line. Also tyrosine residues within the cytoplasmic tail of PfRh4 were essential for Rh4-CR1 interaction, which likely involves phosphorylation (Tham et al., 2015). Further, the thrombospondin-related anonymous protein (TRAP) is essential for sporozoite motility as well as invasion into hepatocytes (Sultan et al., 1997; Kappe et al., 1999). Interestingly, the cytoplasmic tail could be substituted by the one of EBA175 without losing protein functionality (Gilberger et al., 2003). Phosphorylation of TRAP CPD is supposed to be important and it

was shown that the CPD displays multiple phosphorylation sites, including tyrosine residues (Akhouri et al., 2008). Hence it would be interesting to also consider tyrosine residues Y1446 and Y1491 in the cytoplasmic tail of EBA175 as potential target sites for kinases or a possible requirement for receptor binding. Nonetheless, these results clearly indicate that, in contrast to Rh4 and AMA1, none of the putative phosphorylation sites within the cytoplasmic tail (S1448, S1449, T1466, S1473, T1483, S1489) does have any essential impact on the function of EBA175.

### 4.2 Novel putative candidates for erythrocyte invasion

More than 15 years ago the whole *P. falciparum* genome sequence was published (Gardner et al., 2002). This data provided the platform for several bioinformatic tools to predict the localization and function of proteins and diverse network prediction studies previously showed that the localization of proteins indeed allows for functional inference (Date and Stoeckert, 2006; Haase et al., 2008; Hu et al., 2009; Wuchty and Ipsaro, 2007; Zhou et al., 2008). Those prediction tools can be harnessed for screens to identify proteins involved in complex processes such as invasion. An important subset of invasion related proteins was shown to either localize to the surface of invading merozoites or to be stored in the secretory organelles (Cowman and Crabb, 2006). Furthermore, the IMC is implicated in invasion and therefore displays an important compartment for proteins that are involved in this process (Keeley and Soldati, 2004).

Unifying features across all proteins involved in invasion are a late transcription (Le Roch et al., 2003) as well as the presence of a N-terminal signal peptide, which is required for co-translational translocation into the endoplasmic reticulum from where they get transported to their subcellular locations within the secretory pathway (Crabb et al., 2004; Haase et al., 2008). Representing examples are proteins such as MSP1, AMA1, EBA175, and Rh5 that was recently shown to be essential for parasite invasion (Holder

et al., 1992; Peterson et al., 1989; Yap et al., 2014; Camus and Hadley, 1985; Volz et al., 2016).

Haase and collaborators conducted a genome-wide search for invasion related proteins (Haase et al., 2008). In a bioinformatic screen they used transcriptional and structural features such as a N-terminal SP, an obligatory TM, and late expression during the intraerythric cycle. They identified 49 hypothetical proteins with high probability of being located on the surface of merozoites or in the secretory organelles and could show that the selection criteria were sufficient to identify novel invasion related candidate proteins. Nonetheless, not all compounds of the invadome are discovered yet, which demands for another update.

### **4.2.1 Identification of novel candidates**

The chosen 38 genes were endogenously fused to GFP and 29 cell lines could be selected on neomycin using the pSLI system (Birnbaum and Flemming et al., 2017). The 29 obtained stable cell lines were further analysed using fluorescence microscopy in unfixed parasites and subdivided into different categories based on their localization. In total, we identified 15 candidates localizing to invasion related compartments. Among these, we found four proteins at the surface of late stage parasites and free merozoites, two candidate proteins localized to the IMC or BC, and nine fusion proteins were detected at the apical pole of the parasites (Figure 50).

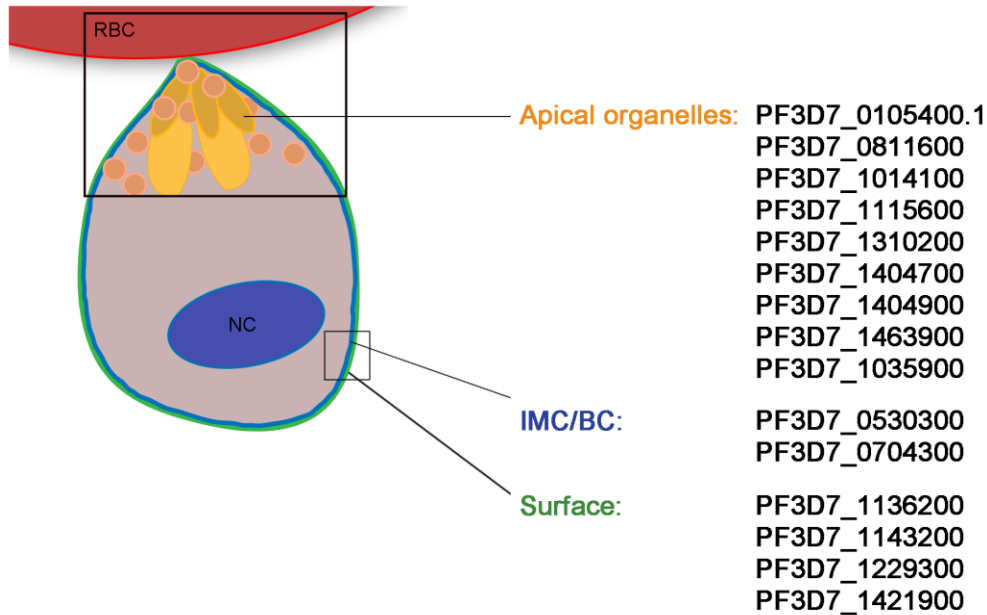


**Figure 50: Schematic representation of a merozoite and candidate genes that were localized to the invasion related compartments.** The invasion relevant compartments are depicted in orange (apical organelles), blue (IMC and BC), and green (surface). RBC, red blood cell; NC, nucleus.

#### 4.2.2 Functional domains within the localized candidate genes

Among the 15 localized proteins four candidates other contained predicted functional domains besides the predicted SP and TMs. The candidates localized to the surface (PF3D7\_1143200 and PF3D7\_1421900) or the apical pole of the parasite (PF3D7\_1035900, and PF3D7\_1463900) (Figure 51), and gene disruption approach revealed at least three of the candidates to be likely essential for parasite growth in blood stage (PF3D7\_1143200, PF3D7\_1035900, and PF3D7\_1463900).

Among the surface candidates we identified a putative copper transporter (PF3D7\_1421900) (Rasoloson et al., 2004; Kenthirapalan et al., 2016) and a putative DnaJ protein (PF3D7\_1143200) (Hiller et al., 2004; LaCount et al., 2005;).



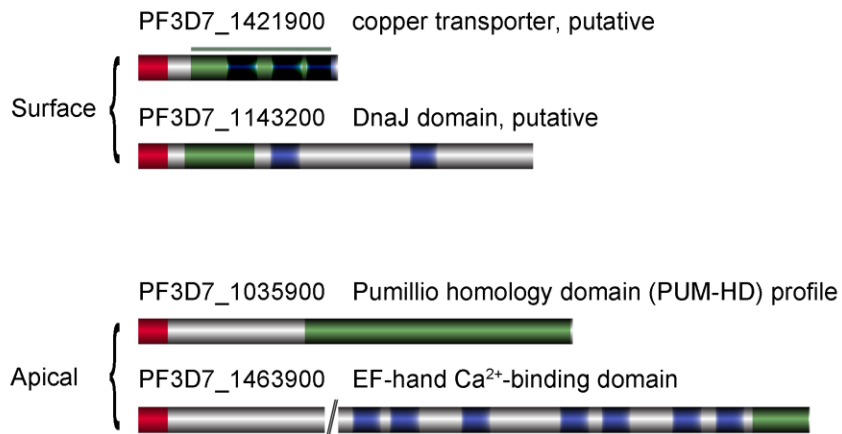


**Figure 51: Annotated functional domains within the 15 localized candidates.** Four of the candidate genes display other predicted functional domains (depicted in green) besides the predicted SP (red) and TMs (blue). Two of the candidates localized to the surface and two to the apical pole of the parasite.

**Candidate PF3D7\_1421900** is a putative copper transporter, harboring a potential copper transporter domain (Rasoloson et al., 2004). Copper is an essential trace element for all organisms and a crucial cofactor for metalloenzymes such as cytochrome-c oxidase (Rasoloson et al., 2004). The copper chelator neocuproine was shown to inhibit the transition of ring stage to trophozoites in *P. falciparum* parasites, which indicates the requirement of copper for parasite development (Rasoloson et al., 2004). Copper catalyses electron transfer reactions as well as the generation of potentially toxic reactive oxygen species (Kenthirapalan et al., 2014). Cuperozymes are able to cycle copper between a stable oxidized ( $\text{Cu}^{2+}$ ) and an unstable ( $\text{Cu}^+$ ) state for diverse redox reactions. As a consequence this reaction makes copper potentially toxic as it generates oxygen radicals via the Fenton reaction. Toxic free ionic copper thus needs to be carefully sequestered by specific cellular mechanisms (Halliwell and Gutteridge, 1984; Wardman and Candeias, 1996; Puig et al., 2002; Rasoloson et al., 2004). The exact sources of copper for parasite growth during blood stage development, however, are unknown. Inside the RBCs high amount of the copper is associated with copper superoxide dismutase (Cu/Zn SOD) (Speisky et al., 2003). Rasoloson and colleagues

therefore suggested an uptake of the erythrocyte derived Cu/Zn SOD along with haemoglobin in the parasite food vacuole as the main source for copper (Rasoloson et al., 2004). Erythrocytes contain 20  $\mu$ M copper and it was shown that copper content in iRBCs decreases during growth of the parasite (Beutler et al., 1995; Rasoloson et al., 2004). Also, extracellular copper chelation does not inhibit parasite growth. These findings support the hypothesis that *P. falciparum* parasites export copper to minimize its toxicity (Rasoloson et al., 2004). Parasitic protozoa such as *P. falciparum* allocate only 2 to 3% of their genome to membrane transporters and only 3 genes encoding for copper transporters are known in *Plasmodium* spp. to date (Rasoloson et al., 2004; Martin et al., 2009; Choveaux et al., 2012; Kenthirapalan et al., 2014). Our localization analysis of PF3D7\_1421900 could situate the GFP fusion protein to the surface of schizont-stage parasites and merozoites. This observation concurs with the localization of other *Plasmodium* copper transporters such as PF3D7\_143900 (Choveaux et al., 2012) and *PbCuTP* (Kenthirapalan et al., 2014), which localize to the erythrocyte and parasite PM. The presence of three TMs is considered definitive for copper transport proteins (De Feo et al., 2009). Also copper transporters in general comprise a specific motif in the second TM such as MxxxM and GxxxG (Aller et al., 2004; Puig et al., 2002). Candidate PF3D7\_1421900 comprises three TMs and a metal binding motif (MxxxM) in the second TM, which, although not restricted to copper transporters, was also shown to be important for copper transporter 1 (CRT1) function (Puig et al., 2002). The presence on the surface of free merozoites strongly suggests implication of the candidate in invasion. The source for copper during blood stage parasite growth might result from erythrocyte derived Cu/Zn SOD as suggested by Rasoloson and colleagues. However, the presence of the copper transporter in the PPM may indicate the requirement during the first hours post invasion as merozoites carry the protein early from the beginning. This presence does not necessarily involve the transporter in invasion but might indicate a function in the regulation of copper homeostasis during invasion or subsequent to the process. As a healthy copper homeostasis is essential for parasite growth and fertility, and thus for

parasite survival (Marva et al., 1989; Kenthirapalan et al., 2014), further functional analyses are currently under progress.

**Candidate PF3D7\_1143200** is a putative DnaJ protein. DnaJ domains are functional domains of all heat shock proteins (Hsps). Hsps in general are molecular chaperones and implicated in many diverse processes such as folding of nascent proteins or the translocation of proteins across membranes (Njunge et al., 2013). According to their molecular weight, which is ~40 kDa for the present candidate, they are grouped into different families. Hsp40s can further be classified into type I-IV based on the presence of other than the DnaJ domain (Botha et al., 2007, review). Lacking of other than the DnaJ domain most probably classifies candidate PF3D7\_1143200 as a type III Hsp40 (Figure 52). This is the biggest group of Hsp40s, however functional information is rare. In *P. falciparum*, Hsps play crucial roles at the host-parasite interface, such as Hsp101, which mediates protein export into the host cell (Shonai and Blatch, 2014; Beck et al., 2014).

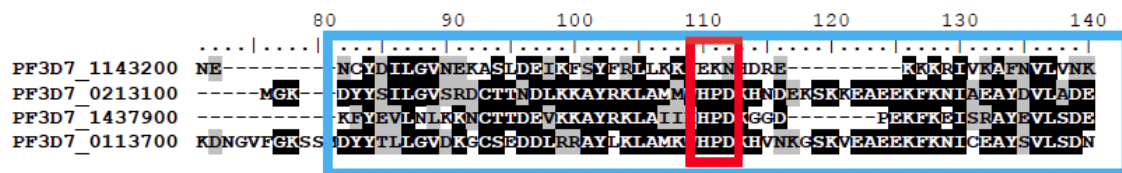


**Figure 52: Alignment of PF3D7\_1143200 with known Hsp proteins.** The presence of a DnaJ domain (blue box) verifies candidate PF3D7\_1143200 as a Hsp40 protein. The absence of HPD domain (red box) most probably classifies the candidate as a type III Hsp40 (with thanks to Tawanda Zininga).

Subsequent to invasion, the parasite starts to remodel its human host, which requires extensive protein folding, complex assembly and disassembly, as well as translocation of proteins to diverse subcellular compartments. Hsp40s and 70s are proposed to play a significant role in the establishment and development of the parasite within the host

cells (Pesce and Blatch, 2014). Further they are important regulators to ensure correct protein folding and transcription under stress conditions such as exposure of the parasite to temperature fluctuation during transmission and regular fever bouts of the human host (Rug and Maier, 2011). Other members of the type III Hsp402 were shown to act in processes such as ER translocation, ER-associated degradation, or display increased mRNA levels upon heat shock (Rug and Maier, 2011; reviewed by Schnell and Hebert, 2003; Hosoda et al., 2010;30, Watanabe, 1997). Direct involvement in the invasion process has not been shown to date. Nonetheless, localization of our candidate protein PF3D7\_1143200 to the surface of late stage parasites and merozoites might be a hint for at least an indirect role in egress from or invasion in RBCs. Further, upon several attempts to disrupt this candidate gene no parasites were obtained, which suggests the candidate to be likely essential. However, pursuing functional characterization will provide more detailed information about its explicit role and interacting partners.

The group of apical candidates comprises a probable protein containing a predicted pumilio homology domain (PUM-HD) profile (PF3D7\_1035900), and a protein of unknown function, which displays a predicted EF-hand  $\text{Ca}^{2+}$ -binding domain (PF3D7\_1463900).

**Candidate PF3D7\_1035900** was annotated as a probable protein with no further definition. Besides the SP it displays a Pumilio homology domain (PUM-HD), which classifies the candidate as member of the Pumilio family of proteins (Puf). Puf proteins are known to regulate translation and mRNA stability in many diverse eukaryotic organisms ranging from plants to fungi, animals and protists (Parisi and Lin, 2000). The signature feature of this protein family is a highly conserved core RNA-binding domain, referred to as the Puf domain, consisting of eight tandem repeats of an approximately 36 aa sequence motif, surrounded by short N- and C-terminal conserved regions (Zamore et al., 1997; B. Zhang et al., 1997). In a bioinformatic survey Reddy and collaborators identified 189 putative RNA-binding proteins (RBPs) in *P. falciparum*,

which can be classified in 13 different families, including the family of Puf proteins (Reddy et al., 2015). The presence of so many RBPs underlines the importance of post-transcriptional regulation in *P. falciparum*. The Pumilio homology domain (PUM-HD) is a sequence specific RNA binding domain and several Puf family members have been shown to bind specific RNA sequences, which are mainly found in the 3'UTR of mRNA. This binding leads to a repression of target mRNA translation and enhances its decay (Souza et al., 1999; Tadauchi et al., 2001; Wharton et al.; B. Zhang et al., 1997). In *P. falciparum* two Puf proteins are found, namely Puf1 and Puf2 (Cui et al., 2002; Fan et al., 2004; Miao et al., 2010). Puf1 and Puf2 are expressed differential in gametocytes during the erythrocytic development. Overexpression and knock down approaches of PfPuf2 resulted in the repression and elevation of gametocytogenesis, respectively. This suggests a role during sexual differentiation and development and therefore in transmission from the human to the mosquito host (Cui et al., 2002; Fan et al., 2004; Gomes-Santos et al., 2011; Miao et al., 2010). In contrast to Puf1 and Pu2, candidate PF3D7\_1035900 expression has its maximum in late erythrocytic stages and fluorescence analysis revealed an apical localization in free merozoites, which suggests a role in invasive stages. Exposure to a different extracellular milieu during the invasion process requires a rapid molecular as well as cellular re-programming. Further, the sequential steps of the invasion process are strictly regulated. The presence of candidate PF3D7\_1035900 in free merozoites therefore suggests an implication in the regulation of mRNA translation and decay of important components of invasion that may be activated or repressed before and during the process.

**Candidate PF3D7\_1463900** was not described in *P. falciparum* before but its *T. gondii* homologue was recently annotated as RON11 (Beck et al., 2013). Calcium ( $\text{Ca}^{2+}$ ) is a second messenger in eukaryotic cell signalling, which is typically released from intracellular stores in response to an (chemical, electrical or mechanical) external stimulus. This release triggers a signalling cascade resulting in an increase of

cytoplasmic-free  $\text{Ca}^{2+}$  (Erxleben et al., 1997). In *T. gondii* and *P. falciparum* increased cytosolic  $\text{Ca}^{2+}$  due to release from intracellular stores has been shown to regulate microneme secretion, which results in driving motility and invasion (Carruthers et al., 1999). Rise in cytosolic  $\text{Ca}^{2+}$  triggers secretion of microneme proteins such as EBA175 to the merozoite surface, which was shown to depend on *PfRh1*-induced  $\text{Ca}^{2+}$  signalling (Singh et al., 2010; Gao et al., 2013). Subsequent decrease of  $\text{Ca}^{2+}$  correlates with rhoptry discharge, for example CLAG3.1 and Rh2b (Singh et al., 2010). The predicted EF-calcium binding domain of candidate PF3D7\_1463900 suggests a role in binding  $\text{Ca}^{2+}$  or sensing  $\text{Ca}^{2+}$  fluctuation. Gene disruption of its homologue *TgRON11* was successful but using an inducible CRISPR/Cas9 system, depletion of the gene did not affect blood stage parasites indicating that RON11 is not essential for parasite survival in *T. gondii* (Wang et al., 2016). Nevertheless, PF3D7\_1463900 candidate was refractory to gene deletion, which indicates the protein to be likely essential for blood stage parasites. But as observed for the *T. gondii* homologue, targeted gene disruption is just a first prediction. Future studies in our lab using inducible KO systems will be performed to investigate the likely essentiality of candidate gene PF3D7\_1463900 for *P. falciparum* parasites.

### 4.2.2.1 Candidates with low expression

The expression of six fusion candidate proteins was too low for localization via fluorescence microscopy. Comparing the expression profiles of those to the 15 genes that could be localized to invasion related compartments (candidates of group I-III) no obvious difference can be detected in the minimum and maximum expression values (Figure 53), which would have been a possible explanation for the absence of GFP signals. Two candidates display a delay of minimum and maximum expression values towards later time points in the parasite life cycle, with the minimum peak at around 38 hpi and the maximum peak at around 48 hpi (Figure 53, left panel). Also, approximately 30% of all genes display a delayed peak of mRNA compared to protein levels (Foth et al., 2011; Le Roch et al., 2004). This might explain why the fusion proteins could not be

detected in late stages, as protein expression would be expected in ring stages. However, as mentioned before, known invasins display an expression maximum during late schizogony and in merozoite stages (Le Roch et al., 2003). Therefore ring stage parasites were not investigated in this approach.

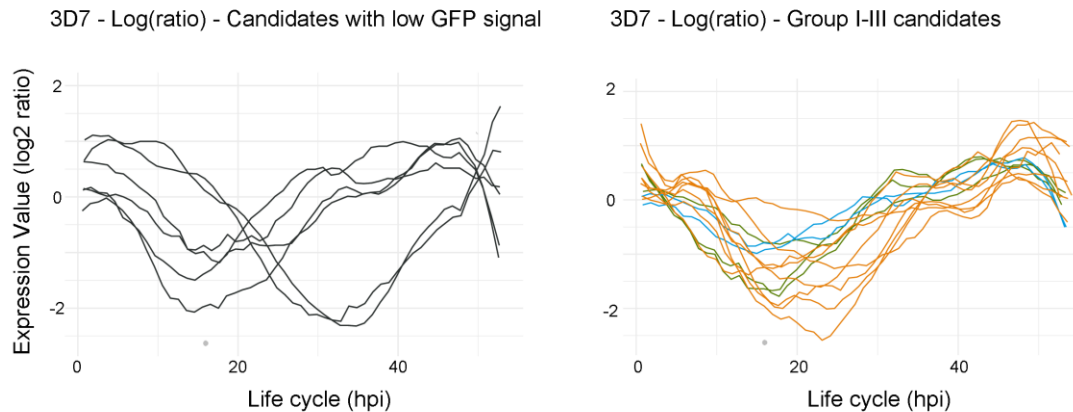


**Figure 53: Expression values of the candidate genes.** **Left panel:** expression values of candidate genes that could not be localized via fluorescence microscopy analysis. **Right panel:** expression levels of candidate genes that could be localized and were subdivided in group I-III depending on their localization. Color code refers to the compartment where the proteins were localized (green, surface; turquoise, IMC/BC; orange, apical). Expression profiles were available on plasmoDB.org.

Different features such as SPs, TMs, rare codons, introns and AT-rich sequences are known to affect recombinant expression of *P. falciparum* proteins (Vedadi et al., 2007). Only one of the six candidates encodes for predicted TMs, but all of them display a SP as we screened exclusively for those genes. Additionally, for unknown reasons, the *P. falciparum* has an exceptionally high AT content (~80% in 3D7 parasites) compared to other eukaryotes and even to other *Plasmodium* spp. (Gardner et al., 2002). This might at least to some extent explain the low expression rate of some candidate proteins.

Further, gene expression is strictly mediated by different mechanisms. These include epigenetic, transcriptional, post-transcriptional as well as post-translational mechanisms such as phosphorylation (Cui et al., 2015; Doerig et al., 2015; Hughes et al., 2010; Voss

et al., 2014; Zhang et al., 2013). It is known that external circumstances such as temperature, pH or other stressors can lead to suppression or activation of a great diversity of genes. Further, stress is one of the most common modes of global mRNA translational repression in eukaryotes (reviewed in Vembar et al., 2016). Accordingly, some of these candidates might only be expressed upon certain external stimuli or circumstances and therefore are silenced under normal conditions. Besides, some proteins are only expressed upon loss of function of others. This is known for important invasins such as EBA175 as described previously, *PfRh4* is upregulated when EBA175 is not functional (Dolan et al., 1990; Reed et al., 2000; Duraisingh et al., 2003; Gilberger et al., 2003a; Stubbs et al., 2005).

Additionally, mass spectrometry data of five out of the six candidates provide expression evidence in stag V gametocytes, sporozoites or ookinets, which might be a hint for a role in transmission and fertilisation. However, mass spectrometry evidence was not taken into account for candidate selection in the present screen. Nonetheless, it would be interesting to investigate into other than blood stages for further characterization of these proteins.

### 4.2.3 Critical aspects

Seven of the selected candidate genes could not be successfully integrated into the appropriate loci and two could not be selected for pSLI-GFP plasmids. Some of the candidates are rather small but it was shown that integration of fragments with a homology region exceeding 200 bp should be feasible as validated by Birnbaum and Flemming et al. (2017). The absence of an amplicon in the seven neomycin resistant transgenic cell lines could be explained by the integration of the plasmid in other than the appropriate loci. Further, previous experience showed that a certain percentage of proteins cannot be C-terminally fused to GFP. This may result from heavy C-terminal modifications such as phosphorylation or other post-translational modification. N-terminal fusion to GFP using a codon optimized SP-sequence would be an option to



circumvent these restrictions. Another chance for successful C-terminal tagging would be the use of smaller protein tags such as TY1, MYC, or HA-sequence. These sequences are significantly shorter than the GFP sequence and may therefore enable the generation of endogenously C-terminal tagged parasite cell lines. Episomal expression as performed by Haase and collaborators would also be an option to circumvent the difficulties of endogenous tagging by homologues recombination (Haase et al., 2008). Late-stage-specific promoters with strong activity such as the *ama1* promoter could be used to drive expression of the proteins. However, overexpression of proteins instead of insertion into the genome results in higher amounts the investigated protein as it occurs on top of the endogenous protein expression. Secretory organelles for instance are rather small compartments, which might not have enough space for a higher amount of proteins than usual. Wild-type localization of the fusion proteins therefore might not be assured. Our approach therefore was to examine expression under conditions as natural as possible.

Also, the original output data set generated by Hu and collaborators (2009) encompassed candidates that did not contain a predicted SP. 11 of the 31 proteins that were predominantly targeted to the secretory organelles or the IMC did neither contain a SP nor a TM. Nevertheless they could be shown to be associated to invasion (Haase et al., 2008). Likewise, the glideosome associated protein 45 (GAP45) was shown to localize to the IMC despite the absence of a N-terminal SP (Ridzuan et al., 2012). It therefore should be considered to reassess selection criteria and further to investigate PTMs such as myristoylation and palmitoylation which have been suggested to drive IMC localization of proteins or at least of GAP45 (Rees-Channer et al., 2006).

As mentioned before, about 30% of all genes display a delayed peak of mRNA compared to protein levels (Foth et al., 2011; Le Roch et al., 2004). One selection criterion for our screen was a maximum expression level in late stages, which refers to a peak around 44 hpi. As also mentioned previously, protein expression is tightly regulated at transcriptional as well as translational levels (Le Roch et al., 2003; Bozdech and Llinas et

al., 2003; Doerig et al., 2015). Delayed translation of proteins due to post-transcriptional as well as -translational modifications such as phosphorylation is a common regulatory mechanism. The selection of candidate genes with maximum expression values earlier in the life cycle therefore might have to be considered to include likely invasion related candidate genes that might have falsely been excluded from our screen.

Further, microarray and RNA sequencing both are methods that allow for high throughput profiling of the whole transcriptome. Nonetheless, it has to be kept in mind that microarray as well as RNA sequencing evidence only provide transcriptional data but do not relay on actual expression of proteins – at all. A critical point as discussed above, which has to be admitted and might explain the absence of some of the candidate fusion proteins when analysed by fluorescence microscopy. Mass spectrometry in contrast provides expression data of proteins that have actually been detected and therefore must have been expressed. A reasonable future approach therefore would implicate evidence derived from mass spectrometry to circumvent the problem of hypothetical proteins that remain hypothetical instead of being actually expressed.

### 4.3 Conclusion and outlook

Merozoite invasion into human erythrocytes is a fast and crucial event. It obliges sequential steps that involve an unidentified number of proteins (LaCount et al., 2005) and needs to be tightly organized.

Performing functional analysis we provided further characterization of the well-known invasion ligand EBA175 and could show that in contrast to other invasion ligands such as AMA1 and Rh4, none of the putative phosphorylation sites that were assessed within the cytoplasmic tail do have any essential impact on the functionality of EBA175.

Further we used a bioinformatic screen to identify new invasion relevant proteins. Combining microarray and RNA sequencing evidence we searched for late transcribed genes that localize to the secretory organelles, the merozoite surface or the IMC, and thus are likely involved in invasion. We identified 15 candidates in those compartments and started to investigate into their essentiality for blood stage parasites, which suggests four of them as likely essential for blood stage growth of the parasite.

However, identification of these 15 putative invasion relevant candidates is just the beginning and paves the way for an update of the invadome. Functional characterization using inducible knock out systems such as Cre recombinase or the *glms* system will show if these candidates could be the next potential therapeutic targets and will help to understand the complex mechanism of erythrocyte invasion.

## Bibliography

- Adams, J. H., Blair, P. L., Kaneko, O., and Peterson, D. S. (2001). An expanding ebl family of *Plasmodium falciparum*. *Trends Parasitol*, *17*(6), 297-299. doi: 10.1016/S1471-4922(01)01948-1
- Adams, J. H., Sim, B. K., Dolan, S. A., Fang, X., Kaslow, D. C., and Miller, L. H. (1992). A family of erythrocyte binding proteins of malaria parasites. *Proceedings of the National Academy of Sciences of the United States of America*, *89*(15), 7085-7089.
- Aguilar, R., Magallon-Tejada, A., Achtman, A. H., Moraleda, C., Joice, R., Cisteró, P., . . . Mayor, A. (2014). Molecular evidence for the localization of *Plasmodium falciparum* immature gametocytes in bone marrow. *Blood*, *123*(7), 959-966. doi: 10.1182/blood-2013-08-520767
- Ahmed, and Cox-Singh. (2015). *Plasmodium knowlesi* – an emerging pathogen. *ISBT Sci Ser.*, *10*(Suppl 1), 134-140.
- Aikawa, M., Hepler, P. K., Huff, C. G., and Sprinz, H. (1966). THE FEEDING MECHANISM OF AVIAN MALARIAL PARASITES. *The Journal of Cell Biology*, *28*(2), 355-373.
- Aikawa, M., Miller, L., Johnson, J., and Rabbege, J. (1978). Erythrocyte entry by malarial parasites. A moving junction between erythrocyte and parasite. *The Journal of Cell Biology*, *77*(1), 72-82. doi: 10.1083/jcb.77.1.72
- Aikawa, M., Miller, L. H., Rabbege, J., and Epstein, N. (1981). Freeze-fracture study of the erythrocyte membrane during malarial parasite invasion. *J Cell Biol*, *92*(55-62).
- Aikawa, M., Torii, M., Sjolander, A., Berzins, K., Perlmann, P., and Miller, L. H. (1990). Pf155/RESA antigen is localized in dense granules of *Plasmodium falciparum* merozoites. *Exp Parasitol.*, *71*, 326-329.
- Akhouri, R. R., Sharma, A., Malhotra, P., and Sharma, A. (2008). Role of *Plasmodium falciparum* thrombospondin-related anonymous protein in host-cell interactions. *Malar J*, *7*, 63. doi: 10.1186/1475-2875-7-63
- Alano, P. (2014). The sound of sexual commitment breaks the silencing of malaria parasites. *Trends Parasitol*, *30*, 509-510.
- Aller, S. G., Eng, E. T., De Feo, C. J., and Unger, V. M. (2004). Eukaryotic CTR Copper Uptake Transporters Require Two Faces of the Third Transmembrane Domain for Helix Packing, Oligomerization, and Function. *J Biol Chem*, *279*(51), 53435-53441. doi: 10.1074/jbc.M409421200
- Aravind, L., Iyer, L. M., Wellems, T. E., and Miller, L. H. (2003). Plasmodium biology: genomic gleanings. *Cell*, *115*(7), 771-785. doi: 10.1016/S0092-8674(03)01023-7
- Ariey, F., Witkowski, B., Amaratunga, C., Beghain, J., Langlois, A.-C., Khim, N., . . . Ménard, D. (2014). A molecular marker of artemisinin-resistant *Plasmodium falciparum* malaria. *Nature*, *505*(7481), 50-55. doi: 10.1038/nature12876
- Ashong, J. O., Blench, I. P., and Warhurst, D. C. (1989). The composition of haemozoin from *Plasmodium falciparum*. *Transition of the Royal Society of Tropical Medicine and Hygiene*, *83*, 167-172.

- Audran, R., Cachat, M., Lurati, F., Soe, S., Leroy, O., Corradin, G., . . . Spertini, F. (2005). Phase I Malaria Vaccine Trial with a Long Synthetic Peptide Derived from the Merozoite Surface Protein 3 Antigen. *Infect Immun*, *73*(12), 8017-8026. doi: 10.1128/IAI.73.12.8017-8026.2005
- Baker, R. P., Wijetilaka, R., and Urban, S. (2006). Two Plasmodium Rhomboid Proteases Preferentially Cleave Different Adhesins Implicated in All Invasive Stages of Malaria. *PLoS Pathog*, *2*(10), e113. doi: 10.1371/journal.ppat.0020113
- Bannister, L., and Mitchell, G. (2003). The ins, outs and roundabouts of malaria. *Trends Parasitol*, *19*(5), 209-213.
- Bannister, L. H., Butcher, G. A., Dennis, E. D., and Mitchell, G. H. (1975). Structure and invasive behaviour of *Plasmodium knowlesi* merozoites *in vitro*. *Parasitology*, *71*, 483-491.
- Bannister, L. H., Hopkins, J. M., Fowler, R. E., Krishna, S., and Mitchell, G. H. (2000). A brief illustrated guide to the ultrastructure of Plasmodium falciparum asexual blood stages. *Parasitology Today*, *16*(10), 427-433. doi: 10.1016/S0169-4758(00)01755-5
- Bannister, L. H., Mitchell, G. H., Butcher, G. A., Dennis, E. D., and Cohen, S. (1986). Structure and development of the surface coat of erythrocytic merozoites of Plasmodium knowlesi. *Cell and Tissue Research*, *245*(2), 281-290. doi: 10.1007/bf00213933
- Barker, D. D., Wang, C., Moore, J., Dickinson, L. K., and Lehmann, R. (1992). Pumilio is essential for function but not for distribution of the Drosophila abdominal determinant Nanos. *Genes & Development*, *6*(12A), 2312-2326. doi: 10.1101/gad.6.12a.2312
- Bartfai, R., Hoeijmakers, W. A., Salcedo-Amaya, A. M., Smits, A. H., Janssen-Megens, E., Kaan, A., . . . Stunnenberg, H. G. (2010). H2A.Z demarcates intergenic regions of the plasmodium falciparum epigenome that are dynamically marked by H3K9ac and H3K4me3. *PLoS Pathog*, *6*(12), e1001223. doi: 10.1371/journal.ppat.1001223
- Bartoloni, A., and Zammarchi, L. (2012). Clinical aspects of uncomplicated and severe malaria. *Mediterr J Hematol Infect Dis*, *4*(1), e2012026. doi: 10.4084/MJHID.2012.026
- Baruch, D. I., Pasloske, B. L., Singh, H. B., Bi, X., Ma, X. C., Feldmann, M., . . . Howard, R. J. (1995). Cloning the *P. falciparum* gene encoding PfEMP1, a malarial variant antigen and adherence receptor on the surface of parasitized human erythrocytes. *Cell*, *82*.
- Baum, J., Chen, L., Healer, J., Lopaticki, S., Boyle, M., Triglia, T., . . . Cowman, A. F. (2009). Reticulocyte-binding protein homologue 5 – An essential adhesin involved in invasion of human erythrocytes by Plasmodium falciparum. *International Journal for Parasitology*, *39*(3), 371-380. doi: <https://doi.org/10.1016/j.ijpara.2008.10.006>
- Baum, J., Gilberger, T. W., Frischknecht, F., and Meissner, M. (2008). Host-cell invasion by malaria parasites: insights from Plasmodium and Toxoplasma. *Trends Parasitol*, *24*(12), 557-563. doi: 10.1016/j.pt.2008.08.006

- Baum, J., Richard, D., Healer, J., Rug, M., Krnajski, Z., Gilberger, T. W., . . . Cowman, A. F. (2006). A conserved molecular motor drives cell invasion and gliding motility across malaria life cycle stages and other apicomplexan parasites. *J Biol Chem*, *281*(8), 5197-5208. doi: 10.1074/jbc.M509807200
- Beck, J. R., Fung, C., Straub, K. W., Coppens, I., Vashisht, A. A., Wohlschlegel, J. A., and Bradley, P. J. (2013). A Toxoplasma palmitoyl acyl transferase and the palmitoylated armadillo repeat protein TgARO govern apical rhoptry tethering and reveal a critical role for the rhoptries in host cell invasion but not egress. *PLoS Pathog*, *9*(2), e1003162. doi: 10.1371/journal.ppat.1003162
- Beck, J. R., Muralidharan, V., Oksman, A., and Goldberg, D. E. (2014). HSP101/PTEX mediates export of diverse malaria effector proteins into the host erythrocyte. *Nature*, *511*(7511), 592-595. doi: 10.1038/nature13574
- Berendt, A., R., Turner, G. D. H., and Newbold, C. I. (1994). Cerebral malaria: the sequestration hypothesis. *Parasitol. Today*, *10*, 412-412.
- Bergman, L. W., Kaiser, K., Fujioka, H., Coppens, I., Daly, T. M., Fox, S., . . . Kappe, S. H. I. (2003). Myosin A tail domain interacting protein (MTIP) localizes to the inner membrane complex of *Plasmodium* sporozoites. *J Cell Sci*, *116*(1), 39-49. doi: 10.1242/jcs.00194
- Besteiro, S., Michelin, A., Poncet, J., Dubremetz, J.-F., and Lebrun, M. (2009). Export of a *Toxoplasma gondii* Rhoptry Neck Protein Complex at the Host Cell Membrane to Form the Moving Junction during Invasion. *PLoS Pathog*, *5*(2), e1000309. doi: 10.1371/journal.ppat.1000309
- Bethke, L. L., Zilversmit, M., Nielsen, K., Daily, J., Volkman, S. K., Ndiaye, D., . . . Wirth, D. F. (2006). Duplication, gene conversion, and genetic diversity in the species-specific acyl-CoA synthetase gene family of *Plasmodium falciparum*. *Molecular and Biochemical Parasitology*, *150*(1), 10-24. doi: <https://doi.org/10.1016/j.molbiopara.2006.06.004>
- Beutler, E., Lichtman, M., Coller, B., and Kipps, T. (1995). Composition of the erythrocyte. *Williams Hematology*, 364-369.
- Billker, O., Lindo, V., Panico, M., Etienne, A. E., Paxton, T., Dell, A., and *al., e.* (1998). Identification of xanthurenic acid as the putative inducer of malaria development in the mosquito. *Nature*, *392*, 289-292.
- Birnbaum, J., Flemming, S., Reichard, N., Soares, A. B., Mesen-Ramirez, P., Jonscher, E., . . . Spielmann, T. (2017). A genetic system to study *Plasmodium falciparum* protein function. *Nat Methods*, *14*(4), 450-456. doi: 10.1038/nmeth.4223
- Blackman, M. J., and Carruthers, V. B. (2013). Recent insights into apicomplexan parasite egress provide new views to a kill. *Current opinion in microbiology*, *16*(4), 459-464. doi: 10.1016/j.mib.2013.04.008
- Blair, P. L., Kappe, S. H. I., Maciel, J. E., Balu, B., and Adams, J. H. (2002). *Plasmodium falciparum* MAEBL is a unique member of the ebl family. *Molecular and Biochemical Parasitology*, *122*(1), 35-44. doi: [https://doi.org/10.1016/S0166-6851\(02\)00067-1](https://doi.org/10.1016/S0166-6851(02)00067-1)
- Bosch, J., Turley, S., Roach, C. M., Daly, T. M., Bergman, L. W., and Hol, W. G. J. (2007). The closed MTIP-MyosinA-tail complex from the malaria parasite invasion

- machinery. *Journal of Molecular Biology*, 372(1), 77-88. doi: 10.1016/j.jmb.2007.06.016
- Botha, M., Pesce, E. R., and Blatch, G. L. (2007). The Hsp40 proteins of *Plasmodium falciparum* and other apicomplexa: Regulating chaperone power in the parasite and the host. *The International Journal of Biochemistry & Cell Biology*, 39(10), 1781-1803. doi: <https://doi.org/10.1016/j.biocel.2007.02.011>
- Boyle, M. J., Wilson, D. W., Richards, J. S., Riglar, D. T., Tetteh, K. K. A., Conway, D. J., . . . Beeson, J. G. (2010). Isolation of viable *Plasmodium falciparum* merozoites to define erythrocyte invasion events and advance vaccine and drug development. *Proceedings of the National Academy of Sciences of the United States of America*, 107(32), 14378-14383. doi: 10.1073/pnas.1009198107
- Bozdech, M., Llinas, M., Pulliam, B., Wong, E., Zhu, J., and DeRisi, J. (2003). The Transcriptome of the Intraerythrocytic Developmental Cycle of *Plasmodium falciparum*. *Plos Biology*. doi: 10.1371/journal.pbio.0000005.st001
- Bruce, M., Alano, P., Duthie, S., and Carter, R. (1990). Commitment of the malaria parasite *Plasmodium falciparum* to sexual and asexual development. *Parasitology*, 100(2), 191-200.
- Bullen, H. E., Tonkin, C. J., O'Donnell, R. A., Tham, W.-H., Papenfuss, A. T., Gould, S., . . . Gilson, P. R. (2009). A Novel Family of Apicomplexan Glideosome-associated Proteins with an Inner Membrane-anchoring Role. *J Biol Chem*, 284(37), 25353-25363. doi: 10.1074/jbc.M109.036772
- Camus, D., and Hadley, T. (1985a). A *Plasmodium falciparum* antigen that binds to erythrocytes and merozoites. *Science*, 230, 553-556.
- Camus, D., and Hadley, T. (1985b). A *Plasmodium falciparum* antigen that binds to host erythrocytes and merozoites. *Science*, 230(4725), 553-556. doi: 10.1126/science.3901257
- Carruthers, V., Giddings, O., and Sibley, L. (1999). Secretion of micronemal proteins is associated with toxoplasma invasion of host cells. *Cell Microbiol*, 1(2), 225-235.
- Carruthers, V. B., and Sibley, L. D. (1999). Mobilization of intracellular calcium stimulates microneme discharge in *Toxoplasma gondii*. *Mol. Microbiol.*, 31, 421-428.
- Carruthers, V. B., and Tomley, F. M. (2008). Receptor-ligand interaction and invasion: Microneme proteins in apicomplexans. *Sub-cellular biochemistry*, 47, 33-45.
- Carter, R., and Miller, L. H. (1979). Evidence for environmental modulation of gametocytogenesis in *Plasmodium falciparum* in continuous culture. *Bull World Health Organ*, 57(Suppl 1), 37-52.
- Cavalier-Smith, T. (1993). Kingdom protozoa and its 18 phyla. *Microbiological Reviews*, 57(4), 953-994. doi: 0146-0749/93/040953-42\$02.00/0
- Cavasini, C. E., Mattos, L. C. d., Couto, Á. A. D. A., Bonini-Domingos, C. R., Valencia, S. H., Neiras, W. C. d. S., . . . Machado, R. L. D. (2007). *Plasmodium vivax* infection among Duffy antigen-negative individuals from the Brazilian Amazon region: an exception? *Transactions of The Royal Society of Tropical Medicine and Hygiene*, 101(10), 1042-1044. doi: 10.1016/j.trstmh.2007.04.011

- Chitnis, C. E., and Miller, L. H. (1994). Identification of the erythrocyte binding domains of *Plasmodium vivax* and *Plasmodium knowlesi* proteins involved in erythrocyte invasion. *The Journal of Experimental Medicine*, *180*(2), 497-506.
- Choveaux, D. L., Przyborski, J. M., and Goldring, J. D. (2012). A *Plasmodium falciparum* copper-binding membrane protein with copper transport motifs. *Malar J*, *11*(1), 397. doi: 10.1186/1475-2875-11-397
- Cova, M., Rodrigues, J. A., Smith, T. K., and Izquierdo, L. (2015). Sugar activation and glycosylation in *Plasmodium*. *Malar J*, *14*(1), 427. doi: 10.1186/s12936-015-0949-z
- Cowman, A. F., Berry, D., and Baum, J. (2012). The cellular and molecular basis for malaria parasite invasion of the human red blood cell. *J Cell Biol*, *198*(6), 961-971. doi: 10.1083/jcb.201206112
- Cowman, A. F., and Crabb, B. S. (2006). Invasion of red blood cells by malaria parasites. *Cell*, *124*(4), 755-766. doi: 10.1016/j.cell.2006.02.006
- Cox, F. E. (2010). History of the discovery of the malaria parasites and their vectors. *Parasit Vectors*, *3*(1), 5. doi: 10.1186/1756-3305-3-5
- Crabb, B., Rug M, Gilberger TW, Thompson JK, Triglia T, Maier AG, and AF., C. (2004). Transfection of the human malaria parasite *Plasmodium falciparum*. *Methods Mol Biol.*, *270*. doi: 10.1385/1-59259-793-9:263
- Crosnier, C., Bustamante, L. Y., Bartholdson, S. J., Bei, A. K., Theron, M., Uchikawa, M., . . . Wright, G. J. (2011). Basigin is a receptor essential for erythrocyte invasion by *Plasmodium falciparum*. *Nature*, *480*(7378), 534-537. doi: 10.1038/nature10606
- Cui, L., Fan, Q., and Li, J. (2002). The malaria parasite *Plasmodium falciparum* encodes members of the Puf RNA-binding protein family with conserved RNA binding activity. *Nucleic Acids Res*, *30*(21), 4607-4617.
- Cui, L., Lindner, S., and Miao, J. (2015). Translational regulation during stage transitions in malaria parasites. *Annals of the New York Academy of Sciences*, *1342*(1), 1-9. doi: 10.1111/nyas.12573
- D'Alessandro, U., and Buttiëns, H. (2001). History and importance of antimalarial drug resistance. *Tropical Medicine & International Health*, *6*(11), 845-848. doi: 10.1046/j.1365-3156.2001.00819.x
- Daneshvar, C., Davis, T. M., Cox-Singh, J., Rafa'ee, M. Z., Zakaria, S. K., Divis, P. C., and Singh, B. (2009). Clinical and laboratory features of human *Plasmodium knowlesi* infection. *Clin Infect Dis*, *49*(6), 852-860. doi: 10.1086/605439
- Date, S. V., and Stoeckert, C. J., Jr. (2006). Computational modeling of the *Plasmodium falciparum* interactome reveals protein function on a genome-wide scale. *Genome Res*, *16*(4), 542-549. doi: 10.1101/gr.4573206
- De Feo, C. J., Aller, S. G., Siluvai, G. S., Blackburn, N. J., and Unger, V. M. (2009). Three-dimensional structure of the human copper transporter hCTR1. *Proceedings of the National Academy of Sciences of the United States of America*, *106*(11), 4237-4242. doi: 10.1073/pnas.0810286106



- de Koning-Ward, T. F., Gilson, P. R., and Crabb, B. S. (2015). Advances in molecular genetic systems in malaria. *Nat Rev Microbiol*, *13*(6), 373-387. doi: 10.1038/nrmicro3450
- De Niz, M., Burda, P.-C., Kaiser, G., del Portillo, H. A., Spielmann, T., Frischknecht, F., and Heussler, V. T. (2016). Progress in imaging methods: insights gained into Plasmodium biology. *Nature Reviews Microbiology*, *15*, 37. doi: 10.1038/nrmicro.2016.158
- Deitsch, K. W., and Wellems, T. E. (1996). Membrane modifications in erythrocytes parasitized by *Plasmodium falciparum*. *Molecular and Biochemical Parasitology*, *76*, 1-10.
- DeSimone, T. M., Bei, A. K., Jennings, C. V., and Duraisingh, M. T. (2009). Genetic analysis of the cytoplasmic domain of the PfRh2b merozoite invasion protein of Plasmodium falciparum. *International Journal for Parasitology*, *39*(4), 399-405. doi: 10.1016/j.ijpara.2008.08.008
- Di Cristina, M., Spaccapelo, R., Soldati, D., Bistoni, F., and Crisanti, A. (2000). Two Conserved Amino Acid Motifs Mediate Protein Targeting to the Micronemes of the Apicomplexan Parasite *Toxoplasma gondii*. *Molecular and Cellular Biology*, *20*(19), 7332-7341. doi: 10.1128/mcb.20.19.7332-7341.2000
- Dixon, M. W., Dearnley, M. K., Hanssen, E., Gilberger, T., and Tilley, L. (2012). Shape-shifting gametocytes: how and why does P. falciparum go banana-shaped? *Trends Parasitol*, *28*(11), 471-478. doi: 10.1016/j.pt.2012.07.007
- Dixon, M. W., Thompson, J., Gardiner, D. L., and Trenholme, K. R. (2008). Sex in *Plasmodium*: a sign of commitment. *Trends Parasitol*, *24*(4), 168-175.
- Doerig, C., Rayner, J., Scherf, A., and Tobin, A. (2015). Post-translational protein modifications in malaria parasites. *Nat Rev Microbiol*, *13*(3), 160-172.
- Dolan, S. A., Miller, L. H., and Wellems, T. E. (1990). Evidence for a switching mechanism in the invasion of erythrocytes by *Plasmodium falciparum*. *The Journal of Clinical Investigation*, *86*, 618-624.
- Dolan, S. A., Proctor, J. L., Alling, D. W., Okubo, Y., Wellems, T. E., and Miller, L. H. (1994). Glycophorin B as an EBA-175 independent Plasmodium falciparum receptor of human erythrocytes. *Molecular and Biochemical Parasitology*, *64*(1), 55-63. doi: [https://doi.org/10.1016/0166-6851\(94\)90134-1](https://doi.org/10.1016/0166-6851(94)90134-1)
- Dondorp, A. M., Nosten, F., Yi, P., Das, D., Phyto, A. P., Tarning, J., . . . White, N. J. (2009). Artemisinin Resistance in Plasmodium falciparum Malaria. *The New England Journal of medicine*, *361*(5), 455-467. doi: 10.1056/NEJMoa0808859
- Duraisingh, M. T., Maier, A. G., Triglia, T., and Cowman, A. F. (2003). Erythrocyte-binding antigen 175 mediates invasion in Plasmodium falciparum utilizing sialic acid-dependent and -independent pathways. *Proc Natl Acad Sci U S A*, *100*(8), 4796-4801. doi: 10.1073/pnas.0730883100
- Duraisingh, M. T., Triglia, T., Ralph, S. A., Rayner, J. C., Barnwell, J. W., McFadden, G. I., and Cowman, A. F. (2003). Phenotypic variation of Plasmodium falciparum merozoite proteins directs receptor targeting for invasion of human erythrocytes. *The EMBO Journal*, *22*(5), 1047-1057. doi: 10.1093/emboj/cdg096

- Dvorak, J. A., and Miller, L. H. (1975). Invasion of erythrocytes by malaria parasites. *Science*, *187*, 748-750.
- Dvorin, J. D., Bei, A. K., Coleman, B. I., and Duraisingh, M. T. (2010). Functional diversification between two related *Plasmodium falciparum* merozoite invasion ligands is determined by changes in the cytoplasmic domain. *Molecular Microbiology*, *75*(4), 990-1006. doi: 10.1111/j.1365-2958.2009.07040.x
- Elford, B. C., and Ferguson, D. J. P. (1993). Secretory processes in *Plasmodium*. *Parasitol. Today*, *9*, 80-81.
- Elmendorf, H., and K., H. (1994). *Plasmodium falciparum* exports the Golgi marker sphingomyelin synthase into a tubovesicular network in the cytoplasm of mature erythrocytes. *The Journal of Cell Biology*, *124*(4), 449-462.
- Elmendorf, H. G., and Haldar, K. (1993). Identification and localization of ERD2 in the malaria parasite *Plasmodium falciparum*: separation from sites of sphingomyelin synthesis and implications for organization of the Golgi. *The EMBO Journal*, *12*(12), 4763-4773.
- EMA, E. M. A. (2015). Assesment Report. Mosuirix (TM)
- Engelberg, K., Paul, A. S., Prinz, B., Kono, M., Ching, W., Heincke, D., . . . Gilberger, T. W. (2013). Specific phosphorylation of the PfRh2b invasion ligand of *Plasmodium falciparum*. *Biochem J*, *452*(3), 457-466. doi: 10.1042/BJ20121694
- Erxleben, C., Klauke, N., Flötenmeyer, M., Blanchard, M.-P., Braun, C., and Plattner, H. (1997). Microdomain Ca<sup>2+</sup> Activation during Exocytosis in Paramecium Cells. Superposition of Local Subplasmalemmal Calcium Store Activation by Local Ca<sup>2+</sup> Influx. *The Journal of Cell Biology*, *136*(3), 597-607. doi: 10.1083/jcb.136.3.597
- Fan, Q., Li, J., Kariuki, M., and Cui, L. (2004). Characterization of PfPuf2, member of the Puf family RNA-binding proteins from the malaria parasite *Plasmodium falciparum*. *DNA Cell Biol.*, *23*, 753-760.
- Farfour, E., Charlotte, F., Settegrana, C., Miyara, M., and Buffet, P. (2012). The extravascular compartment of the bone marrow: a niche for *Plasmodium falciparum* gametocyte maturation? *Malar J*, *11*, 285-285. doi: 10.1186/1475-2875-11-285
- Fidock, D. A., Nomura, T., Talley, A. K., Cooper, R. A., Dzekunov, S. M., Ferdig, M. T., . . . Wellems, T. E. (2000). Mutations in the *P. falciparum* Digestive Vacuole Transmembrane Protein PfCRT and Evidence for Their Role in Chloroquine Resistance. *Molecular Cell*, *6*(4), 861-871. doi: 10.1016/S1097-2765(05)00077-8
- Fidock, D. A., and Wellems, T. E. (1997). Transformation with human dihydrofolate reductase renders malaria parasites insensitive to WR99210 but does not affect the intrinsic activity of proguanil. *Proceedings of the National Academy of Sciences of the United States of America*, *94*(20), 10931-10936.
- Foth, B. J., Zhang, N., Chahal, B. K., Sze, S. K., Preiser, P. R., and Bozdech, Z. (2011). Quantitative Time-course Profiling of Parasite and Host Cell Proteins in the Human Malaria Parasite *Plasmodium falciparum*. *Molecular & Cellular Proteomics : MCP*, *10*(8), M110.006411. doi: 10.1074/mcp.M110.006411
- Foth, B. J., Zhang, N., Mok, S., Preiser, P. R., and Bozdech, Z. (2008). Quantitative protein expression profiling reveals extensive post-transcriptional regulation and post-

- translational modifications in schizont-stage malaria parasites. *Genome Biology*, 9(12), R177-R177. doi: 10.1186/gb-2008-9-12-r177
- Frenal, K., Dubremetz, J. F., Lebrun, M., and Soldati-Favre, D. (2017). Gliding motility powers invasion and egress in Apicomplexa. *Nat Rev Microbiol*, 15(11), 645-660. doi: 10.1038/nrmicro.2017.86
- Frénal, K., Polonais, V., Marq, J.-B., Stratmann, R., Limenitakis, J., and Soldati-Favre, D. (2010). Functional Dissection of the Apicomplexan Glideosome Molecular Architecture. *Cell Host Microbe*, 8(4), 343-357. doi: 10.1016/j.chom.2010.09.002
- Gamain, B., Smith, J., Miller, L., and Baruch, D. (2001). Modifications in the CD36 binding domain of the Plasmodium falciparum variant antigen are responsible for the inability of chondroitin sulfateA adherent parasites to bind CD36. *Blood*, 97(10), 3268-3274. doi: <https://doi.org/10.1182/blood.V97.10.3268>
- Gao, X., Gunalan, K., Yap, S. S. L., and Preiser, P. R. (2013). Triggers of key calcium signals during erythrocyte invasion by Plasmodium falciparum. *Nat Commun*, 4, 2862. doi: 10.1038/ncomms3862
- Gardner, M. J., Hall, N., Fung, E., White, O., Berriman, M., Hyman, R. W., . . . Barrell, B. (2002). Genome sequence of the human malaria parasite Plasmodium falciparum. *Nature*, 419, 498. doi: 10.1038/nature01097
- Garnham, P. (1966). Immunity against the different stages of malaria parasites. *Bull Soc Pathol Exot Filiales*, 59, 549-557.
- Gaskins, E., Gilk, S., DeVore, N., Mann, T., Ward, G., and Beckers, C. (2004). Identification of the membrane receptor of a class XIV myosin in *Toxoplasma gondii*. *The Journal of Cell Biology*, 165(3), 383-393. doi: 10.1083/jcb.200311137
- Gaur, D., Mayer, D. C. G., and Miller, L. H. (2004). Parasite ligand–host receptor interactions during invasion of erythrocytes by Plasmodium merozoites. *International Journal for Parasitology*, 34(13), 1413-1429. doi: <https://doi.org/10.1016/j.ijpara.2004.10.010>
- Gaur, D., Singh, S., Singh, S., Jiang, L., Diouf, A., and Miller, L. H. (2007). Recombinant Plasmodium falciparum reticulocyte homology protein 4 binds to erythrocytes and blocks invasion. *Proceedings of the National Academy of Sciences of the United States of America*, 104(45), 17789-17794. doi: 10.1073/pnas.0708772104
- Gerold, P., Schofield, L., Blackman, M. J., Holder, A. A., and Schwarz, R. T. (1996). Structural analysis of the glycosyl-phosphatidylinositol membrane anchor of the merozoite surface proteins-1 and -2 of Plasmodium falciparum. *Molecular and Biochemical Parasitology*, 75(2), 131-143. doi: [https://doi.org/10.1016/0166-6851\(95\)02518-9](https://doi.org/10.1016/0166-6851(95)02518-9)
- Gibson, D. G., Young, L., Chuang, R.-Y., Venter, J. C., Hutchison Iii, C. A., and Smith, H. O. (2009). Enzymatic assembly of DNA molecules up to several hundred kilobases. *Nat Methods*, 6, 343. doi: 10.1038/nmeth.1318
- Gilberger, T.-W., Thompson, J. K., Triglia, T., Good, R. T., Duraisingh, M. T., and Cowman, A. F. (2003). A Novel Erythrocyte Binding Antigen-175 Parologue from Plasmodium falciparum Defines a New Trypsin-resistant Receptor on

- Human Erythrocytes. *Journal of Biological Chemistry*, 278(16), 14480-14486. doi: 10.1074/jbc.M211446200
- Gilberger, T. W., Thompson, J. K., Reed, M. B., Good, R. T., and Cowman, A. F. (2003). The cytoplasmic domain of the Plasmodium falciparum ligand EBA-175 is essential for invasion but not protein trafficking. *J Cell Biol*, 162(2), 317-327. doi: 10.1083/jcb.200301046
- Gilson, P. R., and Crabb, B. S. (2009). Morphology and kinetics of the three distinct phases of red blood cell invasion by Plasmodium falciparum merozoites. *Int J Parasitol*, 39(1), 91-96. doi: 10.1016/j.ijpara.2008.09.007
- Ginsburg, H. (1990). Some reflections concerning host erythrocyte-malarial parasite interrelationships. *Blood Cells*, 16(2-3), 225-235.
- Goel, V. K., Li, X., Chen, H., Liu, S.-C., Chishti, A. H., and Oh, S. S. (2003). Band 3 is a host receptor binding merozoite surface protein 1 during the Plasmodium falciparum invasion of erythrocytes. *Proceedings of the National Academy of Sciences*, 100(9), 5164-5169. doi: 10.1073/pnas.0834959100
- Golan, D. E., Tashjian, A. H., and Armstrong, E. J. (2011). The principles of pharmacology: The pathophysiologic basis of drug therapy. *Phladelphia: Lippincott Williams & Wilkins*, 1008 p.
- Goldberg, D. E., Slater, A. F., Cerami, A., and Henderson, G. B. (1990). Hemoglobin degradation in the malaria parasite Plasmodium falciparum: an ordered process in a unique organelle. *Proceedings of the National Academy of Sciences of the United States of America*, 87(8), 2931-2935.
- Gomes-Santos, C. S. S., Braks, J., Prudêncio, M., Carret, C., Gomes, A. R., Pain, A., . . . Mota, M. M. (2011). Transition of Plasmodium Sporozoites into Liver Stage-Like Forms Is Regulated by the RNA Binding Protein Pumilio. *PLoS Pathog*, 7(5), e1002046. doi: 10.1371/journal.ppat.1002046
- Gould, S. B., Tham, W.-H., Cowman, A. F., McFadden, G. I., and Waller, R. F. (2008). Alveolins, a New Family of Cortical Proteins that Define the Protist Infrakingdom Alveolata. *Mol Biol Evol*, 25(6), 1219-1230. doi: 10.1093/molbev/msn070
- Green, J. L., Martin, S. R., Fielden, J., Ksagoni, A., Grainger, M., Yim Lim, B. Y. S., . . . Holder, A. A. (2006). The MTIP-Myosin A Complex in Blood Stage Malaria Parasites. *Journal of Molecular Biology*, 355(5), 933-941. doi: https://doi.org/10.1016/j.jmb.2005.11.027
- Grellier, P., Rigomier, D., Clavey, V., Fruchart, J., and J., S. (1991). Lipid traffic between high density lipoproteins and Plasmodium falciparum-infected red blood cells. *The Journal of Cell Biology*, 112(2), 267-277.
- Guerra, C. A., Howes, R. E., Patil, A. P., Gething, P. W., Van Boeckel, T. P., Temperley, W. H., . . . Hay, S. I. (2010). The International Limits and Population at Risk of Plasmodium vivax Transmission in 2009. *PLoS Neglected Tropical Diseases*, 4(8), e774. doi: 10.1371/journal.pntd.0000774
- Guttery, D. S., Roques, M., Holder, A. A., and Tewari, R. (2015). Commit and Transmit: Molecular Players in Plasmodium Sexual Development and Zygote Differentiation. *Trends Parasitol*, 31(12), 676-685. doi: 10.1016/j.pt.2015.08.002

- Haase, S., Cabrera, A., Langer, C., Treeck, M., Struck, N., Herrmann, S., . . . Gilberger, T. W. (2008). Characterization of a conserved rhoptry-associated leucine zipper-like protein in the malaria parasite *Plasmodium falciparum*. *Infect Immun*, *76*(3), 879-887. doi: 10.1128/IAI.00144-07
- Halliwell, B., and Gutteridge, J. M. (1984). Oxygen toxicity, oxygen radicals, transition metals and disease. *Biochemical Journal*, *219*(1), 1-14.
- Hanahan, D. (1983). Studies on transformation of *Escherichia coli* with plasmids. *Journal of Molecular Biology*, *166*(4), 557-580. doi: [https://doi.org/10.1016/S0022-2836\(83\)80284-8](https://doi.org/10.1016/S0022-2836(83)80284-8)
- Hanssen, E., Knoechel, C., Dearnley, M., Dixon, M. W. A., Le Gros, M., Larabell, C., and Tilley, L. (2012). Soft X-ray microscopy analysis of cell volume and hemoglobin content in erythrocytes infected with asexual and sexual stages of *Plasmodium falciparum*. *Journal of Structural Biology*, *177*(2), 224-232. doi: 10.1016/j.jsb.2011.09.003
- Harris, P. K., Yeoh, S., Dluzewski, A. R., O'Donnell, R. A., Withers-Martinez, C., Hackett, F., . . . Blackman, M. J. (2005). Molecular Identification of a Malaria Merozoite Surface Sheddase. *PLoS Pathog*, *1*(3), e29. doi: 10.1371/journal.ppat.0010029
- Hawking, F., Wilson, M. E., and Gammage, K. (1971). Evidence for cyclic development and shortlived maturity in the gametocytes of *Plasmodium falciparum*. *Transactions of the Royal Society of Tropical Medicine and Hygiene*, *65*, 549-559.
- Hayton, K., Gaur, D., Liu, A., Takahashi, J., Henschen, B., Singh, S., . . . Wellems, T. E. (2008). Erythrocyte Binding Protein PfRH5 Polymorphisms Determine Species-Specific Pathways of *Plasmodium falciparum* Invasion. *Cell Host Microbe*, *4*(1), 40-51. doi: 10.1016/j.chom.2008.06.001
- Heintzelman, M. B. Gliding Motility: The Molecules behind the Motion. *Current Biology*, *13*(2), R57-R59. doi: 10.1016/S0960-9822(02)01428-8
- Hiller, N., Bhattacharjee, S., van Ooij, C., Liolios, K., Harrison, T., Lopez-Estraño, C., and Haldar, K. (2004). A host-targeting signal in virulence proteins reveals a secretome in malarial infection. *Science*, *306*(5703), 1934-1937. doi: 10.1126/science.1102737
- Hirtzlin, J., Färber, P., Franklin, R., and Bell, A. (1995). Molecular and biochemical characterization of a *Plasmodium falciparum* cyclophilin containing a cleavable signal sequence. *Eur J Biochem*, *232*(3), 765-772.
- Hoffman, S. L., Vekemans, J., Richie, T. L., and Duffy, P. E. (2015). The March Toward Malaria Vaccines. *Am J Prev Med*, *49*(6 Suppl 4), S319-333. doi: 10.1016/j.amepre.2015.09.011
- Holder, A., Blackman MJ, Burghaus PA, Chappel JA, L. I., McCallum-Deighton N, and S, S. (1992). A malaria merozoite surface protein (MSP1)-structure, processing and function.
- Hosoda, A., Tokuda, M., Akai, R., Kohno, K., and Iwawaki, T. (2010). Positive contribution of ERdj5/JPD1 to endoplasmic reticulum protein quality control in the salivary gland. *Biochemical Journal*, *425*(1), 117-128. doi: 10.1042/bj20091269
- Howard, R. J., Barnwell, J. W., Rock, E. P., Janet, N., Ofori-Adjei, D., Maloy, W. L., . . . Saul, A. (1988). Two approximately 300 kilodalton plasmodium falciparum proteins at

- the surface membrane of infected erythrocytes. *Mol Biochem Parasitol*, 27, 207-224.
- Hu, G., Cabrera, A., Kono, M., Mok, S., Chaal, B. K., Haase, S., . . . Bozdech, Z. (2009). Transcriptional profiling of growth perturbations of the human malaria parasite *Plasmodium falciparum*. *Nat Biotechnol*, 28(1), 91-98. doi: 10.1038/nbt.1597
- Hughes, K. R., Philip, N., Lucas Starnes, G., Taylor, S., and Waters, A. P. (2010). From cradle to grave: RNA biology in malaria parasites. *Wiley Interdisciplinary Reviews: RNA*, 1(2), 287-303. doi: 10.1002/wrna.30
- Iyer, J., Grüner, A. C., Rénia, L., Snounou, G., and Preiser, P. R. (2007). Invasion of host cells by malaria parasites: a tale of two protein families. *Molecular Microbiology*, 65(2), 231-249. doi: 10.1111/j.1365-2958.2007.05791.x
- Jamwal, A., Yogavel, M., Abdin, M. Z., Jain, S. K., and Sharma, A. (2017). Structural and Biochemical Characterization of Apicomplexan Inorganic Pyrophosphatases. *Sci Rep*, 7(1), 5255. doi: 10.1038/s41598-017-05234-y
- Janse C.J., and *al., e.* (1988). DNA synthesis in gametocytes of *Plasmodium falciparum*. *Parasitology*, 96, 1-7.
- Janse, C. J., van der Klooster, P. F., van der Kaay, H. J., van der Ploeg, M., and Overdulve, J. P. (1986). DNA synthesis in *Plasmodium berghei* during asexual and sexual development. . *Mol Biochem Parasitol*, 20, 173-182.
- Johnson, T. M., Rajfur, Z., Jacobson, K., and Beckers, C. J. (2007). Immobilization of the Type XIV Myosin Complex in *Toxoplasma gondii*. *Molecular Biology of the Cell*, 18(8), 3039-3046. doi: 10.1091/mbc.E07-01-0040
- Joice, R., Nilsson, S. K., Montgomery, J., Dankwa, S., Egan, E., Morahan, B., . . . Marti, M. (2014). *Plasmodium falciparum* transmission stages accumulate in the human bone marrow. *Science translational medicine*, 6(244), 244re245-244re245. doi: 10.1126/scitranslmed.3008882
- Kaneko, O., Mu, J., Tsuboi, T., Su, X., and Torii, M. (2002). Gene structure and expression of a *Plasmodium falciparum* 220-kDa protein homologous to the *Plasmodium vivax* reticulocyte binding proteins. *Mol Biochem Parasitol*, 121(2), 275-278.
- Kappe, S., Bruderer, T., Gantt, S., Fujioka, H., Nussenzweig, V., and Ménard, R. (1999). Conservation of a Gliding Motility and Cell Invasion Machinery in Apicomplexan Parasites. *The Journal of Cell Biology*, 147(5), 937-944. doi: 10.1083/jcb.147.5.937
- Kariu, T., Yuda, M., Yano, K., and Chinzei, Y. (2002). MAEBL Is Essential for Malarial Sporozoite Infection of the Mosquito Salivary Gland. *The Journal of Experimental Medicine*, 195(10), 1317-1323. doi: 10.1084/jem.20011876
- Keeley, A., and Soldati, D. (2004). The glideosome: a molecular machine powering motility and host-cell invasion by Apicomplexa. *Trends Cell Biol*, 14(10), 528-532. doi: 10.1016/j.tcb.2004.08.002
- Keeling, P. J., and Rayner, J. C. (2015). The origins of malaria: there are more things in heaven and earth. *Parasitology*, 142 Suppl 1, S16-25. doi: 10.1017/S0031182014000766

- Kenthirapalan, S., Waters, A. P., Matuschewski, K., and Kooij, T. W. (2014). Copper-transporting ATPase is important for malaria parasite fertility. *Mol Microbiol*, *91*(2), 315-325. doi: 10.1111/mmi.12461
- Kenthirapalan, S., Waters, A. P., Matuschewski, K., and Kooij, T. W. (2016). Functional profiles of orphan membrane transporters in the life cycle of the malaria parasite. *Nat Commun*, *7*, 10519. doi: 10.1038/ncomms10519
- Kessler, H., Herm-Götz, A., Hegge, S., Rauch, M., Soldati-Favre, D., Frischknecht, F., and Meissner, M. (2008). Microneme protein 8 – a new essential invasion factor in *Toxoplasma gondii*. *J Cell Sci*, *121*(7), 947-956. doi: 10.1242/jcs.022350
- Kono, M., Herrmann, S., Loughran, N. B., Cabrera, A., Engelberg, K., Lehmann, C., . . . Gilberger, T. W. (2012). Evolution and architecture of the inner membrane complex in asexual and sexual stages of the malaria parasite. *Mol Biol Evol*, *29*(9), 2113-2132. doi: 10.1093/molbev/mss081
- Kyes, S. A., Kraemer, S. M., and Smith, J. D. (2007). Antigenic Variation in *Plasmodium falciparum*: Gene Organization and Regulation of the var Multigene Family. *Eukaryotic Cell*, *6*(9), 1511-1520. doi: 10.1128/EC.00173-07
- LaCount, D., Vignali, M., Chettier, R., Phansalkar, A., Bell, R., Hesselberth, J., . . . Hughes, R. (2005). A protein interaction network of the malaria parasite *Plasmodium falciparum*. *Nature*. doi: 10.1038/nature04104
- Ladda R, Aikawa M, and H., S. (1969). Penetration of erythrocytes by merozoites of mammalian and avian malarial parasites. *J Parasitol.*, *55*(3), 633-644.
- Laemmli, U. K. (1970). Cleavage of Structural Proteins during the Assembly of the Head of Bacteriophage T4. *Nature*, *227*, 680. doi: 10.1038/227680a0
- Lamarque, M., Besteiro, S., Papoin, J., Roques, M., Vulliez-Le Normand, B., Morlon-Guyot, J., . . . Lebrun, M. (2011). The RON2-AMA1 Interaction is a Critical Step in Moving Junction-Dependent Invasion by Apicomplexan Parasites. *PLoS Pathog*, *7*(2), e1001276. doi: 10.1371/journal.ppat.1001276
- Lambros, C., and Vanderberg, J. (1979). Synchronization of *Plasmodium falciparum* erythrocytic stages in culture. *J Parasitol.*, *65*(3), 418-420.
- Langhi, D. M., and Orlando Bordin, J. (2006). Duffy blood group and malaria. *Hematology*, *11*(5-6), 389-398. doi: 10.1080/10245330500469841
- Laveran, A. (1881). Un nouveau parasite trouvé dans le sang de malades atteints de fièvre palustre. Origine parasitaire des accidents de l'impaludisme., *Bull Mém Soc Méd Hôpitaux Paris*.
- Laveran, A. (1884). *Traité des Fièvres Palustres avec la Description des Microbes du Paludisme*.
- Lazarus, M. D., Schneider, T. G., and Taraschi, T. F. (2008). A new model for hemoglobin ingestion and transport by the human malaria parasite *Plasmodium falciparum*. *J Cell Sci*, *121*(11), 1937-1949. doi: 10.1242/jcs.023150
- Le Roch, K., Johnson, J., Florens, L., Zhou, Y., Santrosyan, A., Grainger, M., . . . *al.*, e. (2004). Global analysis of transcript and protein levels across the *Plasmodium falciparum* life cycle. *Genome Res*, *14*, 2308-2318.
- Le Roch, K. G., Yingyao Zhou, Peter L. Blair, Muni Grainger, J. Kathleen Moch, J. David Haynes, . . . Winzeler, E. A. (2003). Discovery of Gene Function by Expression

- Profiling of the Malaria Parasite Life Cycle. *Science*, 301. doi: 10.1126/science.1087025
- Lévêque, M. F., Berry, L., Yamaro - Botté, Y., Nguyen, H. M., Galera, M., Botté, C. Y., and Besteiro, S. (2017). TgPL2, a patatin - like phospholipase domain - containing protein, is involved in the maintenance of apicoplast lipids homeostasis in *Toxoplasma*. *Molecular Microbiology*, 105(1), 158-174. doi: 10.1111/mmi.13694
- Levine, N. D. (1988). The Protozoan Phylum Apicomplexa, Vol. 2. . *Parasitology*, 100(3), 501-501. doi: 10.1017/S0031182000078926
- Leykauf, K., Treeck, M., Gilson, P. R., Nebl, T., Bräulke, T., Cowman, A. F., . . . Crabb, B. S. (2010). Protein Kinase A Dependent Phosphorylation of Apical Membrane Antigen 1 Plays an Important Role in Erythrocyte Invasion by the Malaria Parasite. *PLoS Pathog*, 6(6), e1000941. doi: 10.1371/journal.ppat.1000941
- Liang, H., and Sim, B. (1997). Conservation of structure and function of the erythrocyte-binding domain of *Plasmodium falciparum* EBA-1751. *Molecular and Biochemical Parasitology*, 84(2), 241-245. doi: [https://doi.org/10.1016/S0166-6851\(96\)02791-0](https://doi.org/10.1016/S0166-6851(96)02791-0)
- Lim, L., and McFadden, G. I. (2010). The evolution, metabolism and functions of the apicoplast. *Philosophical Transactions of the Royal Society B: Biological Sciences*, 365(1541), 749-763. doi: 10.1098/rstb.2009.0273
- Lim, W. A., and Pawson, T. (2010). Phosphotyrosine Signaling: Evolving a New Cellular Communication System. *Cell*, 142(5), 661-667. doi: 10.1016/j.cell.2010.08.023
- Lingelbach, K., and Joiner, K. A. (1998). The parasitophorous vacuole membrane surrounding *Plasmodium* and *Toxoplasma*: an unusual compartment in infected cells. *J. Cell Sci.*, 111, 1467-1475.
- Lobo, C.-A., Rodriguez, M., Struchiner, C. J., Zalis, M. G., and Lustigman, S. (2006). Associations between defined polymorphic variants in the PfRH ligand family and the invasion pathways used by *P. falciparum* field isolates from Brazil. *Molecular and Biochemical Parasitology*, 149(2), 246-251. doi: <https://doi.org/10.1016/j.molbiopara.2006.05.011>
- Lopez-Rubio, J. J., Gontijo, A. M., Nunes, M. C., Issar, N., Hernandez Rivas, R., and Scherf, A. (2007). 5' flanking region of var genes nucleate histone modification patterns linked to phenotypic inheritance of virulence traits in malaria parasites. *Molecular Microbiology*, 66(6), 1296-1305. doi: 10.1111/j.1365-2958.2007.06009.x
- Lubell, Y., Dondorp, A., Guérin, P. J., Drake, T., Meek, S., Ashley, E., . . . White, L. J. (2014). Artemisinin resistance – modelling the potential human and economic costs. *Malar J*, 13, 452. doi: 10.1186/1475-2875-13-452
- Mahajan, B., Noiva, R., Yadava, A., Zheng, H., Majam, V., Mohan, K. V. K., . . . Kumar, S. (2006). Protein disulfide isomerase assisted protein folding in malaria parasites. *International Journal for Parasitology*, 36(9), 1037-1048. doi: <https://doi.org/10.1016/j.ijpara.2006.04.012>
- Maier, A. G., Duraisingh, M. T., Reeder, J. C., Patel, S. S., Kazura, J. W., Zimmerman, P. A., and Cowman, A. F. (2003). *Plasmodium falciparum* erythrocyte invasion through



- glycophorin C and selection for Gerbich negativity in human populations. *Nature Medicine*, 9(1), 87-92. doi: 10.1038/nm807
- Malaria vaccine: WHO position paper, January 2016 – Recommendations. (2017). *Vaccine*. doi: <https://doi.org/10.1016/j.vaccine.2016.10.047>
- Malleret, B., Claser, C., Ong, A. S. M., Suwanarusk, R., Sriprawat, K., Howland, S. W., . . . Rénia, L. (2011). A rapid and robust tri-color flow cytometry assay for monitoring malaria parasite development. *Sci Rep*, 1, 118. doi: 10.1038/srep00118
- Marchesi, V. T., Tillack, T. W., Jackson, R. L., Segrest, J. P., and Scott, R. E. (1972). Chemical Characterization and Surface Orientation of the Major Glycoprotein of the Human Erythrocyte Membrane. *Proceedings of the National Academy of Sciences of the United States of America*, 69(6), 1445-1449.
- Marín-Menéndez, A., Monaghan, P., and Bell, A. (2012). A family of cyclophilin-like molecular chaperones in *Plasmodium falciparum*. *Molecular and Biochemical Parasitology*, 184(1), 44-47. doi: <https://doi.org/10.1016/j.molbiopara.2012.04.006>
- Martin, R., Ginsburg, H., and K., K. (2009). Membrane transport proteins of the malaria parasite. *Mol Microbiol.*, 74(3), 519-518.
- Marva, E., Cohen, A., Saltman, P., Chevion, M., and Golenser, J. (1989). Deleterious synergistic effects of ascorbate and copper on the development of *Plasmodium falciparum*: An in vitro study in normal and in G6PD-deficient erythrocytes. *International Journal for Parasitology*, 19(7), 779-785. doi: [https://doi.org/10.1016/0020-7519\(89\)90066-0](https://doi.org/10.1016/0020-7519(89)90066-0)
- Matesanz, F., Téllez, M. a.-d.-M., and Alcina, A. (2003). The *Plasmodium falciparum* fatty acyl-CoA synthetase family (PfACS) and differential stage-specific expression in infected erythrocytes. *Molecular and Biochemical Parasitology*, 126(1), 109-112. doi: [https://doi.org/10.1016/S0166-6851\(02\)00242-6](https://doi.org/10.1016/S0166-6851(02)00242-6)
- Maurer-Stroh, S., Eisenhaber, B., and Eisenhaber, F. (2002). N-terminal N-myristoylation of proteins: refinement of the sequence motif and its taxon-specific differences. Edited by J. Thornton. *Journal of Molecular Biology*, 317(4), 523-540. doi: <https://doi.org/10.1006/jmbi.2002.5425>
- Mayer, D. C. G., Cofie, J., Jiang, L., Hartl, D. L., Tracy, E., Kabat, J., . . . Miller, L. H. (2009). Glycophorin B is the erythrocyte receptor of *Plasmodium falciparum* erythrocyte-binding ligand, EBL-1. *Proceedings of the National Academy of Sciences of the United States of America*, 106(13), 5348-5352. doi: 10.1073/pnas.0900878106
- Mayer, D. C. G., Kaneko, O., Hudson-Taylor, D. E., Reid, M. E., and Miller, L. H. (2001). Characterization of a *Plasmodium falciparum* erythrocyte-binding protein paralogous to EBA-175. *Proceedings of the National Academy of Sciences of the United States of America*, 98(9), 5222-5227. doi: 10.1073/pnas.081075398
- Mayor, A., Bir, N., Sawhney, R., Singh, S., Pattnaik, P., Singh, S. K., . . . Chitnis, C. E. (2005). Receptor-binding residues lie in central regions of Duffy-binding-like domains involved in red cell invasion and cytoadherence by malaria parasites. *Blood*, 105(6), 2557-2563. doi: 10.1182/blood-2004-05-1722
- Mbengue, A., Bhattacharjee, S., Pandharkar, T., Liu, H., Estiu, G., Stahelin, R. V., . . . Halder, K. (2015). A molecular mechanism of artemisinin resistance in

- Plasmodium falciparum malaria. *Nature*, 520(7549), 683-687. doi: 10.1038/nature14412
- Mello, K., Daly, T. M., Morrisey, J., Vaidya, A. B., Long, C. A., and Bergman, L. W. (2002). A Multigene Family That Interacts with the Amino Terminus of Plasmodium MSP-1 Identified Using the Yeast Two-Hybrid System. *Eukaryotic Cell*, 1(6), 915-925. doi: 10.1128/ec.1.6.915-925.2002
- Ménard, D., Barnadas, C., Bouchier, C., Henry-Halldin, C., Gray, L. R., Ratsimbasa, A., . . . Zimmerman, P. A. (2010). Plasmodium vivax clinical malaria is commonly observed in Duffy-negative Malagasy people. *Proceedings of the National Academy of Sciences*, 107(13), 5967-5971. doi: 10.1073/pnas.0912496107
- Meshnick, S. R., Yang, Y. Z., Lima, V., Kuypers, F., Kamchonwongpaisan, S., and Yuthavong, Y. (1993). Iron-dependent free radical generation from the antimalarial agent artemisinin (qinghaosu). *Antimicrobial Agents and Chemotherapy*, 37(5), 1108-1114.
- Meszoely, C., Erbe, E., Steere, R., Trosper, J., and RL., B. (1987). Plasmodium falciparum: freeze-fracture of the gametocyte pellicular complex. *Exp Parasitol.*, 64(3), 300-309.
- Miao, J., Li, J., Fan, Q., Li, X., Li, X., and Cui, L. (2010). The Puf-family RNA-binding protein PfPuf2 regulates sexual development and sex differentiation in the malaria parasite Plasmodium falciparum. *J Cell Sci*, 123(7), 1039-1049. doi: 10.1242/jcs.059824
- Miller. (2002). pathogenic basis of malaria. *Nature*.
- Miller , L. H., Mason , S. J., Clyde , D. F., and McGinniss , M. H. (1976). The Resistance Factor to Plasmodium vivax in Blacks. *New England Journal of Medicine*, 295(6), 302-304. doi: 10.1056/nejm197608052950602
- Miller, L. H., Shiroishi, T., Dvorak, J. A., Durocher J.R., and Schrier, B. K. (1975). Enzymatic modification of the erythrocyte membrane and its effect on malarial merozoite invasion. . *J. Mol. Med.*, 1, 55-63.
- Mok, S., Ashley, E. A., Ferreira, P. E., Zhu, L., Lin, Z., Yeo, T., . . . Bozdech, Z. (2015). Population transcriptomics of human malaria parasites reveals the mechanism of artemisinin resistance. *Science (New York, N.Y.)*, 347(6220), 431-435. doi: 10.1126/science.1260403
- Moreno, A., and Joyner, C. (2015). Malaria vaccine clinical trials: what's on the horizon. *Curr Opin Immunol*, 35, 98-106. doi: 10.1016/j.coi.2015.06.008
- Morrisette, N. S., Murray, J. M., and Roos, D. S. (1997). Subpellicular microtubules associate with an intramembranous particle lattice in the protozoan parasite Toxoplasma gondii. *J Cell Sci*, 110(1), 35-42.
- Morrisette, N. S., and Sibley, L. D. (2002). Cytoskeleton of Apicomplexan Parasites. *Microbiology and Molecular Biology Reviews*, 66(1), 21-38. doi: 10.1128/MMBR.66.1.21-38.2002
- Mota, M. M., Pradel, G., Vanderberg, J. P., Hafalla, J. C. R., Frevert, U., Nussenzweig, R. S., . . . Rodríguez, A. (2001). Migration of Plasmodium Sporozoites Through Cells Before Infection. *Science*, 291(5501), 141-144. doi: 10.1126/science.291.5501.141

- Muh, F., Han, J. H., Nyunt, M. H., Lee, S. K., Jeon, H. Y., Ha, K. S., . . . Han, E. T. (2017). Identification of a novel merozoite surface antigen of *Plasmodium vivax*, PvMSA180. *Malar J*, *16*(1), 133. doi: 10.1186/s12936-017-1760-9
- Mullis, K. B., and Faloona, F. A. (1987). Specific synthesis of DNA in vitro via a polymerase-catalyzed chain reaction *Methods in Enzymology* (Vol. 155, pp. 335-350): Academic Press.
- Njunge, J., M. , Ludewig, M., H. , Boshoff, A., Pesce, E.-R., and Blatch, G., L. (2013). Hsp70s and J Proteins of *Plasmodium* Parasites Infecting Rodents and Primates: Structure, Function, Clinical Relevance, and Drug Targets. *Current Pharmaceutical Design*, *19*(3), 387-403. doi: 10.2174/1381612811306030387
- Nussenzweig, R. S., Vanderberg, J. P., Most, H., and Orton, C. (1969). Specificity of protective immunity produced by x-irradiated *Plasmodium berghei* sporozoites. *Nature*, *222*, 488-489.
- O'Donnell, R. A., Hackett, F., Howell, S. A., Treeck, M., Struck, N., Krnajski, Z., . . . Blackman, M. J. (2006). Intramembrane proteolysis mediates shedding of a key adhesin during erythrocyte invasion by the malaria parasite. *The Journal of Cell Biology*, *174*(7), 1023-1033. doi: 10.1083/jcb.200604136
- O'Neill, P. M., Barton, V. E., and Ward, S. A. (2010). The Molecular Mechanism of Action of Artemisinin—The Debate Continues. *Molecules*, *15*(3), 1705.
- Olivieri, A., Collins, C. R., Hackett, F., Withers-Martinez, C., Marshall, J., Flynn, H. R., . . . Blackman, M. J. (2011). Juxtamembrane Shedding of *Plasmodium falciparum* AMA1 Is Sequence Independent and Essential, and Helps Evade Invasion-Inhibitory Antibodies. *PLoS Pathog*, *7*(12), e1002448. doi: 10.1371/journal.ppat.1002448
- Opitz, C., and Soldati, D. (2002). 'The glideosome': a dynamic complex powering gliding motion and host cell invasion by *Toxoplasma gondii*. *Molecular Microbiology*, *45*(3), 597-604. doi: 10.1046/j.1365-2958.2002.03056.x
- Orlandi, P., Sim, B., Chulay, J., and Haynes, J. (1990). Characterization of the 175-kilodalton erythrocyte binding antigen of *Plasmodium falciparum*. *Mol Biochem Parasitol.*, *40*(2), 285-294.
- Orlandi, P., Sim BK, Chulay JD, and JD., H. (1990). Characterization of the 175-kilodalton erythrocyte binding antigen of *Plasmodium falciparum*. *Mol Biochem Parasitol*, *40*(2), 285-294.
- Orlandi, P. A., Klotz, F. W., and Haynes, J. D. (1992). A malaria invasion receptor, the 175-kilodalton erythrocyte binding antigen of *Plasmodium falciparum* recognizes the terminal Neu5Ac(alpha 2-3)Gal- sequences of glycophorin A. *The Journal of Cell Biology*, *116*(4), 901-909. doi: 10.1083/jcb.116.4.901
- Oyen, D., Torres, J. L., Wille-Reece, U., Ockenhouse, C. F., Emerling, D., Glanville, J., . . . Wilson, I. A. (2017). Structural basis for antibody recognition of the NANP repeats in *Plasmodium falciparum* circumsporozoite protein. *Proc Natl Acad Sci U S A*, *114*(48), E10438-E10445. doi: 10.1073/pnas.1715812114
- Parhizgar, A. R., and Tahghighi, A. (2017). Introducing New Antimalarial Analogues of Chloroquine and Amodiaquine: A Narrative Review. *Iranian Journal of Medical Sciences*, *42*(2), 115-128.

- Parisi, M., and Lin, H. (2000). Translational repression: a duet of Nanos and Pumilio. *Current biology : CB*, 10(2), R81-83. doi: 10.1016/s0960-9822(00)00283-9
- Payne, D. (1987). Spread of chloroquine resistance in *Plasmodium falciparum*. *Parasitology Today*, 3(8), 241-246. doi: [https://doi.org/10.1016/0169-4758\(87\)90147-5](https://doi.org/10.1016/0169-4758(87)90147-5)
- Pesce, E. R., and Blatch, G. L. (2014). Plasmodial Hsp40 and Hsp70 chaperones: current and future perspectives. *Parasitology*, 141(9), 1167-1176. doi: 10.1017/S003118201300228X
- Peterson, M., Marshall, V., Smythe, J., PE., C., Lew, A., Silva, A., . . . Kemp, D. (1989). Integral membrane protein located in the apical complex of *Plasmodium falciparum*. *Molecular and Cellular Biology*, 9(7), 3151-3154. doi: 0270-7306/89/073151-04\$02.00/0
- Pouvelle, B., Spiegel, R., Hsiao, L., Howard, R. J., Morris, R. L., Thomas, A. P., and Taraschi, T. F. (1991). Direct access to serum macromolecules by intraerythrocytic malaria parasites. *Nature*, 353, 73. doi: 10.1038/353073a0
- Preiser, P., Kaviratne, M., Khan, S., Bannister, L., and Jarra, W. (2000). The apical organelles of malaria merozoites: host cell selection, invasion, host immunity and immune evasion. *Microbes and Infection*, 2(12), 1461-1477. doi: [https://doi.org/10.1016/S1286-4579\(00\)01301-0](https://doi.org/10.1016/S1286-4579(00)01301-0)
- Price, R. N., Tjitra, E., Guerra, C. A., Yeung, S., White, N. J., and Anstey, N. M. (2007). Vivax malaria: neglected and not benign. *The American journal of tropical medicine and hygiene*, 77(6 Suppl), 79-87.
- Prinz, B., Harvey, K. L., Wilcke, L., Ruch, U., Engelberg, K., Biller, L., . . . Gilberger, T. W. (2016). Hierarchical phosphorylation of apical membrane antigen 1 is required for efficient red blood cell invasion by malaria parasites. *Sci Rep*, 6, 34479. doi: 10.1038/srep34479
- Puig, S., Lee, J., Lau, M., and Thiele, D. J. (2002). Biochemical and Genetic Analyses of Yeast and Human High Affinity Copper Transporters Suggest a Conserved Mechanism for Copper Uptake. *Journal of Biological Chemistry*, 277(29), 26021-26030. doi: 10.1074/jbc.M202547200
- Ralph, S. A., van Dooren, G. G., Waller, R. F., Crawford, M. J., Fraunholz, M. J., Foth, B. J., . . . McFadden, G. I. (2004). Tropical infectious diseases: metabolic maps and functions of the plasmodium falciparum apicoplast. *Nat Rev Microbiol*, 2(3), 203-216.
- Rasoloson, D., Shi, L., Chong, C., Kafsack, B., and Sullivan, D. (2004). Copper pathways in *Plasmodium falciparum* infected erythrocytes indicate an efflux role for the copper P-ATPase. *Biochem J.*, 381, 803-8011. doi: 10.1042/BJ20040335
- Rayner, J. C., Vargas-Serrato, E., Huber, C. S., Galinski, M. R., and Barnwell, J. W. (2001). A *Plasmodium falciparum* Homologue of *Plasmodium vivax* Reticulocyte Binding Protein (PvRBP1) Defines a Trypsin-resistant Erythrocyte Invasion Pathway. *The Journal of Experimental Medicine*, 194(11), 1571-1582.
- Reddy, B. P. N., Shrestha, S., Hart, K. J., Liang, X., Kemirembe, K., Cui, L., and Lindner, S. E. (2015). A bioinformatic survey of RNA-binding proteins in *Plasmodium*. *BMC Genomics*, 16, 890. doi: 10.1186/s12864-015-2092-1

- Reed, M. B., Caruana, S. R., Batchelor, A. H., Thompson, J. K., Crabb, B. S., and Cowman, A. F. (2000). Targeted disruption of an erythrocyte binding antigen in *Plasmodium falciparum* is associated with a switch toward a sialic acid-independent pathway of invasion. *Proceedings of the National Academy of Sciences*, 97(13), 7509-7514. doi: 10.1073/pnas.97.13.7509
- Rees-Channer, R. R., Martin, S. R., Green, J. L., Bowyer, P. W., Grainger, M., Molloy, J. E., and Holder, A. A. (2006). Dual acylation of the 45kDa gliding-associated protein (GAP45) in *Plasmodium falciparum* merozoites. *Molecular and Biochemical Parasitology*, 149(1), 113-116. doi: <https://doi.org/10.1016/j.molbiopara.2006.04.008>
- Resh, M. D. (1999). Fatty acylation of proteins: new insights into membrane targeting of myristoylated and palmitoylated proteins. *Biochimica et Biophysica Acta (BBA) - Molecular Cell Research*, 1451(1), 1-16. doi: [https://doi.org/10.1016/S0167-4889\(99\)00075-0](https://doi.org/10.1016/S0167-4889(99)00075-0)
- Ridzuan, M. A., Moon, R. W., Knuepfer, E., Black, S., Holder, A. A., and Green, J. L. (2012). Subcellular location, phosphorylation and assembly into the motor complex of GAP45 during *Plasmodium falciparum* schizont development. *PLoS One*, 7(3), e33845. doi: 10.1371/journal.pone.0033845
- Riglar, D. T., Richard, D., Wilson, D. W., Boyle, M. J., Dekiwadia, C., Turnbull, L., . . . Baum, J. (2011). Super-resolution dissection of coordinated events during malaria parasite invasion of the human erythrocyte. *Cell Host Microbe*, 9(1), 9-20. doi: 10.1016/j.chom.2010.12.003
- Roberts, D., J., Craig, A., G., Berendt, A., R., Pinches, R., Nash, G., Marsh, K., and Newbold, C., I. (1992). Rapid switching to multiple antigenic and adhesive phenotypes in malaria. *Nature*, 357(3680), 689-692. doi: 10.1038/357689a0
- Rodriguez, M., Lustigman, S., Montero, E., Oksov, Y., and Lobo, C. A. (2008). PfRH5: a novel reticulocyte-binding family homolog of *plasmodium falciparum* that binds to the erythrocyte, and an investigation of its receptor. *PLoS One*, 3(10), e3300. doi: 10.1371/journal.pone.0003300
- Rogerson, S., Novakovic, S., Cooke, B., and Brown, G. (1997). *Plasmodium falciparum*-infected erythrocytes adhere to the proteoglycan thrombomodulin in static and flow-based systems. *Exp Parasitol*, 86(1), 8-18. doi: DOI: 10.1006/expr.1996.4142
- Rts, S. C. T. P. (2015). Efficacy and safety of RTS,S/AS01 malaria vaccine with or without a booster dose in infants and children in Africa: final results of a phase 3, individually randomised, controlled trial. *Lancet (London, England)*, 386(9988), 31-45. doi: 10.1016/S0140-6736(15)60721-8
- Rug, M., and Maier, A. G. (2011). The heat shock protein 40 family of the malaria parasite *Plasmodium falciparum*. *IUBMB life*, 63(12), 1081-1086. doi: 10.1002/iub.525
- Ryan, J., Stoute, J., Amon, J., Dunton, R., Mtalib, R., Koros, J., . . . Rosenberg, R. (2006). Evidence for transmission of *Plasmodium vivax* among a Duffy antigen negative population in Western Kenya. *Am J Trop Med Hyg*, 75(4), 575-581.

- Salmon, B. L., Oksman, A., and Goldberg, D. E. (2001). Malaria parasite exit from the host erythrocyte: a two-step process requiring extraerythrocytic proteolysis. *Proc Natl Acad Sci U S A*, *98*(1), 271-276. doi: 10.1073/pnas.011413198
- Sanchez, C. P., Rotmann, A., Stein, W. D., and Lanzer, M. (2008). Polymorphisms within PfMDR1 alter the substrate specificity for anti-malarial drugs in *Plasmodium falciparum*. *Molecular Microbiology*, *70*(4), 786-798. doi: 10.1111/j.1365-2958.2008.06413.x
- Schnell, D. J., and Hebert, D. N. Protein Translocons. *Cell*, *112*(4), 491-505. doi: 10.1016/S0092-8674(03)00110-7
- Seder, R. A., Chang, L. J., Enama, M. E., Zephir, K. L., Sarwar, U. N., Gordon, I. J., . . . Hoffman, S. L. (2013). Protection Against Malaria by Intravenous Immunization with a Nonreplicating Sporozoite Vaccine. *Science*, *341*, 1359-1365.
- Siddall, M. E., Reece, K. S., Graves, J. E., and Burreson, E. M. (1997). 'Total evidence' refutes the inclusion of Perkinsus species in the phylum Apicomplexa. *Parasitology*, *115*(2), 165-176. doi: undefined
- Sidhu, A. B. S., Verdier-Pinard, D., and Fidock, D. A. (2002). Chloroquine Resistance in *Plasmodium falciparum* Malaria Parasites Conferred by *pfcr* Mutations. *Science*, *298*(5591), 210-213. doi: 10.1126/science.1074045
- Sidik, S. M., Huet, D., Ganesan, S. M., Huynh, M. H., Wang, T., Nasamu, A. S., . . . Lourido, S. (2016). A Genome-wide CRISPR Screen in *Toxoplasma* Identifies Essential Apicomplexan Genes. *Cell*, *166*(6), 1423-1435 e1412. doi: 10.1016/j.cell.2016.08.019
- Silvestrini, F., Alano, P., and Williams, J. (2000). Commitment to the production of male and female gametocytes in the human malaria parasite *Plasmodium falciparum*. *Parasitology*, *121 Pt*(5), 157-159.
- Sim, B., Toyoshima, T., Haynes, J., and Aikawa, M. (1992). Localization of the 175-kilodalton erythrocyte binding antigen in micronemes of *Plasmodium falciparum* merozoites. *Mol Biochem Parasitol*, *51*(1), 157-159.
- Sim, B. K. L. (1990). Sequence conservation of a functional domain of erythrocyte binding antigen 175 in *Plasmodium falciparum*. *Mol Biochem Parasitol*, *41*, 293-296.
- Sim, B. K. L., Chitnis, C. E., Wasniowska, K., Hadley, T. J., and Millert, L. H. (1994). Receptor and ligand domains for invasion of erythrocytes by *Plasmodium falciparum*. *Science*, *264*, 1941-1944.
- Sim, B. K. L., Orlandi, P., Haynes, J., Klotz, F., Carter, J., Camus, D., . . . Chulay, J. (1990). Primary structure of the 175K *Plasmodium falciparum* erythrocyte binding antigen and identification of a peptide which elicits antibodies that inhibit malaria merozoite invasion. *Journal of Cell Biology*, *111*, 1877-1884.
- Sim, B. K. L., Toyoshima, T., Haynes, J. D., and Aikawa, M. (1992). Localization of the 175-kilodalton erythrocyte binding antigen in micronemes of *Plasmodium falciparum* merozoites. *Mol Biochem Parasitol*, *51*, 157-160.
- Sinden, R. E. (1983). The cell biology of sexual development in *Plasmodium*. *Parasitology*, *86*(4), 7-28.

- Sinden, R. E. (2015). The cell biology of malaria infection of mosquito: advances and opportunities. *Cell Microbiol*, 17(4), 451-466. doi: 10.1111/cmi.12413
- Singh, A. P., Ozwara, H., Kocken, C. H. M., Puri, S. K., Thomas, A. W., and Chitnis, C. E. (2005). Targeted deletion of Plasmodium knowlesi Duffy binding protein confirms its role in junction formation during invasion. *Molecular Microbiology*, 55(6), 1925-1934. doi: 10.1111/j.1365-2958.2005.04523.x
- Singh, S., Alam, M. M., Pal-Bhowmick, I., Brzostowski, J. A., and Chitnis, C. E. (2010). Distinct external signals trigger sequential release of apical organelles during erythrocyte invasion by malaria parasites. *PLoS Pathog*, 6(2), e1000746. doi: 10.1371/journal.ppat.1000746
- Singh, S., and Chitnis, C. E. (2017). Molecular Signaling Involved in Entry and Exit of Malaria Parasites from Host Erythrocytes. *Cold Spring Harb Perspect Med*, 7(10). doi: 10.1101/cshperspect.a026815
- Smith, T. G., Lourenco, P., Carter, R., Walliker, D., and Ranford-Cartwright, L. C. (2000). Commitment to sexual differentiation in the human malaria parasite *Plasmodium falciparum*. *Parasitology*, 121(2), 127-133.
- Souza, G. M., da Silva, A. M., and Kuspa, A. (1999). Starvation promotes Dictyostelium development by relieving PufA inhibition of PKA translation through the Yaka kinase pathway. *Development*, 126(14), 3263-3274.
- Spassov, D. S., and Jurecic, R. (2003). The PUF family of RNA-binding proteins: does evolutionarily conserved structure equal conserved function? *IUBMB life*, 55(7), 359-366. doi: 10.1080/15216540310001603093
- Speisky, H., Navarro, P., Cherian, M. G., and Jiménez, I. (2003). Copper-binding proteins in human erythrocytes: Searching for potential biomarkers of copper over-exposure. *Biomaterials*, 16(1), 113-123. doi: 10.1023/a:1020724331271
- Srinivasan, P., Beatty WL, Diouf A, Herrera R, Ambroggio X, Moch JK, . . . LH., M. (2011). Binding of Plasmodium merozoite proteins RON2 and AMA1 triggers commitment to invasion. *Proc Natl Acad Sci U S A*, 108(32), 13275-13280. doi: 10.1073/pnas.1110303108
- Srinivasan, P., Beatty, W. L., Diouf, A., Herrera, R., Ambroggio, X., Moch, J. K., . . . Miller, L. H. (2011). Binding of *Plasmodium* merozoite proteins RON2 and AMA1 triggers commitment to invasion. *Proceedings of the National Academy of Sciences*, 108(32), 13275-13280. doi: 10.1073/pnas.1110303108
- Storch, V., and Welch, U. (2003). Systematische Zoologie. *Spektrum akademischer Verlag*.
- Striepen, B., Jordan, C. N., Reiff, S., and van Dooren, G. G. (2007). Building the Perfect Parasite: Cell Division in Apicomplexa. *PLoS Pathog*, 3(6), e78. doi: 10.1371/journal.ppat.0030078
- Stubbs, J., Simpson, K. M., Triglia, T., Plouffe, D., Tonkin, C. J., Duraisingh, M. T., . . . Cowman, A. F. (2005). Molecular mechanism for switching of *P. falciparum* invasion pathways into human erythrocytes. *Science*, 309(5739), 1384-1387. doi: 10.1126/science.1115257

- Sturm, A., Amino, R., van de Sand, C., Regen, T., Retzlaff, S., Rennenberg, A., . . . VT, H. (2006). Manipulation of host hepatocytes by the malaria parasite for delivery into liver sinusoids. *Science (New York, NY)*, *313*, 1287-1290.
- Su, X., Heatwole, V. M., Wertheimer, S. P., Guinet, F., Herrfeldt, J. A., Perterson, D. S., . . . Wellems, T. E. (1995). The large gene family var encodes proteins involved in cytoadherence and antigenic variation of plasmodium falciparum-infected erythrocytes *Cell*, *82*, 89-100.
- Sultan, A., Thathy, V., Frevert, U., Robson, K., Crisanti, A., Nussenzweig, V., . . . R., M. (1997). TRAP is necessary for gliding motility and infectivity of plasmodium sporozoites. *Cell*, *90*(3), 511-522.
- Tadauchi, T., Matsumoto, K., Herskowitz, I., and Irie, K. (2001). Post-transcriptional regulation through the HO 3' -UTR by Mpt5, a yeast homolog of Pumilio and FBF. *The EMBO Journal*, *20*(3), 552-561. doi: 10.1093/emboj/20.3.552
- Talevich, E., Tobin, A. B., Kannan, N., and Doerig, C. (2012). An evolutionary perspective on the kinome of malaria parasites. *Philosophical Transactions of the Royal Society B: Biological Sciences*, *367*(1602), 2607-2618. doi: 10.1098/rstb.2012.0014
- Tan, C. S. H., Bodenmiller, B., Pasculescu, A., Jovanovic, M., Hengartner, M. O., Jørgensen, C., . . . Linding, R. (2009). Comparative Analysis Reveals Conserved Protein Phosphorylation Networks Implicated in Multiple Diseases. *Science Signaling*, *2*(81), ra39-ra39. doi: 10.1126/scisignal.2000316
- Tanabe, K., Mackay, M., Goman, M., and Scaife, J. G. (1987). Allelic dimorphism in a surface antigen gene of the malaria parasite Plasmodium falciparum. *Journal of Molecular Biology*, *195*(2), 273-287. doi: [https://doi.org/10.1016/0022-2836\(87\)90649-8](https://doi.org/10.1016/0022-2836(87)90649-8)
- Tardieux, I., and Baum, J. (2016). Reassessing the mechanics of parasite motility and host-cell invasion. *The Journal of Cell Biology*, *214*(5), 507-515. doi: 10.1083/jcb.201605100
- Taylor, H. M., Triglia, T., Thompson, J., Sajid, M., Fowler, R., Wickham, M. E., . . . Holder, A. A. (2001). Plasmodium falciparum Homologue of the Genes for Plasmodium vivax and Plasmodium yoelii Adhesive Proteins, Which Is Transcribed but Not Translated. *Infect Immun*, *69*(6), 3635-3645. doi: 10.1128/IAI.69.6.3635-3645.2001
- Taylor, L. H., and Read, A. F. (1997). Why so few transmission stages? Reproductive restraint by malaria parasites. *Parasitol. Today*, *13*, 135-140.
- Tham, W.-H., Wilson, D. W., Reiling, L., Chen, L., Beeson, J. G., and Cowman, A. F. (2009). Antibodies to Reticulocyte Binding Protein-Like Homologue 4 Inhibit Invasion of Plasmodium falciparum into Human Erythrocytes. *Infect Immun*, *77*(6), 2427-2435. doi: 10.1128/iai.00048-09
- Tham, W. H., Lim, N. T., Weiss, G. E., Lopaticki, S., Ansell, B. R., Bird, M., . . . Cowman, A. F. (2015). Plasmodium falciparum Adhesins Play an Essential Role in Signalling and Activation of Invasion into Human Erythrocytes. *PLoS Pathog*, *11*(12), e1005343. doi: 10.1371/journal.ppat.1005343



- Tham, W. H., Wilson, D. W., Lopaticki, S., Schmidt, C. Q., Tetteh-Quarcoo, P. B., Barlow, P. N., . . . Cowman, A. F. (2010). Complement receptor 1 is the host erythrocyte receptor for *Plasmodium falciparum* PfRh4 invasion ligand. *Proceedings of the National Academy of Sciences*, *107*(40), 17327-17332. doi: 10.1073/pnas.1008151107
- The RTS, S. C. T. P. (2012). A Phase 3 Trial of RTS,S/AS01 Malaria Vaccine in African Infants. *New England Journal of Medicine*, *367*(24), 2284-2295. doi: 10.1056/NEJMoa1208394
- Thompson, J. K., Triglia, T., Reed, M. B., and Cowman, A. F. (2001). A novel ligand from *Plasmodium falciparum* that binds to a sialic acid-containing receptor on the surface of human erythrocytes. *Molecular Microbiology*, *41*(1), 47-58. doi: 10.1046/j.1365-2958.2001.02484.x
- Tonkin, M. L., Roques, M., Lamarque, M. H., Pugnère, M., Douguet, D., Crawford, J., . . . Boulanger, M. J. (2011). Host Cell Invasion by Apicomplexan Parasites: Insights from the Co-Structure of AMA1 with a RON2 Peptide. *Science*, *333*(6041), 463-467. doi: 10.1126/science.1204988
- Trager, W., and Jensen, J. (1976). Human malaria parasites in continuous culture. *Science*, *193*(4254), 673-675. doi: 10.1126/science.781840
- Tran, T. M., Ongoiba, A., Coursen, J., Crosnier, C., Diouf, A., Huang, C.-Y., . . . Crompton, P. D. (2014). Naturally Acquired Antibodies Specific for *Plasmodium falciparum* Reticulocyte-Binding Protein Homologue 5 Inhibit Parasite Growth and Predict Protection From Malaria. *The Journal of Infectious Diseases*, *209*(5), 789-798. doi: 10.1093/infdis/jit553
- Treeck, M., Sanders, J. L., Elias, J. E., and Boothroyd, J. C. (2011). The Phosphoproteomes of *Plasmodium falciparum* and *Toxoplasma gondii* reveal unusual adaptations within and beyond the parasites' boundaries. *Cell Host Microbe*, *10*(4), 410-419. doi: 10.1016/j.chom.2011.09.004
- Treeck, M., Struck, N. S., Haase, S., Langer, C., Herrmann, S., Healer, J., . . . Gilberger, T. W. (2006). A conserved region in the EBL proteins is implicated in microneme targeting of the malaria parasite *Plasmodium falciparum*. *J Biol Chem*, *281*(42), 31995-32003. doi: 10.1074/jbc.M606717200
- Treeck, M., Zacherl, S., Herrmann, S., Cabrera, A., Kono, M., Struck, N. S., . . . Gilberger, T. W. (2009). Functional analysis of the leading malaria vaccine candidate AMA-1 reveals an essential role for the cytoplasmic domain in the invasion process. *PLoS Pathog*, *5*(3), e1000322. doi: 10.1371/journal.ppat.1000322
- Umlas, J., and Fallon, J. N. (1971). New Thick-Film Technique for Malaria Diagnosis. *The American journal of tropical medicine and hygiene*, *20*(4), 527-529. doi: https://doi.org/10.4269/ajtmh.1971.20.527
- Vedadi, M., Lew, J., Artz, J., Amani, M., Zhao, Y., Dong, A., . . . Hui, R. (2007). Genome-scale protein expression and structural biology of *Plasmodium falciparum* and related Apicomplexan organisms. *Molecular and Biochemical Parasitology*, *151*(1), 100-110. doi: https://doi.org/10.1016/j.molbiopara.2006.10.011

- Vembar, S. S., Droll, D., and Scherf, A. (2016). Translational regulation in blood stages of the malaria parasite *Plasmodium* spp.: systems-wide studies pave the way. *Wiley Interdiscip Rev RNA*, *7*(6), 772-792. doi: 10.1002/wrna.1365
- Volz, J. C., Yap, A., Sisquella, X., Thompson, J. K., Lim, N. T., Whitehead, L. W., . . . Cowman, A. F. (2016). Essential Role of the PfRh5/PfRipr/CyRPA Complex during *Plasmodium falciparum* Invasion of Erythrocytes. *Cell Host Microbe*, *20*(1), 60-71. doi: 10.1016/j.chom.2016.06.004
- Voss, T. S., Bozdech, Z., and Bártfai, R. (2014). Epigenetic memory takes center stage in the survival strategy of malaria parasites. *Current opinion in microbiology*, *20*, 88-95. doi: <https://doi.org/10.1016/j.mib.2014.05.007>
- Wahlgren, M., Fernandez, C., Scholander, C., and Carlson, J. (1994). Rosetting. *Parasitol. Today*, *10*, 73-79.
- Walliker, D., Quakyi, I., Wellems, T., McCutchan, T., Szarfman, A., London, W., . . . Carter, R. (1987). Genetic analysis of the human malaria parasite *Plasmodium falciparum*. *Science*, *236*(4809), 1661-1666. doi: 10.1126/science.3299700
- Wang, J., Zhang, C.-J., Chia, W. N., Loh, C. C. Y., Li, Z., Lee, Y. M., . . . Lin, Q. (2015). Haem-activated promiscuous targeting of artemisinin in *Plasmodium falciparum*. *Nat Commun*, *6*, 10111. doi: 10.1038/ncomms10111
- Wang, K., Peng, E. D., Huang, A. S., Xia, D., Vermont, S. J., Lentini, G., . . . Bradley, P. J. (2016). Identification of Novel O-Linked Glycosylated Toxoplasma Proteins by Vicia villosa Lectin Chromatography. *PLoS One*, *11*(3), e0150561. doi: 10.1371/journal.pone.0150561
- Ward, P., Equinet, L., Packer, J., and Doerig, C. (2004). Protein kinases of the human malaria parasite *Plasmodium falciparum*: the kinome of a divergent eukaryote. *BMC Genomics*, *5*, 79-79. doi: 10.1186/1471-2164-5-79
- Wardman, P., and Candeias, L. (1996). Fenton chemistry: an introduction. *Radiat Res.*, *145*(5), 523-531.
- Watanabe, J. (1997). Cloning and characterization of heat shock protein DnaJ homologues from *Plasmodium falciparum* and comparison with ring infected erythrocyte surface antigen1Note: Nucleotide sequence data reported in this paper is available in the DDJB data bases under the accession number D85686.1. *Molecular and Biochemical Parasitology*, *88*(1), 253-258. doi: [https://doi.org/10.1016/S0166-6851\(97\)00073-X](https://doi.org/10.1016/S0166-6851(97)00073-X)
- Wharton, R. P., Sonoda, J., Lee, T., Patterson, M., and Murata, Y. The Pumilio RNA-Binding Domain Is Also a Translational Regulator. *Molecular Cell*, *1*(6), 863-872. doi: 10.1016/S1097-2765(00)80085-4
- White, N., S Pukrittayakamee, TT Hien, MA Faiz, OA Mokuolo, and Dondorp, A. (2014). Malaria. *The Lancet*, *383*, 723-735. doi: [https://doi.org/10.1016/S0140-6736\(13\)60024-0](https://doi.org/10.1016/S0140-6736(13)60024-0)
- WHO. (2016).
- WHO Malaria report. (2016).
- WHO malaria report. (2017).

- Wickham, M. E., Culvenor, J. G., and Cowman, A. F. (2003). Selective Inhibition of a Two-step Egress of Malaria Parasites from the Host Erythrocyte. *J Biol Chem*, 278(39), 37658-37663.
- Williams, J. (1999). Stimulation of *Plasmodium falciparum* gametocytogenesis by conditional medium from parasite cultures. *Am J Trop Med Hyg*, 60, 7-13.
- Winzeler, E. A. (2008). Malaria research in the post-genomic era. *Nature*, 455(7214), 751-756. doi: 10.1038/nature07361
- Wu, Y., Sifri, C. D., Lei, H. H., Su, X. Z., and Wellems, T. E. (1995). Transfection of *Plasmodium falciparum* within human red blood cells. *Proceedings of the National Academy of Sciences of the United States of America*, 92(4), 973-977.
- Wuchty, S., and Ipsaro, J. (2007). A Draft of Protein Interactions in the Malaria Parasite *P. falciparum* *Journal of Proteome Research*, 1461-1470. doi: 10.1021/pr0605769
- Yap, A., Azevedo, M. F., Gilson, P. R., Weiss, G. E., O'Neill, M. T., Wilson, D. W., . . . Cowman, A. F. (2014). Conditional expression of apical membrane antigen 1 in *Plasmodium falciparum* shows it is required for erythrocyte invasion by merozoites. *Cell Microbiol*, 16(5), 642-656. doi: 10.1111/cmi.12287
- Yeoh, S., O'Donnell, R. A., Koussis, K., Dluzewski, A. R., Ansell, K. H., Osborne, S. A., . . . Blackman, M. J. (2007). Subcellular Discharge of a Serine Protease Mediates Release of Invasive Malaria Parasites from Host Erythrocytes. *Cell*, 131(6), 1072-1083. doi: 10.1016/j.cell.2007.10.049
- Zamore, P. D., Williamson, J. R., and Lehmann, R. (1997). The Pumilio protein binds RNA through a conserved domain that defines a new class of RNA-binding proteins. *RNA*, 3(12), 1421-1433.
- Zhang, B., Gallegos, M., Puoti, A., Durkin, E., Fields, S., Kimble, J., and Wickens, M. P. (1997). A conserved RNA-binding protein that regulates sexual fates in the *C. elegans* hermaphrodite germ line. *Nature*, 390, 477. doi: 10.1038/37297
- Zhang, M., Joyce, B. R., Sullivan, W. J., and Nussenzweig, V. (2013). Translational Control in *Plasmodium* and *Toxoplasma* Parasites. *Eukaryotic Cell*, 12(2), 161-167. doi: 10.1128/EC.00296-12
- Zhou, Y., Ramachandran, V., Kumar, K. A., Westenberger, S., Refour, P., Zhou, B., . . . Winzeler, E. A. (2008). Evidence-based annotation of the malaria parasite's genome using comparative expression profiling. *PLoS One*, 3(2), e1570. doi: 10.1371/journal.pone.0001570
- Zuegge, J., Ralph, S., Schmuker, M., McFadden, G. I., and Schneider, G. (2001). Deciphering apicoplast targeting signals – feature extraction from nuclear-encoded precursors of *Plasmodium falciparum* apicoplast proteins. *Gene*, 280(1), 19-26. doi: [https://doi.org/10.1016/S0378-1119\(01\)00776-4](https://doi.org/10.1016/S0378-1119(01)00776-4)

## Appendix

### Oligonucleotides

#### EBA175

Name	Sequence 5'-3'
EBA175_NotI_fwd	GCGCgcgccgcGGAAACAGACAAGATCGGGGGGG
EBA175_NotI_800bp_fwd	GCGCgcgccgcCATGAAGAAATCCCATTAAAAACATGC
EBA175_AvrII_rev	GCGCcttaggTTTCTTAAAATTAATATCATTATATCC
EBA175_S1448A_S1449A_overlap_fwd	CCAAATATCAAgcTgCTGAAGGAGTTATGAATG
EBA175_S1448A_S1449A_overlap_rev	CCTTCAGcAgcTTGATATTTGGCTTG
EBA175_T1466A_S1473A_overlap_fwd	GAATAATTTTTTATTTGAAGTTgCTGATAATTTAGATAAATTAgCCAATATGTTTC
EBA175_T1466A_S1473A_overlap_rev	GAACATATTGGcTAATTTATCTAAATTATCAGcAACTTCAAATAAAAAAATTATTC
EBA175_T1483A_S1489A_AvrII_rev	GCGCcttaggTTTCTTAAAATTAATATCATTATATCCTCATGGTATTTCAGcAAATCGTTGATATTAGcTTCCTGTACTTGTGATTGAAC
EBA175_inte_check 1889 bp fwd	GGGTGAATTCTAAACCTTTATCTG

**Table 3: List of oligonucleotides that were used to generate the EBA175 constructs and for validation of their integration into the endogenous locus.**

#### Bioinformatic screen

Name	Sequence 5'-3'
0105400.1_NotI_fwd	GACTATAGAATACTCgcgccgcATGAGATTATGGTTGATTGTTTG
0105400.1_AvrII/MluI_rev	ACCTCCAGCACCAGCAGCACCTCTAGCagcgtccttaggATTATGCATAGGATTTGGATTAAC
0105400.1_inte check	TTCTGTGCATACCTCTATGC
0105400.1_TGD_NotI_fwd	gctatttaggtgacactatagaataactcgcgcccgcTAAGATTATGGTTGATTGTTGT
0105400.1_TGD_AvrII/MluI_rev	cctccagcaccagcagcagcacctctagcagcgtccttaggAATAGTAGACGCACCTAATGC
0204100_NotI_fwd	GCGCGCGGCCGCTAGATGAACATATATATAATGAAG
0204100_AvrII_MluI_rev	GCGCACGCGTCCTAGGTATAATTTTAAAAAAGATAATATC
0204100_inte check	CATATCATGATACATATGATTTATG
0210800_NotI_fwd	GCGCGCGGCCGCAACAGATTTATATTTAAGGACT
0210800_AvrII_MluI_rev	GCGCACGCGTCCTAGGATAAAAAAGGAAAGAATAAATATC
0210800_inte check	GATATCATAAGTAATAATAAG
0316300.2_NotI_fwd	GCGCGCGGCCGAGCTTTTACCTTGATTGACGAGGGA
0316300.2_AvrII_MluI_rev	GCGCACGCGTCCTAGGAGGTGTCCATATGTTGAGATCTGGC
0316300.2_inte check_sense	GCGCGGAAGCATTATTATTACTGG
0316300.2_TGD_TAA_NotI_fwd	gctatttaggtgacactatagaataactcgcgcccgcTAAGTGTATATGCTTATGTATGCTATGG
0316300.2_TGD_AvrII_MluI_rev	cctccagcaccagcagcagcacctctagcagcgtccttaggaactttcatatgatacataaacgt

	gcg
0404800_NotI_fwd	GCGCGCGGCCGCTAATCATGTATTTTTAGAGGCTGT
0404800_AvrII_Mlul_rev	GCGCACGCGTCTAGGTTCTGTTATAAAATTCATGTAATTTTC
0404800_inte_check_sense	GTTGAGGAGCTCTTCTGTTCG
0410700_NotI_fwd	GCGCGCGGCCGCTAGATTATGTTATCATATTATTG
0410700_AvrII_Mlul_rev	GCGCACGCGTCTAGGCCATCCTATATATTTGTCTGA
0410700_inte_check_sense	CTAAAGCCAATGAAGAATGGGG
0419400_Not_fwd	gacactatagaataactcgcgccgcGGTTGGAATTACGATGGACAAACAG
0419400_AvrII_Mlul_rev	AGCAGCACCTCTAGCagcgtcctaggTAAATCATCTCCATGAAAAAGACC
0419400_inte check	GCGCGGGGAAGAGCAAATGAAAAACATATCCG
0419400_TAA_TGD_NotI_sense	GCGCgcgccgcTAAAGAAAAAGAAGAAAACGTG
0419400_TGD_Mlul_as	GCGCagcgtATTATCATTTTCTATTGTCTG
0419400_TGD_inte_check_s_utr77	GTGTGTGTGTATGCTTATTATCAC
0423300_NotI_fwd	GCGCgcgccgcCTCGTAATTCATTTTTACCACC
0423300_AvrII_Mlul_rev	AGCAGCACCTCTAGCACGCGTCTAGGTTCTTTTGTCTAAAGAATGTAT ATCCGGATATACATTTCTTTAGAAACAAAAAGACCTAGGACGCGTGCTAG AGGTGCTGCT
0423300_inte check	GAACGATAAAGATGGAAAG
0530300_NotI_fwd	GACTATAGAATACTGcgccgcCTCTAGATCTTCATTCATTTGTTATC
0530300_AvrII/Mlul_rev	AGCAGCACCTCTAGCagcgtcctaggCTTCTCAATTTTGATATACTATCA GAG
0530300_inte check	GCGCGTAAAATGCCTTTATTAATG
0530300_TGD_NotI_fwd	GCGCgcgccgcTAAATAAAAGAGAAATTGTTAAAAT
0530300_TGD_Mlul_rev	GCGCagcgtCTTTTTAATTTATTAATAC
0625400_NotI_fwd	GCGCgcgccgcCAATAACGGATATTG
0625400_AvrII_Mlul_rev	GCGCagcgtcctaggTAACTCCATTTTTTTTTGGG
0625400_inte check	GCAAGGGTGTGTAAG
0704300_NotI_fwd	GCGCgcgccgcGATGGTGTAATAAATGATGGTG
0704300_Mlul_rev	GCGCagcgtTTTTTTTTATTTTTTTCTG
0704300_inte check	GATGGTGTAATAAATGATGGTG
0704300_TGD_NotI_fwd	GCGCgcgccgcTAAGAAAAGAATAAATACGATATAG
0704300_TGD_Mlul_rev	GCGCagcgtAGTTAATAATTTGTATTCT
0716300_NotI_fwd	GACTATAGAATACTGcgccgcCAACTGACGATGGTGATAGTC
0716300_AvrII_Mlul_rev	ACCTCCAGCACCAGCAGCAGCACCTCTAGCagcgtcctaggTGAAAATATTT CTTCATAATTTGTATTGTCAACC
0716300_inte check	TGAAGATGAGATAGAGAGGG
0721100_NotI_fwd	GACTATAGAATACTGcgccgcATGTCGAGACTTTTCTTTCTTGTTCT
0721100_AvrII_Mlul_rev	ACCTCCAGCACCAGCAGCAGCACCTCTAGCagcgtcctaggTTCAGTCACAT AACATACTGGATGG
0721100_inte check	CACTTGAAATATGATCCTAAGGC
0725400_NotI_fwd	GCGCgcgccgcATGTGTTTCCTTAAGTATTTCT
0725400_Mlul_rev	GCGCagcgtATTATTCTGTCCTTTTTTCTC
0725400_inte check utr113	CGGTGTATGTTGTTTTAAAAAAGAAG
0730800.1_NotI_fwd	GACTATAGAATACTGcgccgcATGGTTCAATTTACCAAGATTTTAGCA G
0730800.1_AvrII_Mlul_rev	ACCTCCAGCACCAGCAGCAGCACCTCTAGCagcgtcctaggAAATTTTTTTT TTTTCTCTCAATGTAGAAGTACCAGC
0730800.1_inte check	GTAGATTAACGTACTTACAACGG
0806200_NotI_fwd	gacactatagaataactcgcgccgcCCAGAAATTATACCAGATAATACACC
0806200_AvrII_Mlul_rev	AGCAGCACCTCTAGCagcgtcctaggATTGTATATATAAAAAATAATAAAT AATC

0806200_inte check	GCGCGCTTGTCTTCCTTTTAGTGATGGG
0811600_Notl_fwd	GCGCgggccgcGTAATATAGATGATGTAAGTTC
0811600_Avrll/Mlul_rev	GCGCacgcgtcctaggTTCGTCTACCTTAAATAAAATAAAGAAGACG
0811600_inte check	GAAACTGATAACAGTAATGAAG
0811600_TGD_Notl_fwd	GCGCgggccgcTAATCATAATATTTTTATTATTAC
0811600_TGD_Mlul_rev	GCGCacgcgtCATAATATTCATCTATACTTC
1014100_Notl_fwd	GCGCgggccgcCTCTCACCTTTGATATAAAATTATG
1014100_Avrll_Mlul_rev	GCGCacgcgtcctaggTGGATTTCTAAAATCTAGTGCATCTCC
1014100_inte check	GGAAGAGGATATGAATGAG
1030200_Notl_fwd	GCGCGCGGCCCAAGGTAATAAATAGTG
1030200_Avrll_Mlul_rev	GCGCACGCGTCTAGGAAATTTATATGGTTTCTGTGAATCAAATG
1035100_Notl_fwd	GCGCgggccgcGAATAAAGATAACAG
1035100_Avrll_Mlul_rev	GCGCacgcgtcctaggCTTATAATCACTAAATAAATTTATTATAG
1035100_inte check	GTCATCCTGAAGCACTTGTGGGTGGAGAG
1105300_Notl_fwd	GCGCgggccgcGGATTCAATAAATGAAATATCC
1105300_Mlul_rev	GCGCacgcgtATGGCCTACAGTCGAGGGAC
1105300_inte check	CATCTGTTAATCAGTATACAGC
1105300_TGDI_TAA_Not_fwd	GCGCgggccgcTAAAGAAAAATAATACCTCTTTTGTACTCGG
1105300_TGD_Mlul_rev	GCGCacgcgtGGAAGAATTAAGAATTATTATAATAATTG
1115600_Notl_fwd	GACACTATAGAATACTGcggccgcTATGCTTTATGCGCCGAGGAAC
1115600_Avrll/Mlul_rev	ACCTCCAGCACCAGCAGCAGCACCTCTAGCacgcgtcctaggCAATGGCAAT TCTCCTGATTC
1115600_inte check	TATAAAGGAGGAAAAATGGG
1115600_TGD_Not_fwd	gctatttagtgacactatagaataactcggccgcTAAgtatctaattagatctcataattta atacatac
1115600_TGD_Avrll/Mlul_rev	cctccagcaccagcagcagcacctctagcagcgtcctaggGTGGGTATTTATTATTAT CC
1122700_Notl_fwd	GCGCgggccgcATGAAGCTGAATAAATTTTTGATCG
1122700_Mlul_rev	GCGCacgcgtGTAAAAATCTTTATTATAATCATC
1122700_inte_check_sense_utr15 7	CCAATTCTTGCCCTTATCC
1136200_Notl_fwd	GCGCgggccgcCTATTATGCTAAACAATAGTTCTTC
1136200_Mlul_rev	GCGCacgcgtTAAAAATAATATATATGTAATTATAG
1136200_inte check	CAGGTGCAGCTATCAGCGGAC
1136200_TGD_TAA_Notl_fwd	GCGCgggccgcTAAAATTTAAACAAAATTTCTGTCC
1136200_TGD_Mlul_rev	GCGCacgcgtCGTGTATTATCATCTACATTGTC
1136200_TGD_inte check	CCAAAAGGCAGCGGATCAC
PF3D7_1143200_Notl_fwd	GCGCgggccgcATGAGAATACATTGTTTTTC
PF3D7_1143200_Mlul_rev	GCGCacgcgtATCGTTGTAATTAACCTAAACC
PF3D7_1143200_5'utr_inte check	CCCTTATTAATTGTTACATATC
PF3D7_1143200_TGD_Notl_fwd	GCGCgggccgcTAAAGAATACATTGTTTTTC
PF3D7_1143200_TGD_Mlul_rev	GCGCacgcgtCAAATATACTAAATTCAAAAAAC
PF3D7_1200700_Notl_fwd	GCGCgggccgcGAATATATAGAACTGAAATG
PF3D7_1200700_Avrll_Mlul_rev	GCGCacgcgtcctaggTACATTTACTTGTAGTTCTTG
PF3D7_1200700_inte check	CACGAATGATGGTATTTTAAACGGGAGATATTG
PF3D7_1229300_Notl_fwd	GCGCgggccgcCAATGATACTACTAAGAATAACC
PF3D7_1229300_Mlul_rev	GCGCacgcgtTGCCATGTCAAGTGAATTTTC
PF3D7_1229300_inte check	CGGAGAAAAGTGTGAGAAGG
PF3D7_1229300_TGD_Notl_fwd	GCGCgggccgcTAAAAGTTGAAATATCATTTATTTTTTC
PF3D7_1229300_TGD_Mlul_rev	GCGCacgcgtCTTAAATGATTTCTTAAATAAATTG
PF3D7_1310200_Notl_fwd	GACACTATAGAATACTGcggccgcATGAAAATACAATACATGATAATAATA

	TATTTTATCATTTTGATCTGCG
PF3D7_1310200_AvrII/Mlul_rev	ACCTCCAGCACCAGCAGCAGCACCTCTAGCacgctcctaggACTGTTTCATAA ATTTACAGTGTTTTACATG
PF3D7_1310200_inte check	ATTTATATAGCCTCTCTCTGG
PF3D7_1310200_TGD_NotI_fwd	GCGCgcgccgcTAAATAATAATATATTTTATCATTTTG
PF3D7_1310200_TGD_Mlul_rev	GCGCacgctCATTGCACCACCAGAATTTCTC
PF3D7_1334600_NotI_fwd	GACACTATAGAATACTCgcgccgcAGGACTTATTTTTATTTGTTTATATGC
PF3D7_1334600_AvrII/Mlul_rev	ACCTCCAGCACCAGCAGCAGCACCTCTAGCacgctcctaggACTATATAAAC CATACATTACCTTTTAAATTC
PF3D7_1334600_inte check	ATTTATATAGCCTCTCTCTGG
PF3D7_1334600_TGD_NotI_fwd	gctatttagtgacactatagaataactcgcgccgcTAAGGACTTATTTTTATTTGTT TATATGC
PF3D7_1334600_TGD_AvrII/Mlul_rev	cctccagcaccagcagcagcacctctagcagcctcctaggATAATCGTCCACATTTG ACC
1352500_NotI_fwd	GACACTATAGAATACTCgcgccgcATGGCTATATTTAAGAAGAG
1352500_AvrII_Mlul_rev	ACCTCCAGCACCAGCAGCAGCACCTCTAGCacgctcctaggATCCTTTTTCT TAGCAACTTTCGATGCTCC
1352500_inte check	AAAGCATATTTTACAACCTCC
PF3D7_1358000_NotI_fwd	GCGCgcgccgcGAAGAAGAAATTAATTCCTCC
PF3D7_1358000_Mlul_rev	GCGCacgctTGTTCTTTTTTAAAAAAGAAACATC
PF3D7_1358000_inte check	GCCAAACAGAAAATCGAAAAGATTC
PF3D7_1404700_NotI_fwd	GACACTATAGAATACTCgcgccgcGAAAATATCATAGGGCAGGATGAGA
PF3D7_1404700_AvrII_Mlul_rev	ACCTCCAGCACCAGCAGCAGCACCTCTAGCacgctcctaggTTTAGAAAATA TAAATGTTATGTTTGC
PF3D7_1404700_inte check	GAGTCCTCCTAATTACAGTAC
PF3D7_1404700_NotI_fwd	GACACTATAGAATACTCgcgccgcGAAAATATCATAGGGCAGGATGAGA
PF3D7_1404800_NotI_fwd	GACACTATAGAATACTCgcgccgcGAGAAATTAGGATATGCTTATAGAG
PF3D7_1404800_AvrII_Mlul_rev	ACCTCCAGCACCAGCAGCAGCACCTCTAGCacgctcctaggTGTAGAATAA AATTTTGATATAACACGGGATGGC
PF3D7_1404800_inte check	CGTTTAGATATTGTTGTTGATGTACC
PF3D7_1404900.1_NotI_fwd	GACACTATAGAATACTCgcgccgcATGTTGAGTGTTAACAAAGTTACCGC
PF3D7_1404900.1_AvrII_Mlul_rev	ACCTCCAGCACCAGCAGCAGCACCTCTAGCacgctcctaggGAGTTCATCTG AACTGTTAAGTAG
PF3D7_1404900.1_inte check	GAATATAATTTACTTCAGACAGTTGAGAG
PF3D7_1404900.1_TGD_TAA_NotI_fwd	gctatttagtgacactatagaataactcgcgccgcTAATTGAGTGTTAACAAAGTTA CC
PF3D7_1404900.1_TGD_AvrII_Mlul_rev	cctccagcaccagcagcagcacctctagcagcctcctaggTCCATAGCTTCTTTGCTG G
PF3D7_1463900_NotI_fwd	GACACTATAGAATACTCgcgccgcTGGACATAAATGCTGTTCCAGGT
PF3D7_1463900_AvrII/Mlul_rev	ACCTCCAGCACCAGCAGCAGCACCTCTAGCacgctcctaggTTTCGAATCAG ATGCTGActgta
PF3D7_1463900_inte check	TAACATCTGAACATGATATTAGGG
PF3D7_1463900_TGD_NotI_fwd	GCGCgcgccgc cTAATTGTATCTTCATATTTTGTATGT
PF3D7_1463900_TGD_Mlul_rev	GCGCacgctAGGTTTCATAATAATTCCTTTTTGTTT
PF3D7_1472600_NotI_fwd	GCGCgcgccgcGATTTCTTATAAATATAAGCCACAAAG
PF3D7_1472600_AvrII_Mlul_rev	CGCGCacgctcctaggTAATCTTCATAATTTTCAAATAGTTG
PF3D7_1472600_inte check	CTGGTACGACACAAATTTTTGAAAAGCGATTACTC
PF3D7_1035900_NotI_fwd	GACACTATAGAATACTCgcgccgcTGTGAAGCCAATGGAACACT
PF3D7_1035900_AvrII_Mlul_rev	ACCTCCAGCACCAGCAGCAGCACCTCTAGCacgctcctaggTGGATATAAA GTGCTTAAATGC
PF3D7_1035900_inte check	GTGCACACAAAAGATGCTTATATTTGTAC

PF3D7_1035900_TGD_TAA_NotI_fwd	GCGCgcgccgcTAATTGAATATTTTAAATATAATTTTC
PF3D7_1035900_TGD_MluI_rev	GCGCacgcgtTACTTCTTCAGCTACTTTTTC

**Table 4: List of oligonucleotides that were used for cloning and integration analysis of the candidate gene constructs.**

### Sequencing primer

Name	Sequence 5'-3'
pA55sense	GGAATTGTGAGCGGATAACAATTCACACAGG
pA_as	CAGTTATAAATACAATCAATTGG
FKBP39rev	TTGACCTCTTTTGGAAATGTACG
GFP272as	CCTTCGGGCATGGCACTC

**Table 5: List of oligonucleotides that were used for sequencing of the plasmids that were generated for this study.**

### Control genes

Name	Reference
EBA175	Orlandi, P.A., Sim, B.K., Chulay, J.D., and Haynes, J.D., 1990, <i>Mol Biochem Parasitol</i> 40, 285-294
EBA181 (JESEBL)	Adams, J.H., Blair, P.L., Kaneko, O., and Peterson, D.S., 2001, <i>Trends Parasitol</i> 17, 297-299; Gilberger et al., 2003 (see References)
AMA1	Crewther, P.E., Culvenor, J.G., Silva, A., Cooper, J.A., and Anders, R.F., 1990, <i>Exp Parasitol</i> 70, 193-206
RH4	Triglia, T., Thompson, J., Caruana, S.R., Delorenzi, M., Speed, T., and Cowman, A.F., 2001, <i>Infect Immun</i> 69, 1084-1092
Rh2b	Duraisingh et al., 2003 (see References)
MSP1	Tanabe, K., Mackay, M., Goman, M., and Scaife, J.G., 1987, <i>J Mol Biol</i> 195, 273-287
MTRAP	Baum, J., Richard, D., Healer, J., Rug, M., Krnajska, Z., Gilberger, T.W., Green, J.L., Holder, A.A., and Cowman, A.F., 2006, <i>J Biol Chem</i> 281, 5197-5208
MSP7	Pachebat J.A., Ling I.T., Grainger M., et al., 2001, <i>Mol Biochem Parasitol.</i> ; 117: 83-89
EBL1	Adams, J.H., Blair, P.L., Kaneko, O., and Peterson, D.S., 2001, <i>Trends Parasitol</i> 17, 297-299
RopH3	Brown, H.J., and Coppel, R.L., 1991, <i>Mol Biochem Parasitol</i> 4, 99-110
SERA5	Delplace, P., Fortier, B., Tronchin, G., Dubremetz, J.F., and Vernes, A., 1987, <i>Mol Biochem Parasitol</i> 23, 193-201; Miller et al., 2002 (see References)
RAP2	Howard, R.F., Stanley, H.A., Campbell, G.H., and Reese, R.T., 1984, <i>Am J Trop Med Hyg</i> 33, 1055-1059; Bushell et al., 1988
MSP9	Sharma, P., Kumar, A., Singh, B., Bharadwaj, A., Sailaja, V.N., Adak, T., Kushwaha, A., Malhotra, P., and Chauhan, V. S., 1998, <i>Infect Immun</i> 66, 2895-2904; Kushwaha et al., 2000



**Table 6: List of genes that were used as control for the expression profiles of candidate genes selected in the bioinformatic screening approach and the according reference publications.**

### Genes identified by the bioinformatic screening approach

Gene ID	Product Description
PF3D7_0102500	erythrocyte binding antigen-181
PF3D7_0102700	merozoite-associated tryptophan-rich antigen
PF3D7_0104000	thrombospondin-related sporozoite protein
PF3D7_0104200	StAR-related lipid transfer protein
PF3D7_0105400	conserved Plasmodium protein, unknown function
PF3D7_0105400	conserved Plasmodium protein, unknown function
PF3D7_0106600	conserved Plasmodium protein, unknown function
PF3D7_0106900	2-C-methyl-D-erythritol 4-phosphate cytidyltransferase, putative
PF3D7_0109850	phosphatidate cytidyltransferase, putative
PF3D7_0111500	UMP-CMP kinase, putative
PF3D7_0202500	early transcribed membrane protein 2
PF3D7_0204100	conserved Plasmodium protein, unknown function
PF3D7_0206900	merozoite surface protein 5
PF3D7_0207400	serine repeat antigen 7
PF3D7_0207500	serine repeat antigen 6
PF3D7_0207600	serine repeat antigen 5
PF3D7_0207700	serine repeat antigen 4
PF3D7_0207800	serine repeat antigen 3
PF3D7_0207900	serine repeat antigen 2
PF3D7_0208000	serine repeat antigen 1
PF3D7_0210600	conserved Plasmodium protein, unknown function
PF3D7_0210800	conserved Plasmodium protein, unknown function
PF3D7_0211600	UDP-N-acetylglucosamine transferase subunit ALG14, putative
PF3D7_0212000	GDP-fructose:GMP antiporter, putative
PF3D7_0212600	secreted protein with altered thrombospondin repeat domain
PF3D7_0214900	rhoptry neck protein 6
PF3D7_0215900	palmitoyltransferase DHHC11, putative
PF3D7_0216800	TMEM121 domain-containing protein, putative
PF3D7_0217000	conserved Plasmodium membrane protein, unknown function
PF3D7_0220800	cytoadherence linked asexual protein 2
PF3D7_0221700	Plasmodium exported protein, unknown function
PF3D7_0302200	cytoadherence linked asexual protein 3.2
PF3D7_0302500	cytoadherence linked asexual protein 3.1
PF3D7_0303900	phosphatidylethanolamine-binding protein, putative
PF3D7_0304700	conserved Plasmodium protein, unknown function
PF3D7_0307400	ATP-dependent Clp protease proteolytic subunit

PF3D7_0310400	parasite-infected erythrocyte surface protein
PF3D7_0311200	valine--tRNA ligase, putative
PF3D7_0314000	co-chaperone p23
PF3D7_0316300	inorganic pyrophosphatase, inorganic pyrophosphatase, putative
PF3D7_0316300	inorganic pyrophosphatase, inorganic pyrophosphatase, putative
PF3D7_0320200	CPW-WPC family protein
PF3D7_0323400	Rh5 interacting protein
PF3D7_0402100	Plasmodium exported protein (PHISTb), unknown function
PF3D7_0402300	reticulocyte binding protein homologue 1
PF3D7_0404700	dipeptidyl aminopeptidase 3
PF3D7_0404800	conserved Plasmodium protein, unknown function
PF3D7_0404900	6-cysteine protein
PF3D7_0405900	apical sushi protein
PF3D7_0408600	sporozoite invasion-associated protein 1
PF3D7_0410700	ribosome biogenesis GTPase A, putative
PF3D7_0413800	50S ribosomal protein L10, putative
PF3D7_0415700	conserved Plasmodium protein, unknown function
PF3D7_0419200	protein transport protein GOT1, putative
PF3D7_0419400	conserved Plasmodium protein, unknown function
PF3D7_0419700	apical merozoite protein
PF3D7_0422800	serpentine receptor, putative
PF3D7_0423300	conserved Plasmodium protein, unknown function
PF3D7_0423400	apical asparagine-rich protein AARP
PF3D7_0423700	early transcribed membrane protein 4
PF3D7_0423800	cysteine-rich protective antigen
PF3D7_0424100	reticulocyte binding protein homologue 5
PF3D7_0424200	reticulocyte binding protein homologue 4
PF3D7_0424300	erythrocyte binding antigen-165, pseudogene
PF3D7_0500600	stevor, pseudogene
PF3D7_0501500	rhoptry-associated protein 3
PF3D7_0501600	rhoptry-associated protein 2
PF3D7_0504500	MOLO1 domain-containing protein, putative
PF3D7_0505400	conserved Plasmodium protein, unknown function
PF3D7_0506400	conserved Plasmodium protein, unknown function
PF3D7_0507400	conserved Plasmodium protein, unknown function
PF3D7_0507500	subtilisin-like protease 1
PF3D7_0508000	6-cysteine protein
PF3D7_0508200	longevity-assurance (LAG1) protein, putative
PF3D7_0511600	apical rhoptry neck protein
PF3D7_0522500	50S ribosomal protein L17, apicoplast, putative
PF3D7_0522600	inner membrane complex protein

PF3D7_0525700	conserved Plasmodium protein, unknown function
PF3D7_0530200	phosphoenolpyruvate/phosphate translocator
PF3D7_0530300	conserved Plasmodium membrane protein, unknown function
PF3D7_0606800	VFT protein
PF3D7_0607300	uroporphyrinogen III decarboxylase
PF3D7_0611100	succinate dehydrogenase subunit 3, putative
PF3D7_0612300	transmembrane protein 234, putative
PF3D7_0612700	6-cysteine protein
PF3D7_0613200	conserved Plasmodium protein, unknown function
PF3D7_0613400	50S ribosomal protein L18, apicoplast, putative
PF3D7_0620400	merozoite surface protein 10
PF3D7_0624700	N-acetylglucosaminylphosphatidylinositol deacetylase, putative
PF3D7_0625400	conserved Plasmodium protein, unknown function
PF3D7_0629300	phospholipase, putative
PF3D7_0630400	conserved Plasmodium protein, unknown function
PF3D7_0702000	Plasmodium exported protein (hyp12), unknown function
PF3D7_0704300	conserved Plasmodium membrane protein, unknown function
PF3D7_0704900	peptide chain release factor 2
PF3D7_0707300	rhoptry-associated membrane antigen
PF3D7_0709100	Cg1 protein
PF3D7_0709800	conserved protein, unknown function
PF3D7_0715200	conserved Plasmodium protein, unknown function
PF3D7_0716300	conserved Plasmodium protein, unknown function
PF3D7_0719400	conserved Plasmodium protein, unknown function
PF3D7_0721100	conserved Plasmodium protein, unknown function
PF3D7_0722200	rhoptry-associated leucine zipper-like protein 1
PF3D7_0725400	conserved Plasmodium protein, unknown function
PF3D7_0727100	conserved Plasmodium protein, unknown function
PF3D7_0730800	Plasmodium exported protein, unknown function, unspecified product
PF3D7_0730800	Plasmodium exported protein, unknown function, unspecified product
PF3D7_0731500	erythrocyte binding antigen-175
PF3D7_0731600	acyl-CoA synthetase
PF3D7_0804400	methionine aminopeptidase 1c, putative
PF3D7_0806200	C-mannosyltransferase, putative
PF3D7_0808200	plasmepsin X
PF3D7_0811600	conserved Plasmodium protein, unknown function
PF3D7_0817800	conserved Plasmodium protein, unknown function
PF3D7_0820600	conserved Plasmodium membrane protein, unknown function
PF3D7_0825200	translation initiation factor IF-3
PF3D7_0827500	apicoplast ribosomal protein L21 precursor, putative
PF3D7_0828800	GPI-anchored micronemal antigen

PF3D7_0829600	early transcribed membrane protein 8
PF3D7_0831600	cytoadherence linked asexual protein 8
PF3D7_0900500	rifin
PF3D7_0902800	serine repeat antigen 9
PF3D7_0904400	signal peptidase complex subunit 3, putative
PF3D7_0904700	bacterial histone-like protein
PF3D7_0905400	high molecular weight rhoptry protein 3
PF3D7_0908100	apicoplast integral membrane protein, putative
PF3D7_0908300	conserved protein, unknown function
PF3D7_0908300	conserved protein, unknown function
PF3D7_0909600	conserved Plasmodium protein, unknown function
PF3D7_0911600	conserved Plasmodium protein, unknown function
PF3D7_0913500	protease, putative
PF3D7_0916300	conserved Plasmodium protein, unknown function
PF3D7_0917200	conserved Plasmodium membrane protein, unknown function
PF3D7_0918000	glideosome-associated protein 50
PF3D7_0918400	conserved Plasmodium protein, unknown function
PF3D7_0919400	protein disulfide isomerase
PF3D7_0920600	conserved Plasmodium protein, unknown function
PF3D7_0929400	high molecular weight rhoptry protein 2
PF3D7_0929900	conserved Plasmodium protein, unknown function
PF3D7_0930300	merozoite surface protein 1
PF3D7_0932100	protein MAM3, putative
PF3D7_0932500	palmitoyltransferase DHHC6, putative
PF3D7_0935800	cytoadherence linked asexual protein 9
PF3D7_1001500	early transcribed membrane protein 10.1
PF3D7_1001700	Plasmodium exported protein (PHISTc), unknown function
PF3D7_1005900	conserved Plasmodium protein, unknown function
PF3D7_1008500	conserved Plasmodium membrane protein, unknown function
PF3D7_1012200	rhoptry associated adhesin
PF3D7_1014100	merozoite surface protein MSA180, putative
PF3D7_1017100	rhoptry neck protein 12
PF3D7_1021000	conserved Plasmodium protein, unknown function
PF3D7_1021300	apicoplast integral membrane protein, putative
PF3D7_1022800	4-hydroxy-3-methylbut-2-en-1-yl diphosphate synthase (ferredoxin), putative
PF3D7_1028700	merozoite TRAP-like protein
PF3D7_1030200	claudin-like apicomplexan microneme protein, putative
PF3D7_1030900	ookinete surface protein P28
PF3D7_1034100	conserved Plasmodium protein, unknown function
PF3D7_1034200	apicoplast ribosomal protein L27 precursor, putative
PF3D7_1035100	probable protein, unknown function

PF3D7_1035200	S-antigen
PF3D7_1035300	glutamate-rich protein GLURP
PF3D7_1035400	merozoite surface protein 3
PF3D7_1035700	duffy binding-like merozoite surface protein
PF3D7_1035900	probable protein, unknown function
PF3D7_1036000	merozoite surface protein
PF3D7_1036300	duffy binding-like merozoite surface protein 2
PF3D7_1038000	antigen UB05
PF3D7_1038000	antigen UB05
PF3D7_1102700	early transcribed membrane protein 11.1
PF3D7_1102800	early transcribed membrane protein 11.2
PF3D7_1105300	conserved Plasmodium protein, unknown function
PF3D7_1105600	translocon component PTEX88
PF3D7_1106100	apicoplast ribosomal protein S15 precursor, putative
PF3D7_1108600	endoplasmic reticulum-resident calcium binding protein
PF3D7_1114800	glycerol-3-phosphate dehydrogenase, putative
PF3D7_1115100	conserved Plasmodium protein, unknown function
PF3D7_1115600	peptidyl-prolyl cis-trans isomerase
PF3D7_1115900	palmitoyltransferase DHHC9
PF3D7_1116000	rhoptry neck protein 4
PF3D7_1117000	conserved Plasmodium membrane protein, unknown function
PF3D7_1117300	conserved Plasmodium protein, unknown function
PF3D7_1122100	GPI transamidase component GPI16, putative
PF3D7_1122700	conserved Plasmodium protein, unknown function
PF3D7_1124000	endoplasmic reticulum oxidoreductin, putative
PF3D7_1125000	conserved Plasmodium protein, unknown function
PF3D7_1127500	protein disulfide-isomerase, putative
PF3D7_1128700	GPI-anchor transamidase, putative
PF3D7_1132800	aquaglyceroporin
PF3D7_1133000	conserved Plasmodium protein, unknown function
PF3D7_1133400	apical membrane antigen 1
PF3D7_1134100	protein disulfide isomerase
PF3D7_1136200	conserved Plasmodium protein, unknown function
PF3D7_1136900	subtilisin-like protease 2
PF3D7_1137500	apicoplast ribosomal protein S14p/S29e precursor, putative
PF3D7_1143000	alpha/beta hydrolase, putative
PF3D7_1143200	DnaJ protein, putative
PF3D7_1144700	apicoplast import protein Tic20, putative
PF3D7_1200700	acyl-CoA synthetase
PF3D7_1201300	liver stage associated protein 1
PF3D7_1201600	NIMA related kinase 3

PF3D7_1204900	probable protein, unknown function
PF3D7_1205300	conserved Plasmodium protein, unknown function
PF3D7_1206000	shewanella-like protein phosphatase 2
PF3D7_1214000	conserved Plasmodium protein, unknown function
PF3D7_1218000	thrombospondin-related apical membrane protein
PF3D7_1228600	merozoite surface protein 9
PF3D7_1228700	conserved Plasmodium protein, unknown function
PF3D7_1229300	conserved Plasmodium protein, unknown function
PF3D7_1229600	conserved Plasmodium protein, unknown function
PF3D7_1232700	conserved Plasmodium protein, unknown function
PF3D7_1234600	protein TOC75, putative
PF3D7_1236800	protein-S-isoprenylcysteine O-methyltransferase, putative
PF3D7_1237900	conserved Plasmodium protein, unknown function
PF3D7_1240100	early transcribed membrane protein 12
PF3D7_1242000	conserved Plasmodium protein, unknown function
PF3D7_1247800	dipeptidyl aminopeptidase 2
PF3D7_1248600	conserved Plasmodium protein, unknown function
PF3D7_1252100	rhoptry neck protein 3
PF3D7_1252400	reticulocyte binding protein homologue 3, pseudogene
PF3D7_1252900	Plasmodium exported protein, unknown function
PF3D7_1253300	Plasmodium exported protein (PHISTa), unknown function, pseudogene
PF3D7_1253400	acyl-CoA synthetase
PF3D7_1253500	Plasmodium exported protein, unknown function
PF3D7_1301600	erythrocyte binding antigen-140
PF3D7_1301700	CX3CL1-binding protein 2
PF3D7_1301900	Plasmodium exported protein, unknown function
PF3D7_1305100	conserved Plasmodium protein, unknown function
PF3D7_1306200	conserved Plasmodium protein, unknown function
PF3D7_1308800	tyrosine recombinase
PF3D7_1310200	conserved Plasmodium protein, unknown function
PF3D7_1318000	conserved Plasmodium membrane protein, unknown function
PF3D7_1320100	ATP-dependent Clp protease adapter protein ClpS
PF3D7_1321900	conserved Plasmodium protein, unknown function
PF3D7_1322000	nucleoside-diphosphatase, putative
PF3D7_1330100	conserved Plasmodium protein, unknown function
PF3D7_1330200	conserved Plasmodium protein, unknown function
PF3D7_1331600	protein tyrosine phosphatase-like protein, putative
PF3D7_1332100	conserved Plasmodium membrane protein, unknown function
PF3D7_1334600	MSP7-like protein
PF3D7_1334700	MSP7-like protein
PF3D7_1334800	MSP7-like protein

PF3D7_1335000	MSP7-like protein
PF3D7_1335100	merozoite surface protein 7
PF3D7_1338600	conserved Plasmodium protein, unknown function
PF3D7_1338900	serine/threonine protein kinase, putative
PF3D7_1340000	secreted ookinete protein, putative
PF3D7_1340800	mitochondrial pyruvate carrier protein 1, putative
PF3D7_1344600	lipoyl synthase
PF3D7_1345100	thioredoxin 2
PF3D7_1347600	conserved Plasmodium protein, unknown function
PF3D7_1352500	thioredoxin-related protein, putative
PF3D7_1352900	Plasmodium exported protein, unknown function
PF3D7_1358000	patatin-like phospholipase, putative
PF3D7_1358300	rhomboid protease ROM7
PF3D7_1364100	6-cysteine protein
PF3D7_1364600	aldehyde reductase, putative
PF3D7_1367500	NADH-cytochrome b5 reductase, putative
PF3D7_1368000	conserved Plasmodium protein, unknown function
PF3D7_1371600	erythrocyte binding like protein 1, pseudogene
PF3D7_1372100	Plasmodium exported protein (PHISTb), unknown function
PF3D7_1372300	Plasmodium exported protein (PHIST), unknown function
PF3D7_1372400	acyl-CoA synthetase
PF3D7_1401400	early transcribed membrane protein 14.1
PF3D7_1404700	conserved Plasmodium protein, unknown function
PF3D7_1404800	conserved Plasmodium protein, unknown function
PF3D7_1404900	conserved Plasmodium protein, unknown function
PF3D7_1410400	rhoptry-associated protein 1
PF3D7_1410700	conserved Plasmodium protein, unknown function
PF3D7_1412000	p1/s1 nuclease, putative
PF3D7_1413400	30S ribosomal protein S9, putative
PF3D7_1413500	FeS assembly ATPase SufC
PF3D7_1416000	conserved Plasmodium protein, unknown function
PF3D7_1421900	copper transporter, putative
PF3D7_1422500	ERAD-associated E3 ubiquitin-protein ligase HRD1
PF3D7_1429600	conserved Plasmodium protein, unknown function
PF3D7_1430200	plasmepsin IX
PF3D7_1430700	NADP-specific glutamate dehydrogenase
PF3D7_1431400	conserved Plasmodium protein, unknown function
PF3D7_1436300	translocon component PTEX150
PF3D7_1437100	conserved Plasmodium protein, unknown function
PF3D7_1439000	copper transporter
PF3D7_1443700	dephospho-CoA kinase, putative

PF3D7_1452000	rhoptry neck protein 2
PF3D7_1452300	DER1-like protein
PF3D7_1459900	rhoptry protein, putative
PF3D7_1460900	apicoplast ribosomal protein S10, putative
PF3D7_1460900	apicoplast ribosomal protein S10, putative
PF3D7_1463900	EF-hand calcium-binding domain-containing protein, putative
PF3D7_1468500	derlin-1
PF3D7_1469200	shewanella-like protein phosphatase 1, putative
PF3D7_1470800	conserved Plasmodium protein, unknown function
PF3D7_1472600	protein disulfide-isomerase
PF3D7_1472800	conserved Plasmodium protein, unknown function
PF3D7_1477700	Plasmodium exported protein (PHISTa), unknown function
PF3D7_1478100	Plasmodium exported protein (hyp13), unknown function
PF3D7_1479000	acyl-CoA synthetase
PF3D7_API02400	probable protein, unknown function
mal_mito_1	cytochrome c oxidase subunit 3

**Table 7: List of all 289 genes that were identified by the bioinformatics screen.**



## Danksagung

Zuerst möchte ich mich bei Prof. Tim Gilberger für Betreuung und die Möglichkeit bedanken, an einem so spannenden Thema und interessantem Forschungsumfeld zu arbeiten. Es war eine sehr lehrreiche Zeit aus der ich für die Zukunft sehr viel mitnehmen werde. Vielen Dank auch für die spannende Zeit in Kanada, eine der besten Erfahrungen, die ich während meines Studiums machen durfte.

Besonders möchte ich auch Dr. Tobias Spielmann für die Co-Betreuung meiner Arbeit danken. Es war eine große Hilfe, mit jeder Frage zu dir kommen zu können! Vielen Dank dafür und für meinen Malaria-Einstieg!

Ganz besonders möchte ich mich bei allen alten und neuen Spielbergern bedanken! Ihr wart die allerbeste Arbeitsgruppe, die es für eine Doktorarbeit geben kann!

Sven und Maya vielen Dank für eure Zeit und die Einarbeitung! Danke an Bärbel, Sarah und Ulrike dafür, dass ihr uns so viel Arbeit abnehmt! Und Bärbel, dir ganz besonders für alles was darüber hinausging! Sarah, vielen Dank ausserdem für die vielen Glitzer-Blots und PCRs in den letzten Monaten! Du warst mir wirklich eine große Hilfe in schwierigen METT-Zeiten!

Darüber hinaus muss ich mich noch bei Swagetti Yolonese bedanken! Ihr habt das letzte Jahr zu einem besonders guten gemacht! Vielen, vielen Dank dafür! ☺ Und Marius, danke für Kaffee, Schokolade und die ausdauernde Unterstützung in den letzten Monaten! Und danke an Freunde, die absolut nichts mit der Arbeit zu tun haben und wirklich einfach immer da sind!

Ein unglaubliches Dankeschön geht an meine Familie! Vielen Dank für all die Unterstützung und das Vertrauen, das ihr mir bei allem entgegenbringt! Falls es auch noch keiner gesagt hat: ihr seid die Besten!